BLAKE PLATEAU: MID-DEPTH AND BOTTOM CURRENT MEASUREMENTS

FINAL REPORT
(Year One)

Contract No. AA851-CT0-35

Submitted to: Bureau of Land Management
OCS Office, New York, NY

Submitted by: C. Casagrande, Program Manager
General Oceanics, Inc.
Miami, Florida

September 1982

This report has been reviewed by the Bureau of Land Management and approved for publication. Approval does not signify that the contents necessarily reflect the views and policies of the Bureau, nor does mention of trade names or commercial products constitute endorsement or recommendation for use.

TABLE OF CONTENTS

LIST OF FIGURES

LIST OF TABLES

EXECUTIVE SUMMARY

General Oceanics, Inc., under a Bureau of Land Management contract, anchored five moorings instrumented with current meters across the Blake Plateau along latitude 30°N. The water depts range from 75 to 970 meters.

The data collected from the 12 month field study is to be used to verify the performance of a numerical model, also supported by the Bureau of Land Management, representing circulation in the South Atlantic Bight.

One current meter was placed near the anchor of each mooring. Two of the moorings intended for anchorage under the Gulf Stream had an additional current meter attached at 200 meters and another at 400 meters above the bottom current meter.

The data from these upper meters clearly indicated the Gulf Stream as a strong northward flow whose meanders created speed and temperature fluctuations representing 40-70% of the total variance recorded. Many of these meanders appear to have been produced by energy fluctuations occurring at 2 to 14 day intervals. These results agree remarkably well with those of Richardson et al. (1968).

Near-bottom flows on the two Blake Plateau moorings east of the Gulf Stream displayed prolonged southward flow events lasting up to 42 days and reaching speeds in excess of 30 cm sec^{-1}. These events did not correlate with flows at the other three sites. The generating mechanism behind these southward flows is not clear and further work will have to be performed in order to characterize the responsible mechanism.

I. INTRODUCTION

1.1 Program Objectives

After determining that few organized or systematic area-wide observations were available for the Blake Plateau region, the Bureau of Land Management (BLM) initiated a field study of "Mid-depth and bottom currents on the Blake Plateau - 30°N" under contract number AA851-CTO-35 with General Oceanics, Inc.

In the past three to four years, it has become apparent that oil and gas interests would be capable of exploring for and, if found, developing economically viable reserves in the deep water seaward of the South Atlantic Bight (SAB) continental shelf, i.e., on the Blake Plateau (BP) in Figure 1-1. In anticipation of leases in this area, the BLM started a several pronged effort to assure that appropriate information was available to make sound environmental management decisions regarding all aspects of oil and gas activities. The different elements in the BLM effort included: (1) making operational a full three-dimensional prognostic numerical model of SAB/BP processes, and (2) establishing a physical oceanographic data base to provide both information for initializing and calibrating the above model and independent estimates of key processes active in the area. The numerical model results will be used in conjunction with the USGS oil spill trajectory model. A major component of Item (2) is the long term measurement of BP subsurface currents described in this report. A very preliminary analysis and examination of the BP data was also undertaken.

1.2 Program Tasks and Personnel

The organization for this program is presented in Figures 1-2. General Oceanics, Inc. (GO) was responsible for program management as well as all instrumentation and field work. Current meter mooring design, fabrication, deployment, and recovery were conducted by the University of Miami under the supervision of Dr. Tom Lee and Philip Bedard. Dr. Lee was also responsible for data synthesis and interpretation. Science Applications, Inc. (SAI/Raleigh) provided data management and provided most data analysis and data products. Under the direction of GO, SAI also assisted in certain aspects of program and technical management.

1.3 Report Organization

Chapter II presents a discussion of observational methods. General Oceanics current meters are described and their calibration and use in this program discussed. Chapter III gives a summary of the data processing and analysis methods used by SAI to produce the data products. Chapter IV contains a technical discussion of the data and analysis products by Dr. Tom Lee of University of Miami using representative data examples. Dr. E. Waddell of SAI also contributed to this chapter. Chapter V gives a brief summary and future recommendations. Appendix A presents data products created.

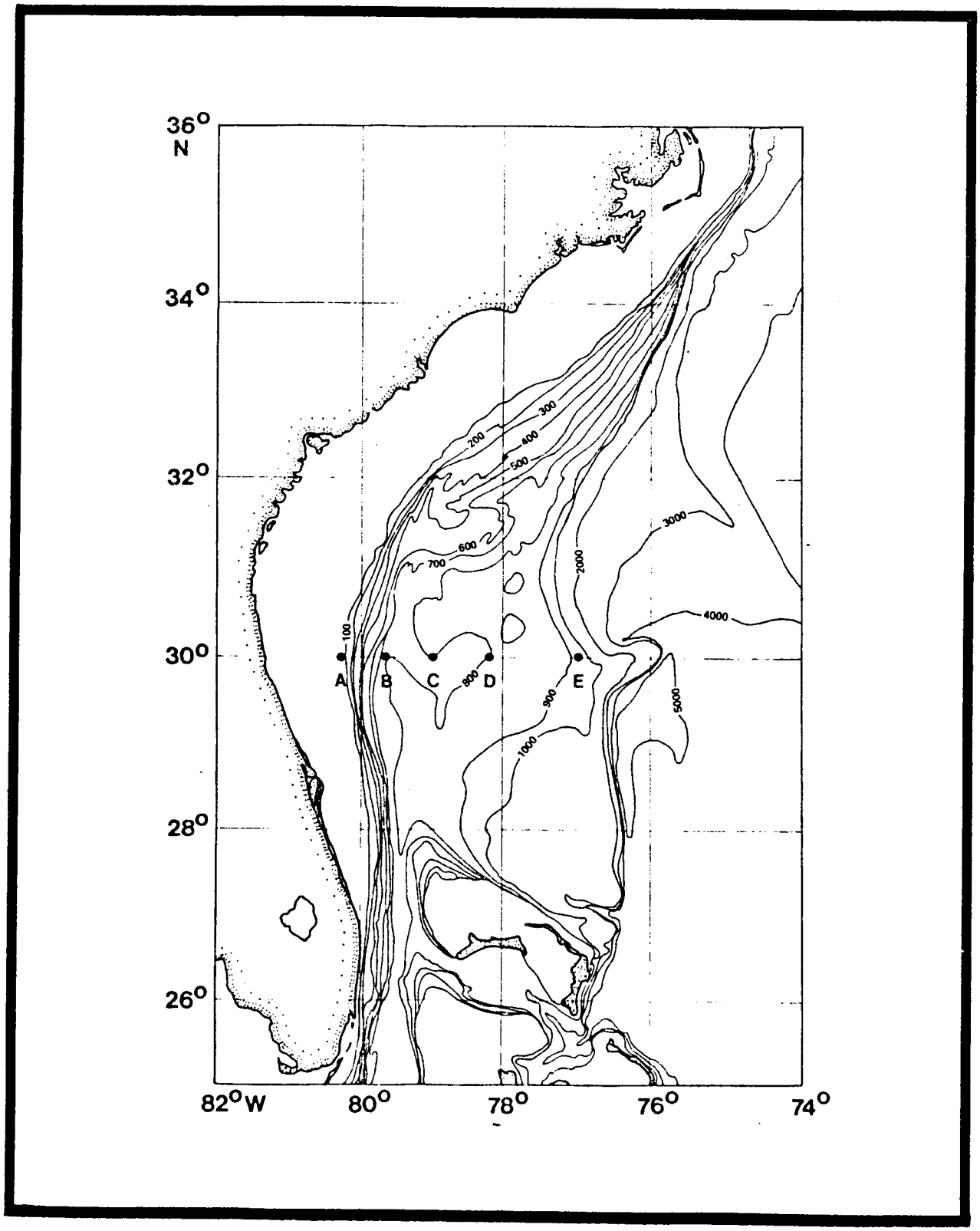

Figure 1-1 Blake Plateau study area.

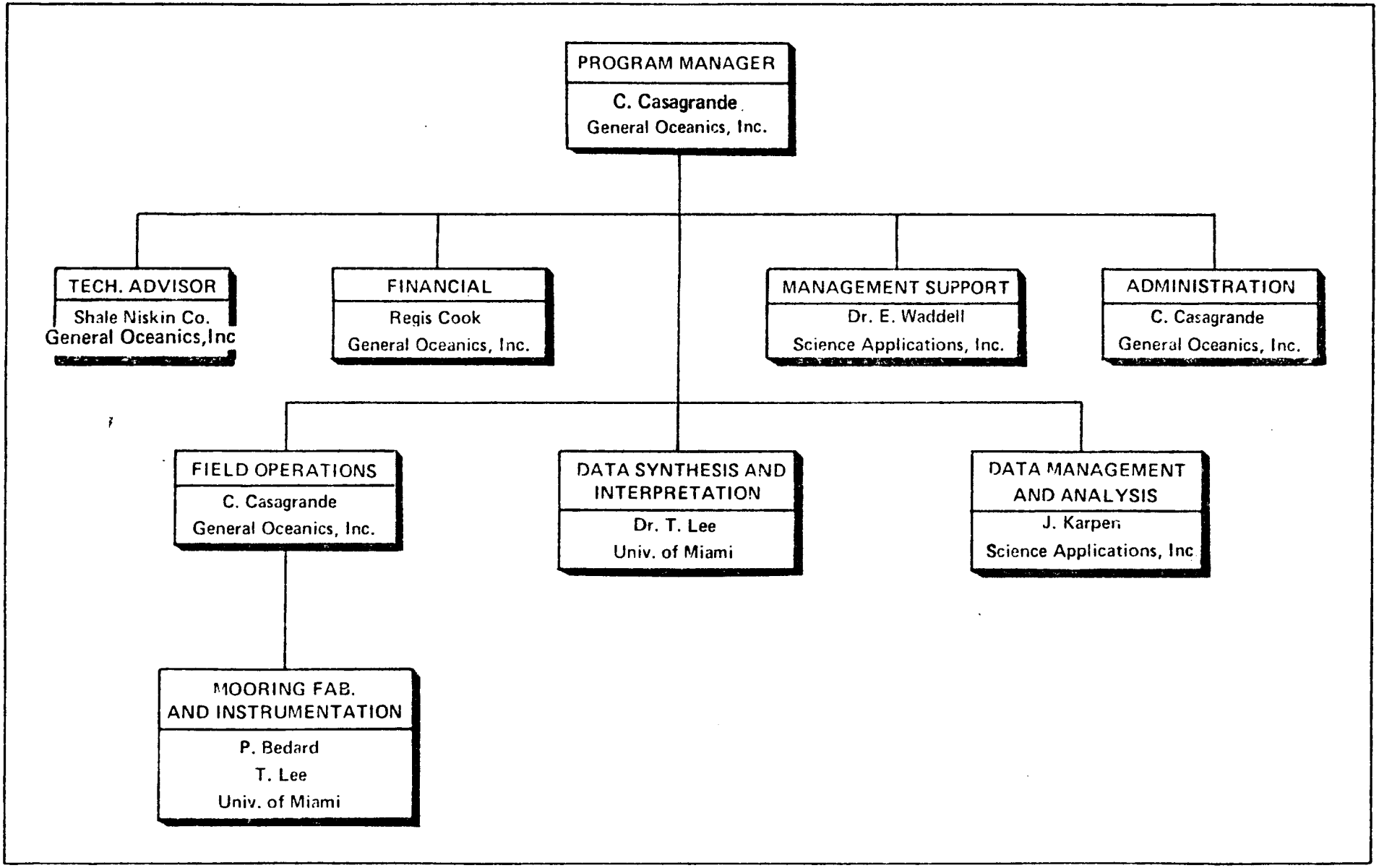

Figure 1-2 Organizational chart of the Blake Plateau subsurface current study.

II. OBSERVATIONAL METHODS

2.1 General Description

Current and temperature variability over the Blake Plateau at 30°N was measured with a cross-stream array of 5 subsurface taut-wire current meter moorings (Figure 2-1). The vertical distribution of instruments is shown superimposed on a temperature section made across the array on September 8 and 9, 1980 (Figure 2-2a); and on a velocity section made by Richardson, et al. (1969) 37 km north of the array (Figure 2-2b). The mooring array was in place for a total of 13 months from August 27, 1980 to October 6, 1981 with a mooring exchange in March, 1981. The array was equipped with 9 Niskin wing current meters. Instrument configuration and relevant information is given in Table 2-1. The mooring array extended from the shelf edge (80°15'W) to the Blake Escarpment (77°W). The shelf edge mooring (#A) was deployed at the 75 m isobath with a single current meter 3 m above the bottom. Moorings B and C were installed in water depths of about 800 m with instruments located near depths of 400, 600 and 797 m. Mooring B was located near the subsurface extension of the Gulf Stream axis and Mooring C was near the seaward edge of the GS as shown in Figure 2-2b. Moorings D and E were near bottom moorings with current meters located 3 m above the bottom in water depths of about 800 and 970 m respectively. Mooring E was located at the seaward edge of the Blake Plateau on the Blake Spur. The 600 m level current meter on Mooring C did not operate properly during the first deployment so is not listed. The lower layer instrument on Mooring B lost a fin at the start of the second deployment giving low speeds. Also temperature from the top meter on Mooring B of the second deployment was in error.

2.2 Equipment Selection and Mooring Design

2.2.1 Current Meter Selection and Description

The Model 6011 Niskin Winged Current Meter (NWCM) was used at all locations due to its reliability and high quality data return. Two additional meters considered were the Aanderaa and the VACM, but both of these instruments utilize Savonious rotors which can become problematic in regions of high currents and are sensitive to high mooring tilt. Therefore, the decision was made in favor of the NWCM.

In addition, the NWCM offer these desirable features:

- The amount of mooring tile does not affect the instrument speed and direction sensing capabilities, and no data corrections are needed for excessive inclination of the mooring.

- Instrument calibration basically consists of a compass check since the housing dimensions and buoyant weight remain constant.

- The 20 inch length and 20 pound weight in air can be handled by one person. Whereas the VACM is 77 inches long and weighs 160 pounds in air. The Aanderaa is 55 inches long and weighs 56 pounds in air.

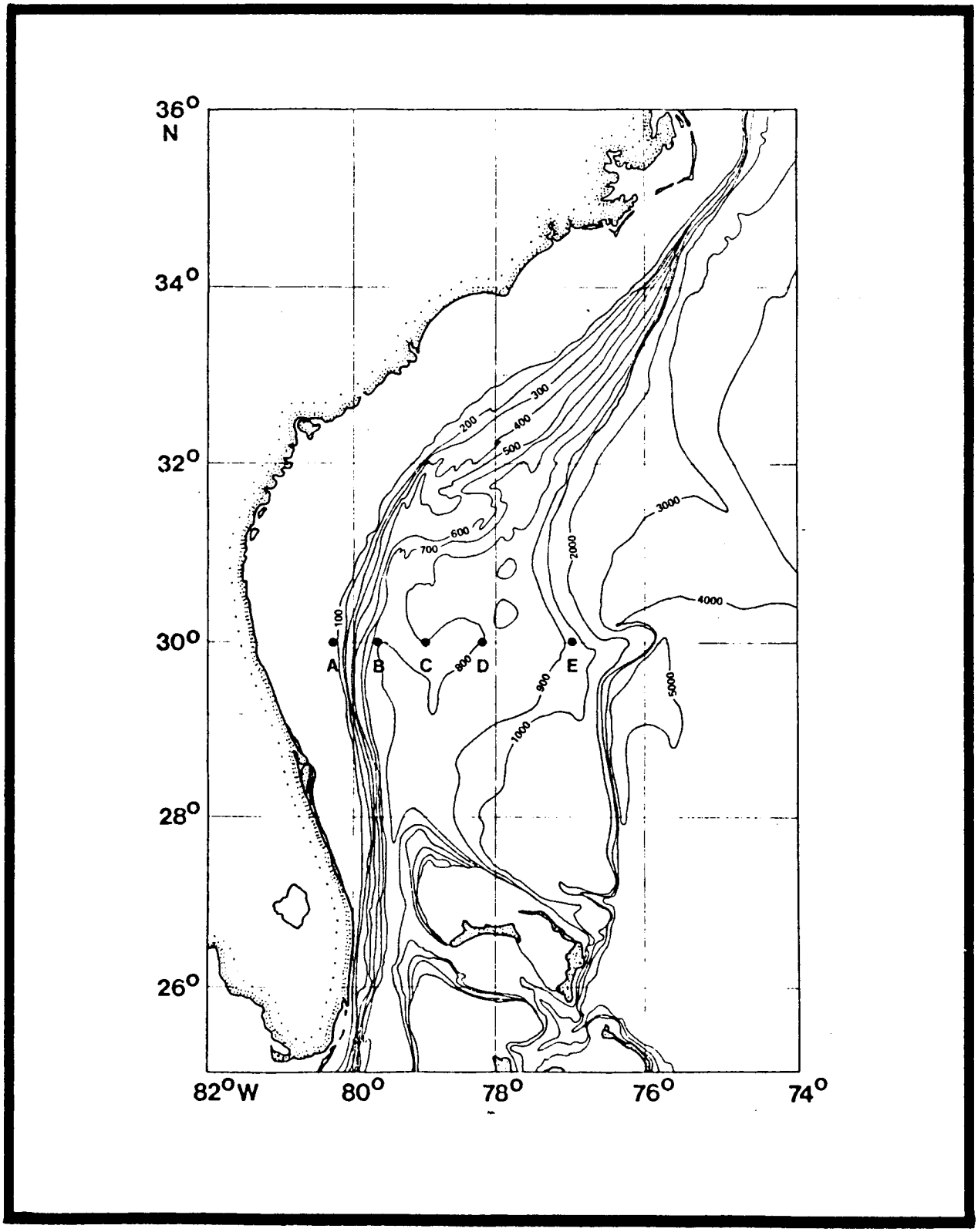

Figure 2-1 Location of Blake Plateau current meter mooring sites; August 26, 1980 to October 6, 1981.

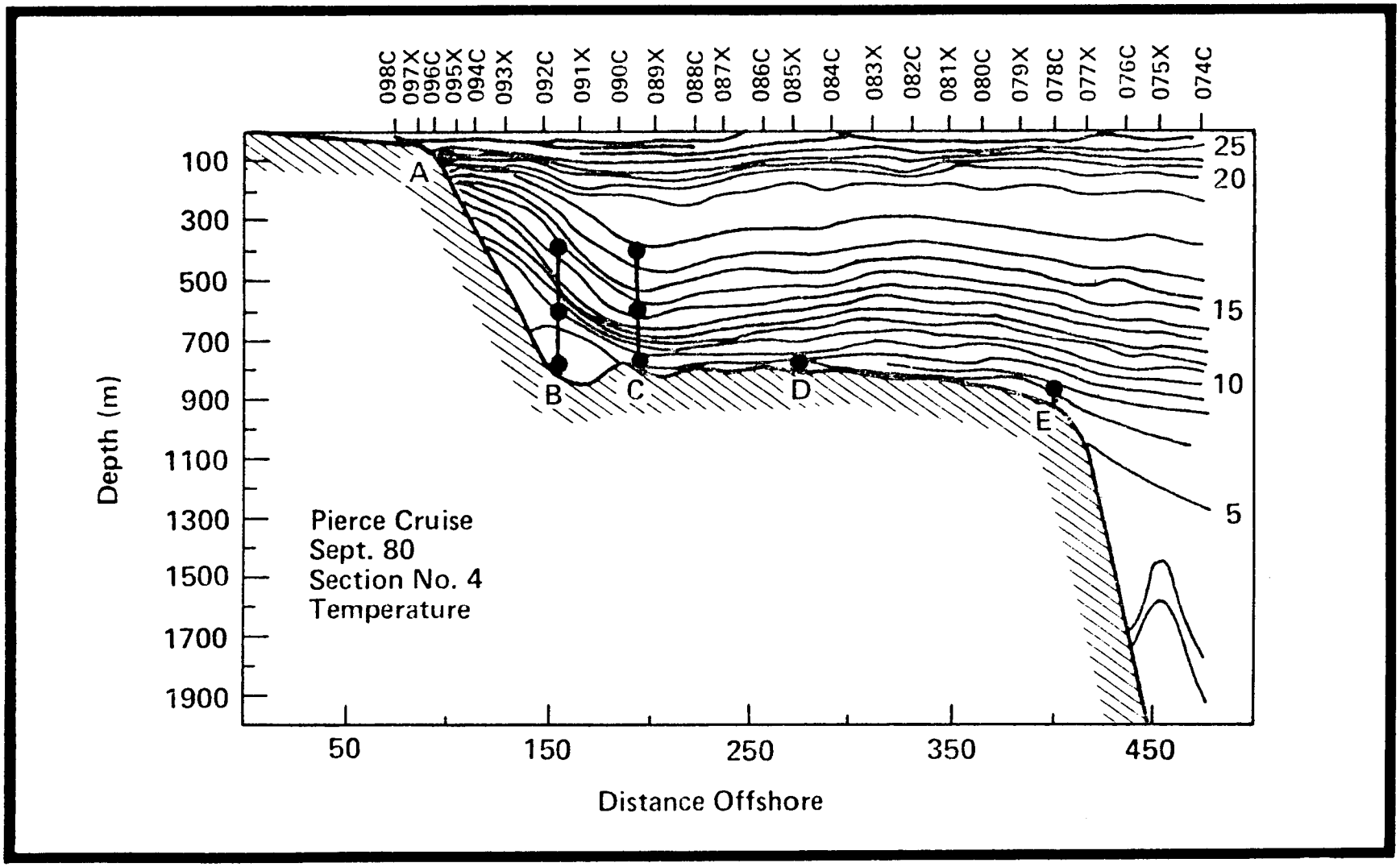

Figure 2-2a Vertical configuration of current meters superimposed on a temperature section of September 8 and 9, 1980 made by Skidaway Institute of Oceanography.

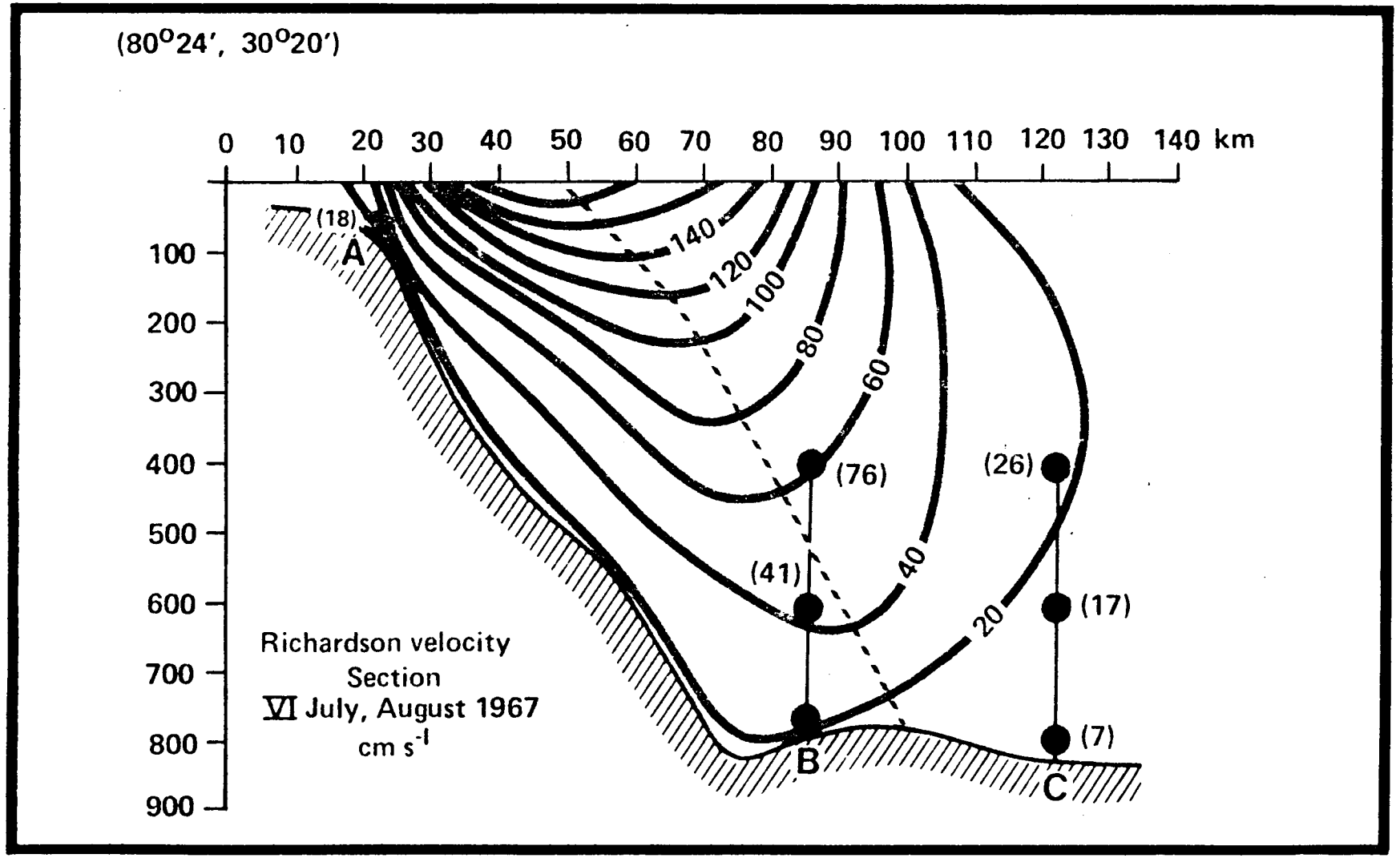

Figure 2-2b Vertical configuration of moorings A, B and C superimposed on a velocity section made by Richardson et al. (1969) during July and August 1967. Mean downstream velocities at each current meter during the 2nd deployment are shown in parenthesis.

	Mooring Site	Lat.	Long.	Mooring No.	Current Meter No.	Instrument Depth (m)	Water Depth (m)	Deployed (GMT)	Recovered (GMT)
1st Deployment	A	30°N	80°15'W	120	12001	73	76	8/28/80 0035	3/15/81 1430
	B	"	79°40'	121	12101	397	797	8/27/80 1952	3/16/81 1810
					12102	597		" 2005	" 1820
					12103	794		" 2020	" 1830
	C	"	79°20'	122	12201	406	806	8/27/80 1602	3/16/81 0010
					12203	803		" 1625	" 0025
	D	"	78°10'	123	12301	801	804	8/27/80 0736	3/15/81 1225
	E	"	77°00'	124	12401	969	972	8/26/80 2233	3/15/80 0010
2nd Deployment	A	30°N	80°15'W	129	12901	72	75	3/15/81 1530	10/4/81 2145
	B	"	79°40'	130	13001	397	797	3/16/81 1910	10/6/81 1414
					13002	597		" "	" 1424
					13003	794		" "	" 1437
	C	"	79°20'	131	13101	415	815	3/16/81 0107	10/6/81 1115
					13102	615		" "	" 1125
					13103	812		" "	" 1137
	D	"	78°10'	132	13201	796	799	3/15/81 1325	10/5/81 2217
	E	"	77°00'	133	13301	965	968	3/15/81 0103	10/5/81 1550

Table 2-1 Mooring Information.

- The standoff supporting the NWCM is clamped onto the mooring line. There is no mooring line segmentation and, therefore, no strength requirements other than to withstand the water pressure. Operational depth is 6000 m.

Comparison between the NWCM Model 6011 and the VACM indicates excellent agreement between them (Bonde, 1978).

The GO Model 6011 is a solid state recording meter with no external moving parts. Specifications are given in Table 2-2. The meter is attached with a swivel on a mooring standoff and hangs vertically in the absence of a current. In the presence of a current, the instrument is tilted downstream (Figure 2-3). The angle of tilt varies with the speed of the current. The greater the current, the greater the angle of tilt.

The instrument is fitted with a wing-like structure which stabilizes and orients the instrument in the direction of current flow. The housing contains a tilt sensor (a force balanced inclinometer), three orthogonally mounted hall effect sensors for compass direction, and a thermistor (optional) for temperature.

During the mooring period, signals from the sensors are digitized and placed in a 64-bit parallel-in/serial-out shift register together with an associated time code and instrument serial number. The information is then recorded in binary code on a Phillip style magnetic tape cassette.

The cassette is read and input directly to a computer where GO software calculates current velocity directly from instrument tilt by converting this tilt angle to current speed using an experimentally determined calibration curve. The three vector components of the earth's magnetic field provided by the hall effect sensors are combined in an appropriate equation to produce magnetic headings.

The results are displayed on strip charts and/or transcribed to a 9 track magnetic tape for further processing and analysis.

2.2.2 Mooring Design

2.2.2.1 Mooring Criteria

The criteria defined in this section have been used in the design of the moorings shown in Figures 2-4a and 2-4b.

Moorings B and C were designed according to the following criteria:

a) The angle of the inclination of each mooring does not exceed 25° from the vertical in order to ensure the quality.

b) All instruments are shackled to flotation sufficient to raise the instrument and associated hardware in the event of a mooring failure at any location along the mooring line.

Table 2-2 Niskin Winged Current Meter Model 6011 Specifications

Designation:	Niskin Winged Current Meter (NWCM) Model 6011-T
Manufacturer:	General Oceanics, Inc., Miami, Florida
Current Speed:	Sensor: Housing tilt Threshold: 2 cm s^{-1} Maximum: 225 cm s^{-1}
Current Direction:	Compass: 3 hall generation; resolution 1^{o}, accuracy $\pm 2^{o}$
Temperature:	Yellow Springs aged linear thermistor; resolution $\pm$ 1/64°C, accuracy $\pm$ .25°C
Time Base:	Source: Crystal oscillator Accuracy $\pm$ 10 sec per day Sampling Interval: 1 to 512 readings per hour
Data Storage:	Tape Recorder: Digital Capacity: 10,000 readings
Mechanical:	Pressure Housing: 51.3 mm long x 10.5 mm diameter 7075-T6 aluminum, hard coat anodized 6000 meter operating depth
Weight:	20 Lbs in air, 10.7 Lbs in water
Corrosion protection:	Zinc Anode
Sampling Rate:	Since wave contamination will not be a problem, burst sampling will not be used. A 15 minute sample rate (Δt=15 min) is to be used. This sampling interval will assure resolution of all pertinent velocity fluctuations. A 15 minute interval produces a Nyquist frequency of 48 cycles day^{-1}. This will easily accommodate resolution of tides, any meteorological forcing, eddies, and Gulf Stream fluctuations.

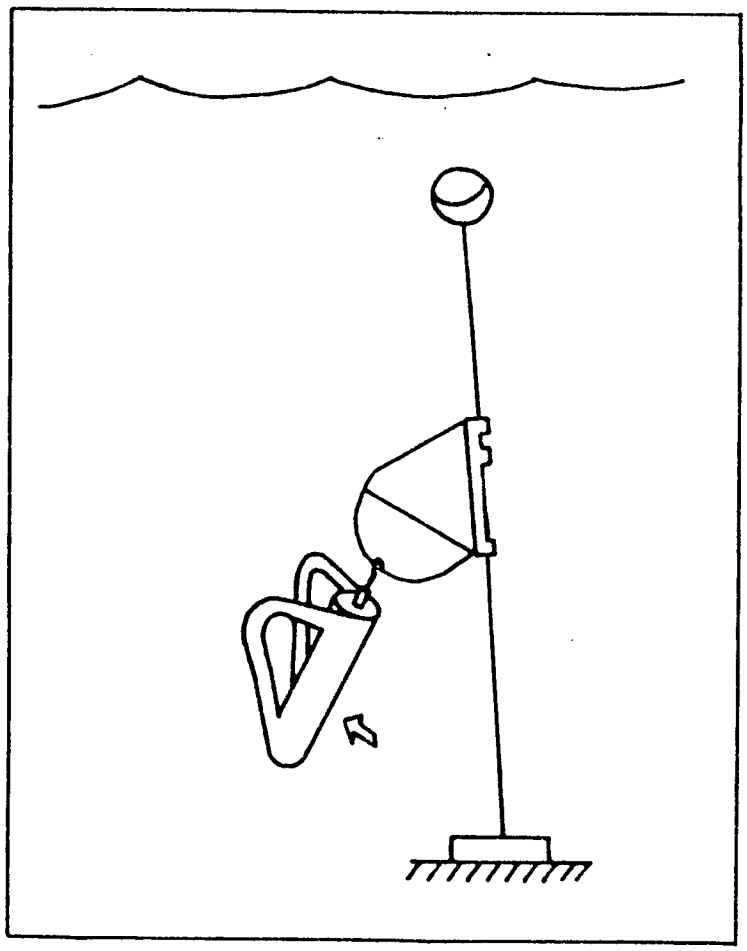

Figure 2-3 Niskin Winged Current Meter (NWCM) Model 6011 tilting downstream and independent of mooring inclination.

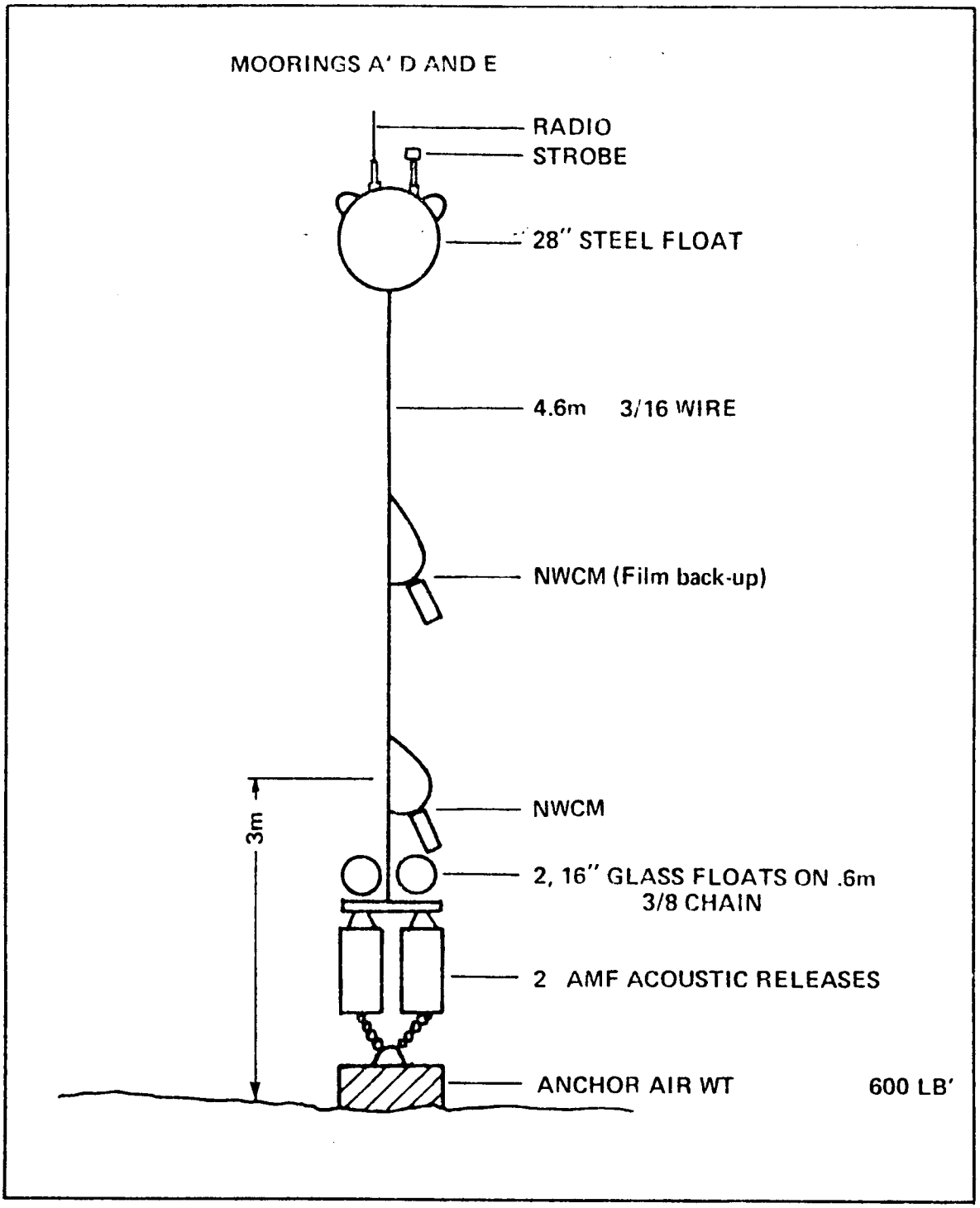

Figure 2-4a Schematic of Blake Plateau current meter moorings A, D and E.

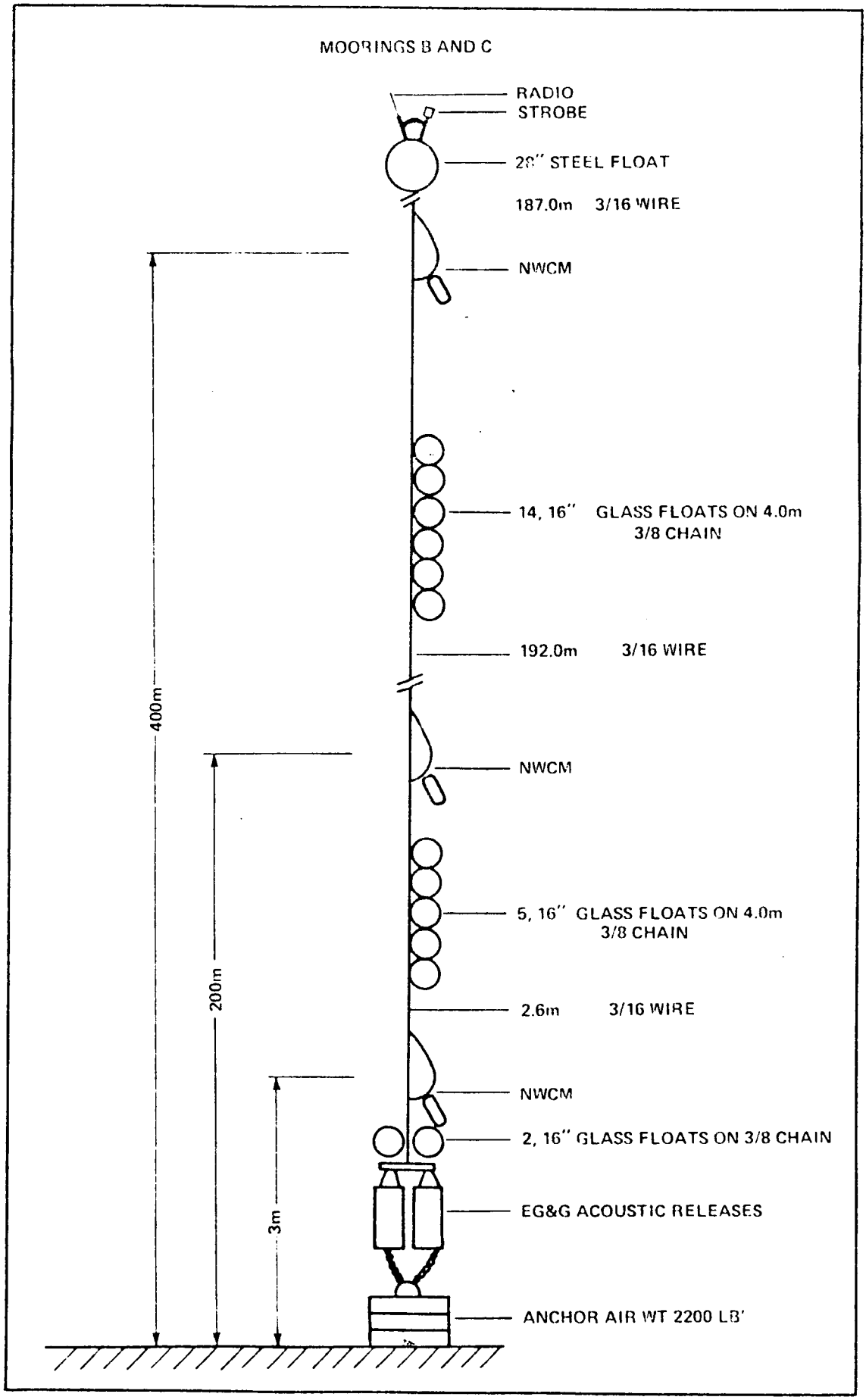

Figure 2-4b Schematic of Blake Plateau current meter moorings B and C.

c) Insofar as possible, galvanized steel was used in the mooring components. Where not possible, dissimilar materials were isolated from one another.

d) Acoustically actuated release devices were used to detach the anchor from the rest of the mooring system in order to recover the instruments. Two acoustic release mechanisms are employed in a parallel arrangement, such that release can be effected if only one of the releases functions.

The flotation devices were subsurface steel buoys manufactured by Ocean Research Equipment (ORE) Company and glass spheres. The weight of the anchor is designed to insure that the mooring will drag before the mooring wire is subjected to a strain near its elastic limit.

2.2.2.2 Mooring Design Methodology

Mooring design involved a process of successive interaction. The first step consists of defining representative vertical current profiles likely to prevail at the sites. This task requires a review of existing literature relevant to the area of interest and of data sets actually collected at the sites or in their near vicinity, or in dynamically similar environments. It is clear that, short of processing actual current meter time series at various depths at the mooring site, one can only make an educated estimate of expected current profiles. Fortunately, there was current profile data available from a Richardson transport section taken near 30°N (Table 2-3; Richardson, Schmitz and Niiler, 1969). These data were entered as inputs to the mooring design computer program described below and used for the definition of the static configuration of the first mooring to be deployed. The second step in the design consists of defining a theoretical mooring configuration suitable for the environment in which it will be launched, based on the experience of the design team at the University of Miami.

In the third step, adequacy of the mooring design defined in second step is checked by running a computer program originally developed by WHOI (Moller, 1976) which calculates the deflection of the current meter array when submitted to the current profiles defined in step 1, and the tensile load and reserve buoyancy at the elevation of every mooring element.

If some criteria (e.g. maximum allowable inclination) are violated, the mooring configuration will be modified (step two), and step three repeated until the final configuration is such that criteria on instrument inclination, reserve buoyancy, and tensile loads are all met for the input current profiles selected in step one.

Final mooring designs are shown in Figures 2-4a and 2-4b. Three moorings are short with each supporting only one current meter and a back-up film recording current meter to be used in case of failure of the primary instrument, and two releases in addition to flotation and anchors. The two longer moorings each support three current meters and more extensive flotation in addition to two releases and anchorage.

Table 2-3. Current Profile. The ± values represent the amplitude of traveling barotropic waves. A maximum profile would be obtained by adding 50 cm s^{-1} to the velocities at all levels. To obtain the minimum profile subtract 50 cm s^{-1} which indicates that deep current reversals are possible.

Depth (m)	Downstream Current Speed (cm s^{-1})
0	140 ± 50
100	110 ± 50
200	95 ± 50
300	80 ± 50
400	65 ± 50
500	55 ± 50
600	40 ± 50
700	30 ± 50
800	20 ± 50

The current profile used in this static configuration test is given in Table 2-3. With this as input, maximum inclination of the mooring line for the short mooring was less than 1°. The longer moorings had a maximum mooring line inclination of 24.4°, however, this occurred on the long mooring line sections between instruments. At depths where current meters are located, maximum inclination was less than 19°, well under the maximum allowable.

2.2.3 Release Mechanisms

Release mechanisms used to separate moorings A, B, C and D from their anchors at the end of the deployment period were the shallow water Models 314 and 722A Recoverable Acoustic Transponders manufactured by EG&G SeaLink, Herndon, VA (formerly AMF). Mooring E required the deep water Model 723A manufactured by the same firm. These instruments were used side-by-side in a parallel arrangement allowing a mooring to be released from the anchor by either unit. In addition to the release function, performed by firing a small explosive squib, these units are equipped for the following functions:

- Reply Pinger - Upon receipt of appropriate command, unit transmits acoustic pulses for a period of 90 seconds.

- Tilt Switch - A tilt switch was incorporated to give an indication of the attitude of the mechanisms. If the release exceeds 45° from vertical, then the pulse rate from the reply pinger is doubled. This feature will determine whether or not a mooring failure has occurred.

- Transponder - This enables the recovering vessel to obtain an accurate slant range to the release mechanism, both before and after

the release has been activated. Confirmation of release is obtained by the underwater unit transmitting a double pulse in return to the interrogating pulse. After the release has been activated and release confirmation received, the ranging information is used to locate the surface mooring.

2.3 Quality Assurance

A quality assurance (QA) program is recognized as essential to a productive field measurement operation since success is judged by the quality and amount of data taken. Our QA involved a careful conformance both to predeployment testing and to detailed post-retrieval performance evaluation. This detailed before and after evaluation assures problem identification and resolution. Steps and procedures minimizing data degradation and/or equipment loss have been developed for all components of field equipment.

GO's quality assurance manager had the responsibility to inspect all current meters, to insure their checkout/calibration and maintenance prior to deployment and after retrieval. Further the QA manager coordinated with the University of Miami (P. Bedard) to insure all current meter moorings were assembled according to design specifications; that trained personnel were on duty for retrieval and redeployment; to inspect the ship and make certain that all ship equipment, davits, cranes, cables, etc. were adequate to handle the instruments in poor weather conditions; and that these operations were thoroughly documented. He was also responsible for reviewing the data reduction procedures used and, with the assistance of the program manager, make certain that all procedures were adequate.

2.3.1 Current Meters

Before a current meter was used it underwent a testing and checking procedure described below. Many of the checked items verify correct operation of the sensors and sequencing and recording system. An important check in any instrument which must operate reliably for long periods on an internal battery is the power consumption.

A "Compass Error Table" is produced for each meter by mounting the meter in a test jig which allows it to be tilted at angles of zero, 30° and 60° while at the same time point in various directions relative to magnetic north. The meter is thus subject in turn to the same conditions produced by zero current, a mid-range current and a current near to maximum for each of eight different directions round the compass.

Signals picked off from a special monitor connector mounted near the tape recording head on the current meter are fed into a minicomputer. The minicomputer then calculated and displayed the tilt and direction angles actually sensed by the current meter so that they could be recorded in the Compass Error Table.

2.3.2 Release Mechanisms

Of prime importance to subsurface current measurements is the operation of acoustic release mechanisms. Maintenance procedures used in this study

rely heavily on those developed at WHOI in which each release is divided into two main sections: the command receiver and the transponder section.

After being received, the first step in the maintenance procedure is to connect the two receiver batteries and to power up the release for 24 to 36 h. After that period, the battery voltages are read and recorded, as well as the standby current drains. The command receiver is then checked for the proper response to test signals using an AMF model 210 Release Mechanism Test Set. If necessary, the circuits are adjusted for the proper timing values at this time. The same tests are repeated for all three receiver commands. Each release is capable of responding to three commands: Release, Timed Pinger/Transponder Enable, and Transponder Disable.

The transponder section, upon receipt of an interrogation pulse, transmits a return pulse with a known turn-around time. The timing and pulse relationship of this circuit are checked and adjusted, if necessary. The time pinger, transponder enable/disable circuit, and firing circuit are checked for proper operation.

All the above tests are repeated at 5°C, to determine proper operation under low temperatures. Prior to sealing the electronics chassis in its pressure housing, the transducer is connected and a signal from the test set is acoustically coupled to the release mechanism to give a final end-to-end check of all functions. After assembly into its housing, the release mechanism is purged with freon to insure a dry operating environment for the electronics. All new release mechanisms are fired at least one prior to deployment on a mooring.

When the release is returned from the field, the first step is to thoroughly clean and re-arm the squib firing assembly. After that has been done, the electronic tests are performed as above.

2.4 Mooring Deployment and Retrieval

2.4.1 Mooring Deployment Procedures

Mooring launching procedures followed are similar to those described by Heinmiller (1976). The methodology for mooring deployment implemented is briefly described below.

Deployment of the moorings was accomplished by the anchor-last method, where the top of the mooring is paid out over the stern, while the ship is usually moving upwind or upcurrent at low speed (< 2 kts). Payout of the line, instruments, and flotation proceeds under moderate tension in the line until the bottom end of the mooring is finally reached. The anchor is then attached to the lower end of the mooring and released, free-falling to the bottom. This free fall procedure is considered the safest mode of deployment for it involves a minimum handling time of anchors. If a problem develops on the mooring assembly, then it can be brought aboard with ease. This also reduces the time of maximum mooring load so that the duration of peak transient loads due to wave and ship motions are reduced.

Anchor-last deployment streams the mooring away from the ship which lessens the danger of mooring fouling with the ship. It also provides greater

ship maneuverability which helps in station keeping and allows final adjustments in the mooring location to be made if necessary. Experience has shown that the mooring is not damaged on impact after a free fall. The buoyancy of the components and subsurface flotation is sufficient to hold the mooring upright during free fall. Deployments conducted by Nova University demonstrated the feasibility of this method where scientific considerations dictated that a precision pressure gauge be mounted directly on the anchor, with the release mechanism 1 m or less above. In all instances, there was no indication that the release mechanism impacted on the anchor, or the bottom. The impact of the mooring on contact with the bottom is actually the same on an anchor last or anchor first development since terminal velocity is reached soon after release.

Deploying a mooring at a selected location or depth requires a great deal of at-sea experience in similar deployments to maintain line tension within an acceptable range and in selecting the starting point of the deployment procedure with respect to the mooring site. In doing this the ship's motion relative to the water, mooring length, complexity of the configuration of the mooring to be deployed must be taken into account. Knowledge of the ship response to a combination of wave action, wind and surface currents is essential to a successful operation.

Following deployment of a mooring the transponders were interrogated and then disabled. Proper receipts of the disable command is indicated when the transponder no longer responds to an interrogate pulse.

2.4.2 Mooring Retrieval Procedures

The major problem associated with mooring recovery is to locate the mooring, and to establish good acoustic contact with the release mechanisms. Once the mooring is released from its anchor and located as it floats to the surface, the operation becomes fairly straightforward.

Typically, the ship will be brought into the immediate vicinity of the mooring, using Loran-C for positioning. The acoustic ranging system will then be immersed to determine range to the mooring. Once the distance between the mooring and the ship is reduces to 1 km or less, release mechanisms will be actuated. The entire scientific party will be on deck to act as spotters. After breaking the surface, the mooring is located either by sight or with a Radio Direction Finder, depending on nearness to the ship and sea conditions. If necessary, an acoustic range measurement will be made to determine if the mooring flotation should be visible from the ship's upper deck. Once located, the ship converges on the mooring, keeping the latter on the lee side.

The general mooring recovery procedure consists of grabbing the subsurface float with a Renfroe hook working from the starboard "A" frame in conjunction with a hydraulic winch. This hook is attached to the end of a line wound on the winch. A static length of chain (or stopper) approximately 4 m long is attached to the top ot the "A" frame with a stainless steel snap hook attached to the free end. Once the surface marker is hooked, the ship is positioned so that the mooring is trailing behind the ship. The actual recovery operation can then begin.

The actual mooring hauling procedures for in-line moorings are fairly straightforward. The subsurface buoy is lifted up with the winch and drawn on board by the "A" frame. Load is then transferred from the winch wire to the stopper and snap hook. The section on deck is dismantled and stored. The winch line is reattached below the snap hook and drawn in until the winch has taken up the load. The snap hook is removed and wire is taken up until the next instrument package is landed on the deck. This procedure is repeated until the whole mooring is on board. Because the instrument to be used in this study is a clamp-on, there was no winch line reattachment and time on station was reduced.

A post-recovery inspection was made of each mooring, noting the condition of instruments, biofouling, corrosion, and any unusual signs of stress. Photographs were taken of the wire and housing assembly of each current meter upon recovery, to give a qualitative assessment of the amount of biological fouling present on the sensors.

2.5 Data Reduction

Instruments in the General Oceanics 6000 series record their data on a standard Philips style data cassette in a binary coded format. This format makes for simplicity and reliability in the recording instrument.

GO provides the service of translating the data from these cassettes into engineering units and then recording them on 9-track magnetic tape in a format which meets IBM and ANSI standards. The following describes the formats on the tapes and the procedure used for converting the numbers on the cassette tape into current speed, direction and, if that option was fitted, temperature.

2.5.1 Current Meter and Tape Format

Data are recorded on the instrument cassette as a 64-bit binary work - one for each reading - in the format shown in Table 2-4. In the translating process the 64-bit word is read by the computer which then calculates the corresponding value of current velocity (east-west and north-south components). Temperature and time values are also calculated.

A file number and reading numbers are added, together with space and carriage return characters. Unless otherwise requested by the customer, a file number of 001 is assigned to data from the first cassette recorded on the reel, 002 to that from the second etc.

This process results in a 38-character word representing the original 64-bit binary word. The final stage combines eight of these words into a 304-character data block. Data from three fully recorded cassettes may be stored on one 7-inch reel of 9-track tape.

Table 2-4. Format of recorded data on cassette of the NWCM, Model 6011.

Sensor	No. of Bits on Cassette	Range
Y-Magnetic	8	0-255
Z-Magnetic	8	0-255
X-Magnetic	8	0-255
Tilt	8	0-255
Instrument SN	6	0-63
Hour Code	10	0-1023
Temperature	12	0-4095
Filler	4	-
TOTAL	64	

*Records all 1's or 4095 when no temperature option is fitted.

2.5.2 Procedure for Computing Speed and Direction

To compute current speed and direction, or alternatively north-south and east-west components, readings from four sensors are used - X, Y and Z from the three magnetic sensors and T from the tilt sensor. Each of these readings, as recorded on the cassette tape, has a value between 0 and 235. The computation procedure may be summarized as follows:

1. Readings required: X, Y, Z, T. Each ranges from 0 to 255.

2. Convert T to angle of tilt using

$$\theta = \text{ARCSIN } (T-G)/H. \qquad (1)$$

3. Convert angle to current magnitude M using calibration curve.

4. Determine Hy using $Hy = E(Y-B)$.

5. Determine H_n using equation 1 above.

6. Determine east-west component C_{EW} using

7. Determine north-south component C_{NS} using

$$C_{EW} = \frac{(H_y)(M)}{(H_y^2 + H_h^2)^{\frac{1}{2}}} \qquad (2)$$

$$\frac{(H_h)(M)}{(H_y^2 + H_h^2)^{\frac{1}{2}}} \qquad (3)$$

Current speed is calculated directly from the tilt reading using equation 1 and the calibration curve of tilt angle as a function of current speed.

To obtain current direction the three magnetic sensor readings have to be combined with the inclinometer reading in the following procedure. A conventional compass, such as a ship's compass, determines direction by responding only to the horizontal component of the earth's magnetic field. To insure this the compass magnets are suspended below the pivot point so that they remain horizontal for any reasonable tilt of the instrument. The range of allowable tilt is extended by mounting the compass in a gimbal system. Any response to the vertical component, such as occurs when the vehicle in which the compass is mounted turns or accelerates rapidly, leads to an error in reading.

With a solid state compass, direction is determined by using two hall effect sensors mounted in a horizontal plane. To avoid the complexity of the necessary gimbal system, however, the method chosen in the Model 6011 is to use three Hall effect sensors, fixed rigidly to the frame of the instrument, and to correct for the effect of the vertical component using the inclinometer reading.

Since the instrument always tilts towards the wings, the so-called Y-axis sensor always remains horizontal. This sensor measures a horizontal component Hy. The horizontal component perpendicular to this is H_h and can be obtained from the readings of the X and Z sensor by using the relation

$$H_\eta = D(X-A)\ \text{Cos}\ \theta + F(Z-C)\ \text{Sin}\ \theta. \qquad (4)$$

Here A, C, D, and F are offset and scale factors whose values are given and θ is the angle of tilt. Direction is then a simple function of ARCTAN H_y/H_h.

2.5.3 Procedure for Computing Time and Temperature

The hour code is a number ranging from 0 to 1023. It represents directly the time in hours since the instant of clock reset prior to the deployment of the instrument. To determine the actual time of a particular reading one should bear in mind that in any hour the first reading occurs half a sampling period after the hour mark. For example, with a sampling rate of four per hour there will be four readings with the same hour code; the time of these readings being 7-1/2, 22-1/2, 37-1/2 and 52-1/2 minutes after the hour.

After 1024 hours the hour code restarts at zero. Therefore, for long deployments the user has to keep track of the multiples of 1024-hour periods to be used to compute the total time. Since 1024 hours is about six weeks this is not difficult.

The temperature reading as a number in the range 0 to 4095. It is converted to degrees centigrade using

$$\text{Temperature} = (\text{Reading}/64) - 8°\text{C}. \qquad (5)$$

III. DATA ANALYSIS

3.1 Introduction

As a result of the field program described previously, 18 current velocity/temperature time series were created (two deployments x nine instruments per deployment).

Initially a standard set of analyses and associated data products were created and provided to General Oceanics, Inc. and Dr. Thomas Lee (University of Miami). These included:

(1) printout or plots of time series
(2) stack plots of data filtered to remove tidal and higher frequencies (stick plot form of vector data).
(3) spectra of filtered current components
(4) progressive vector diagrams (PVD) of filtered velocities
(5) biweekly and total means
(6) data tapes (NODC formats).

In addition to the above six items, SAI has worked with Chris Casagrande, the program manager, and Dr. T. Lee to provide additional data products. A complete set of the above data products are presented in Appendices A and B for the first and second deployment periods respectively.

3.2 General Procedures

Instruments sample velocity and temperature at half hourly intervals ($\Delta t = \frac{1}{2}$hr.). These time series are recorded on magnetic tape cassettes. Following retrieval, data is transcribed (by GO) from cassettes to nine track tapes and sent to SAI. When received at SAI, the data are evaluated for quality with routines which check the number of observations, and flag zero and unexpectedly high velocities. All flagged data are evaluated for validity by SAI physical oceanographers. Fortunately, there have only been a few short data gaps on the order of several hours. When identified, synthetic (usually linearly interpolated) values are inserted. This "fix" has very little impact on derived values such as spectra, means, and variances.

All velocity time series are decomposed into orthogonal components (N-S, E-W). Since the direction of each component is fixed, its magnitude is evaluated as a scalar time series. Each component time series is demeaned and progressively filtered with 3- and 40-hour low pass (HLP) filters. A Lanscos filter is used. The 40-HLP filter eliminates tidal and inertial motions from the velocity record.

The filtered component vectors are recombined to create a filtered velocity vector. This is then plotted as a time series of vectors in which the vertical is positive "v" to the north and horizontally to the right is positive "u" to the east.

Spectra of the time series of component velocity magnitude is computed using an fast Fourier transform (FFT). The transformation is given by

$$X(f) = \frac{1}{T} \int_0^T x(t)e^{-jwt}dt \qquad (1)$$

where $x(t)$ = original time series, $X(f)$ = Fourier Transform $\omega = 2\pi/T$, $-j = (-1)^{\frac{1}{2}}$, t = time.

The spectral density or variance density is given by the magnitude squared of $S(f)$ and partitions velocity variance as a function of frequency. Thus

$$\sigma_x^2 = \int_0^\infty X(f)df \qquad (2)$$

where σ_x^2 = variance of original time series, $x(t)$. The integral of $X(f)$ between two frequencies (f_1, f_2) represents that portion of the original record variance produced by fluctuations having frequencies, f, between f_1 and f_2.

Progressive vector diagrams (PVD) represent the vector addition of Eulerian velocities. It is important to remember that PVD's do not represent water parcel movement since the velocities represented were measured at only a point in the horizontal. With this visualization of currents it is possible to see easily differences in velocities occurring at several points. Biweekly and total record length means are computed as are standard deviations and maximums and minimums for a given time series.

Identification of measurement sites is given by mooring sites (A, B, C, D, E) and location on the mooring: top, mid, bottom. "Top" was at mid depth in the water column. "Mid" was half way between the "top" and "bottom" meter. "Bottom" was 3 meters above the local bottom. These sites were occuppied twice, once during each of two deployments.

On some data products, data identification is by instrument number. The correspondence between measurement sites and instrument numbers is shown below.

Site Identifier	INSTRUMENT NUMBER First Deployment	Second Deployment
A		
(bottom)	12001	12901
B		
top	12101	13001
mid	12102	13002
bottom	12103	13003
C		
top	12201	13101
mid	12202	13102
bottom	12203	13103
D		
bottom	12301	13201
E		
bottom	12401	13301

IV. TECHNICAL DISCUSSION

4.1 Introduction

The Gulf Stream is a highly variable, dynamic current system that emerges from the Florida Straits and generally follows the continental slope northward to Cape Hatteras. The mean downstream flow is in approximate geostrophic balance with cross-stream pressure gradients over a large portion of the current structure (Wust, 1924). However, within the cyclonic shear zone ageostrophic conditions prevail (Brooks and Niiler, 1977).

4.1.1 Transport

Richardson, Schmitz and Niiler (1969) measured the velocity structure and volume transport of the Gulf Stream with seven dropsonde sections between the Florida Keys and Cape Fear. Downstream velocities were strongly sheared in the vertical and horizontal with a baroclinic jet (current axis) located in the western half of the flow. Volume transports were northward and increased from a minimum of $29.6 \times 10^6 m^3 s^{-1}$ off the Florida Keys to a maximum of $53.0 \times 10^6 m^3 s^{-1}$ off Cape Fear. Knauss (1969) found the volume transport to nearly double from Miami ($33 \times 10^6 m^3 s^{-1}$) to Cape Hatteras ($63 \times 10^6 m^3 s^{-1}$). The transport measured near the 30°N mooring transect was found to be $37 \times 10^6 m^3 s^{-1}$ (Richardson et al., 1969).

Niiler and Richardson (1973) estimated mean transport off Miami at $32.0 \times 10^6 m^3 s^{-1}$ with energetic fluctuations occurring on seasonal, 2-14 day and tidal time scales. There appeared to be little energy between the 15 day and seasonal periods. The total fluctuation bound was about $19 \times 10^6 m^3 s^{-1}$ with a maximum of $38.2 \times 10^6 m^3 s^{-1}$ in summer and a minimum of $19.0 \times 10^6 m^3 s^{-1}$ in winter. Seasonal variations were on the order of $\pm 3 \times 10^6 m^3 s^{-1}$ and accounted for about 45% of the observed variability. Fluctuations within the 2-15 day period band also had amplitudes of ± 3 to $4 \times 10^6 m^3 s^{-1}$ and appear to produce 40 to 50% of the total variance. Tidal fluctuations in the Florida Straits occurred with both diurnal and semi-diurnal periods, again with amplitudes of ± 3 to $4 \times 10^6 m^3 s^{-1}$ and accounted for 10-20% of the variability (Schmitz and Richardson, 1968; Brooks, 1979).

4.1.2 Meanders and Eddies

A large part of the Gulf Stream variability occurs with periods of 2-14 days. These fluctuations were first observed by Pillsbury (1890) and later by Parr (1937). Webster (1961a) made a 1-month Geomagnetic Electro Kinetograph (GEK) and baththermograph study off Onslow Bay; he found the surface front and Gulf Stream axis to be meandering in the onshore-offshore direction over a distance of 10 km on a time scale of 4 to 7 days, having wave lengths on the order of 100 km. He also noted a strong apparent correlation with the onshore/offshore wind component, but estimated the wind effect to be one or two orders of magnitude less than that required for the meanders energy source.

Schmitz and Richardson (1968) reported east-west meanders of the Florida Current occurring on a 1-week time scale with amplitudes of about 5 km. Düing (1975) analyzed 2 weeks of current profiles sampled from 4 ships anchored off Miami and noted a barotropic current meander with a 4 to 6 day time scale.

Comparison of the ship measured transport data with that estimated from the electrical potential on a submarine cable off Jupiter, FL, indicates that the several day "meander" was produced by a wave traveling to the north at 47 cm s^{-1} and wave length of 200 km. Düing described two cases for meanders: deep southward flow appeared to occur over the Miami Terrace during an offshore meander (current axis displaced to the east) and deep northward flow occurred over the Terrace during an onshore meander stage (axis displaced to the west). In general it appeared that flow variations on the cyclonic shear side of the axis were about 180° out of phase with those on the anticyclonic side.

More recently Brooks (1979) found similar results from detailed dropsonde transects of the Florida Current off Miami over an 83 day period in the summer of 1974. Transport fluctuations with periods of 2-14 days were highly coherent and in phase at stations in the cyclonic shear region as were stations in the anticyclonic region but the two regions were 180° out of phase. Brooks also found fluctuations in the total transport that were visually coherent and in phase with the variations on the anticyclonic side. During the experiment, the current axis meandered a total distance of approximately 24 km. An offshore (onshore) meander was associated with a transport increase (decrease) on the eastern side of the current, a transport decrease (increase) on the western side and an increase (decrease) of total transport.

Current records from an array of near bottom current meters, spanning the Florida Straits at the same location and time as the Brooks dropsonde measurements, showed energetic fluctuations of the downstream component with well defined spectral peaks at periods of 9 to 12 days that were coherent across the entire Florida Straits (Düing et al., 1977). The downstream coherence scale of these fluctuations was estimated at 55 km from a current meter array along the continental slope (Lee et al., 1977).

Brooks and Bane (1981) and Bane el al., (1981) used current meter data from the continental slope, satellite infrared images and AXBT temperature profiles to describe Gulf Stream meanders off Onslow Bay. Their results are consistent with Webster's (1961a) findings and indicate that the meanders were produced by northward propagating skewed waves with a weekly period. Approaching wave crests (shoreward excursions of the SST front) produced in-phase increases in northward speeds and temperature at the mooring locations. Decreasing speeds and temperatures occurred following the crest's passage.

Cyclonic, cold-core eddies have been observed embedded in the Gulf Stream front in the Florida Straits region (Lee et al., 1977) and along the Florida/Georgia outer shelf (Lee, Atkinson and Legeckis, 1981; Lee and Atkinson, 1982). These eddies occur during periods of offshore meanders and have horizontal dimensions equivalent to the meander. They propagate to the north at the same phase speed as the meander (30 to 70 cm s^{-1}) and appear to grow as the meander develops. Upwelling in the cold-core has been observed to uplift the density structure of the front in the upper 200 m. Eddies occur on the average of about 1 per week and have a life span of about 1 to 3 weeks. Satellite images (Legeckis, 1975; Stumpf and Rao, 1975) suggest that these eddies evolve from growing frontal meanders. Their surface manifestation is similar to the "shingle" structure observed by Von Arx et al. (1955).

Satellite imagery shows that wave-like meanders and eddies which are a consistent feature of the Gulf Stream front all along the southeast U.S., appear to undergo size increases north of Jupiter, FL, and again north of Charleston in the region of the Carolina Capes. North of Jupiter, where the shelf widens eddy dimensions increase to 100 to 200 km in length and meander amplitudes of 30 km are observed (Lee et al., 1981; Bane and Brooks, 1979). A second elongation is observed north of the "Charleston bump", a topographic anomaly of the slope extending seaward into the Gulf Stream, where downstream dimensions can reach 300 km (Legeckis, 1979) and meanders with 100 km displacements can occur from waves propagating to the north at an average speed of about 40 cm s^{-1} in the 2 to 14 day period band (Legeckis, 1979: Bane and Brooks, 1979; Brooks and Bane, 1981; Bane et al,, 1981).

The Gulf Stream is observed to have a quasi-persistent eastward displacement downstream of the "bump", which is believed to be the cause of the larger meanders and eddies between the "bump" and the Cape Hatteras (Pietrafesa et al, 1978; Brooks and Bane, 1978, Bane and Brooks, 1979; Legeckis, 1979). East of Cape Hatteras, Gulf Stream meanders are no longer restricted by the continental shelf as along the southeast U.S. coast and the well known warm-core and cold-core "rings" develop north and south of the Stream, respectively.

4.1.3 Theory

Current spectra from the Florida Straits and continental slope region south of Cape Hatteras generally show a decrease of energy toward the very low frequencies (Düing et al., 1977; Lee and Atkinson, 1982), which appears to be typical of continental shelves (Niiler, 1976) and in contrast to spectra from the deep ocean (e.g. from the site D, Thompson, 1971). The most energetic motions in the Florida Current and along the continental slope appear to occur with periods of 7 to 12 days, with smaller but still significant fluctuations occurring at periods of 4 to 5 and 2 to 3 days (Düing, et al., 1977; Mooers and Brooks, 1977; Brooks, 1979). In the open, ocean subinertial motions are largely governed by planetary Rossby waves, whereas, along continental margins topographic Rossby waves or continental shelf waves (CSW's) can occur, and have a greater high-frequency cut-off than do planetary Rossby waves.

Brooks (1975) investigated stable barotropic CSW's in the Florida Straits using a realistic bottom profile with a baroclinic, horizontally sheared steady current. The lowest mode wave properties appeared to agree with observations reasonably well, i.e., period of 10-12 days, wave length of 200 km and southward propagation of 20 cm s^{-1}. Schott and Düing (1976) found that a barotropic CSW with similar wave properties produced the best fit to current observations from an along-axis array of lower layer moorings in the Florida Straits. Approximately 70% of the observed variance could be attributed to the barotropic mode. Similar results were found by Mooers and Brooks (1977) and Düing (1975).

Continental shelf wave theory predicts a 180° cross-stream phase difference between currents on the shallow Miami Terrace and the deep region of the Florida Straits, which was observed by Düing et al. (1977). In the presence of the horizontally sheared Florida Current northward propagating CSW's are also possible (Brooks, 1975; Niiler and Mysak, 1971). The most probable generating mechanism for CSW's is usually attributed to Ekman suction

due to wind stress curl over the Straits (Brooks, 1975; Schott and Düing, 1976; Düing et at., 1977). Significant coherence was found by Düing et al. (1977) between the downstream flow and wind stress curl in the 10 to 13 day period band, with the curl being nearly in quadrature with the downstream current.

Several theoretical studies have addressed GS meandering motion off the southeast U.S. Niiler and Mysak (1971) considered subinertial waves in a barotropic Gulf Stream with horizontal shear and variable cross-stream bottom topography; that is, they considered a model with potential vorticity gradients commensurate with the magnitude and form of the depth-integrated Florida Current. They concluded that long waves could propagate northward and were unstable. The most unstable waves had a period of about 10 days and wave lengths of 150 to 200 km in the vicinity of the Blake Plateau. Schott and Düing (1976) reported that rescaling the Niiler and Mysak dispersion relation for topography and current conditions in the Florida Straits indicated only stable waves with lengths of 100 km for the 10 day period.

Orlanski (1969) considered a model with 2 "active" layers and bottom topography and found baroclinic instabilities possible for the parametric range observed in the Blake Plateau. The most unstable waves had a period of about 10 days and wave lengths of about 220 km. Orlanski also noted the need for observations through the water column to determine the various energy exchanges. Orlanski and Cox (1973) carried out analoguous calculations for a continuously stratified system with similar results. Additionally, finite-amplitude effects reducted the growth rate; maximum amplitudes were reached in 1 week.

4.1.4 Energy Transfers

Webster (1961b) demonstrated that on the 1 day to 1 week time scale kinetic energy was transfered from fluctuations to the mean current on the surface in the cyclonic shear zone of the Gulf Stream in the Florida Straits and off Onslow Bay. On the cross-stream average from Miami to Onslow Bay, he found a net flux to the mean Gulf Stream that could rapidly double the average surface speed. Such an acceleration is not observed so it may be that work of opposite sign is done by the pressure gradients near the surface.

Sturges (1974) estimated the mean downstream pressure gradient from coastal sea level along the southeast U.S. and the Florida Straits and found the gradient to be large enough to provide an energy flux, at least along the shelf break, sufficient to balance the work done on the eddies. Following Webster's analysis, Oort (1964), using the thermal flux data corresponding to Webster's momentum flux data, found a counter-gradient heat flux that would sharpen the surface layer front. He also raised the question of a lower-layer source for both a flux of heat and an intense potential energy release.

Blanton (1971) combined a few short current meter records at the shelf break off Onslow Bay with hydrographic sections and interpreted the results in a two-dimensional vertical plane sense. He found near-bottom intrusions of Gulf Stream water, followed by vertical mixing with shelf waters and subsequent offshore flow of nearsurface shelf water, which would give a counter-gradient heat flux near the surface. Schmitz and Niiler (1969) analyzed dropsonde data in an analogous fashion as Webster. They concluded

that negligible net transfer of kinetic energy existed between the fluctuations and the mean Gulf Stream motion in the surface layer on the cross-stream average; instead an internal redistribution of kinetic energy was believed to occur.

Brooks and Niiler (1977) conducted an intense dropsonde experiment during the summer of 1974. They measured Florida Current volume transport off Miami on 41 occasions during an 83 day period. These data substantiated their earlier findings for the surface layer and indicate that an intense internal energy adjustment takes place without any significant net energy conversion over the total section area. Mean perturbation kinetic and potential energy conversion had complicated horizontal and vertical structure with no clear indication of a dominant barotropic or baroclinic instability process at work. Mean perturbation kinetic energy appears in general to provide energy to the mean Florida Current in the upper 100 to 200 m and at depths greater than 500 m and in a narrow region of the cyclonic shear zone. The distribution of the average perturbation potential energy transfer suggests that the potential energy of the mean flow is the energy source for the growing meanders, which indicates a baroclinic instability process. However, over the cross-sectional average these energy transfers appear to compensate each other, resulting in little net energy conversion. Brooks and Niiler conclude that pressure forces must locally balance the energy flow so that an equilibrium exists between the fluctuations and the mean Florida Current. Current and temperature time series from the shelf break north of Cape Canaveral (Lee and Atkinson, 1982) and in the vicinity of the current axis off Onslow Bay (Brooks and Bane, 1981) indicate that perturbation kinetic energy transfer to the mean current is a characteristic feature of the Gulf Stream cyclonic shear zone.

4.1.5 Tidal Variability

Current and transport fluctuations in the tidal/inertial period band account for approximately 10 to 20% of the observed total variability of the Florida Current (Schmitz and Richardson, 1968; Kielman and Düing, 1974; Mooers and Brooks, 1977; Brooks, 1979). Both diurnal (K_1, O_1) and semi-diurnal (M_2, S_2) periods occur and produce transport fluctuations with amplitudes of ± 3 to $4 \times 10^6 \, m^3 s^{-1}$. Smith, Zetler and Broida (1969) and Zetler and Hansen (1970) hypothesized that since tidal sea level variations in the Florida Straits were primarily semi-diurnal then the observed diurnal component of the flow is produced by a standing wave with a node near Miami. Amplitudes of the K_1 and O_1 components of downstream currents or transport were found to be greater than or equal to the M_2 component (Schmitz and Richardson, 1968; Smith et al., 1969; Kielman and Düing, 1974; Brooks, 1979).

Energy spectra of downstream (v) and cross-stream (u) velocity components from the lower layer over the Miami Terrace clearly show larger variance for the diurnal fluctuations. The O_1 constituent was largest for the v component and K_1 was the greatest u tidal constituent. The downstream component accounted for about 25% of the total variance and 6% for the cross-stream component. The harmonic constants (amplitude and phase) for K_1, O_1, M_1 and S_2 computed from surface current speed records (Smith et al., 1969) were found to agree quite well with those computed for lower layer currents by Kielman and Düing, indicating a strong barotropic structure to the tides.

Brooks (1970) used a Munk/Cartwright technique to remove the tidal signal from station transport data and found little effect; however, the small changes at each station accumulated to produce a large effect on the total transport through the section. Brooks reported that the semi-diruanl and diurnal tides accounted for about 20% of the total transport variance. The diurnal component produced most of the tidal variance over the Miami Terrace and near the Bahama Bank. The semi-diurnal component had a larger effect in the interior flow. The phase of the diurnal component was relatively constant between Miami and the Bahamas, again indicating a standing wave with a node near Miami.

Mooers and Brooks (1977) analyzed thermistor arrays and tide gauge records from both sides of the Florida Current. They found appreciable diurnal and semi-diurnal internal tidal energy that was as large as the surface tides. The diurnal internal tide was dominant. Near-inertial motions were apparent at some depths at the effective inertial frequency which varied as a function of horizontal shear (20 hours near Miami and 35 hours near Bimini). They found that low-frequency fluctuations can modulate all near-inertial motions including diurnal and semi-diurnal internal tides causing time-varying amplitudes. The modulation time scale was monthly and longer for the diurnal internal tides and fortnightly and longer for the semi-diurnal internal tides. Mooers and Brooks also found that the cross-channel phase of the diurnal and semi-diurnal internal tides indicated that internal seiches could exist in the Florida Straits as these periods.

4.2 Observations

4.2.1 Time Domain

Examples of the 40-HLP current vector time series and temperature across the Blake Plateau during each season are shown in Figure 4-1 through Figure 4-8. The first order statistics of these data are given in Table 4-1a and 4-1b for the first and second deployment periods, respectively. Moorings B and C were apparently located within the Gulf Stream judging from the strong persistent northward flow at both locations. Downstream mean velocities agree remarkably well with the Richardson et al. (1969) velocity section shown in Figure 2-2b indicating that mooring B was located near the subsurface extension of the current axis and mooring C was located near the eastern edge of the current. Mean downstream velocities were about 62 cm s^{-1} at B (top) during the first deployment and 76 cm s^{-1} during the second deployment, which suggests a seasonal trend consistent with the summer transport maximums observed by Niiler and Richardson (1973). Mean flows at C were about half as strong as at B and showed little change between the deployment periods. Mean vertical shears were about -1.7×10^{-3} s^{-1} at B and -0.5×10^{-3} s^{-1} at C over both deployment periods, indicating little seasonal change in baroclinic transport between B and C. Maximum downstream flow at B reached 109 cm s^{-1} at mid-depth during the second deployment and maximum flow at C was 87 cm s^{-1} during the first deployment. Standard deviations of the cross-stream and downstream components were approximately equal at each instrument of moorings B and C during both deployments and ranged from a minimum of ± 7 cm s^{-1} near the bottom to a maximum of ± 18 cm s^{-1} at mid-depth.

Low frequency velocity and temperature fluctuations appear to be visibly well correlated over the 400 m vertical separation at both moorings B and C

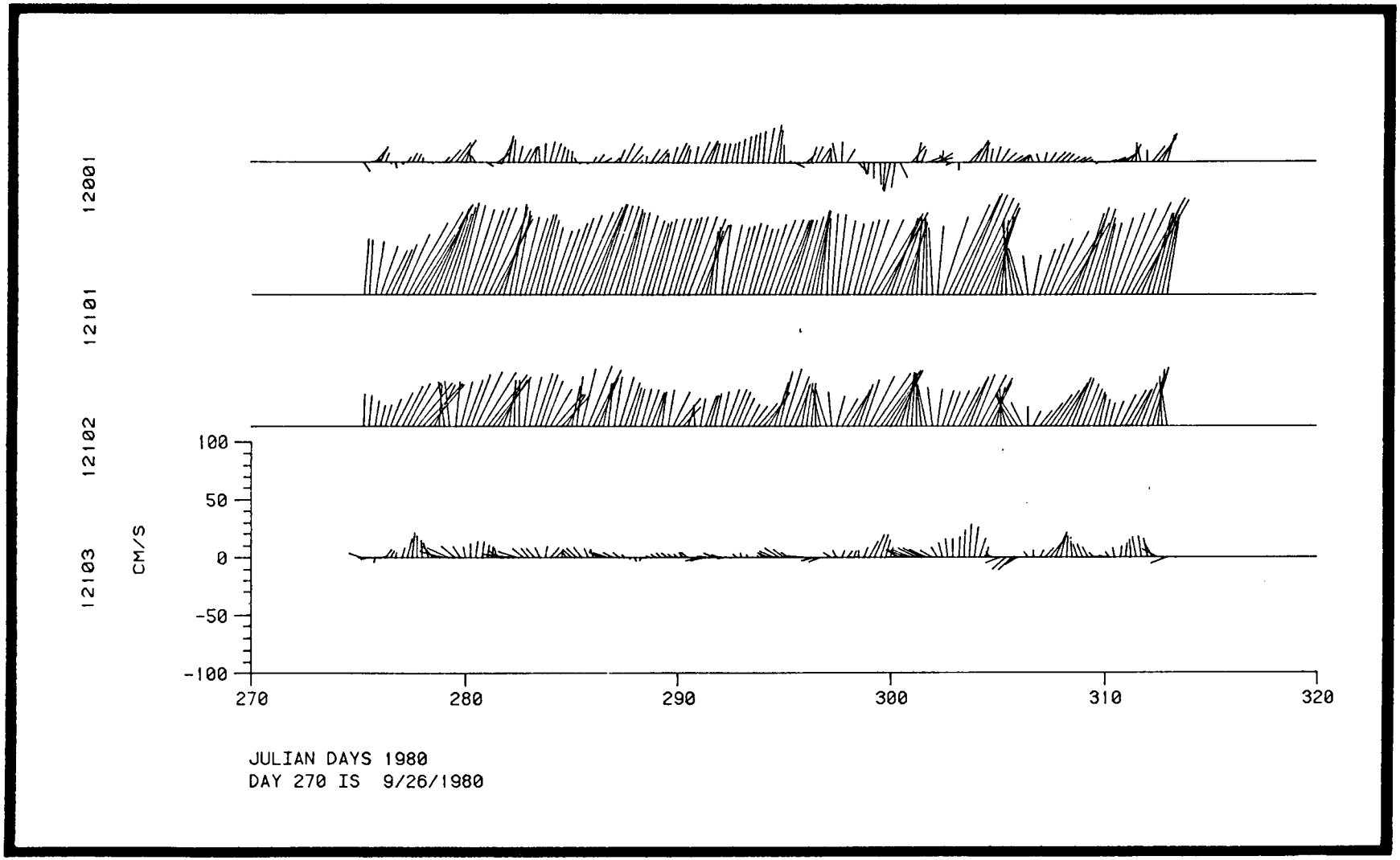

Figure 4-1 Stick plots of 40-HLP data for the indicated time period. Velocities on a given mooring are visually coherent.

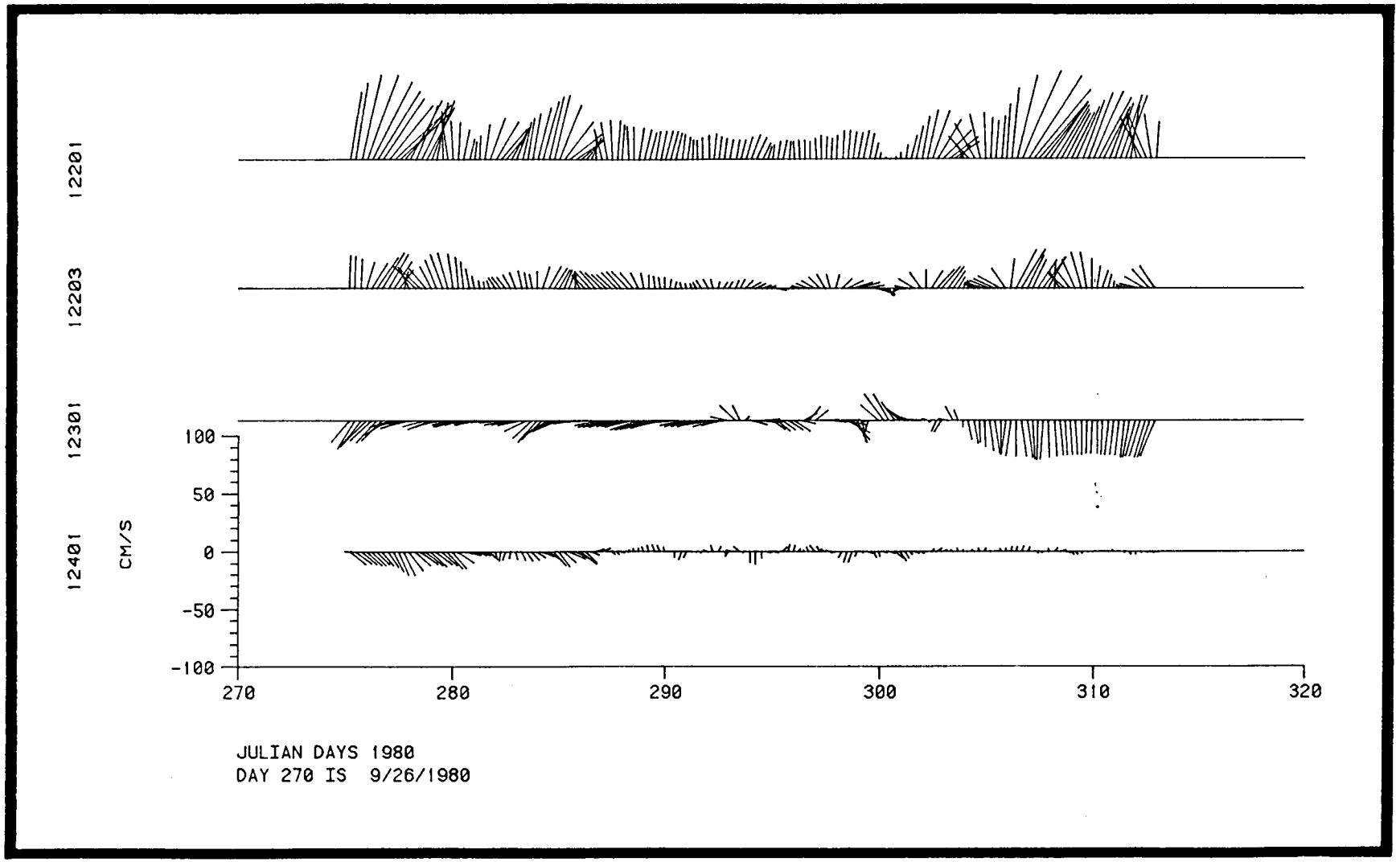

Figure 4-1 Continued.

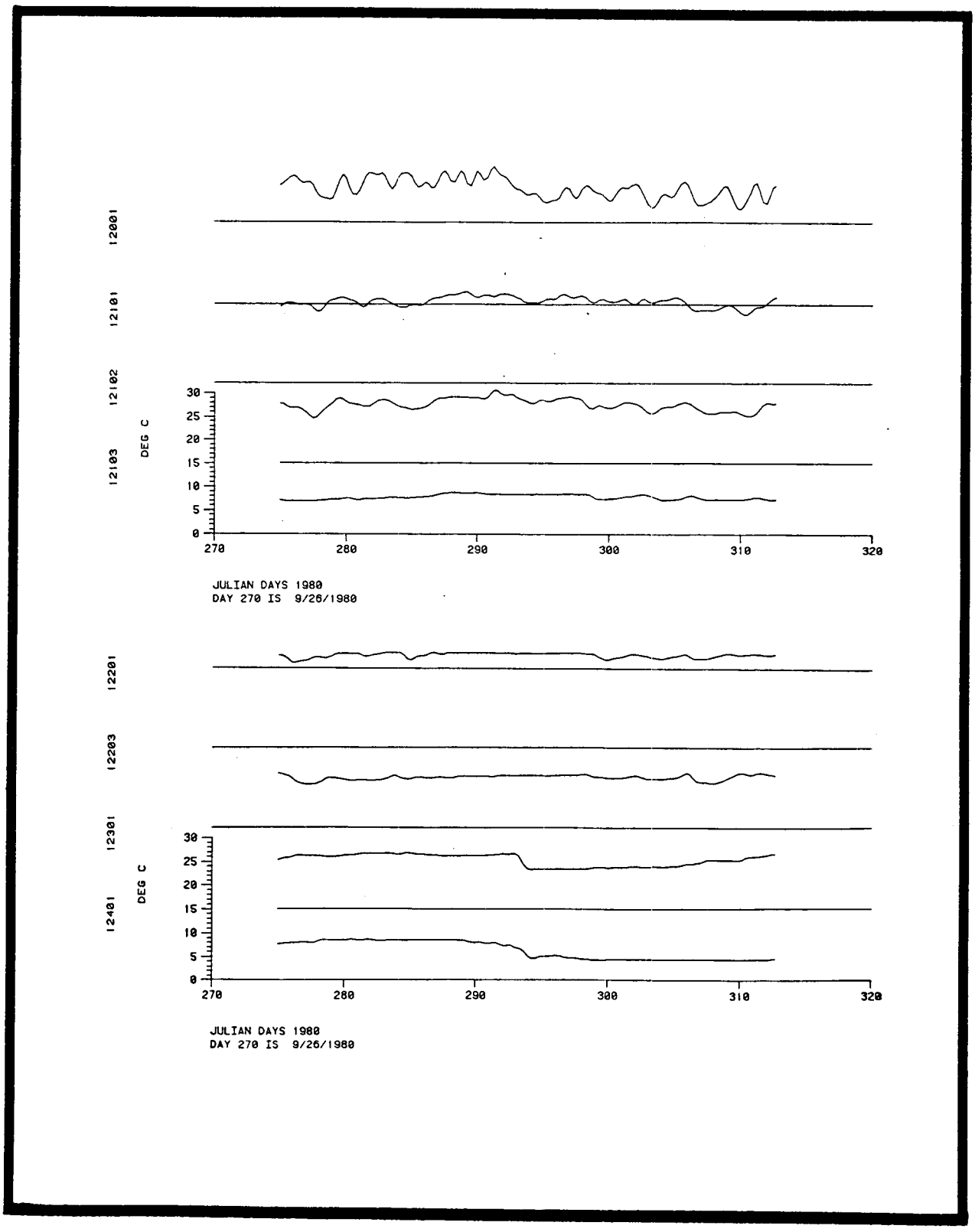

Figure 4-2 Time series plots of 40-HLP filtered temperature at the indicated sites and periods.

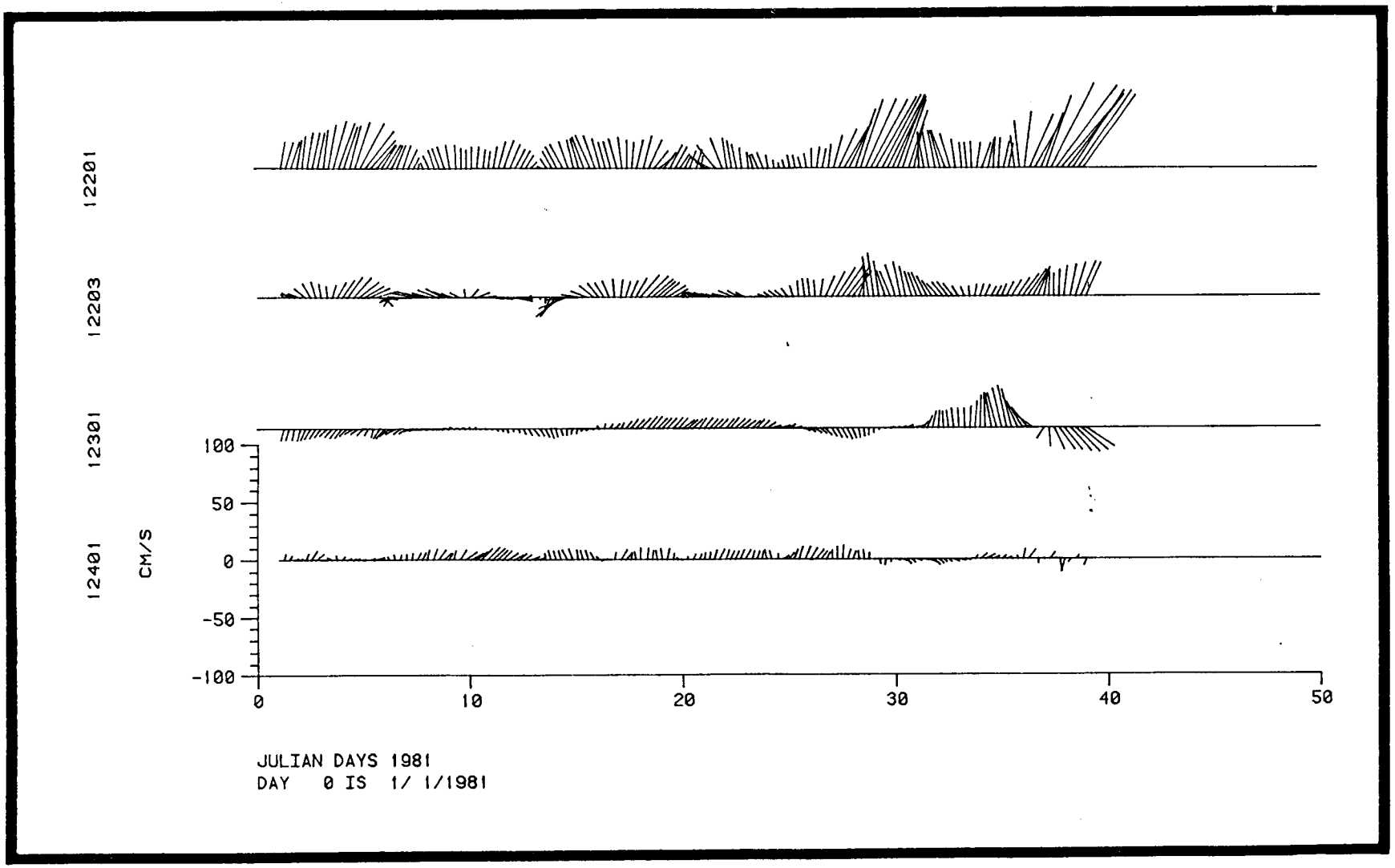

Figure 4-3 Stick plot of 40-HLP velocity data for the indicated time period.

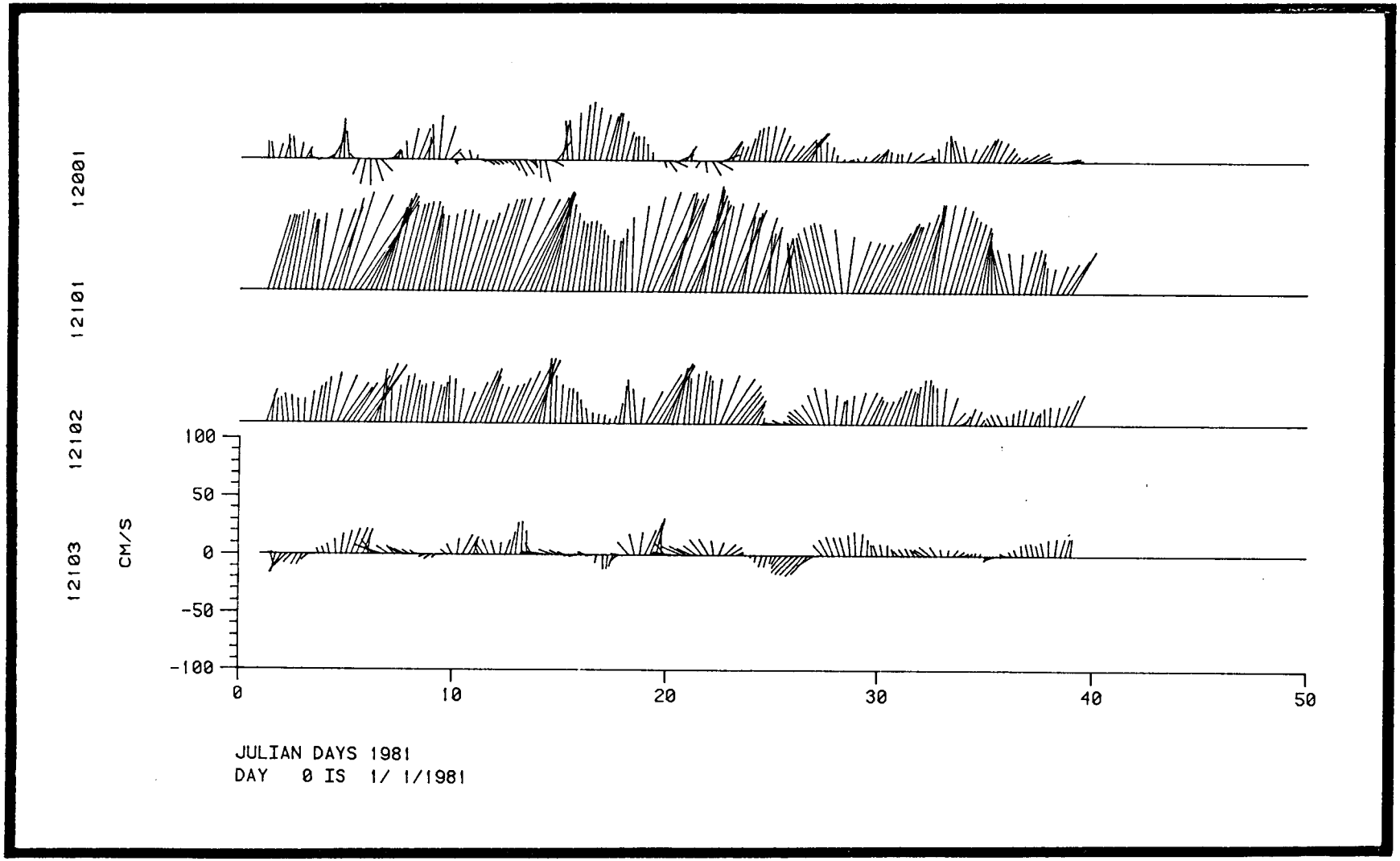

Figure 4-3. Continued.

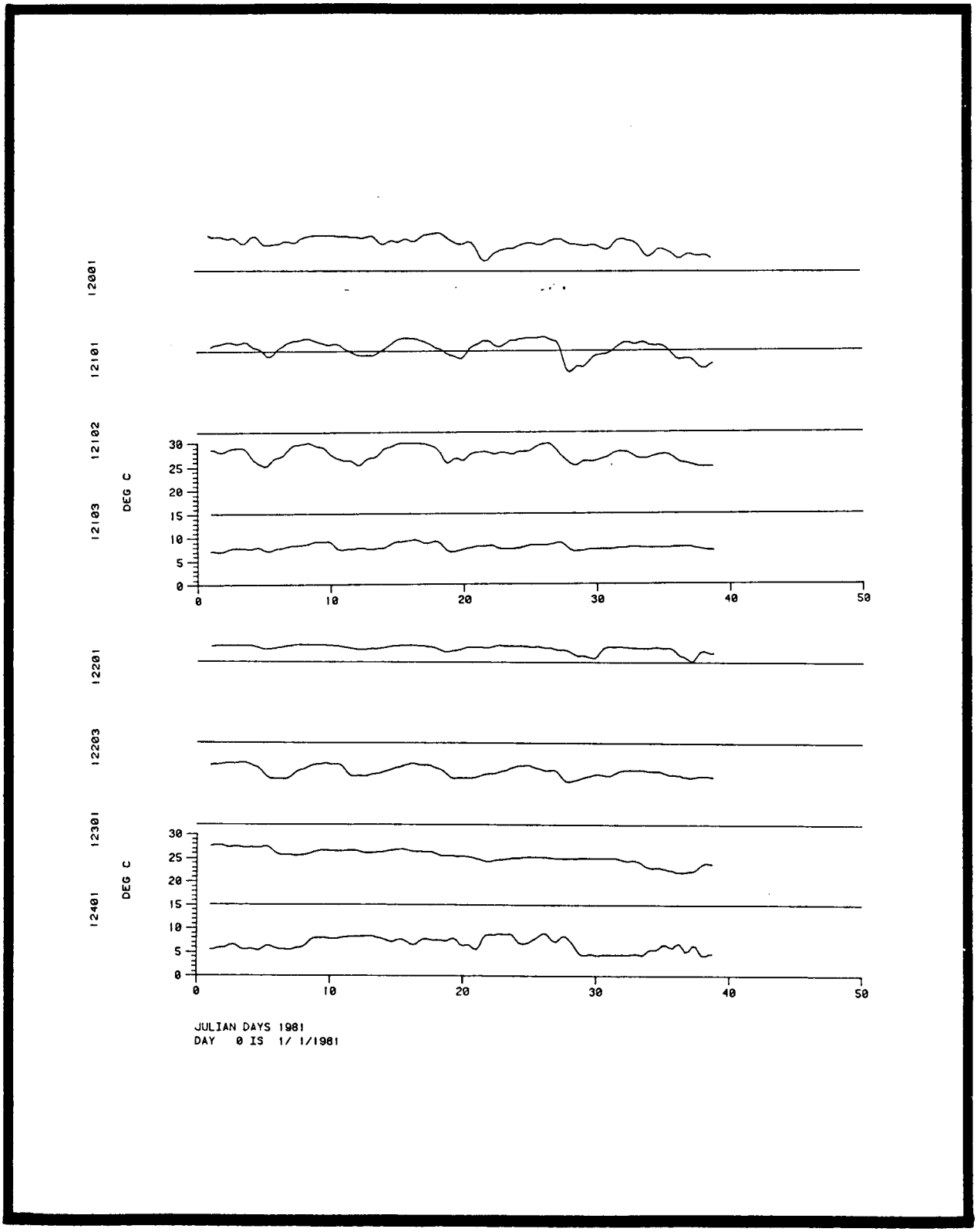

Figure 4-4 Time series plot of 40-HLP filtered temperature for the indicated sites and periods.

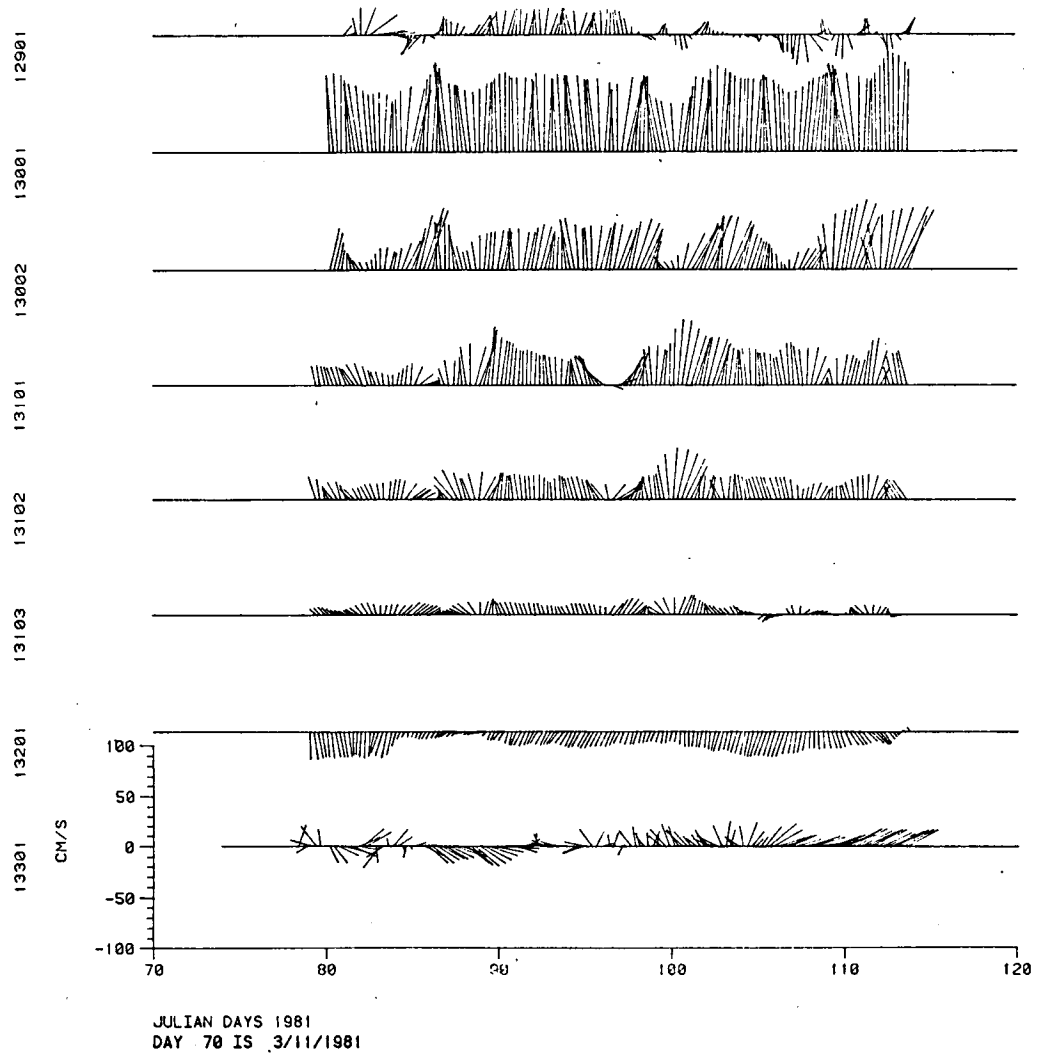

Figure 4-5 Stick plots of 40-HLP current data for the indicated portion of the second deployment period.

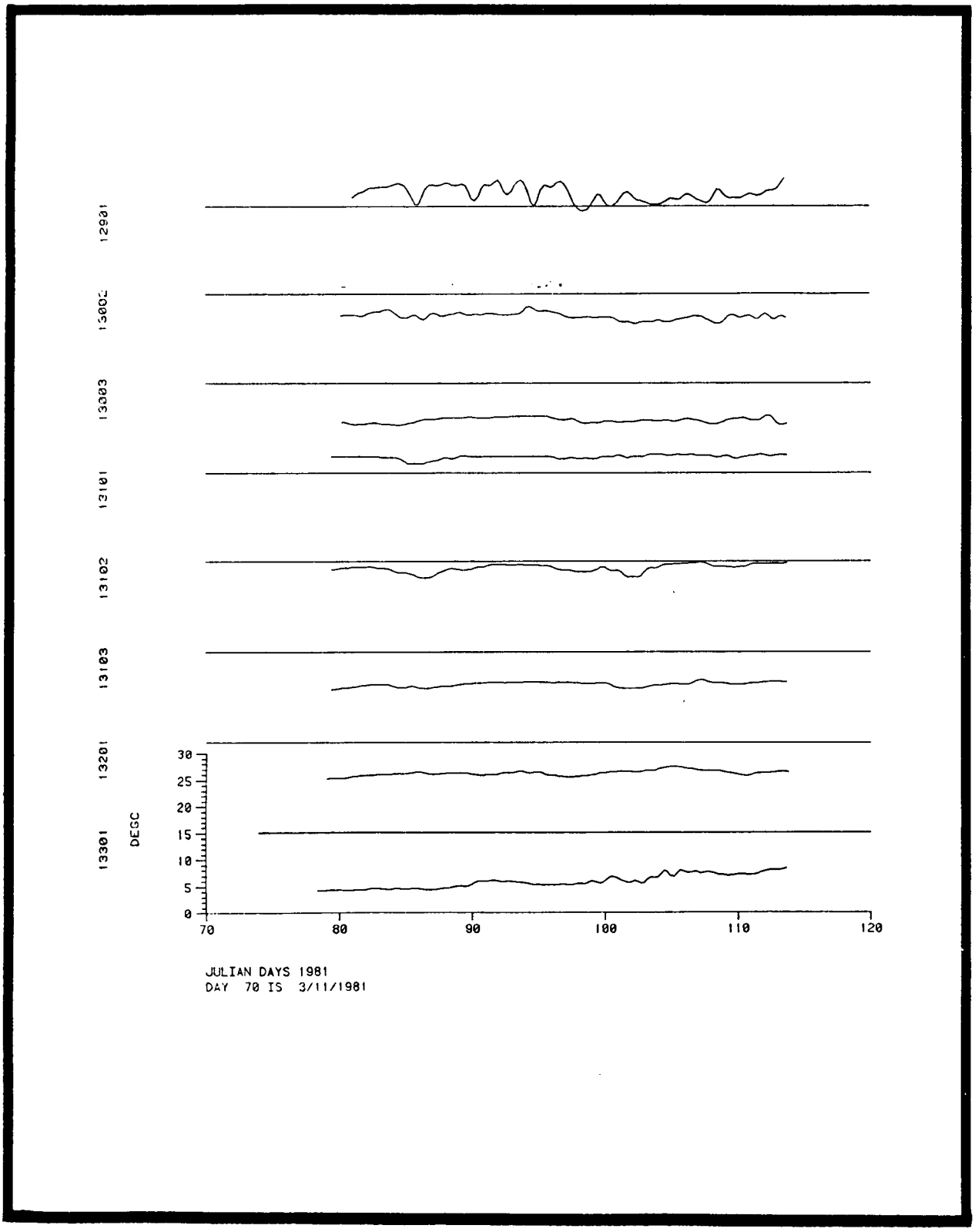

Figure 4-6 Time series plot of 40-HLP filtered temperatures observed at the indicated sites and times.

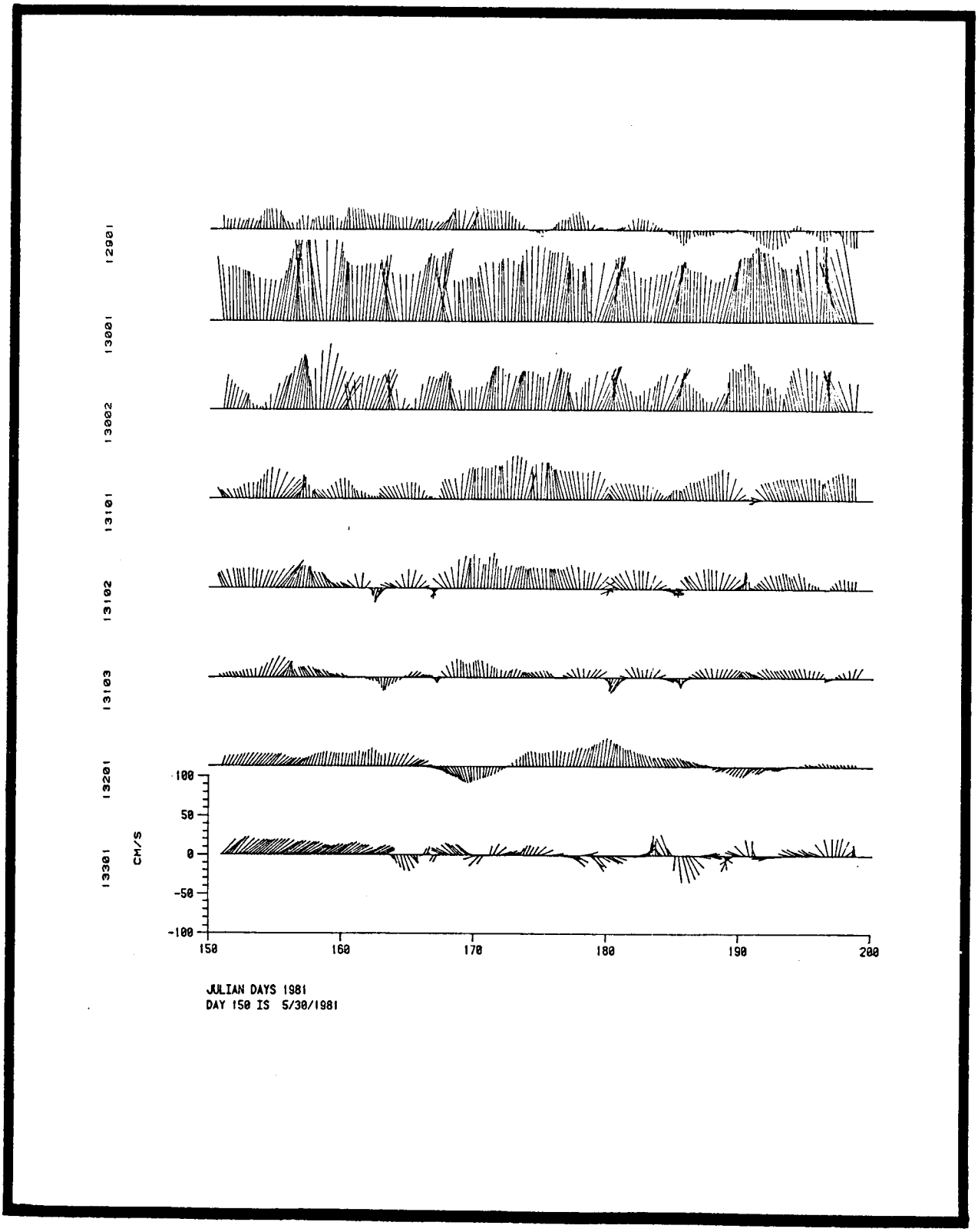

Figure 4-7 Stick plots of 40-HLP current data for the indicated portion of the second deployment period.

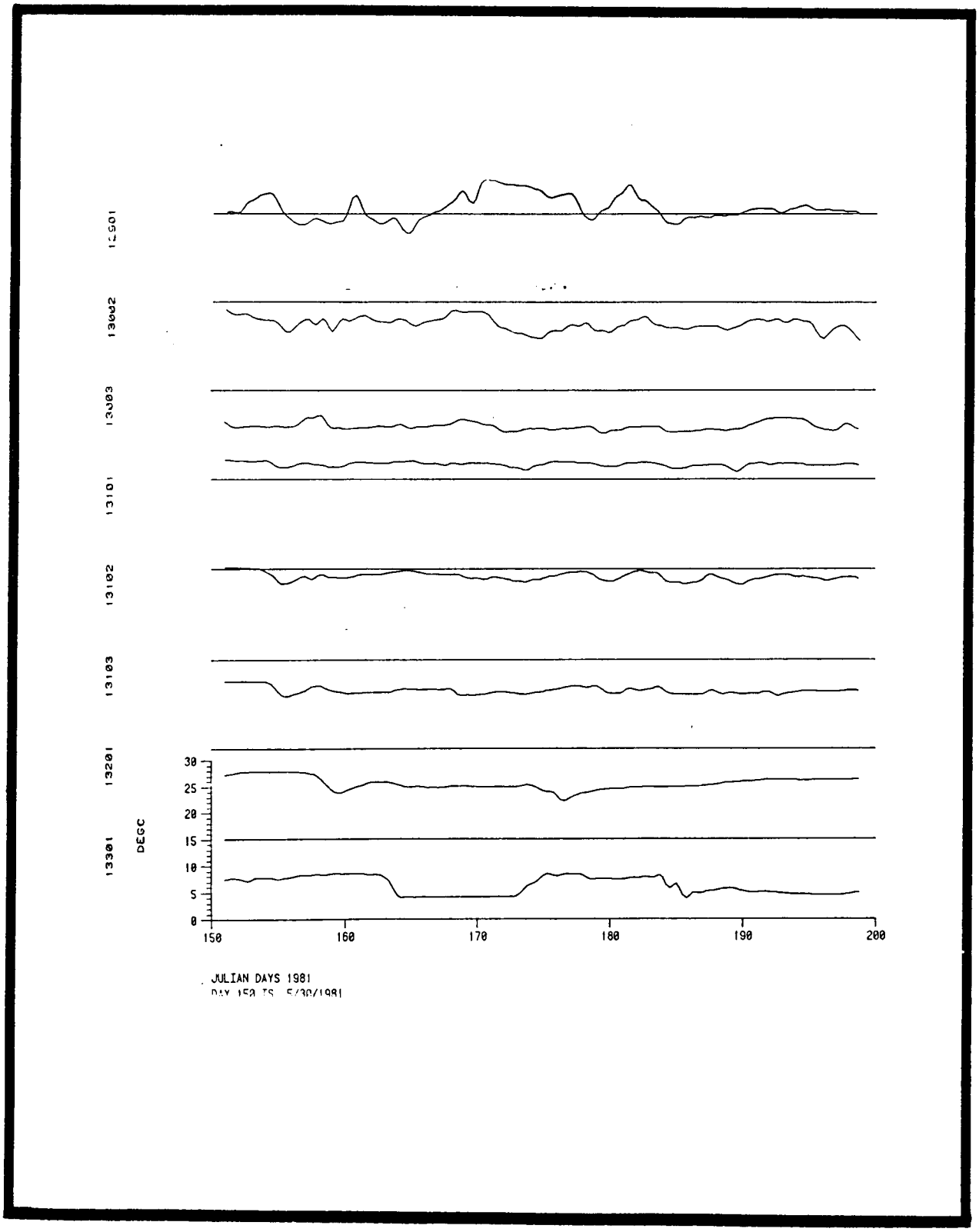

Figure 4-8 Time series plots of 40-HLP temperatures at the indicated times and sites. Note the rapid, relatively large increases and decreases occurring at Moorings D(13201) and E(13301).

Current Meter I.D.	Variable	Minimum	Maximum	Mean	Standard Deviation
A (bot)	T	11.8	26.8	21.2	2.3
	u	-10.6	26.9	5.8	6.1
	v	-40.9	49.6	6.9	13.7
B (top)	T	9.2	18.0	15.3	1.8
	u	-34.3	59.6	20.3	14.6
	v	-20.2	101.1	61.8	17.1
B (mid)	T	7.2	13.9	10.2	1.5
	u	-20.5	39.8	9.6	10.5
	v	-5.8	56.4	28.8	12.0
B (bot)	T	6.3	9.6	7.6	0.6
	u	-27.4	12.5	-4.3	8.1
	v	28.6	30.9	5.4	8.6
C (top)	T	10.7	19.2	17.7	1.2
	u	-22.0	51.9	10.2	14.8
	v	-1.6	87.3	30.2	18.0
C (bot)	T	6.7	10.9	8.7	1.0
	u	-27.8	15.5	-0.8	10.8
	v	-17.1	44.6	10.9	9.9
D (bot)	T	4.5	11.0	8.1	1.7
	u	-32.2	21.0	-2.7	13.9
	v	-38.4	38.3	-7.1	15.3
E (bot)	T	4.2	9.0	6.0	1.3
	u	-18.8	20.7	5.2	7.6
	v	-25.3	20.7	0.3	7.4

Table 4-1a First order statistics of 40-HLP time series for first deployment period: September 2, 1980 to March 13, 1981; temperature (T) in ^{o}C, velocity components (u and v) in cm s^{-1}.

Current Meter I.D.	Variable	Minimum	Maximum	Mean	Standard Deviation
A (bot)	T	11.2	25.9	18.1	2.8
	u	-20.2	35.1	2.7	6.3
	v	-31.4	61.1	5.0	15.4
B (top)	u	-42.2	38.7	1.2	11.8
	v	46.6	108.7	75.9	11.8
B (mid)	T	7.7	13.9	10.9	1.2
	u	32.2	41.8	6.6	11.1
	v	1.2	84.6	40.6	13.4
B (bot)	T	6.8	10.2	8.1	0.6
C (top)	T	16.5	18.9	18.1	0.4
	u	-26.3	38.6	1.6	8.8
	v	-5.4	64.7	26.3	12.6
C (mid)	T	11.4	16.2	14.0	0.9
	u	-28.3	39.9	0.2	9.5
	v	-18.1	52.7	17.2	10.6
C (bot)	T	7.2	11.4	9.2	0.9
	u	-19.6	23.9	-1.3	8.6
	v	-18.8	27.1	6.8	7.1
D (bot)	T	5.2	11.0	8.6	1.3
	u	-20.4	19.8	-1.1	8.1
	v	-26.6	35.3	-1.9	11.9
E (bot)	T	3.9	9.5	5.8	1.6
	u	-26.0	35.6	7.4	15.4
	v	-34.5	27.8	3.1	10.4

Table 4-1b First order statistics of 40-HLP time series for second deployment period: March 22, 1981 to September 30, 1981; temperature (T) in ^{o}C, velocity component (u and v) in cm s^{-1}.

(Figure 4-1 and Figure 4-8). Both cyclonic and anticyclonic perturbations occur with cyclonic perturbations more common at mooring B and anticyclonic more prevalent at C. At times cyclonic perturbations at B appear to occur simultaneously with anticyclonic events at C and cyclonic events at A (Figures 4-3 and 4-4). Cold, cyclonic fluctuations at the shelf edge have been shown to be produced by northward propagating cyclonic, cold-core eddies embedded in the Gulf Stream front (Lee and Atkinson, 1982). These type of events appear to be a common feature at A throughout the year.

Near bottom flow at site D shows little visual similarity to the currents at sites C or E. Prolonged southward flows occurred that persisted for periods up to 42 days and reached speeds in excess of 30 cm s^{-1} (Figures 4-1 and 4-5). Mean flows at D were southward at -7 and -2 cm s^{-1} during the first and second deployments respectively. The near bottom mean flow at the seaward edge of the Plateau (site E) was primarily in the offshore direction at about 5 cm s^{-1} during the first deployment and 7 cm s^{-1} during the second deployment. Maximum currents at E reached speeds of about 35 cm s^{-1} in the offshore and southerly directions. Standard deviations ranged form ± 7 to ± 15 cm s^{-1}. Prolonged southward and northward flow events occurred that were not well correlated to temperature. Occasionally higher frequency events occurred such as the cold, cyclonic perturbation on about day 186 of 1981. Cold-core, cyclonic rings have been observed to cross the Plateau in this region and coalesce with the Gulf Stream (Cheney and Richardson, 1976; Perkins and Wimbush, 1976; Vukovich and Grissman, 1978).

4.3.2 Energy Partitioning

If the velocity field is decomposed into mean and fluctuating components, i.e. $u = \bar{u} + u'$, then the total kinetic energy can be estimated from

$$\frac{1}{T}\int_0^T |V|^2 dt = (\sigma_u^2 + \sigma_v^2) + (\bar{u}^2 + \bar{v}^2) \qquad (1)$$

where V = velocity vector and σ^2 = variance. In this decomposition the second bracketed term on the right is approximately proportional to the energy of the mean flow and the first term is proportional to kinetic energy due to velocity fluctuations, i.e. eddy or perturbation kinetic energy (PKE). The various major components in Eq. 1 are shown in Tables 4-2 and 4-3 for the first and second approximately equal length measurement periods.

The locally dominant GS influence is apparent at Moorings B and C from the large total kinetic energy levels observed away from the bottom. Division into time varying and steady components shows this GS contribution results substantially from mean flow having strong vertical shear, i.e., baroclinicity in the mean. In contrast, perturbation kinetic energy is of lower relative magnitude near the GS core and has weaker vertical gradients. Away from the GS, only near bottom measurements were made so it is not possible to determine the importance of mean interior flows to energetics at non-GS sites. However, even near the GS, the time varying velocity dominated energetics at the bottom.

Because of the overall importance of the time varying velocity component, the kinetic energy was partitioned as a function period (Tables 4-4 and 4-5).

TABLE 4-2

FIRST DEPLOYMENT PERIOD

CURRENT METER ID	PERTURBATION KINETIC ENERGY	+	MEAN KINETIC ENERGY	=	TOTAL KINETIC ENERGY
A (bottom)	435 (84%)		80 (16%)		515 (100%)
B (top)	519 (11%)		4104 (89%)		4623 (100%)
B (mid)	295 (25%)		884 (75%)		1179 (100%)
B (bottom)	178 (80%)		44 (20%)		222 (100%)
C (top)	560 (37%)		945 (63%)		1505
C (mid)	———		NO DATA		———
C (bottom)	255 (69%)		116 (31%)		371 (100%)
D (bottom)	520 (92%)		48 (8%)		568 (100%)
E (bottom)	184 (88%)		26 (12%)		210 (100%)

Table 4-2 Table showing estimates of indicated contributions to kinetic energy at each measurement site for the first deployment period.

TABLE 4-3

SECOND DEPLOYMENT PERIOD

CURRENT METER ID	PERTURBATION KINETIC ENERGY	+	MEAN KINETIC ENERGY	=	TOTAL KINETIC ENERGY
A (bottom)	463 (93%)		35 (7%)		498 (100%)
B (top)	319 (5%)		5742 (95%)		5961 (100%)
B (mid)	346 (17%)		1635 (83%)		1981 (100%)
B (bottom)	_____		NO DATA		_____
C (top)	257 (27%)		690 (77%)		947 (100%)
C (mid)	238 (44%)		299 (56%)		537 (100%)
C (bottom)	142 (74%)		50 (26%)		192 (100%)
D (bottom)	247 (97%)		8 (3%)		255 (100%)
E (bottom)	497 (90%)		57 (10%)		554 (100%)

Table 4-3 Table showing estimates of indicated contributions to kinetic energy at each measurement site - second deployment period.

TABLE 4-4

FIRST DEPLOYMENT PERIOD
DECOMPOSITION OF PERTURBATION KINETIC ENERGY (PKE) INTO PERIODICITIES

CURRENT METER ID	PERIOD BAND (3-40 HR) +	(40 HR-14 DAY) +	(>14 DAY) =	PKE
A (bottom)	210 (48%)	180 (41%)	45 (10%)	435 (100%)
B (top)	17 (3%)	236 (45%)	266 (52%)	519 (100%)
B (mid)	42 (14%)	174 (59%)	79 (27%)	295 (100%)
B (bottom)	28 (16%)	111 (62%)	39 (22%)	178 (100%)
C (c)	18 (3%)	221 (39%)	321 (57%)	560 (100%)
C (mid)	———	NO DATA	———	
C (bottom)	50 (20%)	158 (70%)	47 (18%)	255 (100%)
D (bottom)	91 (18%)	89 (17%)	340 (65%)	520 (100%)
E (bottom)	72 (39%)	18 (10%)	94 (51%)	184 (100%)

Table 4-4 Decomposition of Perturbation Kinetic Energy (PKE) into relevant period bands - first deployment period.

TABLE 4-5

SECOND DEPLOYMENT PERIOD
DECOMPOSITION OF PERTURBATION KINETIC ENERGY (PKE) INTO THE PERIODICITIES

CURRENT METER ID	PERIOD BANDS (3-40 HRS) +	(40 HRS-14 DAYS) +	(>14 DAYS) =	FKE
A (bottom)	188 (41%)	149 (32%)	128 (28%)	463 (100%)
B (top)	42 (13%)	213 (67%)	64 (20%)	319 (100%)
B (mid)	44 (13%)	246 (71%)	56 (16%)	346 (100%)
B (bottom)	———	NO DATA	———	
C (top)	20 (9%)	122 (47%)	115 (45%)	257 (100%)
C (mid)	36 (15%)	140 (59%)	62 (26%)	238 (100%)
C (bottom)	17 (12%)	99 (70%)	26 (18%)	142 (100%)
D (bottom)	35 (14%)	40 (16%)	172 (70%)	247 (100%)
E (bottom)	149 (30%)	137 (28%)	211 (42%)	497 (100%)

Table 4-5 Decomposition of Perturbation Kinetic Energy (PKE) into relevant period bands - second deployment period.

The high frequency component containing tidal and inertial fluctuations was a major contributor to PKE only at those sites close to a topographic break (Moorings A and E) at the continental slope and the Blake Escarpment respectively. At those sites having a substantial GS influence (Moorings B and C) the middle period band (2-14 days) tended to be the major contributor to PKE. Available data suggests this relative contribution increased with depth as might be expected for a barotropic flow.

The lowest frequency component (period >14 days) was significant only for interior flow in the vicinity of the GS and near bottom flow on the middle and outer Blake Plateau. During the first deployment, the low frequencies contributed the majority of velocity variance observed at mid depth locations on Moorings B and C. In contrast, during the second deployment only a relatively smaller component of velocity variance occurred in this low frequency band at those measurement positions under strong mean GS influence.

At the mid- and outer Blake Plateau stations (Moorings D and E) and for interior positions near or in the GS, approximately six month records do not produce stationary means or variance although the patterns do generally seem to be consistent. This is clearly evident in the magnitude of the mean and fluctuating components of kinetic energy. It is important that continuous records be spatially dense enough and long enough for weak sense stationarity to occur if such things as energy content and distribution are to be used in evaluating appropriateness of numerical model results.

4.2.3 Frequency Domain

Spectra, coherence squared and phase computed for the 40-HLP time series of cross-stream and along-stream velocity components from each mooring site of the first deployment are shown in Figures 4-9 through 4-13. Similar results were obtained from the second deployment. Energetic fluctuations of the cross-stream and along-stream velocity components at mid-depth of sites B and C, which were within the Gulf Stream flow regime, were coherent for periods greater than 8 days and over a band of 2 to 4 days. At site B the phase was positive at these periods, therefore cross-stream fluctuations were leading in phase, which would occur for cyclonic motion (Figure 4-10). At site C the phase was negative over the 2 to 4 day period band indicating anticyclonic motion and positive for periods greater than 8 days, indicative of cyclonic fluctuations (Figure 4-11). Anticyclonic motion also appeared to occur in the near bottom flow at site D (Figure 4-12), whereas the coherent part of the bottom flow near the Blake Escarpment (site E) appeared to occur as cyclonic fluctuations (Figure 4-13).

At the shelf-edge location (site A) the low-frequency velocity variations occurred as cyclonic motions that were coherent at periods of about 5, 3.5, 2.5 and 2 days (Figure 4-9). Along-stream fluctuations at the shelf edge had well-defined energy peaks with about an order of magnitude higher energy levels than the cross-stream fluctuations for periods longer than 3 days. In contrast, energy spectra from the Blake Plateau sites continued to increase with decreasing frequencies without well-resolved energy peaks. Also, the level of energy was nearly the same for the cross- and along-stream components.

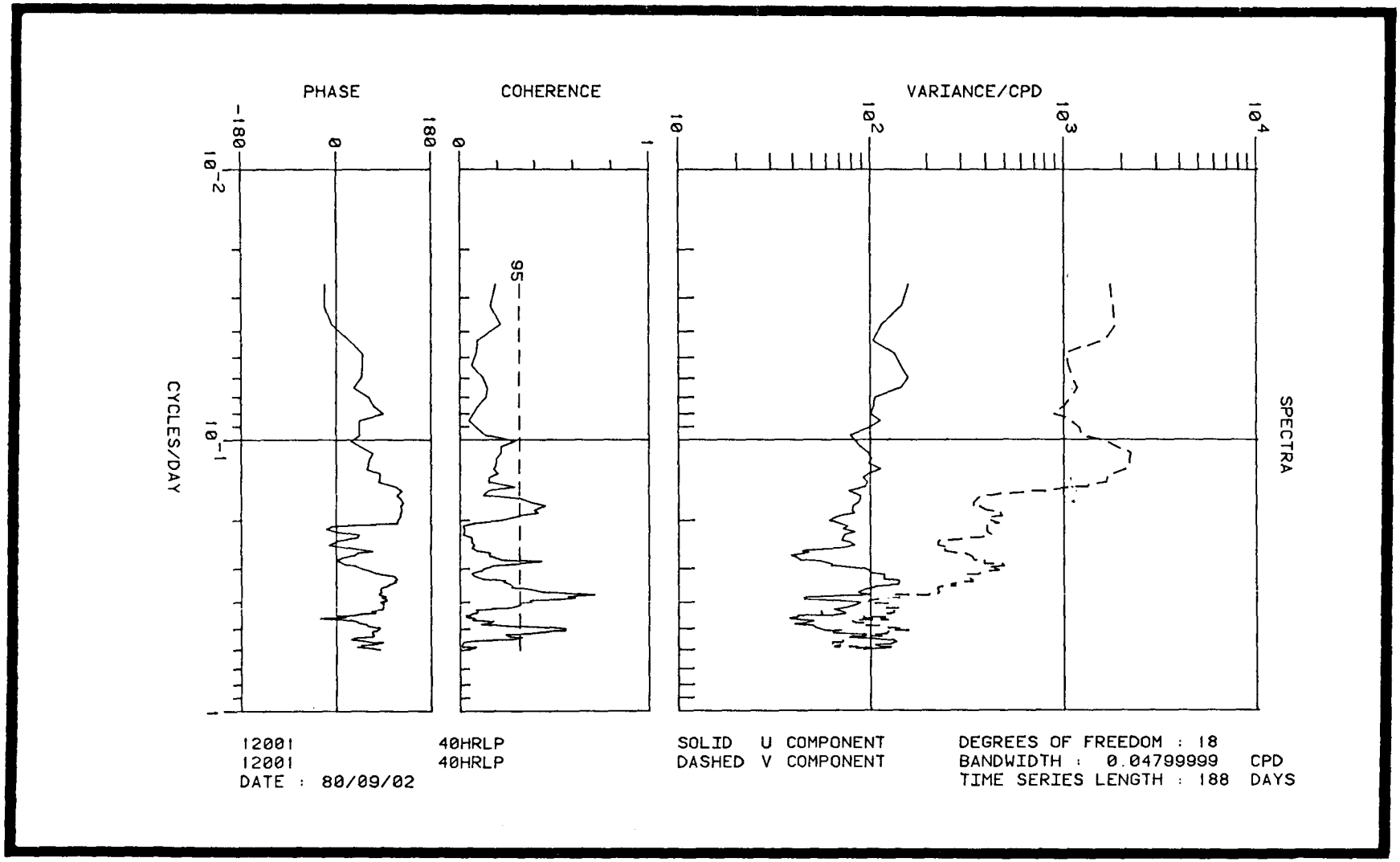

Figure 4-9 Spectra, coherence and phase of u and v velocity components at Mooring A-bottom (12001).

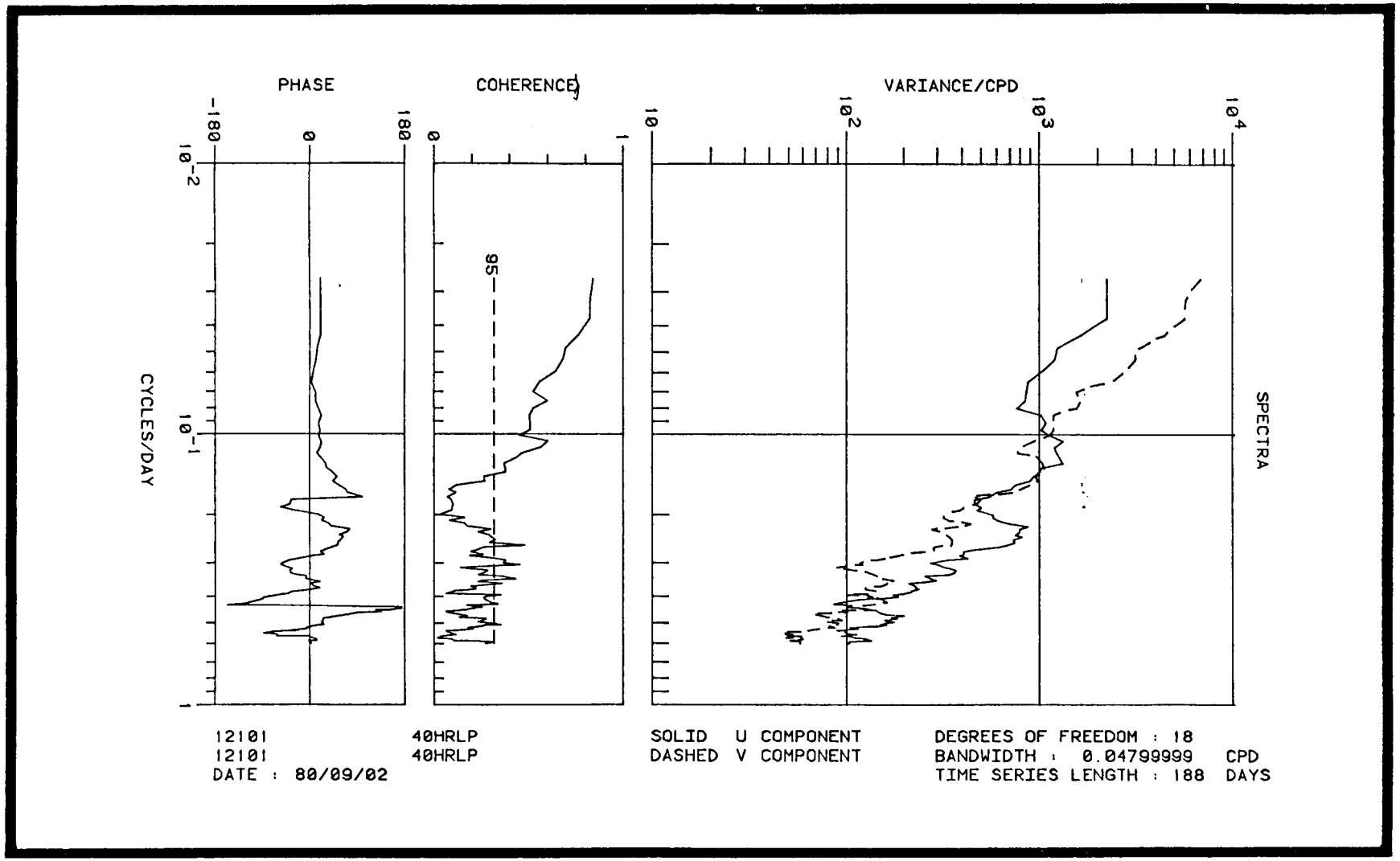

Figure 4-10. Spectra, coherence and phase for velocity at Mooring B: Top (12101).

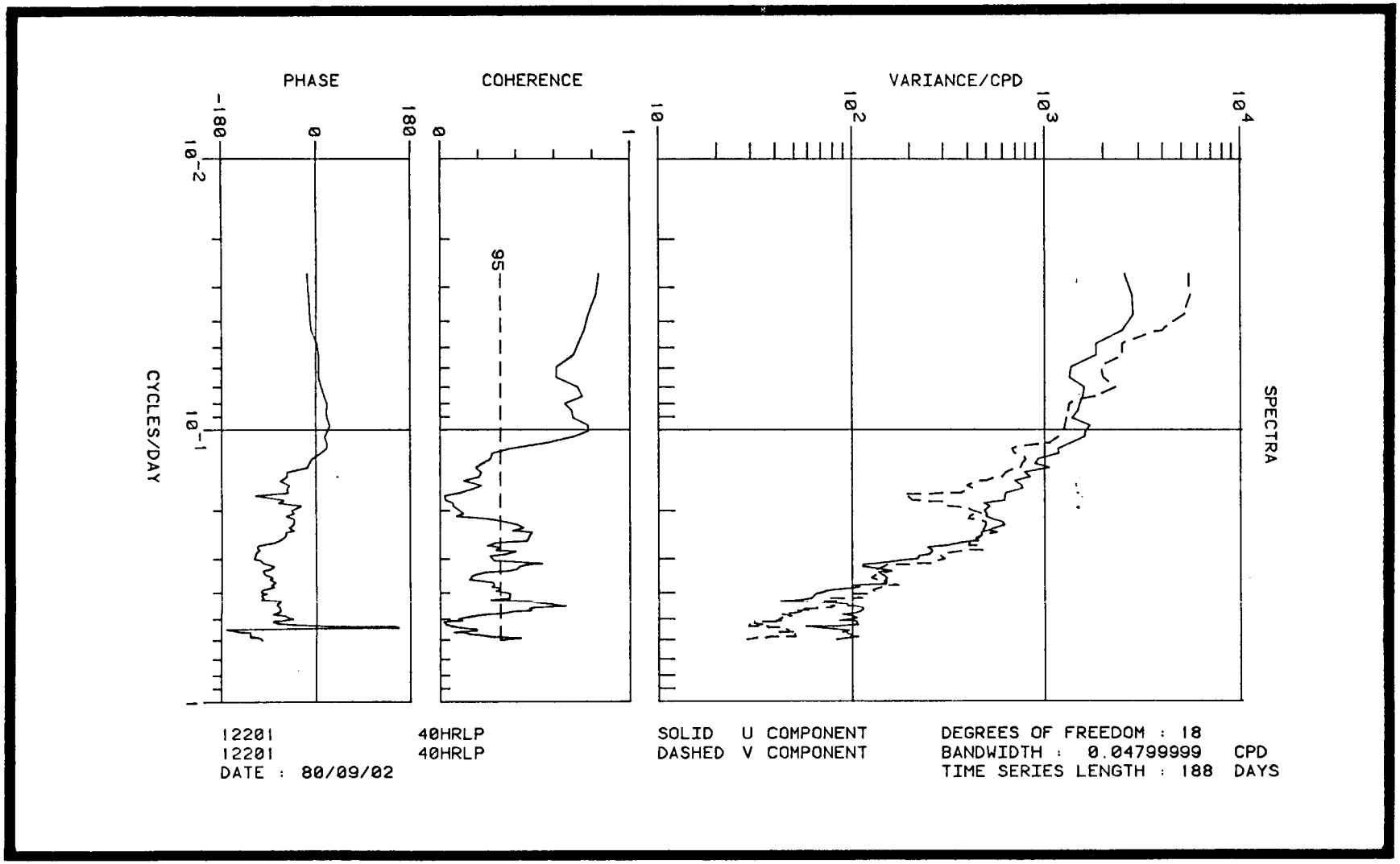

Figure 4-11 Spectra, coherence and phase for currents at Mooring C: Top (12201).

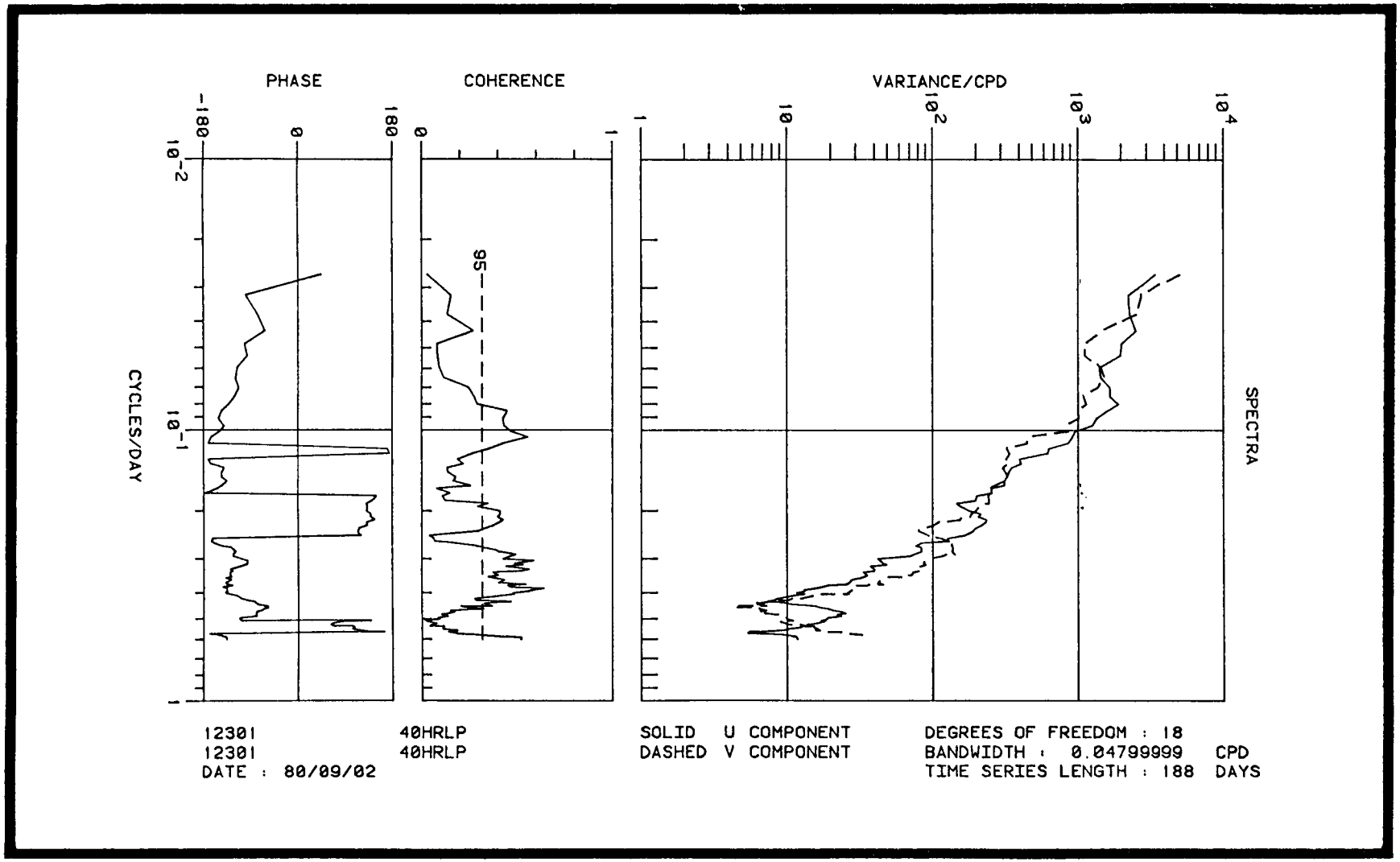

Figure 4-12 Spectra, coherence and phase for current velocity at Mooring D: Bottom (12301).

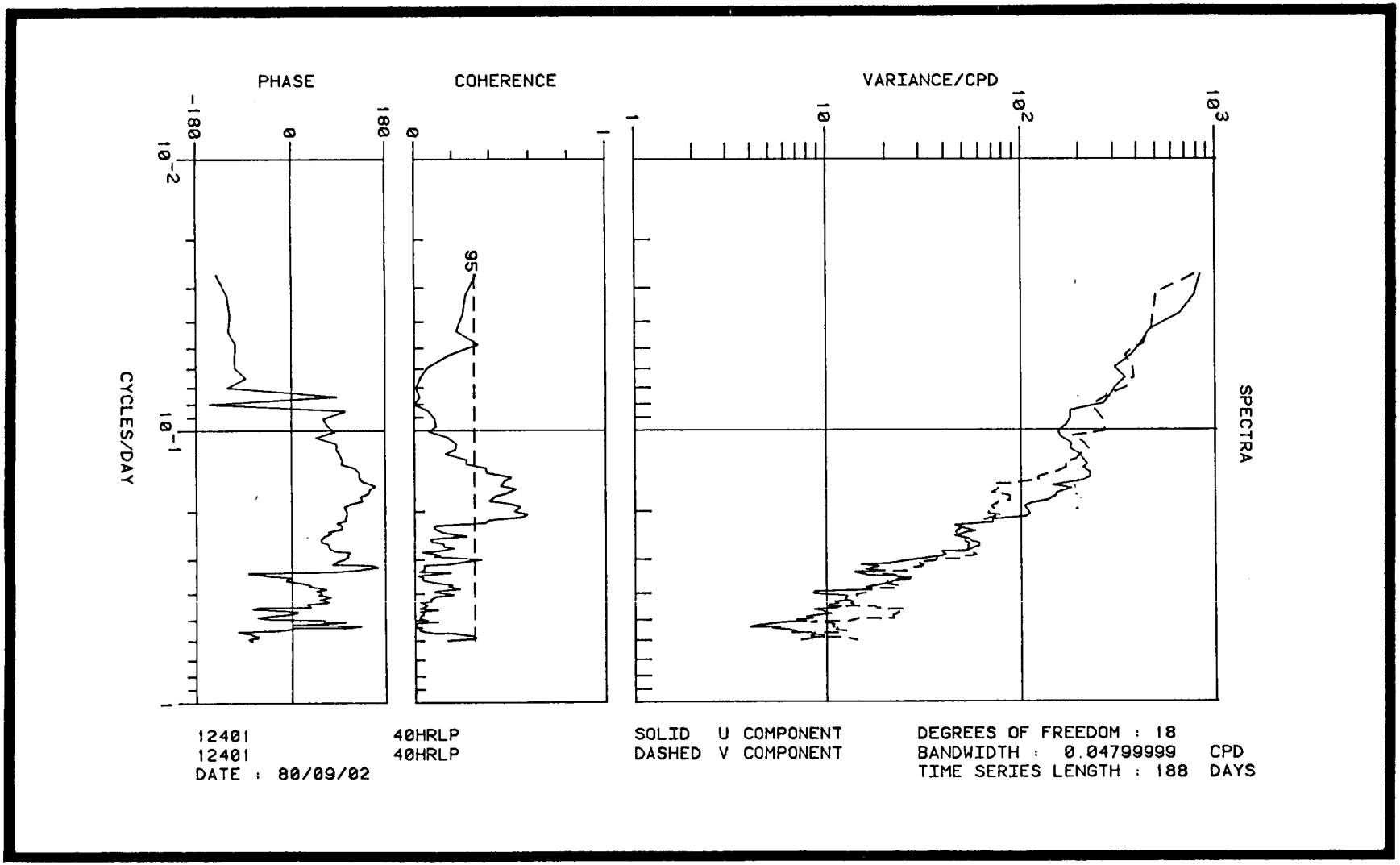

Figure 4-13 Spectra, coherence and phase for current velocity at Mooring E: Bottom (12401).

The cross-stream coherence and phase of velocity components and temperature at the 400 m level between sites B and C separated by a distance of 37 km are shown in Figures 4-14 through 4-16. Fluctuations in the 3 to 4 and 8 to 12 day period bands were coherent in all 3 variables. Cross-stream current variations at C appear to lead those at B by about 45° phase in the 3 to 4 day band and about 90° phase in the 8 to 12 day band. Along-stream current fluctuations were almost 180° out of phase for periods less than one week. Temperature was nearly in phase over these periods. Similar results were found for the lower layer between sites B and C except that fluctuations in the cross-stream components were nearly in phase and along-stream variations at C lead those at B by about 90° in phase.

Coherence of low-frequency velocity and temperature records from near bottom were generally weak between sites A and B. Between sites C and D there was a band of coherence at periods of 8 to 12 days in the near bottom along-stream velocity and temperature records, with the currents being 180° out of phase and temperature nearly in phase. Coherence between sites D and E was not significant for any variable.

Significant coherence was observed over the 400 m vertical separation at site B for the cross-stream components at periods of 3 to 5 days; for the along-stream component at periods longer than 1 week; and for temperature at periods of 2.5 and 5 to 10 days with small phase lags for all variables. At site C significant coherence was observed over the 400 m vertical separation at periods of 2 to 7 days for u, 4 to 5 and 7 to 12 days for v and 4 to 12 days for T, again with small phase lags.

4.3 Discussion

Low-frequency time series and spectra of current and temperature from the Gulf Stream region indicate that cold, cyclonic perturbations of the basic northward flow at site B tend to be coherent and 180° out of phase with anticyclonic flow events at site C. Fluctuations of this type appear to occur at periods of 2 to 7 days and are more clearly recognizable after removing the effect of the strong northward Gulf Stream mean flow by band-pass filtering the data over a 40 hour to 2 week period band. This removes fluctuations with periods less than 40 hours and greater than 2 weeks. Figures 4-17 and 4-18 show examples of band-pass filtering. Current perturbations at sites A and B generally show a cyclonic sense of rotation and are at least 180° out of phase. At site C anticyclonic rotation that is 180° out of phase with the flow at site B tends to be more common. Current amplitudes were approximately equal at sites A, B and C resulting in weak vertical shear on the order of 10^{-4} s^{-1} which is about an order of magnitude less than the mean shears and indicates a strong barotropic component to the fluctuations. Temperature fluctuations were nearly in phase between sites B and C and visibly coherent. Temperature fluctuations were approximately 180° out of phase with the cross-stream velocity component at sites B and C.

During days 27 to 40 temperature was in phase with the along-stream velocity at site B and out of phase at site C and appears to be a reasonably clear example of an offshore/onshore/offshore Gulf Stream meander with a period of about 8 to 9 days. Assuming the current axis was located near mooring B as indicated in Figure 2-1 than a meander of the Stream (east/west shift of the velocity and temperature fields) could account for the observed

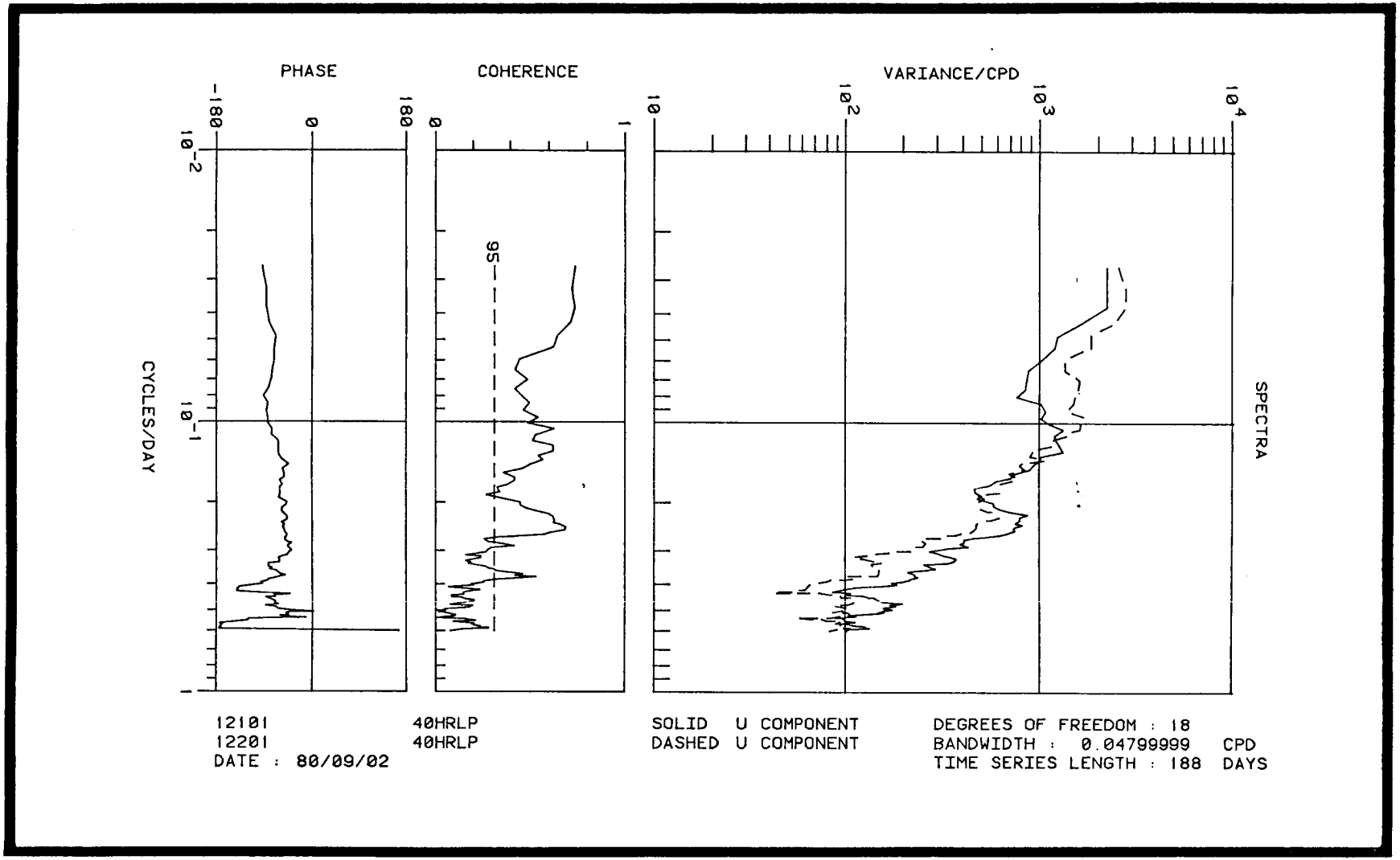

Figure 4-14 Spectra, coherence and phase between u components at Moorings B and C: Top measurement position.

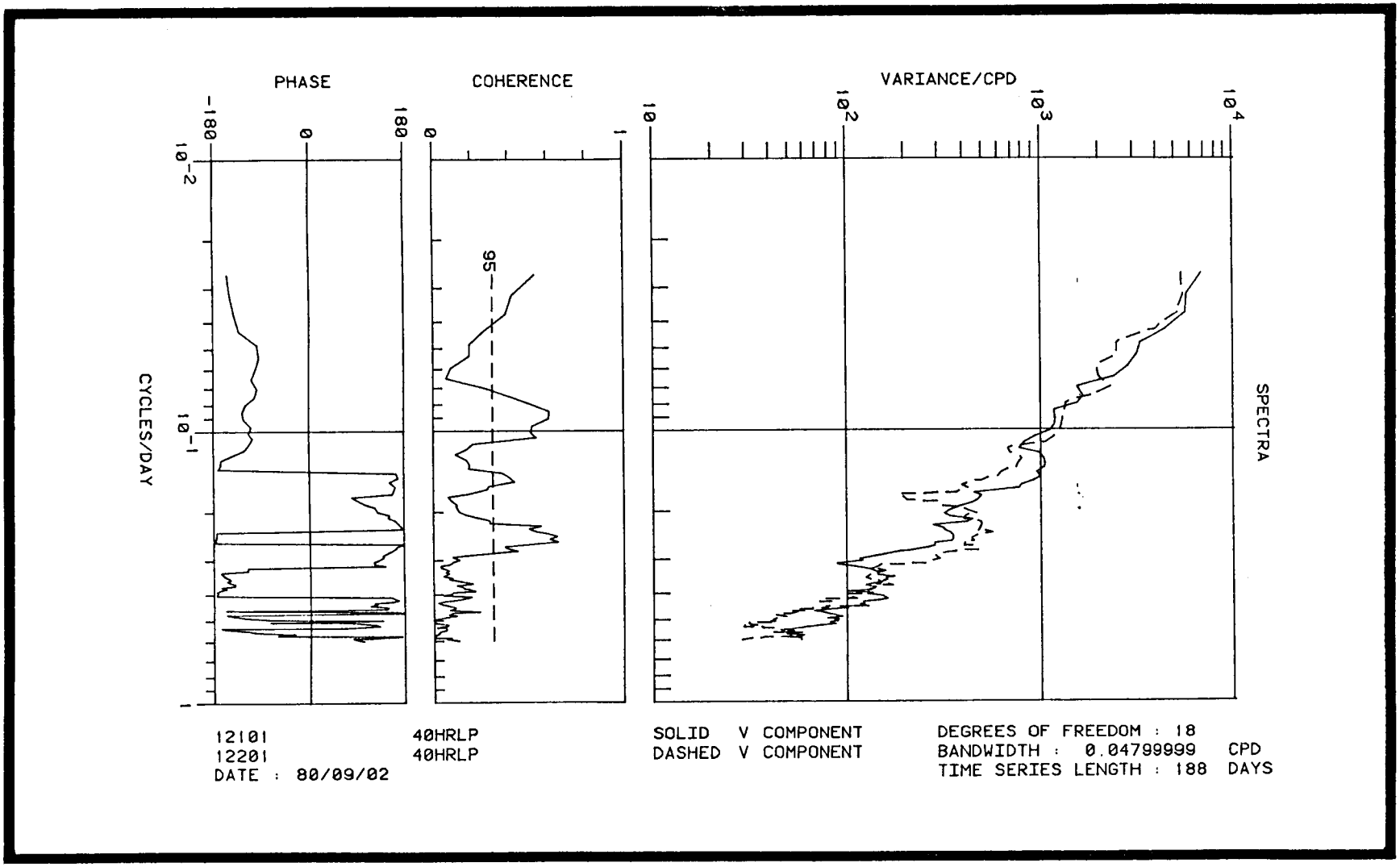

Figure 4-15 Spectra, coherence and phase for v components of velocity at Moorings B and C: Top (12101 vs 12201).

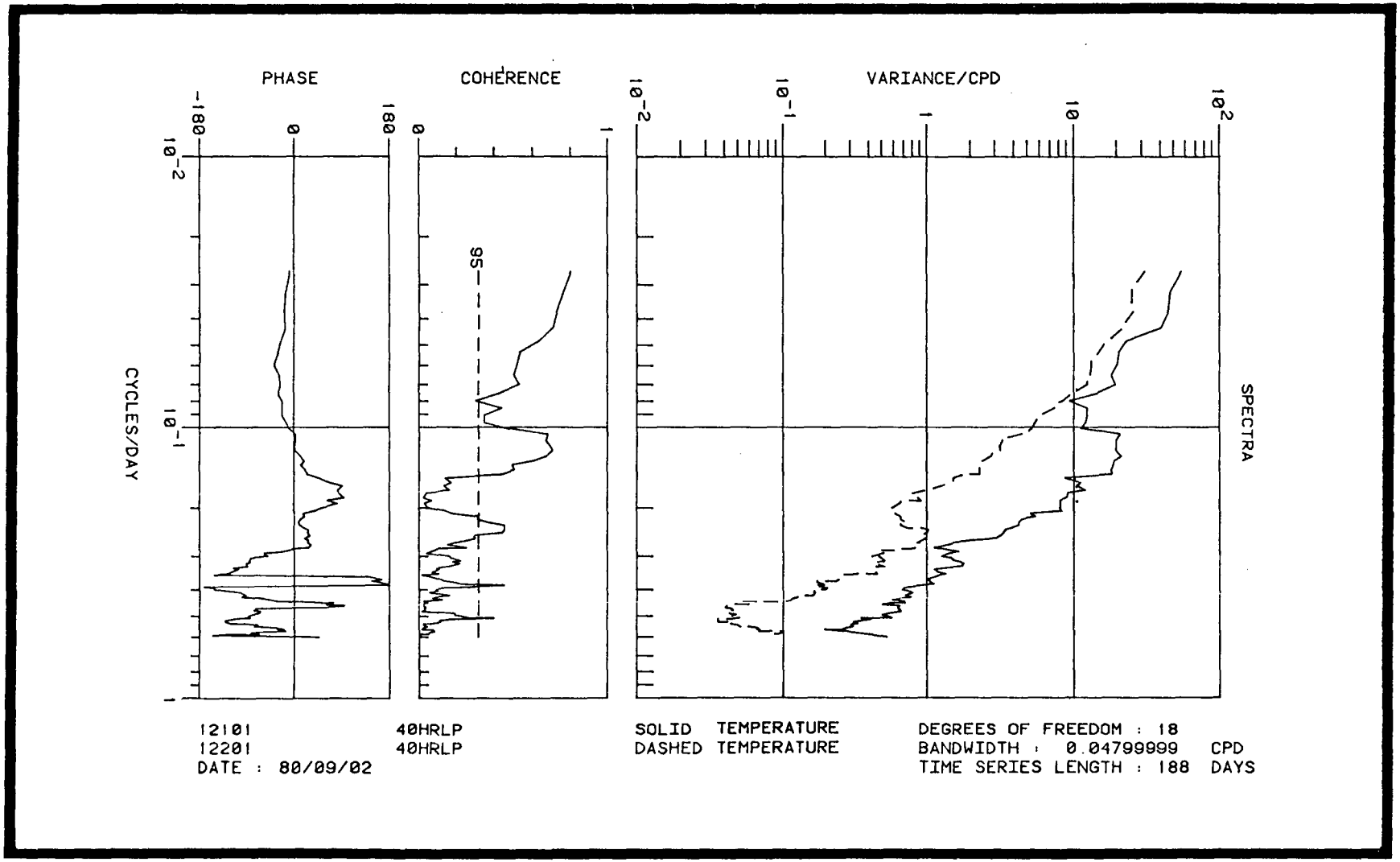

Figure 4-16 Spectra, coherence and phase between temperatures at Moorings B and C: Top.

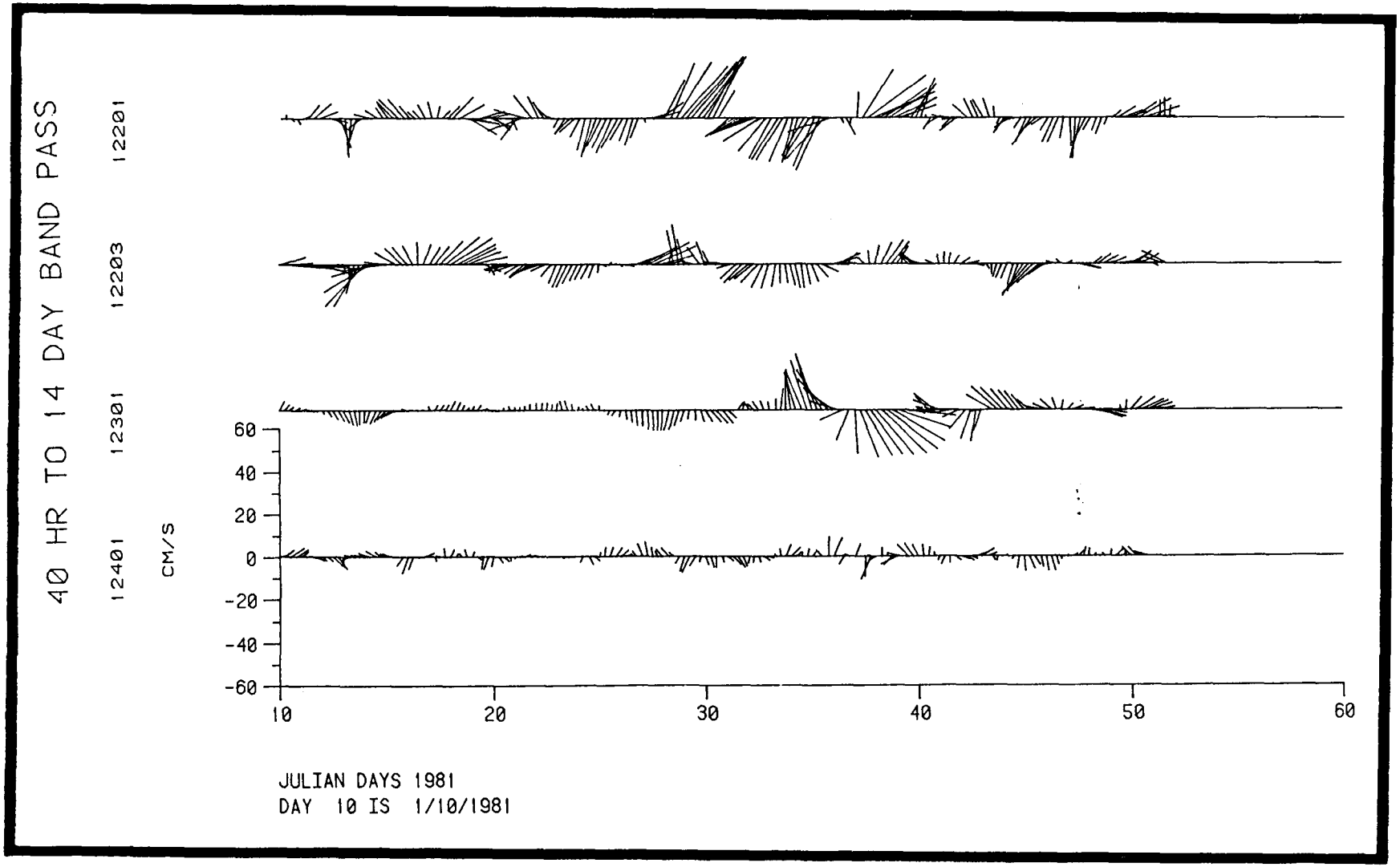

Figure 4-17 Stick plots of band passed (40 HLP - 14 day) velocity for the indicated sites and period.

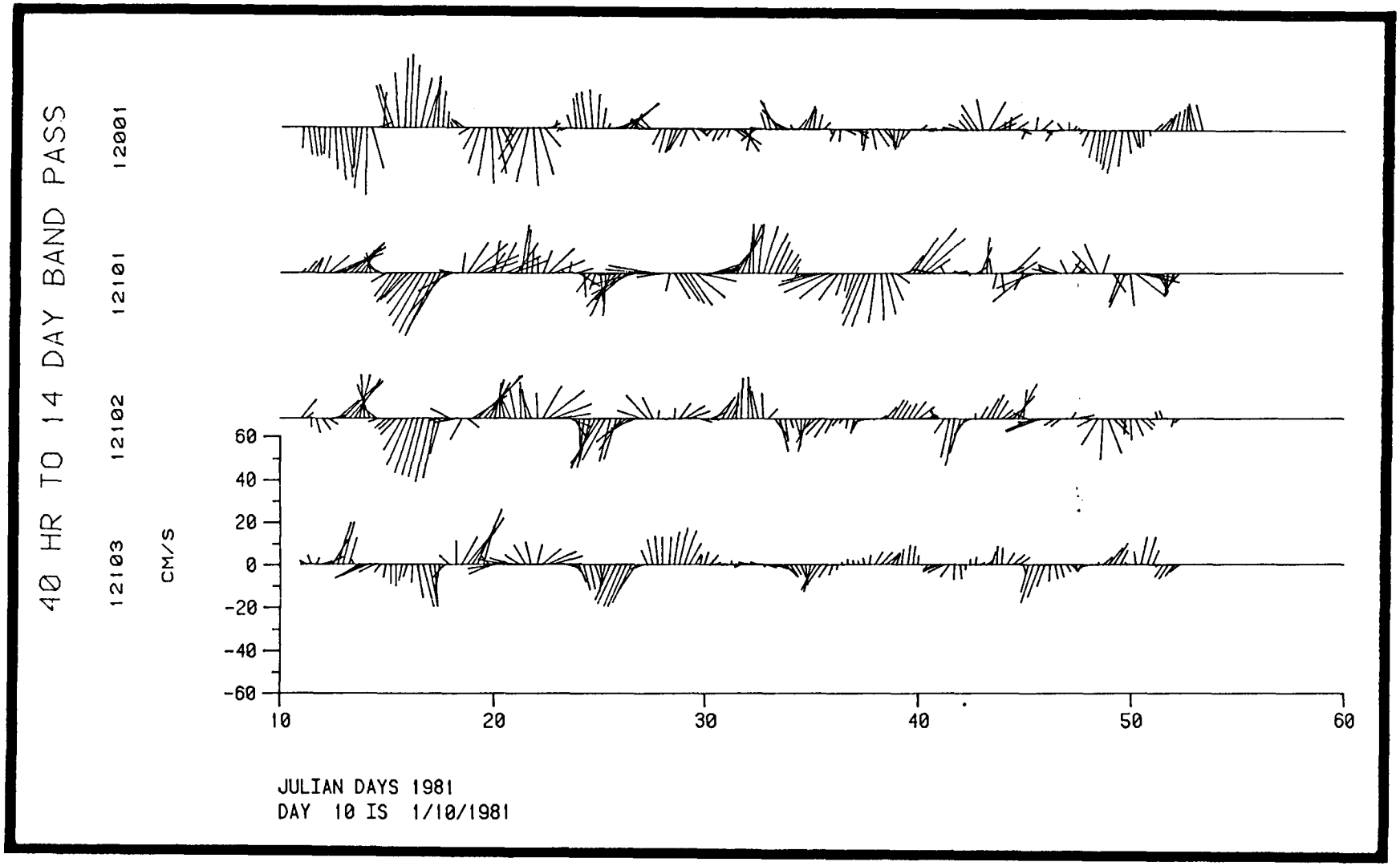

Figure 4-17 Continued.

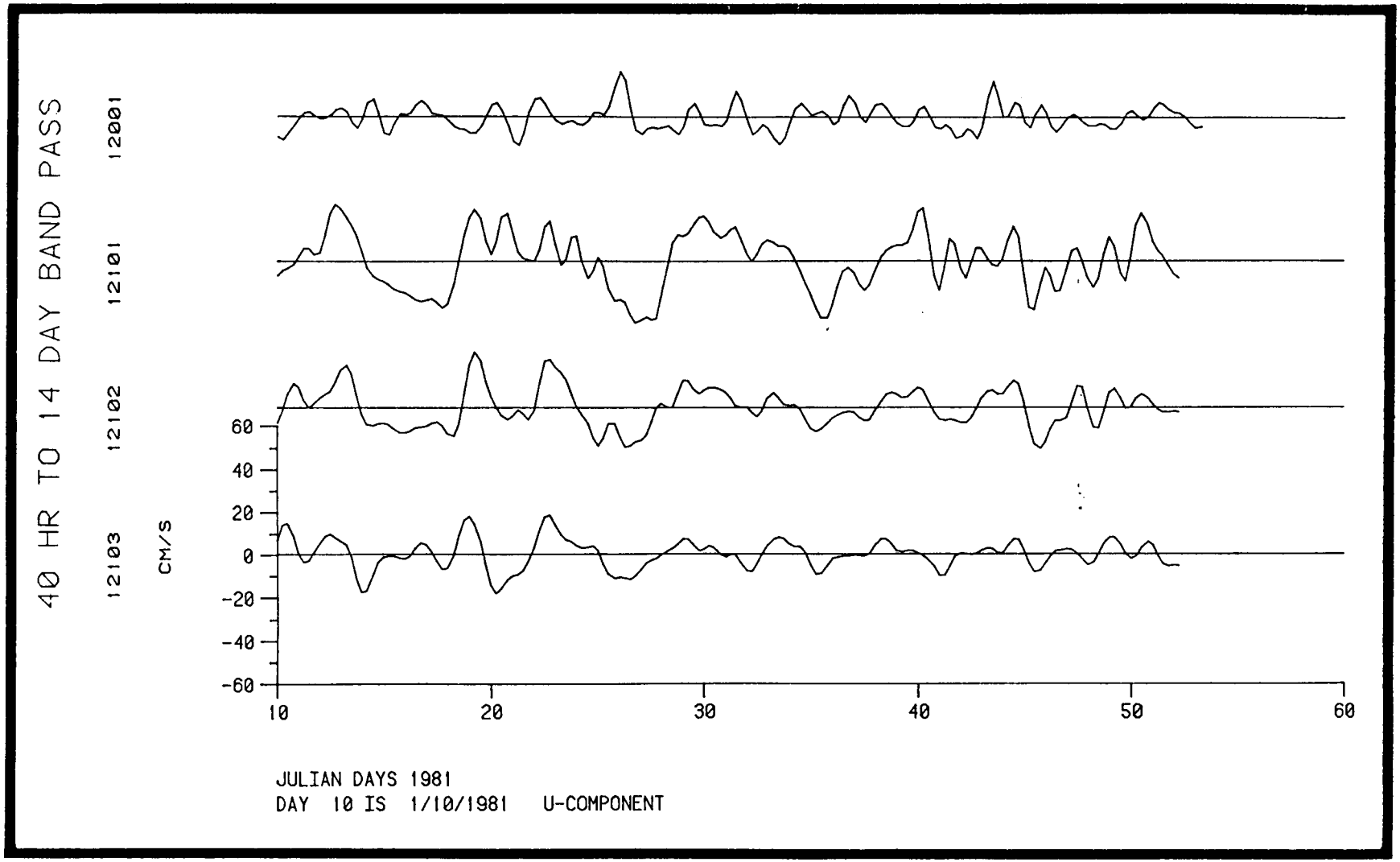

Figure 4-18a Band pass filtered velocity for the indicated component sites and period.

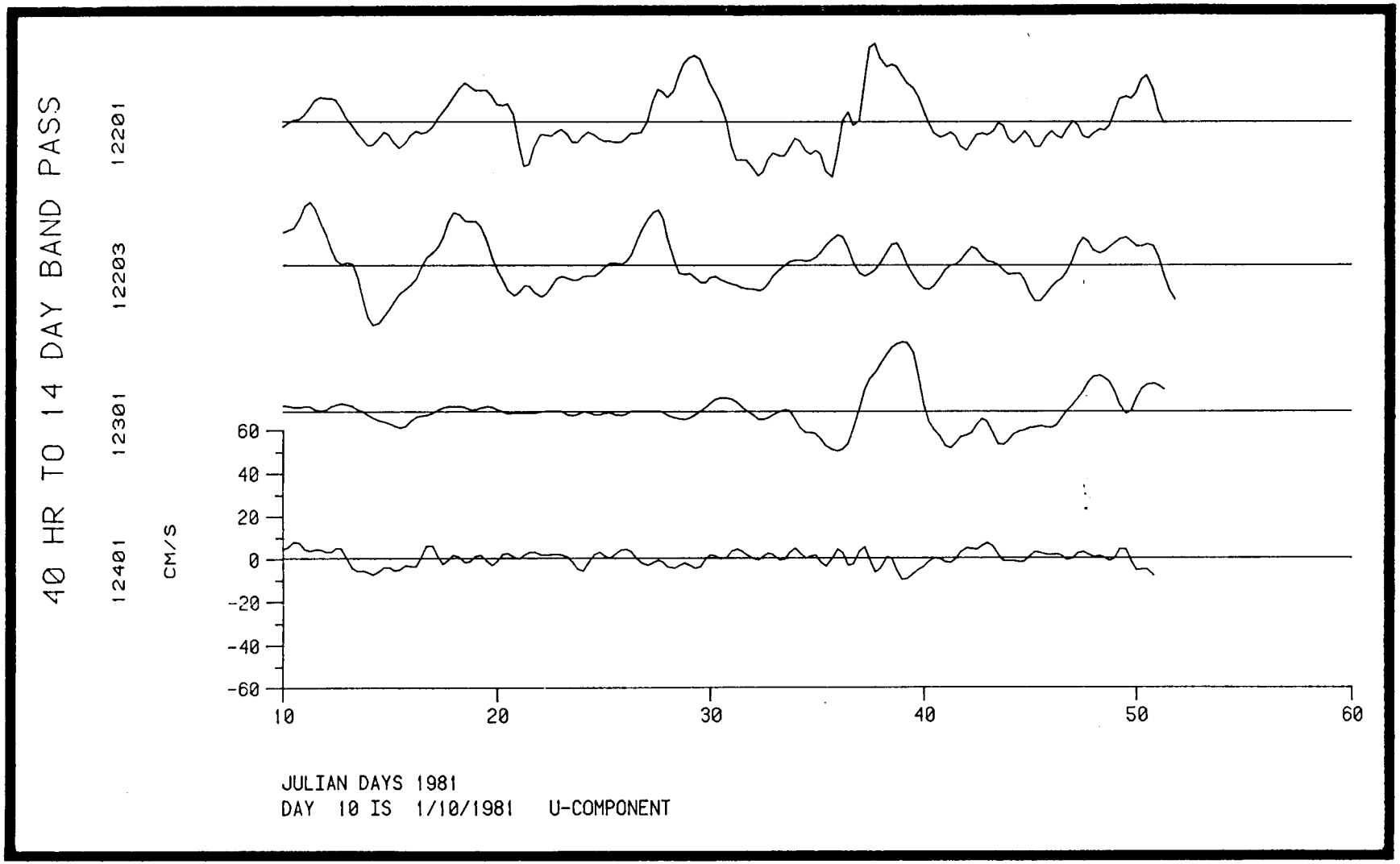

Figure 4-18b Band pass filtered velocity for the indicated component, sites and periods.

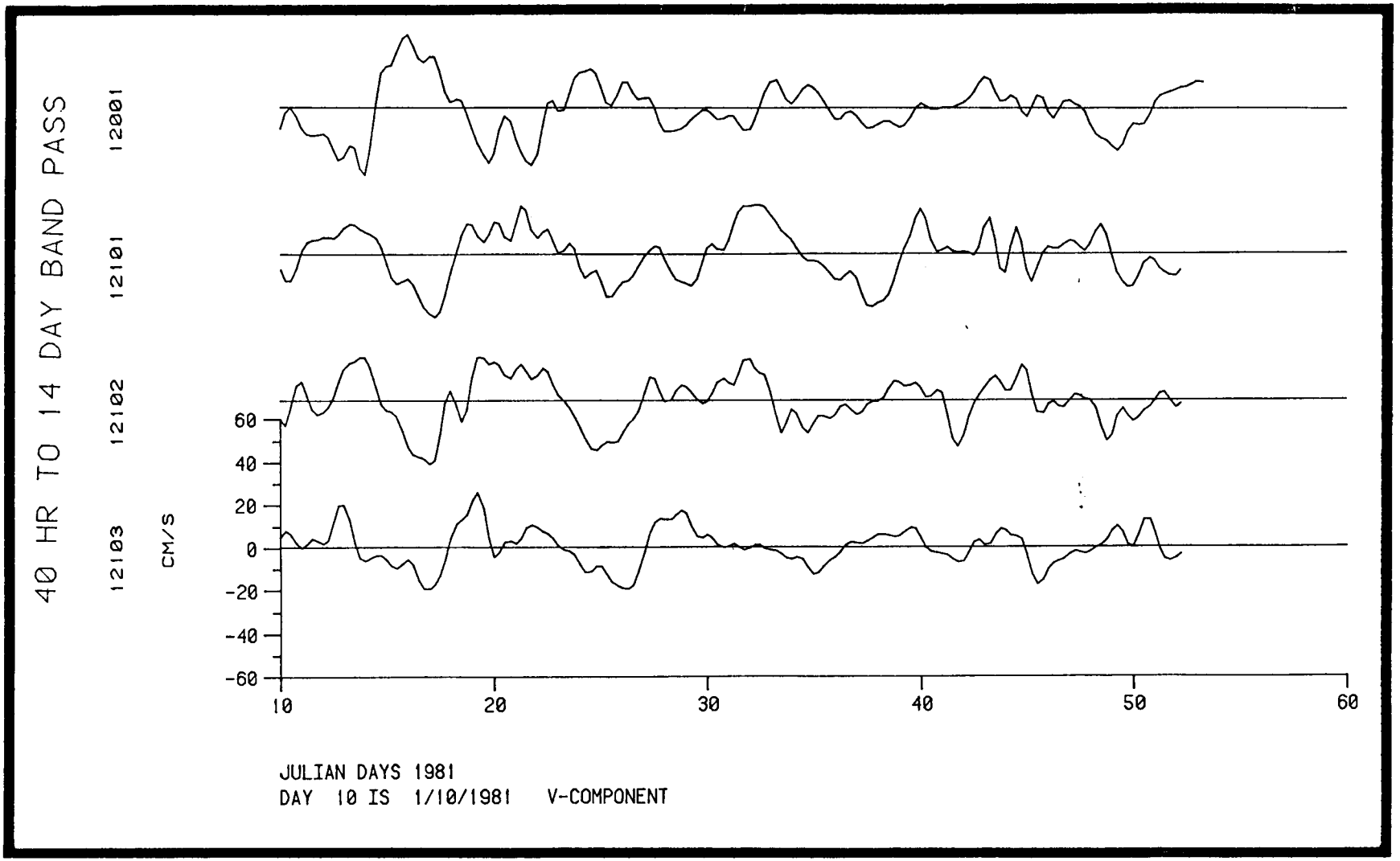

Figure 4-18c Band pass filtered velocity for the indicated component, sites and periods.

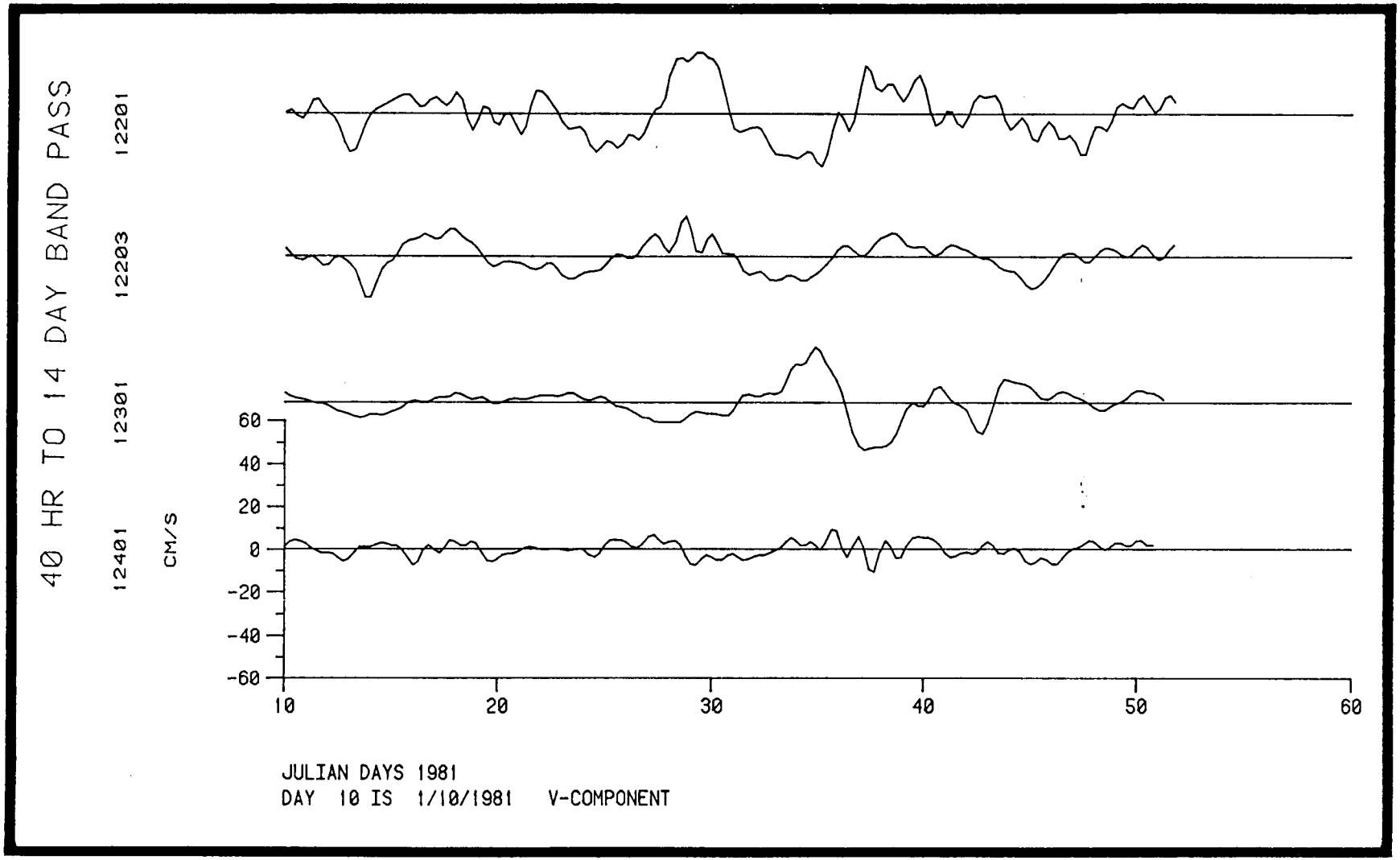

Figure 4-18d Band pass filtered velocity for the indicated component, sites and periods.

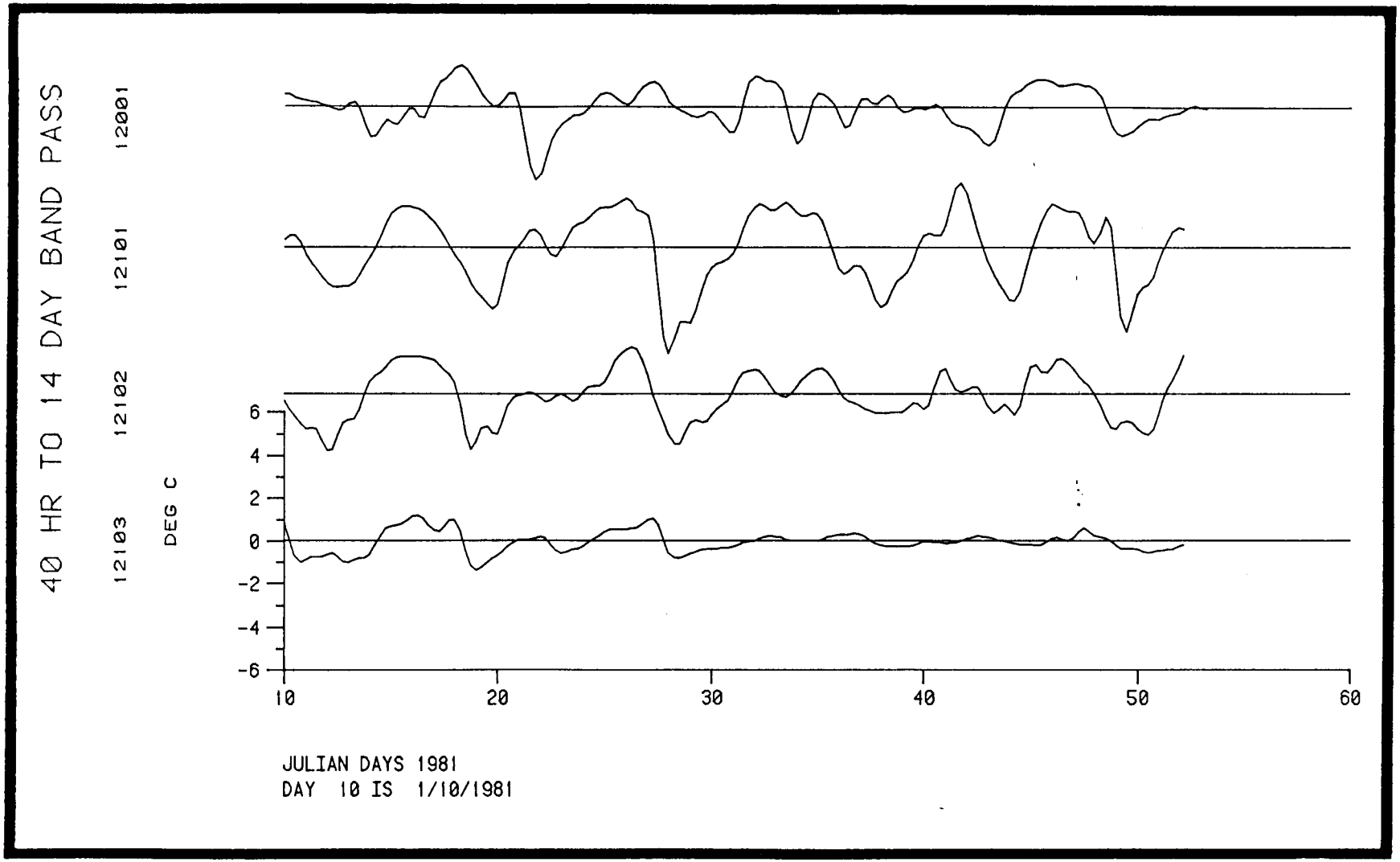

Figure 4-18e Band pass filtered temperature for indicated sites and periods.

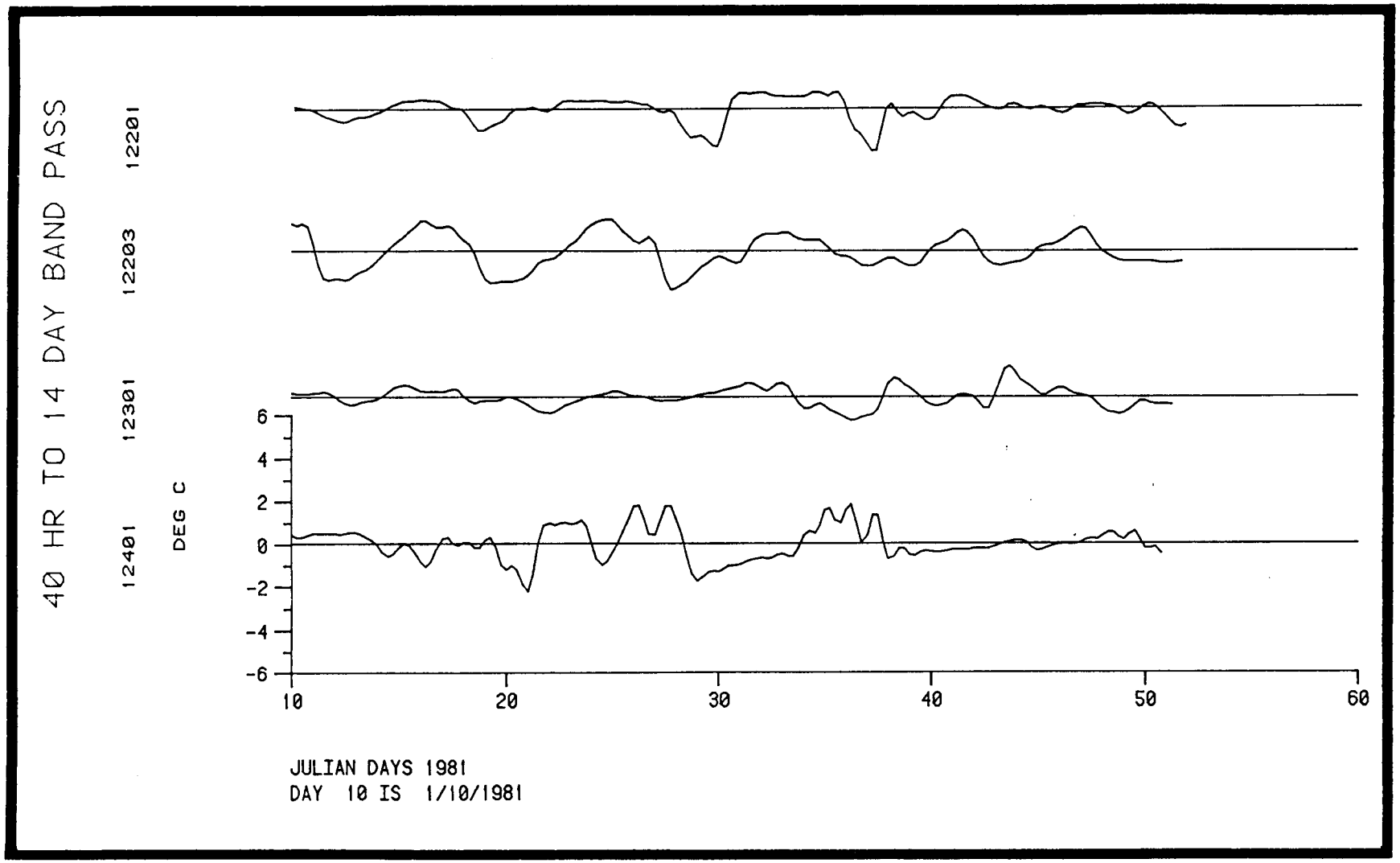

Figure 4-18f Band pass filtered temperature for the indicated sites and period.

changes in velocity and temperature. An offshore meander could cause an offshore component in flow and decreasing temperatures at B and C coupled with an increase in along-stream flow at C (as the axis approaches) and decrease at B. The observations on days 27 to 31 and 35 to 40 are typical examples of this type of offshore meander behavior. An onshore meander would result in an onshore current component and increasing temperatures at B and C while the along-stream flow increased at B, with the approaching axis, and decreased at C. The observations on days 31 to 35 are representative of the changes that occur during an onshore meander.

Brooks and Bane (1981) and Bane et al., (1981) observed weekly period Gulf Stream meanders off Onslow Bay with moored current meters, satellite thermal imagery and AXBT surveys. These meanders produces current and temperature fluctuations at stations located on the cyclonic side of the axis that were quite similar to the observed fluctuations at site B. Brooks (1979) observed the Florida Current axis to meander up to 24 km in the Florida Straits within a period band of 2-14 days. Transport fluctuations on the cyclonic side of the Current were 180° out of phase with transport on the anticyclonic side (similar to our findings for sites B and C) and were shown to be produced by east-west shifts of the current axis. The meanders did not affect the total transport but were coupled to mass flow variations on the anticyclonic side.

Bane and Brooks (1979) investigated east-west movements of the Gulf Stream surface thermal front and found meander amplitudes of ± 15 km upstream of the Charleston bump and ± 40 km downstream of the bump. Legeckis (1979) showed from time sequences of satellite thermal images that these meanders were produced by northward traveling waves that appear to amplify downstream of the Charleston bump. Lee, Atkinson and Legeckis (1981) and Lee and Atkinson (1982) have shown that cyclonic, cold-core eddies form in the Gulf Stream frontal region in connection with the growth of an offshore meander. These features can produce the cyclonic perturbations observed at site A during the periods of offshore meander (Figures 4-17 and 4-18).

A significant fraction of the low-frequency current and temperature variability at sites A, B and C was produced by fluctuations of the type described above. Comparisons with previous investigations indicates that east-west Gulf Stream meanders generated by northward traveling waves are the most likely mechanisms responsible for producing the observed fluctuations. Theoretical investigations indicate that both barotropic and baroclinic instabilities can occur for the Gulf Stream flow in this region (Niiler and Mysak, 1971; Orlanski, 1969; Orlanski and Cox, 1973). Theory predicts wave lengths of 100 to 200 km and wave periods of about 10 days for the fastest growing northward propagating waves, which appears to match reasonably well with satellite observations of the surface thermal front (Legeckis, 1979); current meter data from the shelf edge upstream of the Charleston bump (Lee and Atkinson, 1982); on the continental slope downstream of the bump (Brooks and Bane, 1981); and those data presented here. However without additional current meter data or supporting hydrographic and satellite data taken at a sufficiently high frequency to resolve several day period motions, we can only speculate as to the nature of the observed fluctuations.

Near-bottom flows at sites D and E do not appear to be significantly correlated between sites nor with near-bottom flows at the other locations.

At site D prolonged southward flows occurred that were not observed at any other station (Figure 4-5). The cause of this flow is uncertain but it may be related to the southward flowing undercurrent beneath the Gulf Stream off Cape Hatteras and over the Blake Escarpment (Stommel, 1965). Curiously these prolonged southward flow events were not observed at site E, the seaward edge of the Blake Plateau. Current amplitudes at sites D and E were not significantly different from the flows beneath the Gulf Stream, and commonly reached speeds of 20 to 30 cm s^{-1} that lasted for several days (Figures 4-1, 4-3, 4-7 and 4-17).

Cyclonic, cold-core eddies are known to travel across the BP and merge with the Gulf Stream in the region of the current meter array. Cheney and Richardson (1976) observed a ring move from relatively deep water of the Sargasso Sea onto shallower Blake Plateau in the vicinity of site E and finally coalesce with the Gulf Stream off Cape Canaveral. The ring traveled to the southwest at about 2 km day^{-1}. The ring extended to a depth of at least 3000 m in the deep water and presumably interacted strongly with the bottom as it moved into shallower water of the Blake Plateau, judging from a four fold increase in decay rate.

Satellite thermal imagery often show cold eddies on the east side of the Gulf Stream that are sometimes connected to the Stream by elongated warm streamers (Vukovich, 1978). Figures 4-19 and 4-20 show examples of cyclonic eddies in the vicinity of sites D and E on about February 10 and July 7, 1981, respectively. The February event was observable in the NOAA/VHRR products in the vicinity of site D for about a 10 day period during which a significant cold, cyclonic flow event was observed (Figures 4-3, 4-4, 4-17 and 4-18). The July eddy was observed to drift southwest by mooring E at about 1 to 2 km day^{-1} from May 12 to July 21. It appeared to be nearest mooring E at about July 7. Low-frequency current and temperature time series indicate a cold, cyclonic event occurred during Julian days 183 to 188 (July 1 to 6). From single near-bottom current meter measurements one cannot be certain if there is any real connection between the observed flow events and the cyclonic eddies indicated in the satellite images. Indeed the duration of the flow events of about 6 days appears too short for it would take on the order of 50 days for a 100 km diameter eddy to pass completely over a mooring.

4.3.1 Energy Transfer

Meanders have been shown to play an important role in the flux of momentum and heat and redistribution of kinetic and potential energy within the Gulf Stream. The transfer of eddy kinetic energy was found to be distributed horizontally across the Stream off Miami, whereas the transfer of perturbation potential energy was vertically distributed (Brooks and Niiler, 1977). Perturbation kinetic energy was transferred from the fluctuations to the mean flow in the cyclonic shear region of the current, and from the mean to the fluctuations in the anticyclonic shear region (Webster, 1961b; Schmitz and Niiler, 1969; Brooks and Niiler, 1977). Perturbation potential energy was transferred from the mean to the fluctuations in the lower half of the current and in the vicinity of the current axis (Brooks and Niiler, 1977). Orlanski (1969) and Orlanski and Cox (1973) concluded that energy transfers of this type can best be explained by a baroclinic instability process where disturbances can grow by feeding on the potential energy of the mean current and then transfer their kinetic energy back to the mean flow.

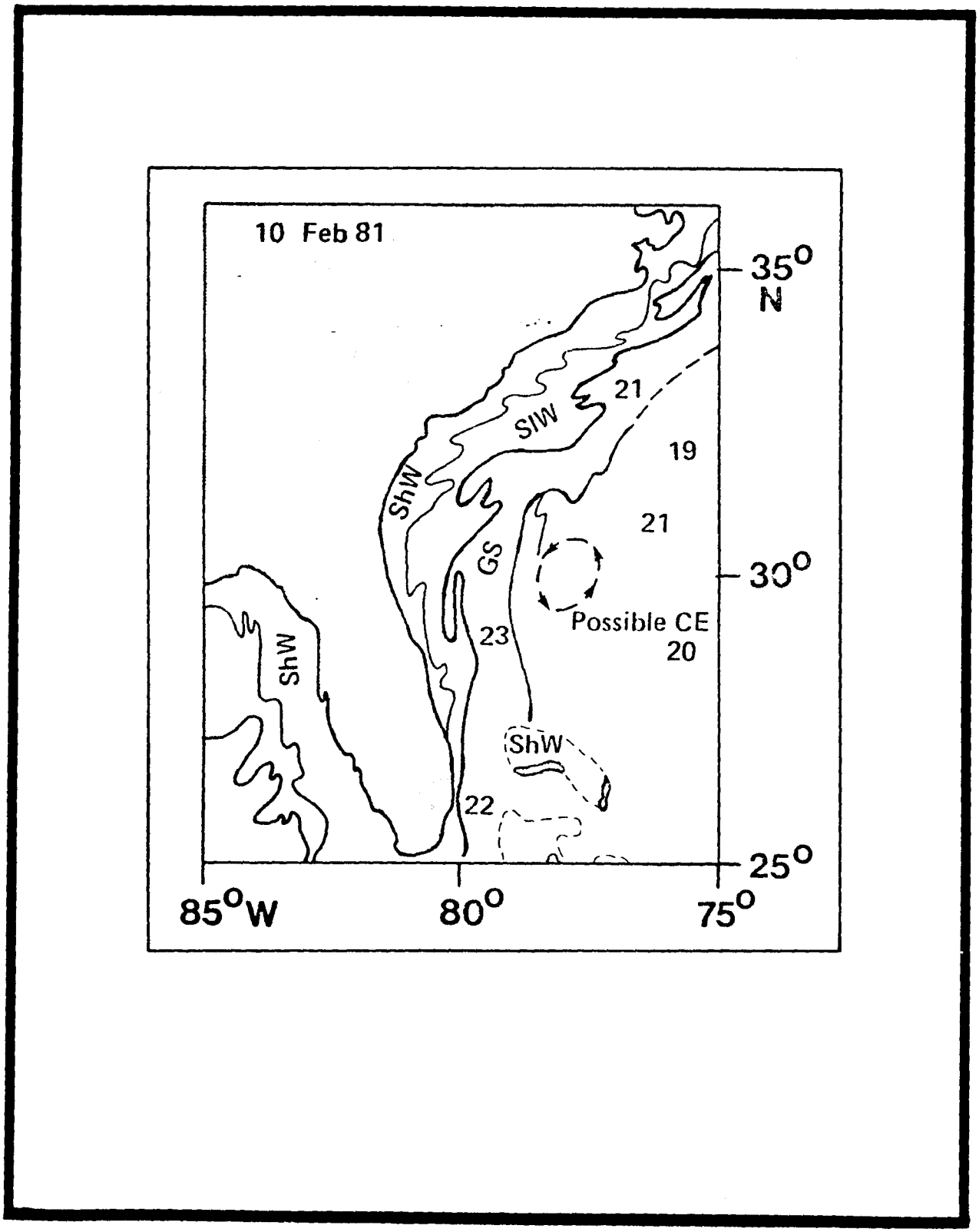

Figure 4-19 NOAA VHRR image of sea surface temperature on February 10, 1981. CE stands for cold eddy, GS is Gulf Stream, SIW is shelf intermediate water and ShW is shelf water.

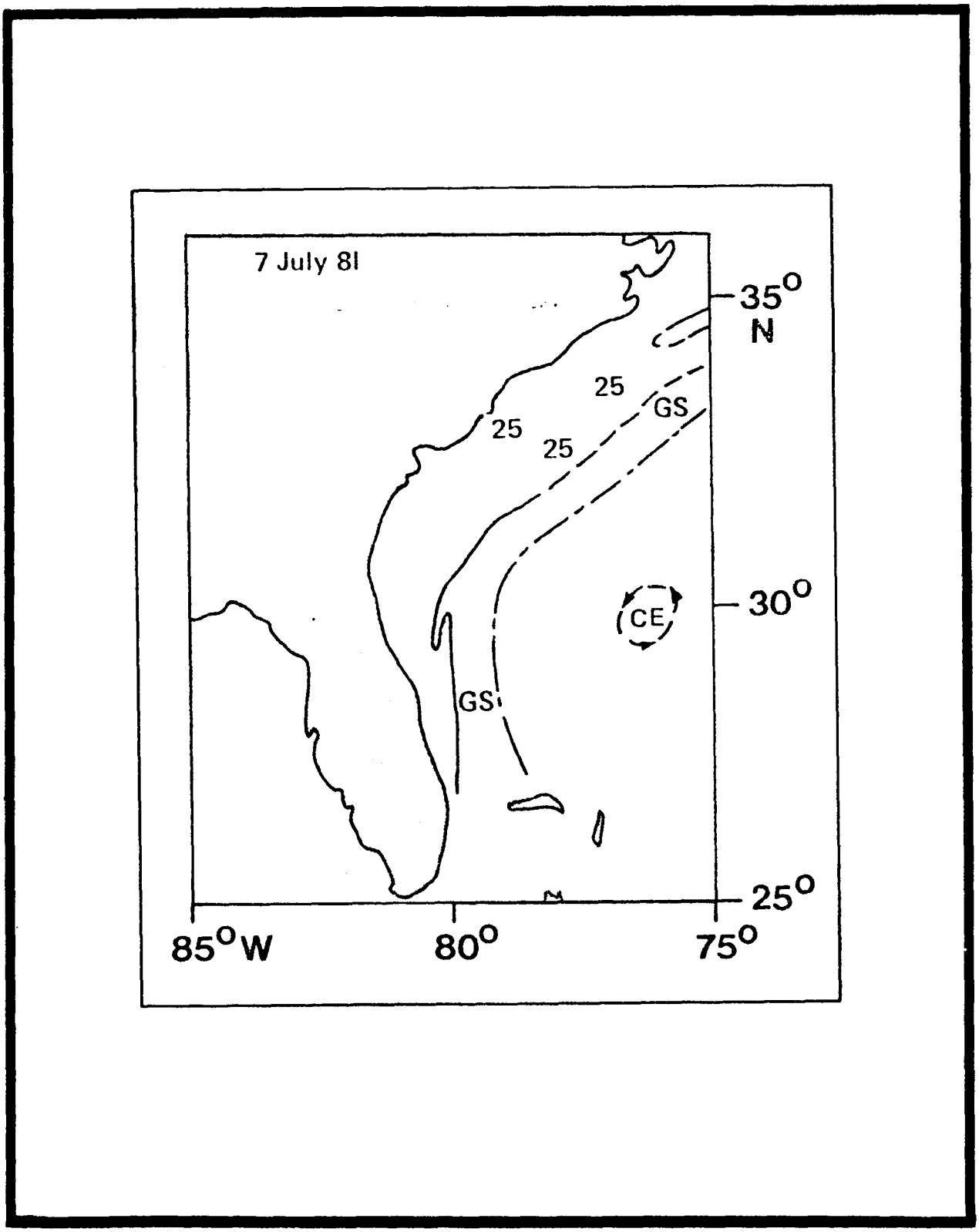

Figure 4-20 NOAA VHRR image of sea surface temperature on July 17, 1981. CE stands for cold eddy, GS is Gulf Stream, SIW is shelf intermediate water and ShW is shelf water.

Brooks and Niiler (1977) determined that Gulf Stream fluctuations caused an internal redistribution of energy with no appreciable net energy transfer over the current cross-sections average. They showed that the net conversion rate of perturbation kinetic energy can be estimated from:

$$\frac{d}{dt}\left[\frac{1}{2}\left(\overline{u'^2} + \overline{v'^2}\right)\right] = -\left[\overline{u'^2}\,\frac{\partial \bar{u}}{\partial x} + \overline{v'^2}\,\frac{\partial \bar{v}}{\partial y} + \overline{u'v'}\,\frac{\partial \bar{v}}{\partial x}\right] \quad (2)$$

where the overbar represents a time average and the primes are deviations from the mean. The first and third terms on the right hand side of (Eq. 2) were evaluated from the 400 m and near bottom depts at sites B and C. The second term involves downstream derivative of $\bar{v}$ which could not be calculated from the cross-stream array. However, since the cross-stream and along-stream current fluctuations (u',v') were about the same magnitude and $\partial\bar{v}/\partial x >> \partial\bar{v}/\partial y$, then the second term should be small compared to the third. The results for these calculations are given in Table 4-6. The dominant term in the energy transfer is $\bar{u}'\bar{v}'\ \partial\bar{v}/\partial x$. The negative sign indicates that there was a net transfer of perturbation kinetic energy from the mean flow to the fluctuations over the 7 month averaging period. This is consistent with the finding of Schmitz and Niiler (1968) and Brooks and Niiler (1977) for the anticyclonic shear zone. The rate of transfer was about 140×10^{-4} cm s^{-3} at mid-depth and was insignificant near the bottom. The net transfer of perturbation energy to the fluctuations in this region was produced by the combined effects of a net offshore flux of northward momentum of 1.4×10^{3} cm^2 s^{-2} occurring in a zone of mean anticyclonic shear of about -9×10^{-6} s^{-1}. Using these values the horizontal eddy exchange coefficient, $A_h = -\bar{u}'\bar{v}' / \partial\bar{v}/\partial x$, is estimated at 2×10^{8} cm^2 s^{-1}. Co-spectra of the velocity components from 400 m at sites B and C indicates that the offshore flux of northward momentum was distributed rather evenly over the total low-frequency range at both sites, without any well-defined peaks (Figure 4-21). This suggests that either the energy transfer was distributed over a broad range of periodicites or that the record lengths were too long, causing the energy density of near-periodic motions to merge, producing a red spectrum.

Co-spectra of the cross-stream velocity component and temperature from sites B and C at the 400 m depth (Figure 4-22) shows that the heat flux (u'T') was negative over the 2 to 14 day period range. This condition would occur for east-west meanders of a current with a positive horizontal temperature gradient. Onshore flows are correlated with increasing temperatures and offshore flows with decreasing temperatures. These co-spectra can be used to estimate the sense of perturbation potential energy transfer. The net conversion rate of perturbation potential energy can be determined from:

$$\frac{d}{dt}\left[\frac{g}{2}\overline{\rho'^2} + \frac{\partial\bar{\rho}}{\partial z}\,\rho_o\right] = -\left[g\,\overline{u'\rho'}\,\frac{\partial\bar{\rho}}{\partial x}\Big/\rho_o\left|\frac{\partial\bar{\rho}}{\partial z}\right| + \overline{gv'\rho'}\,\frac{\partial\rho}{\partial y}\Big/\rho_o\left|\frac{\partial\bar{\rho}}{\partial z}\right|\right] \quad (3)$$

We assume that downstream gradients of density (ρ) are small. Since temperature and density have a strong inverse relationship in the Gulf Stream

Quantity	Units	Net value mid-depth (400 m)	Net value near-bottom (800 m)
$\overline{u'^2}$	cm^2s^{-2}	624	84
$\overline{v'^2}$	cm^2s^{-2}	4114	104
$\overline{u'v'}$	cm^2s^{-2}	1394	-10
$\frac{\partial \bar{u}}{\partial x}$	s^{-1}	-2.7×10^{-6}	0.9×10^{-6}
$\frac{\partial \bar{v}}{\partial x}$	s^{-1}	-8.6×10^{-6}	1.5×10^{-6}
$\bar{\rho}\,\overline{u'^2}\,\frac{\partial \bar{u}}{\partial x}$	ergs $cm^{-3}s^{-1}$	-16.8×10^{-4}	0.8×10^{-4}
$\bar{\rho}\,\overline{u'v'}\,\frac{\partial \bar{v}}{\partial x}$	ergs $cm^{-3}s^{-1}$	-119.9×10^{-4}	-0.2×10^{-4}

Table 4-6 Net kinetic energy exchange rate at sites B and C for the period September 2, 1980 to March 13, 1981.

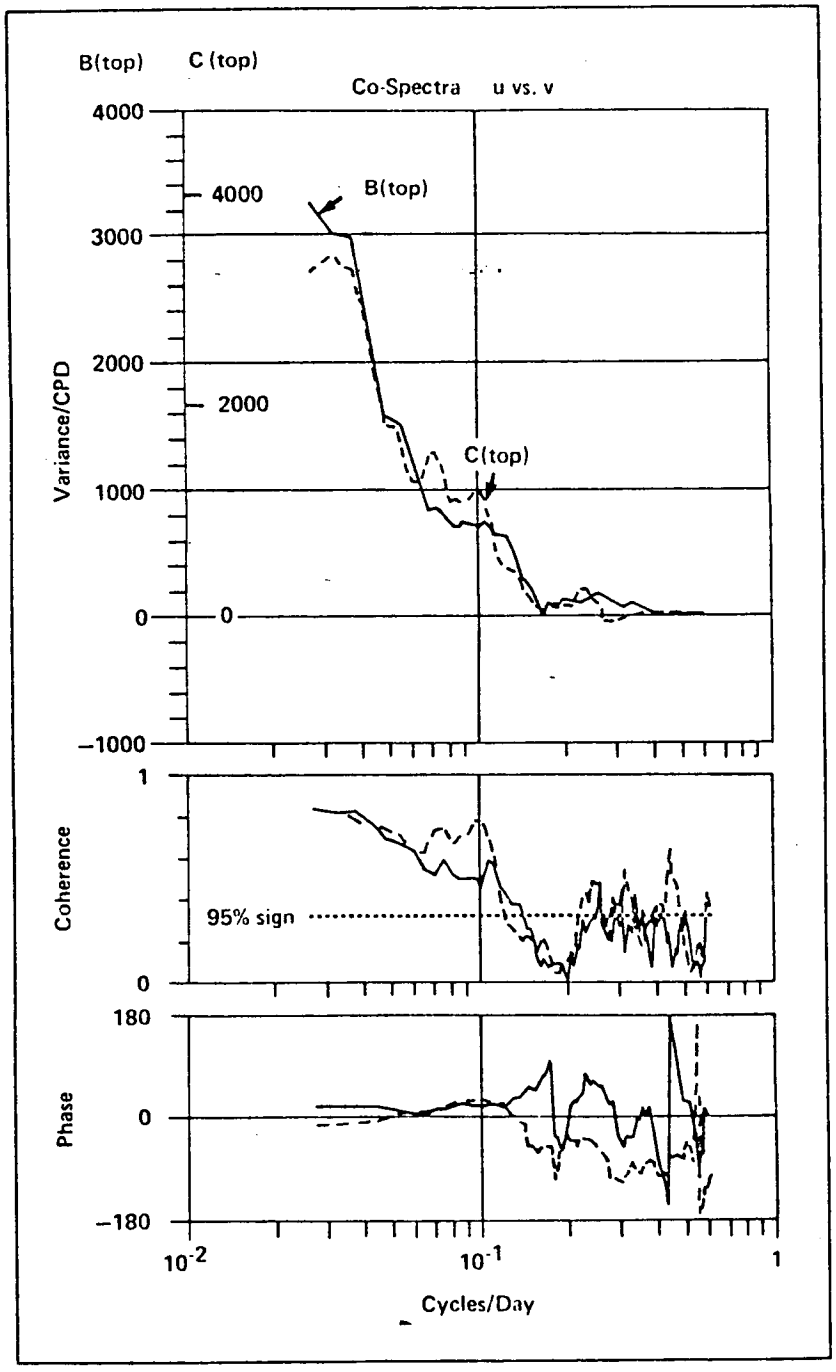

Figure 4-21 Co-spectra, coherence squared and phase of u and v components from current meters B (top) (solid lines) and C (top)(dashed lines). Degrees of freedom = 18; bandwidth = 0.048; data length = 188 days.

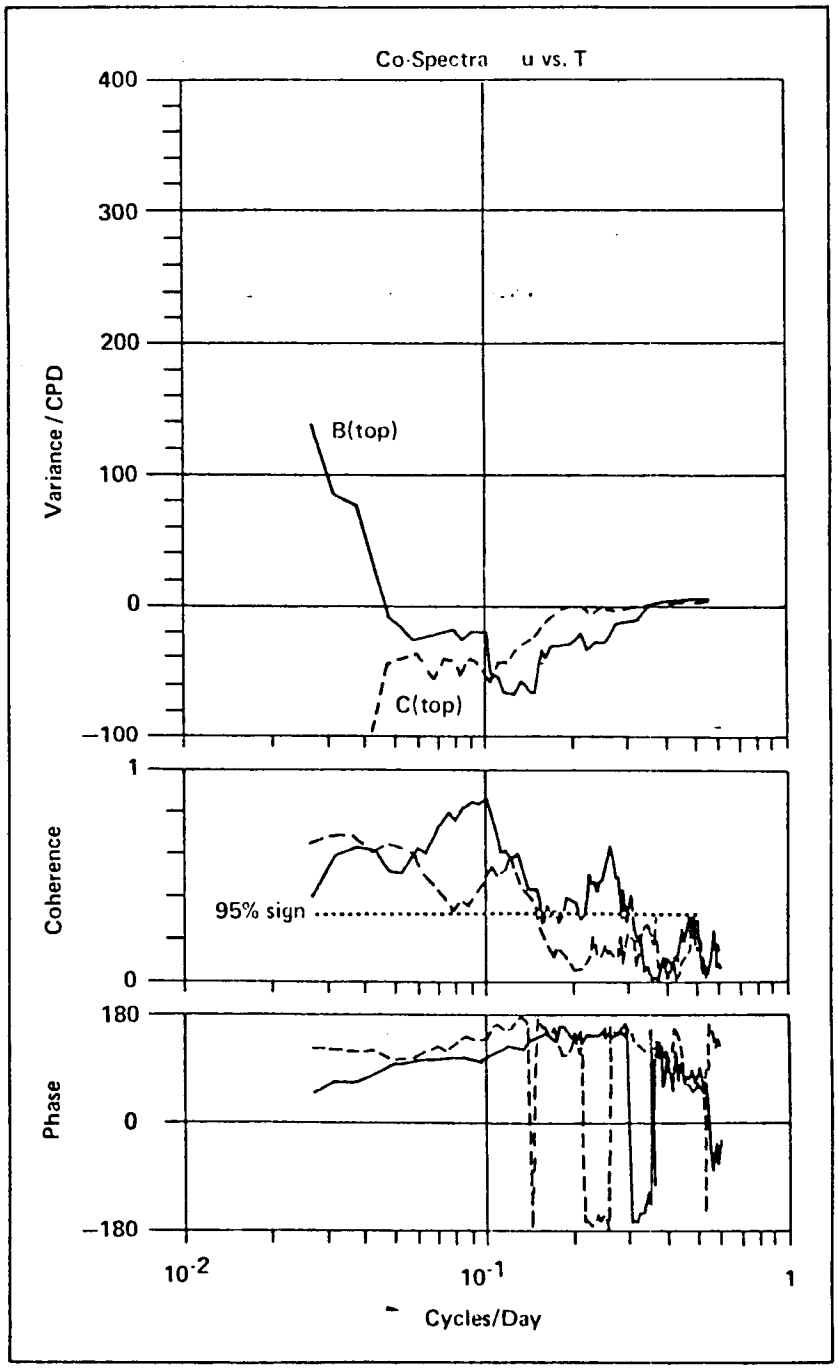

Figure 4-22 Co-spectra, coherence squared and phase of u and T from current meters B (top) (solid lines) and C (top) (dashed lines). Degrees of freedom = 18; bandwidth = 0.048; data length = 188 days.

then a negative heat flux would give a positive density flux ($u'\rho'$) which is multiplied times a negative horizontal density gradient giving a negative term inside the brackets. Therefore perturbation potential energy is transferred from the mean flow to the low-frequency fluctuations in the anticyclonic shear zone at 400 m, in the same manner as the transfer of perturbation kinetic energy.

4.3.2 Seasonality

Niiler and Richardson (1973) determined from transport sections between Miami and Bimini that there was a seasonal variation in volume transport of the Florida Current that could account for about 45% of the total transport variability. A seasonal maximum transport of $33.6 \times 10^6 m^3 s^{-1}$ was observed during early summer and a minimum of $25.4 \times 10^6 m^3 s^{-1}$ was found during December. Overall, the seasonal cycle results in a fluctuation bound of about $8 \times 10^6 m^3 s^{-1}$.

Seasonal variations in the Gulf Stream at mooring sites B and C were investigated by computing 2-weekly averages of the along-stream velocity components which were then used to construct a time series of the 2-weekly along-stream transport (M_y) flowing through the 15 km^2 area between the moorings. These data are shown in Figure 4-23 along with estimates of the 2-weekly averaged vertical and horizontal shear for the 400 to 600 m level between sites B and C, and the vertically averaged current at site B over the 400 to 600 m levels.

The mean annual transport between moorings B and C was about $4 \times 10^6 m^3 s^{-1}$, which is only about 10% of the Gulf Stream transport estimated by Richardson et al (1969) for this region. Even though the moorings encompassed only a small fraction of the total transport there still appears to be a seasonal trend consistent with that found by Niiler and Richardson (1973). Amplitude of the seasonal cycle was approximated $\pm$ $1 \times 10^6 m^3 s^{-1}$ with minimum values occurring during the fall and winter months and maximum values during spring and summer. This variation appears to have been produced by a summertime increase in the barotropic component of the flow at site B (increase in $\bar{v}$). The baroclinic component ($\partial\bar{v}/\partial z$) of the flow at site B appears to have remained relatively constant for the year except for a large event during the first two weeks. The flow at site C shows a slight decrease during the summer. Interestingly, horizontal shear ($\partial\bar{v}/\partial x$) at the 400 m depth also shows a general decreasing trend.

4.4 Summary and Conclusions

Subtidal current and temperature variability was investigated over the Blake Plateau at 30°N with a subsurface array of 5 current meter moorings extending from the shelf edge to the eastern edge (Blake Escarpment). The array was in place for a 13 month period from August 28, 1980 to October 6, 1981. Two of the moorings reached mid-depth levels in the high speed region of the Gulf Stream and the rest measured near-bottom flow.

Energetic current and temperature fluctuations occurred over a period band of 2 to 14 days at all locations. Flow perturbations on the cyclonic side of the Gulf Stream generally had a cyclonic sense of rotation, whereas on

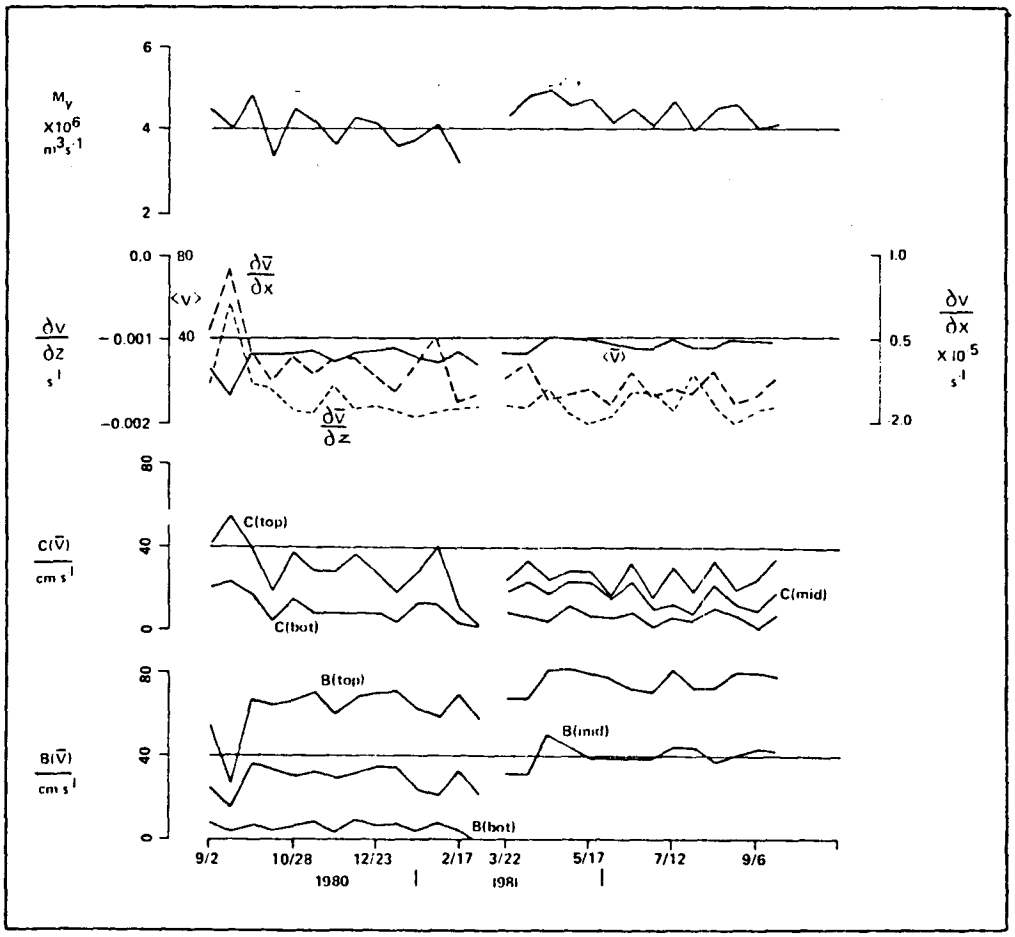

Figure 4-23 Two-weekly averages of along-stream currents from moorings B and C; vertical shear ($\partial\bar{v}/\partial z$) at B over the 400 to 100 m depths; horizontal shear ($\partial\bar{v}/\partial x$) between B (top) and C (top); vertically averaged currents (<v>) at B over the 400 to 600 m depths; and volume transport (M_y) between moorings B and C.

the anticyclonic side the fluctuations were anticyclonic and 180° out of phase with flow variations on the cyclonic side. These events appear to account for a significant fraction of the total observed variability throughout the year. Fluctuations of this type can be explained by east-west meanders of the Gulf Stream. A offshore meander results in an offshore flow and decreasing temperature at locations on both sides of the axis, coupled with increasing downstream flow in the anticyclonic shear region and decreasing downstream flow in cyclonic shear zone. The opposite occurs for an onshore meander: onshore flow and increasing temperature in both regions correlated to increasing downstream flow in the cyclonic zone and decreasing downstream flow in the anticyclonic shear region.

Gulf Stream meanders appear to be produced by waves propagating to the north at speeds of 30 to 70 cm s^{-1}, wave lengths of 100 to 200 km and periods of several days to one week. Indications are that these waves may be unstable through either a barotropic or baroclinic instability process which tends to redistribute the kinetic and potential energy between the fluctuations and the mean flow. Fluctuations on the anticyclonic side of the GS appear to derive perturbation kinetic and potential energy from the mean flow, whereas on the cyclonic side fluctuations tend to supply energy to the mean flow.

Low frequency flow variability near the bottom at the shelf edge appears to be related to Gulf Stream meanders. Indication are that cold, cyclonic perturbations occur at times of offshore meanders due to the formation of cyclonic eddies in the frontal region. During the onshore meander stage the western edge of the Stream is closer to the shelf and northward near-bottom flows occur with increased temperatures.

Near-bottom flows on the Blake Plateau east of the Gulf Stream show prolonged southward flow events that lasted up to 42 days and reached speeds in excess of 30 cm s^{-1}. These events were not correlated with flows at any other site and it is not clear as to the nature of the generating mechanism. A possible explanation may be the southward undercurrent that has been observed beneath the Gulf Stream off Cape Hatteras. Near bottom flows at this location and at the seaward edge of the BP may at times be affected by cyclonic, cold-core eddies that are observed to move across the BP and merge with the GS in this region. However, without additional current measurements and supporting hydrographic and satellite data, it is difficult to be more specific.

Mean flows in the vicinity of the Gulf Stream axis were toward the north at about 60 to 75 cm s^{-1} at the 400 m level. A maximum downstream current of 109 cm s^{-1} also occurred at this location. The mean vertical shear near the axis was approximately -2×10^{-3} s^{-1} and showed little variation with season. The mean transport through the mooring array was 4×10^{6} m^{3} s^{-1} which is about 10% of the total transport observed at 30°N. A seasonal change in transport of about 2×10^{6} m^{3} s^{-1} was observed with minimum transport occurring in late fall-early winter and maximum values in late spring-early summer, consistent with the seasonal change in total transport observed by Niiler and Richardson (1973). The seasonal change in transport appeared to be produced by an increase in the barotropic component of the flow.

REFERENCES

Bane, J.M., Jr., and D.A. Brooks, 1979: Gulf Stream meanders along the continental margin from the Florida Straits to Cape Hatteras. Geophys. Res. Lett., 6, 280-282.

Bane, J.M., Jr., D.A. Brooks and K.R. Lorenson, 1981: Synoptic observations of the three-dimensional structure, propagation and evolution of Gulf Stream meanders along the Carolina continental margin. J. Geophys. Res. (in press).

Blanton, J., 1971: Exchange of Gulf Stream water with North Carolina shelf water in Onslow Bay during statified conditions. Deep-Sea Res., 18, 167-178.

Bonde, L., 1978: Comparative testing of Niskin and vector averaging current meters. Tech. Rept for ONR, Contract No. N00014-74-C-0146. 41 pp.

Brooks, D.A., 1975: Wind-forced continental shelf waves in the Florida Current. U. of Miami/RSMAS Technical Report No. 75026, 268 pp.

Brooks, D.A., and J.M. Bane, Jr., 1978: Gulf Stream deflection by a bottom feature off Charleston, S.C. Science, 201, 1225-1226.

Brooks, D.A., 1979: Fluctuations in the transport of the Florida Current at periods between tidal and two weeks. J. Phys. Oceanogr., 9, 1048-1053.

Brooks, D.A., and J.M. Bane, Jr., 1981: Gulf Stream fluctuations and meanders over the Onslow Bay upper continental slope. J. Phys. Oceanog., 11, 247-256.

Brooks, I., and P.P. Niiler, 1977: Energetics of the Florida Current. J. Mar. Res., 35, 163-191.

Cheney, R.E. and P.L. Richardson, 1976: Observed decay of a cyclonic Gulf Stream ring. Deep-Sea Res, 23, 143-155.

Düing, W., 1975: Synoptic studies of transients in the Florida Current. J. Mar. Res., 33, 53-73.

Düing, W, C.N.K. Mooers and T.N. Lee, 1977: Low-frequency variability in the Florida Current and relations to atmospheric forcing from 1972 to 1974. J. Mar. Res., 35, 129-161.

Heinmiller, R.H., Jr., 1976: Mooring Operations Techniques of the Buoy Project at the Woods Hole Oceanographic Institution. Woods Hole Technical Report No. WHOI-76-69.

Kielmann, J. and W. Düing, 1974: Tidal and subinertial fluctuations in the Florida Current. J. Phys. Oceanogr., 4, 227-236.

Knauss, J.A., 1969: A note on the transport of the Gulf Stream. Deep-Sea Res.,Supplement to Vol. 16, 117-123.

Lee, T.N., 1975: Florida current spin-off eddies. Deep-Sea Res., 22, 753-765.

Lee, T.N., and D. Mayer, 1977: Low-frequency current variability and spin-off eddies on the shelf off southeast Florida. J. Mar. Res., 35, 193-220.

Lee, T.N., I. Brooks and W. Düing, 1977: The Florida Current - its structure and variability. U. of Miami Technical Report/RSMAS 77003, 275 pp.

Lee, T.N., L.P. Atkinson and R. Legeckis, 1981: Observations of a Gulf Stream frontal eddy on the Georgia continental shelf, April 1977. Deep-Sea Res., 28A, 347-348.

Lee, T.N., and L.P. Atkinson, 1982: Low-frequency current variability from Gulf Stream frontal eddies and atmospheric forcing along the southeast U.S. outer continental shelf. (Submitted to special issue of J. Geophys. Res. of the South Atlantic Bight.)

Legeckis, R., 1975: Applications of synchronous meteorological satellite data to the study of time dependent sea surface temperature changes along the boundary of the Gulf Stream. Geophys. Res. Lett., 2, 435-438.

Legeckis, R., 1979: Sattellite observations of the influence of bottom topography on the seaward deflection of the Gulf Stream off Charleston, S.C. J. Phys. Oceanogr., 9, 483-497.

Moller, D.A., 1976: A Computer Program for the design and static analysis of single-point subsurface mooring systems: NOYFB. WHOI Tech. Rpt. WHOI-76-59, unpublished manuscript, 106 pp.

Mooers, C.N.K., and D.A. Brooks, 1977: Fluctuations in the Florida Current, summer 1970. Deep-Sea Res., 24, 399-425.

Niiler, P.P. and L.A. Mysak, 1971: Barotropic waves along an eastern continental shelf. Geophys. Fluid Dynamics, 2, 273-278.

Niiler, P.P. and W.S. Richardson, 1973: Seasonal variability of the Florida Current. J. Mar. Res., 31, 144-167.

Niiler, P.P., 1976: Observations of low-frequency currents on the Western Florida Continental Shelf. Mémories Société Royale des Sciences de Liège, Series 6, 10, 331-358.

Oort, A.H., 1964: Computations of eddy heat and density transports across the Gulf Stream. Tellus, 16, 55-63.

Orlanski, I., 1969: The influence of bottom topography on the stability of jets in abaroclinic fluid. J. Atmos. Sci., 26, 1216-1232.

Orlanski, I. and M.D. Cox, 1973: Baroclinic instability in ocean currents. Geophys. Fluid Dynamics, 4, 197-221.

Parr, A.E., 1937: Report of hydrographic observations at a series of anchor stations across the Straits of Florida. Bull. of the Bingham Oceanographic Laboratory, Yale University, 6, 1-63.

Perkins, H., and M. Wimbush, 1976: A cyclonic mini-eddy near the Blake Escarpment. Geophys. Res. Lett., 3, 625-628.

Pietrafesa, L.J., L.P. Atkinson and J.O. Blanton, 1978: Evidence for deflection of the Gulf Stream by the Charleston Rise. Gulf Stream, IV, 3-7.

Pillsbury, 1890: The Gulf Stream. Report of the U.S. Coast and Geodetic Survey for 1890. Appendix No. 10. 461-620.

Richardson, W.S., W.J. Schmitz, Jr. and P.P. Niiler, 1969: The velocity structure of the Florida Current from the Straits of Florida to Cape Fear. Deep-Sea Res., 16, 225-231.

Schmitz, W.J., Jr. and W.S. Richardson, 1968: On the transport of the Florida Current. Deep-Sea Res., 15, 679-693.

Schmitz, W.J., Jr. and P.P. Niiler, 1969: A note on the kinetic energy exchange between fluctuations and mean flow in the surface layer of the Florida Current. Tellus XXI, 6, 814-819.

Schott, F., and W. Düing, 1976: Continental shelf waves in the Florida Straits. J. Phys. Oceanogr., 6, 451-460.

Smith, J.A., B.D. Zetler and S. Broida, 1969: Tidal modulation of the Florida Current surface flow. Marine Tech. Soc. J., 3, 41-46.

Stommel, H.M., 1965: The Gulf Stream. University of California Press, 248 pp.

Stumpf, H.G. and P.K. Rao, 1975: Evolution of Gulf Stream eddies as seen in satellite infrared imagery. J. Phys. Oceanogr., 5, 388-393.

Sturges, W., 1974. Sea level slope along continental boundaries. J. Geophys. Res., 79, 825-830.

Thompson, R., 1971: Topographic Rossby waves at a site north of the Gulf Stream. Deep-Sea Res., 18, 1-19.

Von Arx, W.S., D.F. Bumpus and W.S. Richardson, 1955: On the fine-structure of the Gulf Stream front. Deep-Sea Res., 3, 46-65.

Vukovich, F.M. and B.W. Grissman, 1978: Further studies of a cold eddy on the eastern side of the Gulf Stream using satellite data and ship data. J. Phys. Oceanogr., 8, 838-843.

Webster, F.A., 1961a: A description of Gulf Stream menaders off Onslow Bay. Deep-Sea Res., 8, 130-143.

Webster, F.A., 1961b: The effect of meanders on the kinetic energy balance of the Gulf Stream. Tellus, 13, 391-401.

Wust, G., 1924: Florida and Antillenstrom, eine hydrodynamische untersuchung, Veroff. Inst. Meeresk, Univ. Berlin, NFA 12, 48pp.

Zetler, B.D. and D.V. Hansen, 1970: Tides in the Gulf of Mexico - a review and proposed program. Bull. Marine Sci., 20, 57-69.

APPENDIX A

DATA PRODUCTS
FIRST DEPLOYMENT

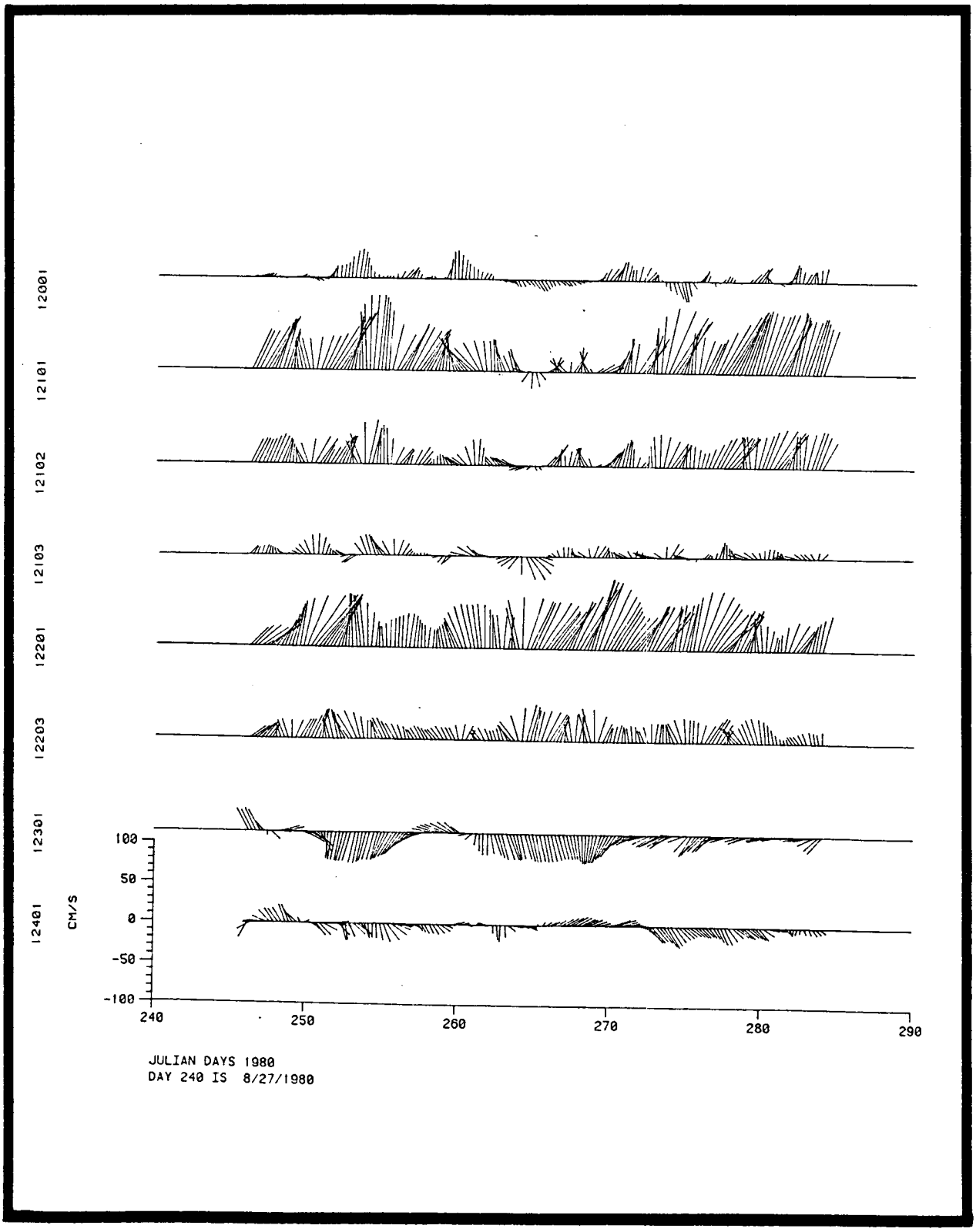

Figure A-1. Stick plot of currents during indicated period of first deployment (40-HLP data).

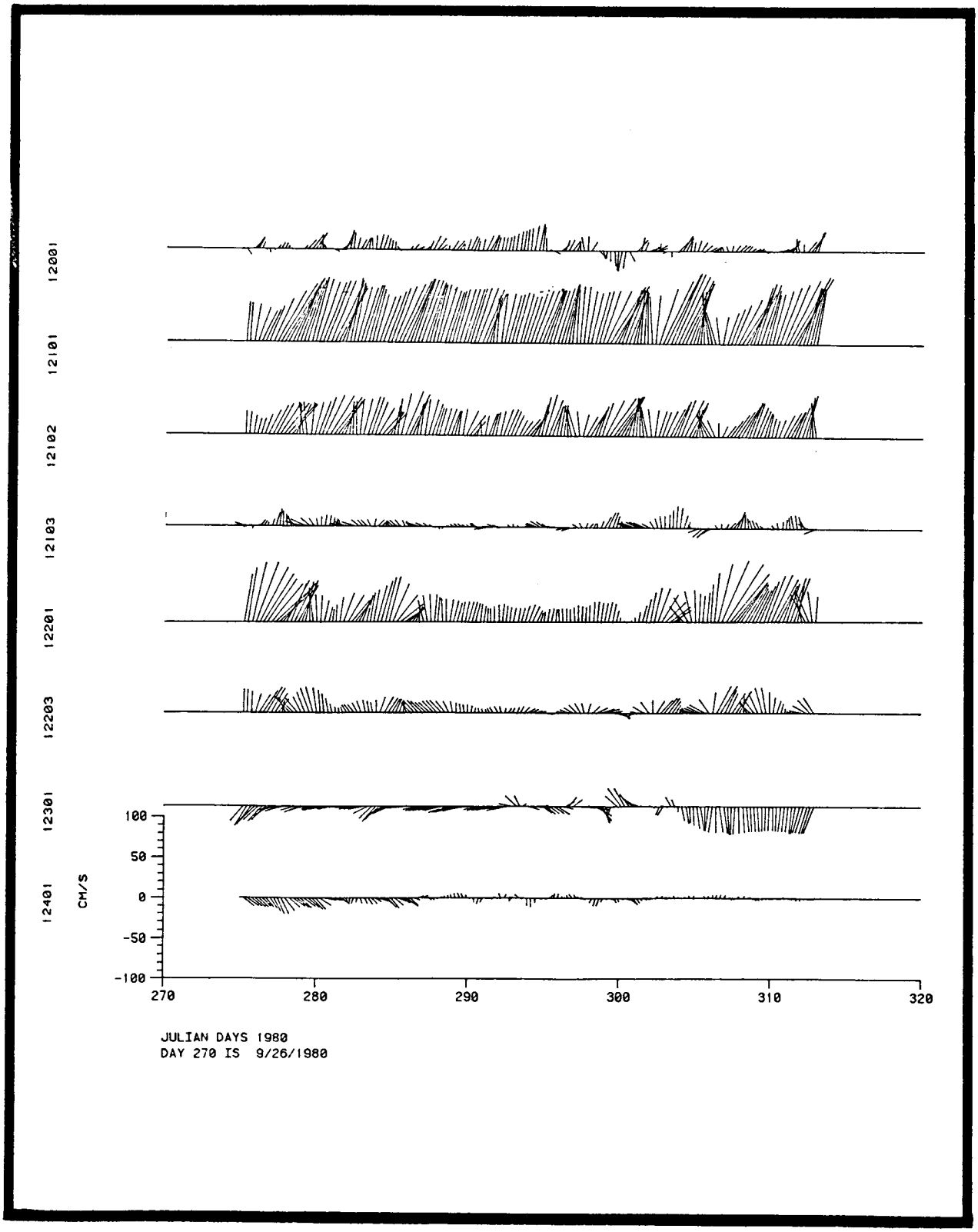

Figure A-2. Stick plot of currents during indicated period of first deployment (40-HLP data).

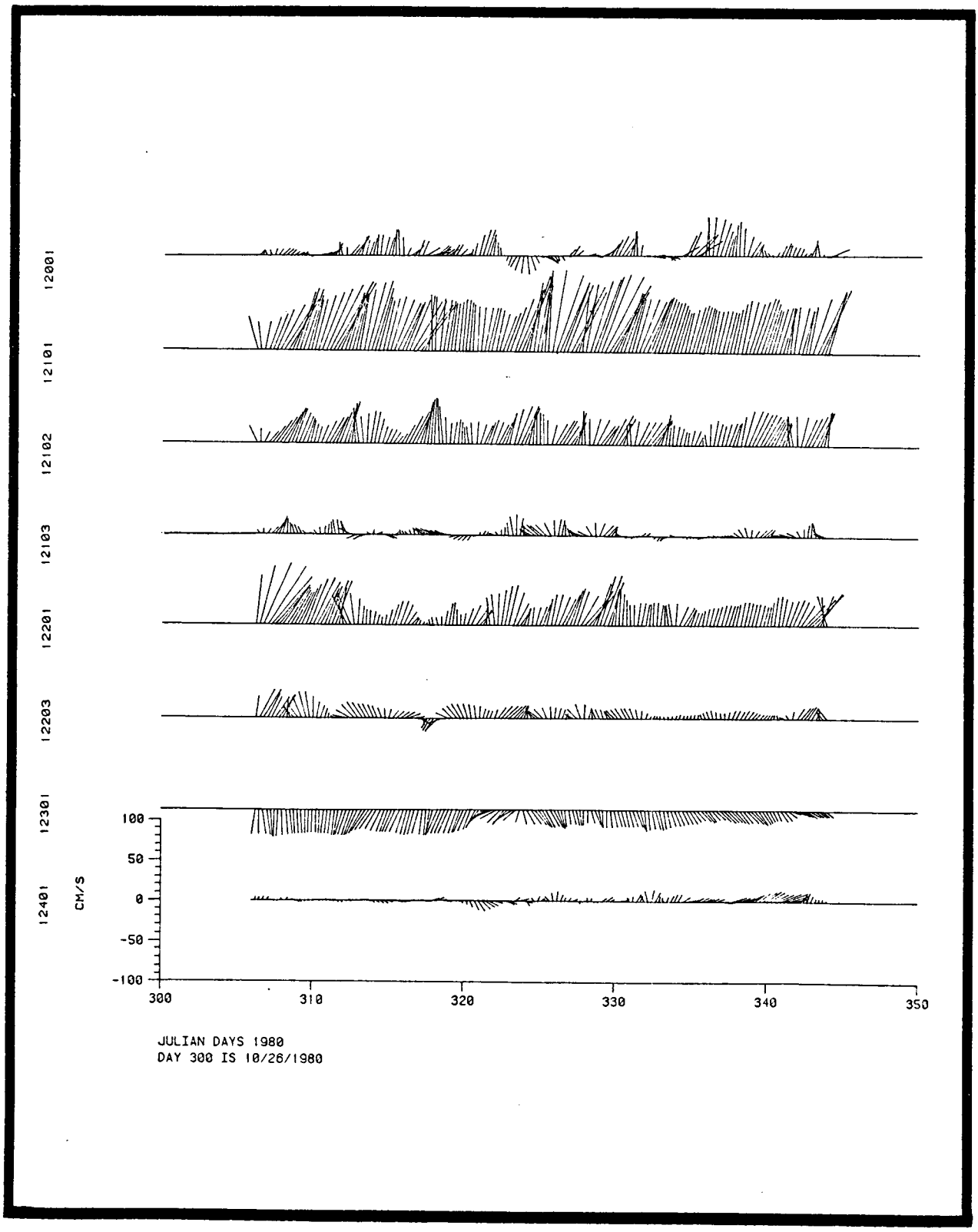

Figure A-3. Stick plot of currents during indicated period of first deployment (40-HLP data).

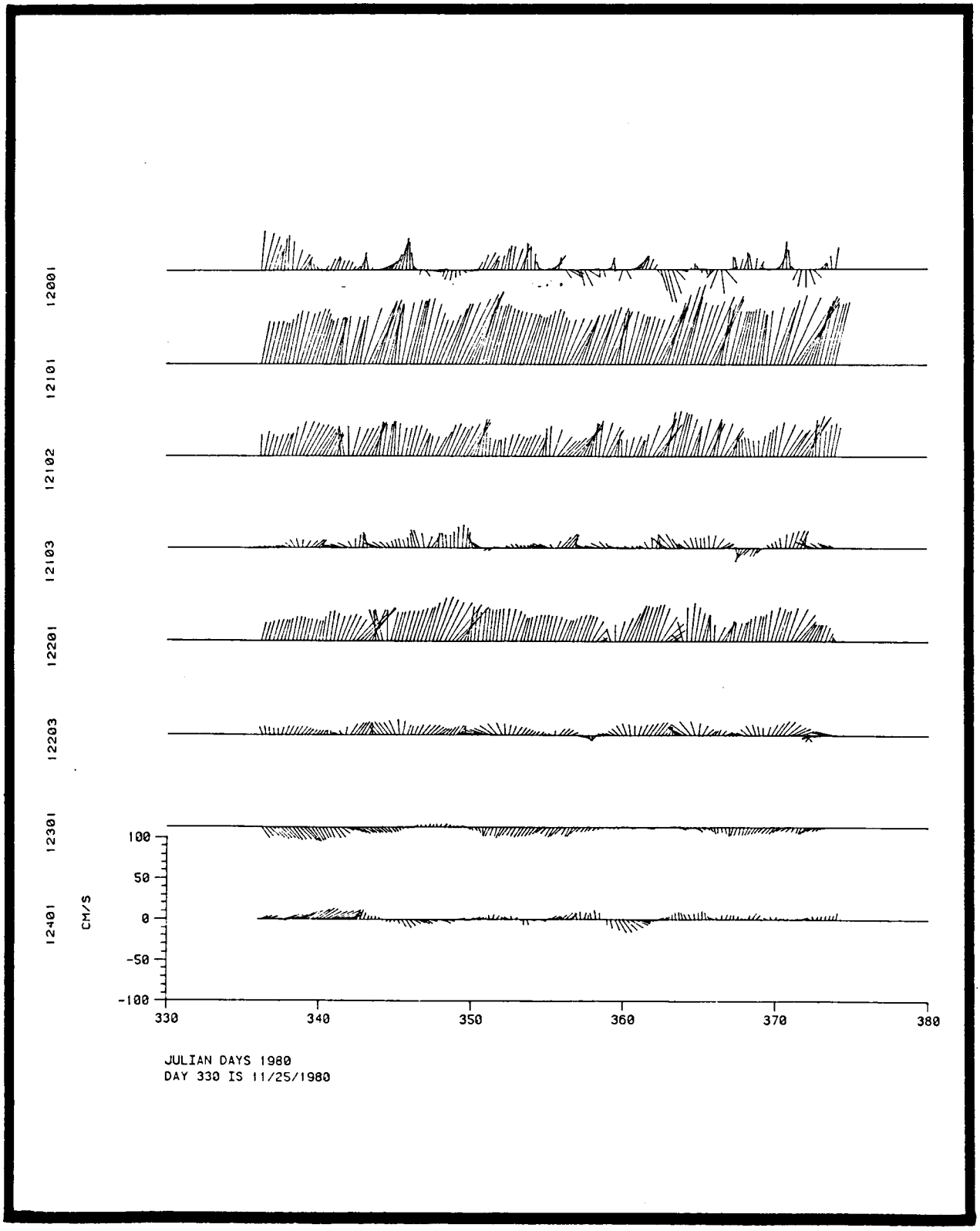

Figure A-4. Stick plot of currents during indicated period of first deployment (40-HLP data).

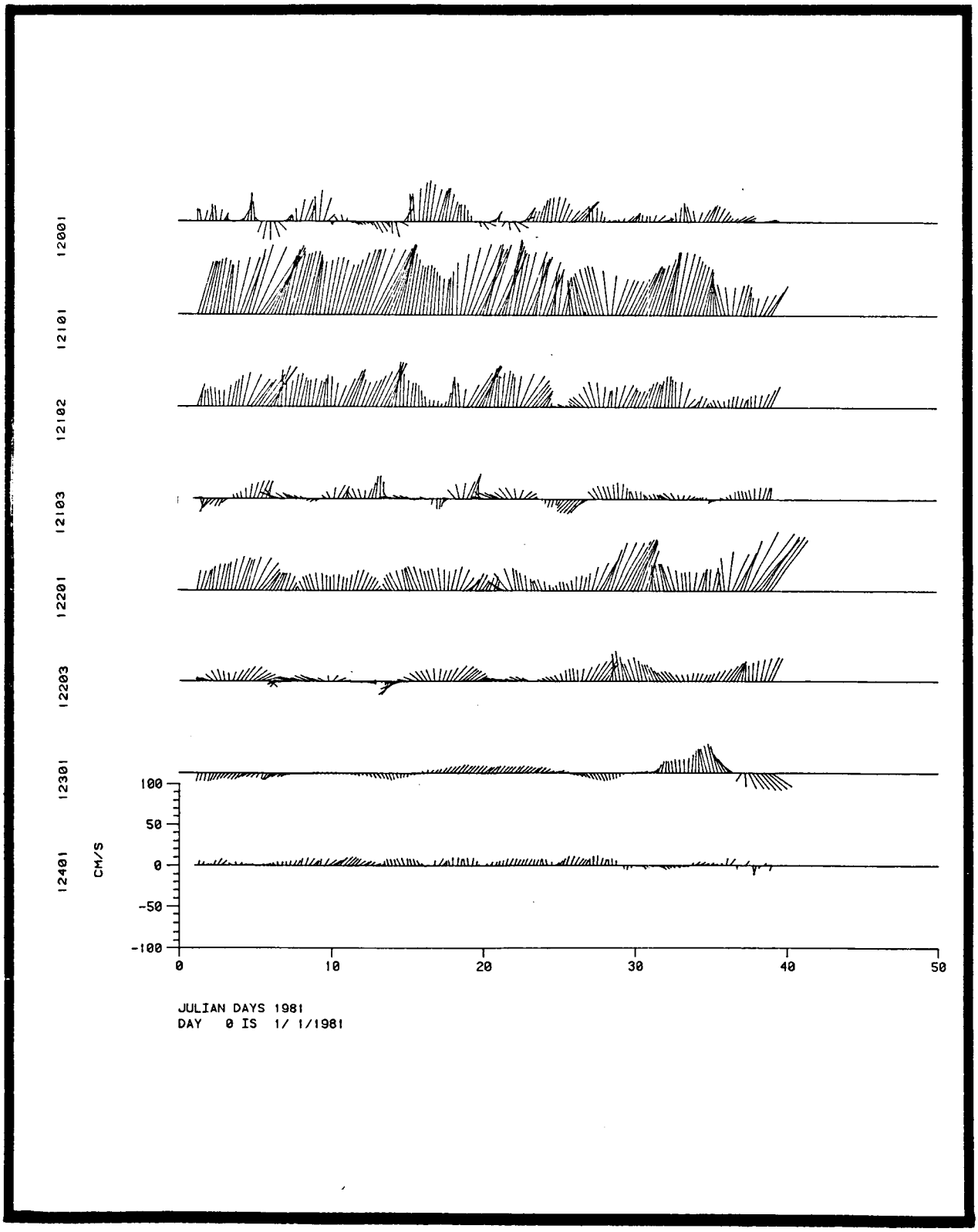

Figure A-5. Stick plot of currents during indicated period of first deployment (40-HLP data).

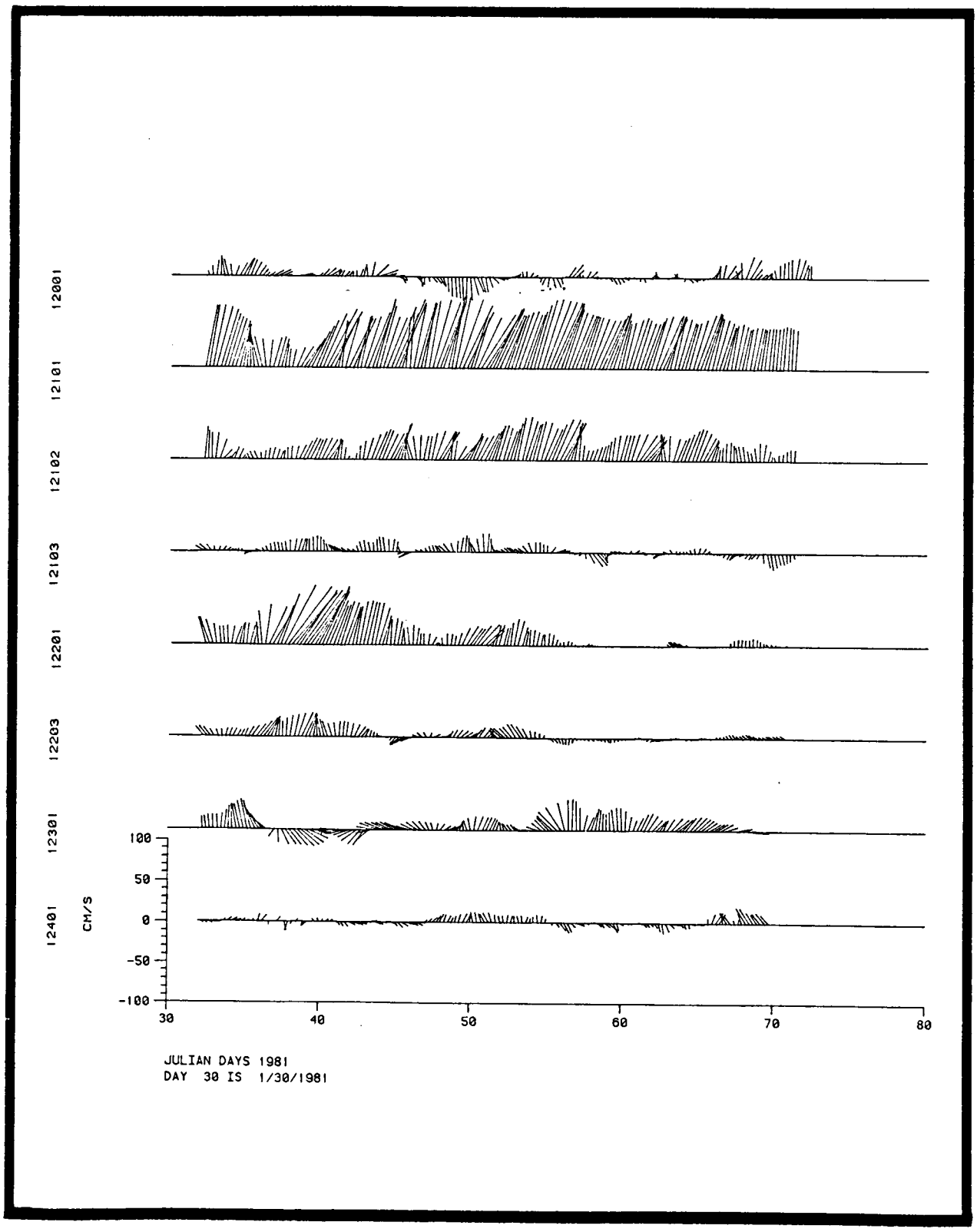

Figure 4-6. Stick plot of currents during indicated period of first deployment (40-HLP data).

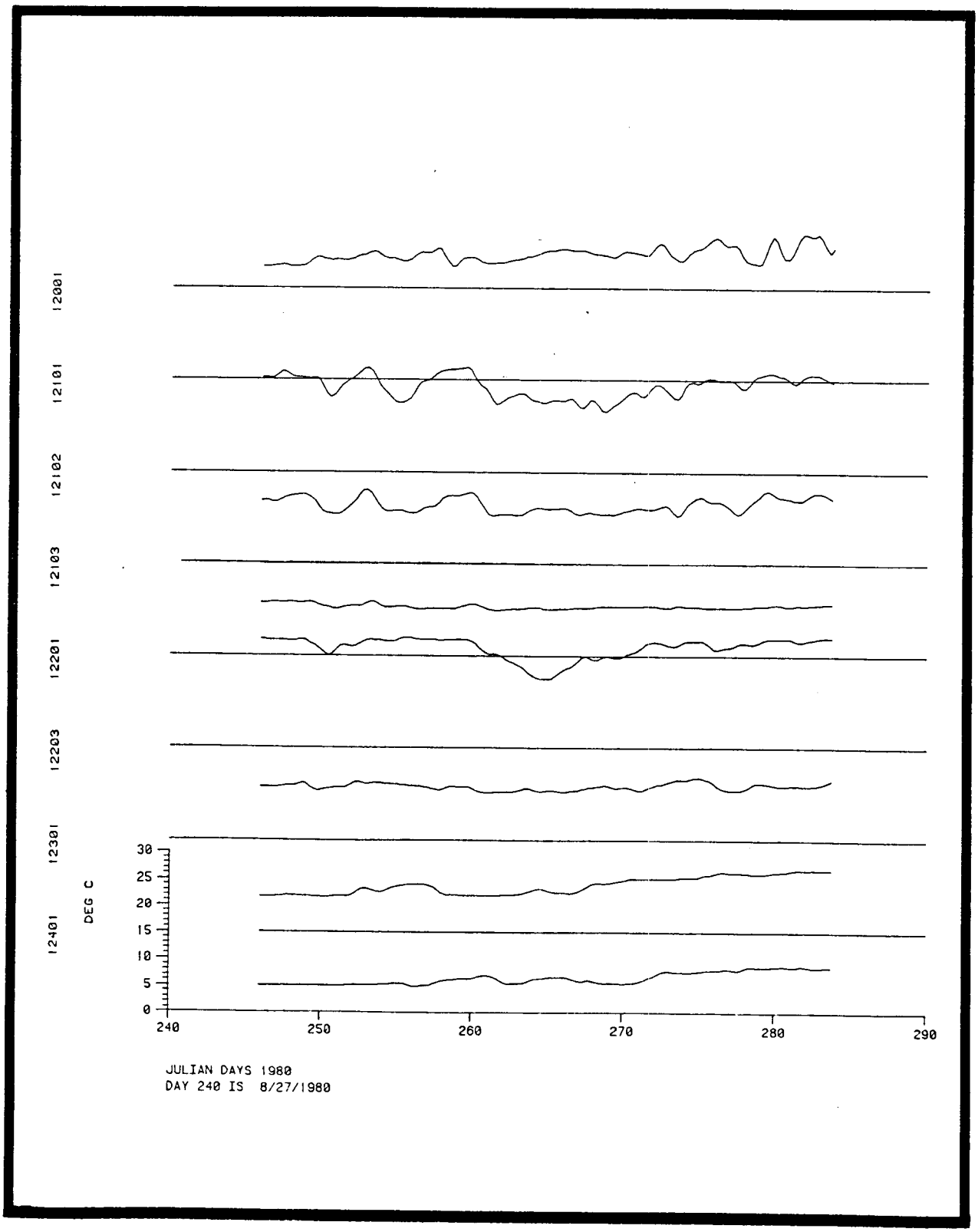

Figure A-7. Temperature time series plot during indicated period of first deployment (40-HLP data).

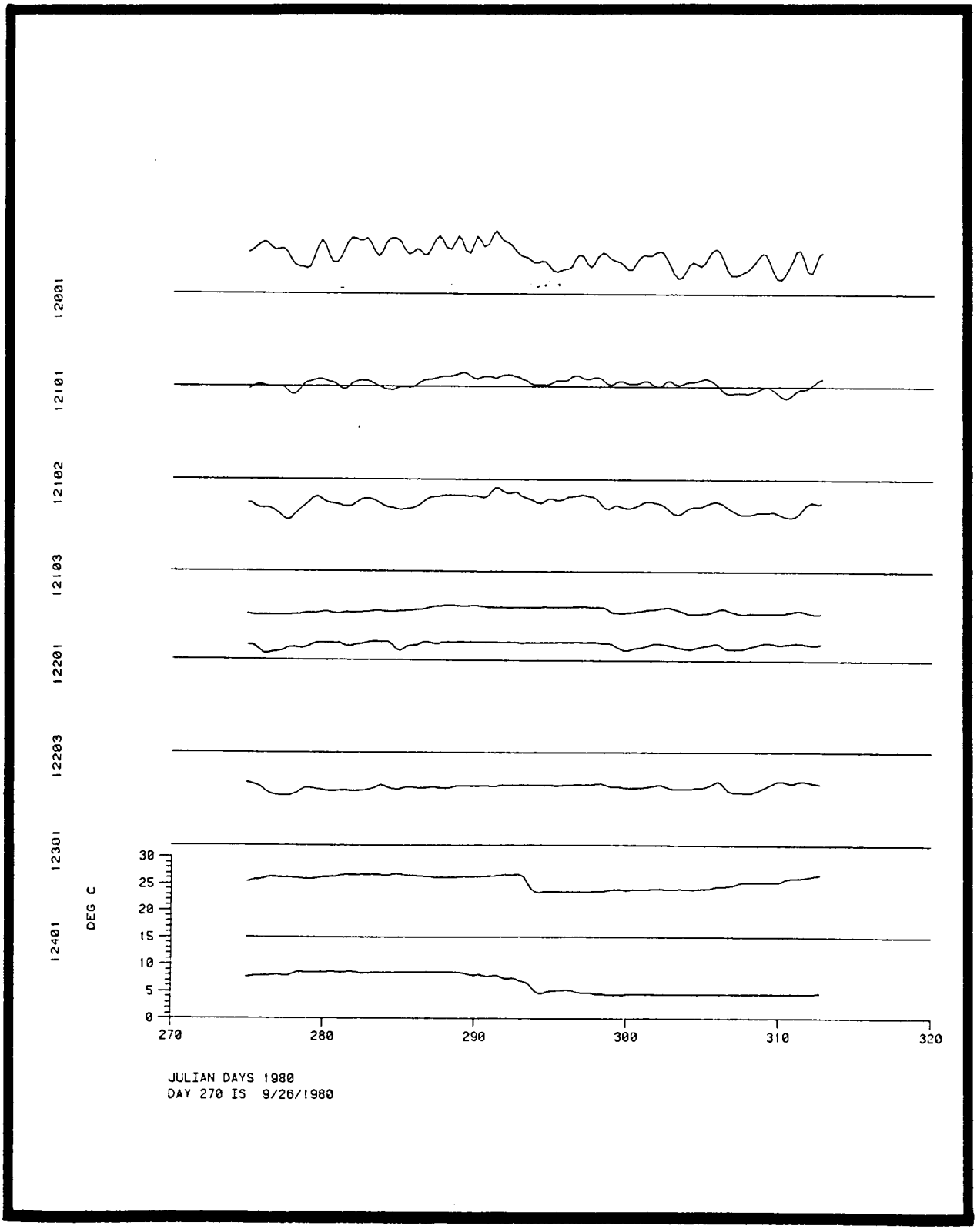

Figure A-8. Temperature time series plot during indicated period of first deployment (40-HLP data).

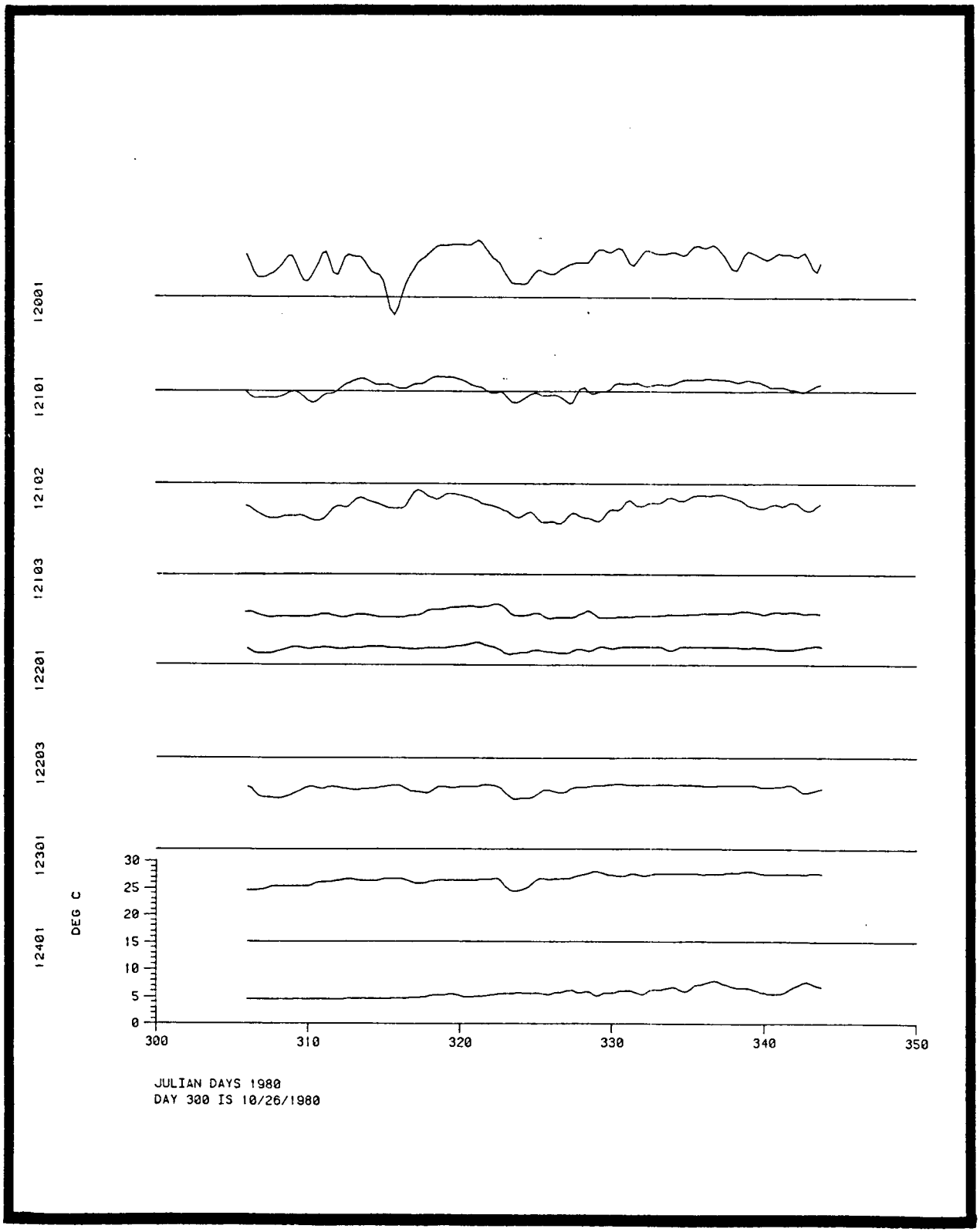

Figure A-9. Temperature time series plot during indicated period of first deployment (40-HLP data).

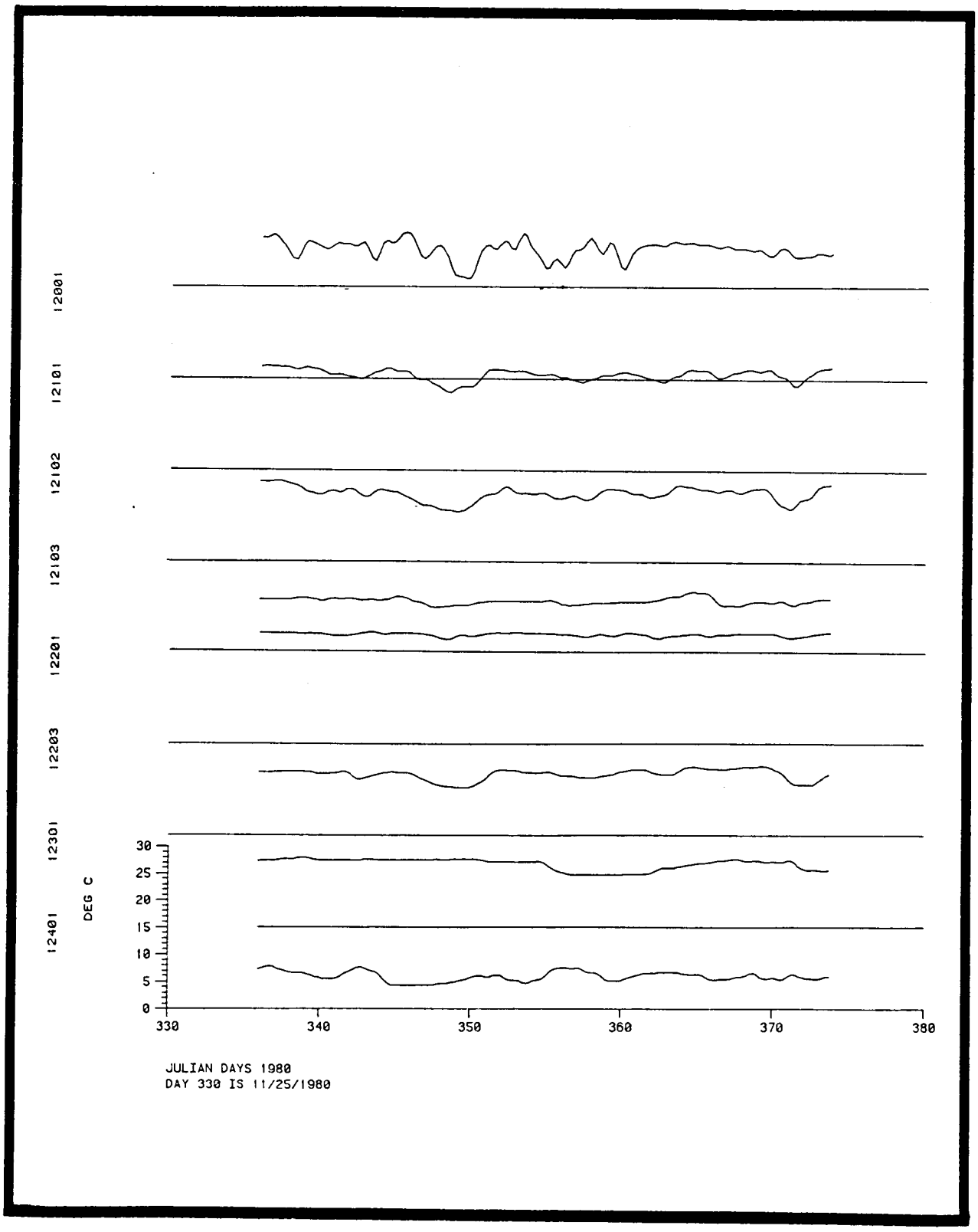

Figure A-10. Temperature time series plot during indicated period of first deployment (40-HLP data).

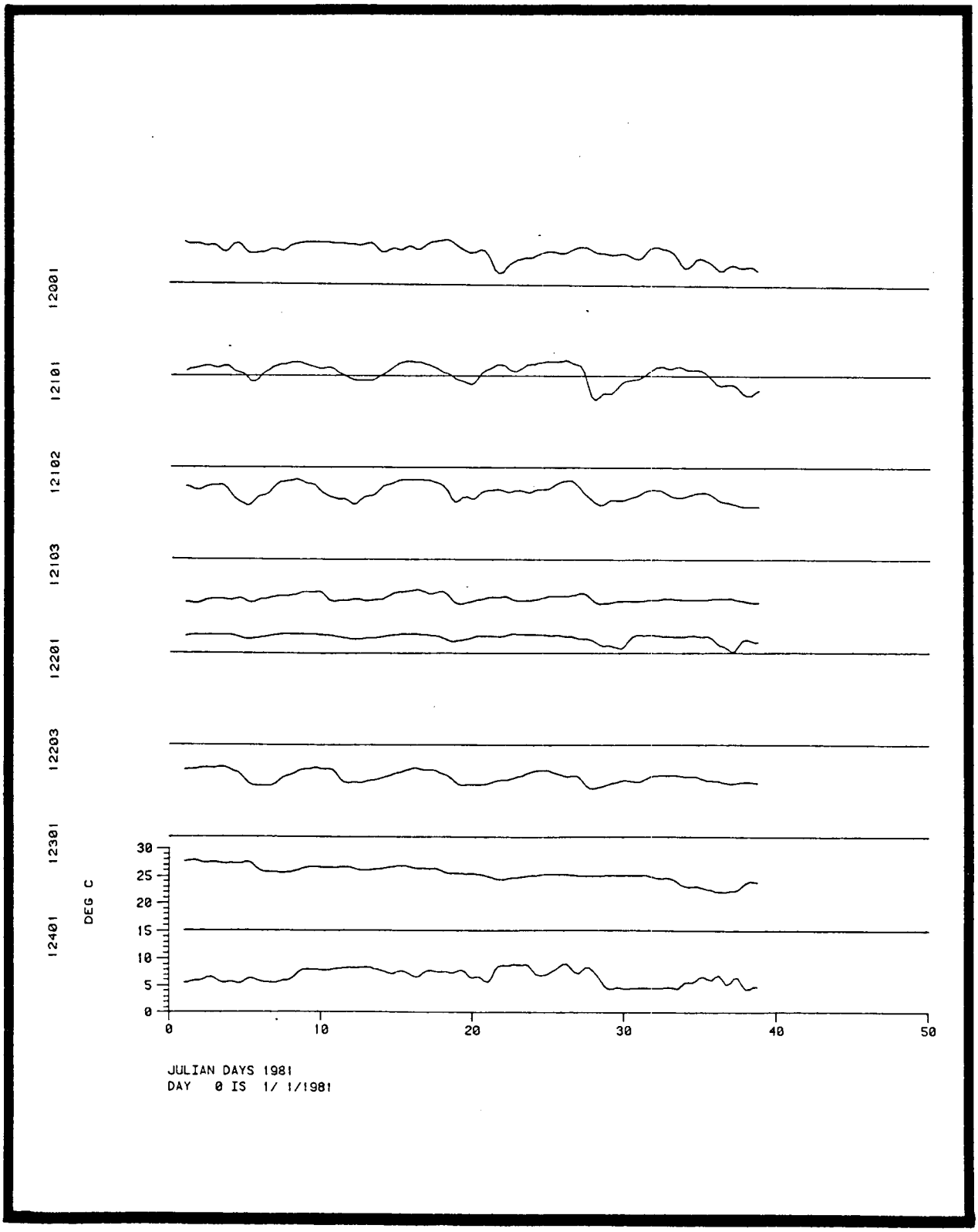

Figure A-11. Temperature time series plot during indicated period of first deployment (40-HLP data).

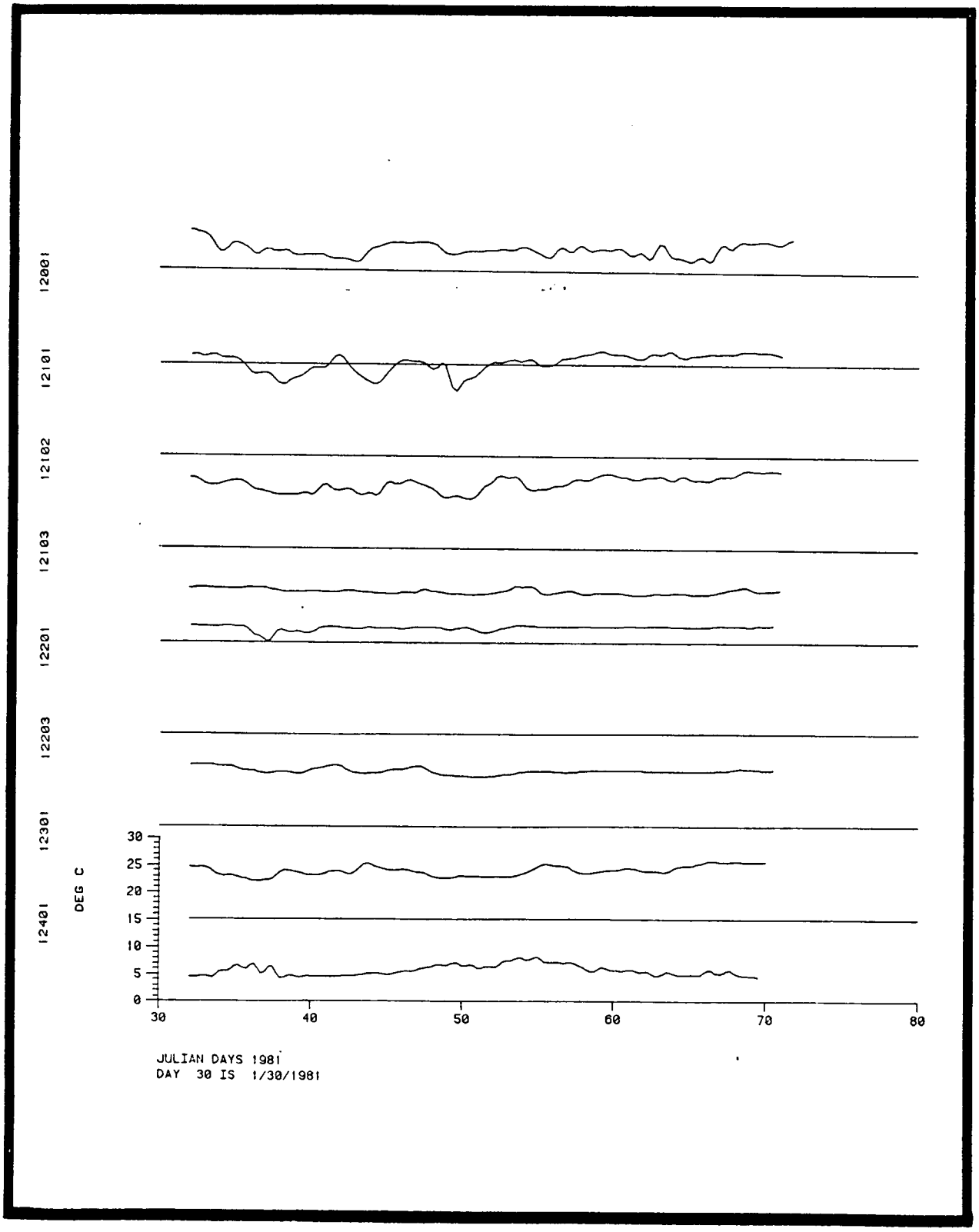

Figure A-12. Temperature time series plot during indicated period of first deployment (40-HLP data).

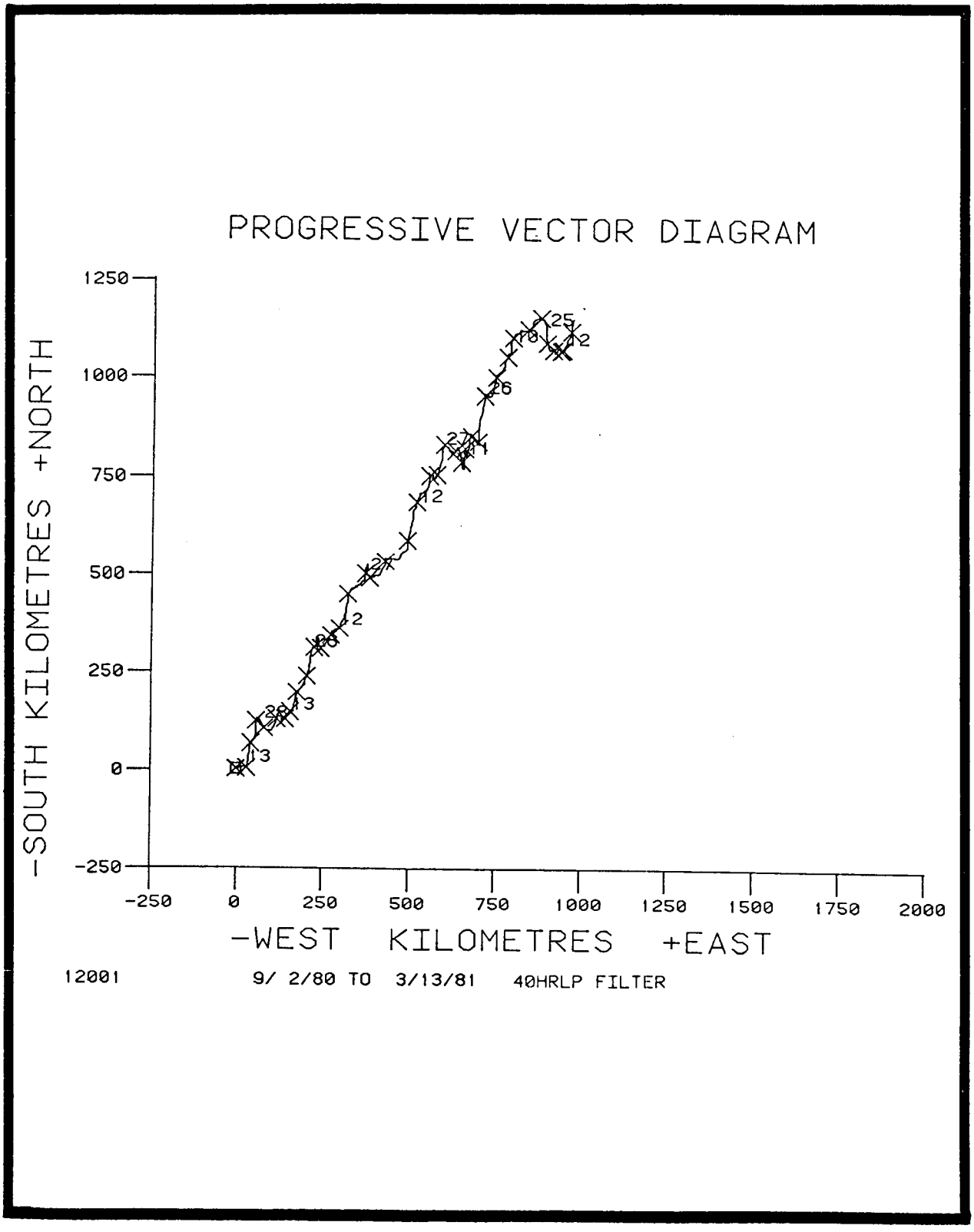

Figure A-13. Progressive vector diagram of currents measured by current meter 12001 during first deployment.

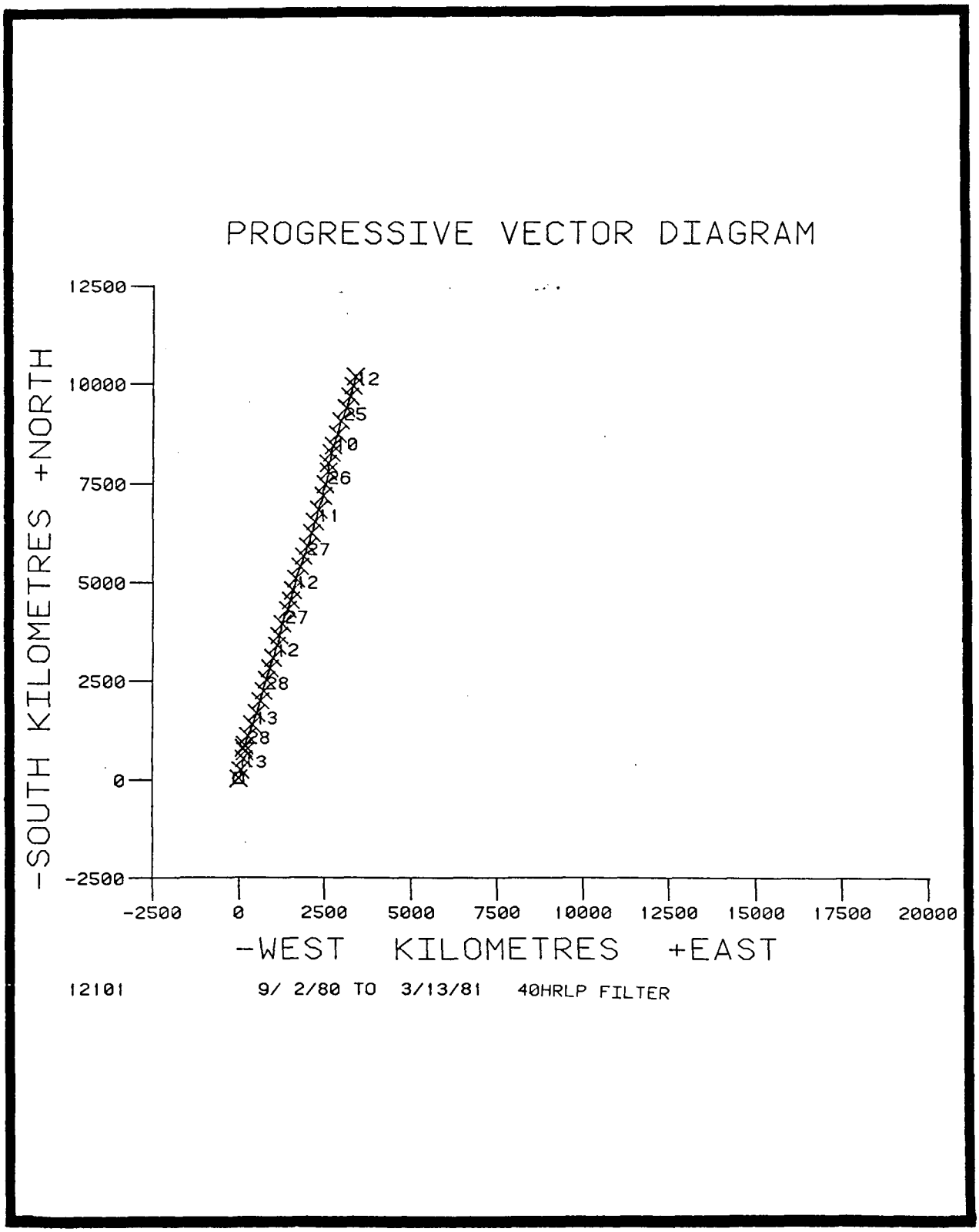

Figure A-14. Progressive vector diagram of currents measured by current meter 12101 during first deployment.

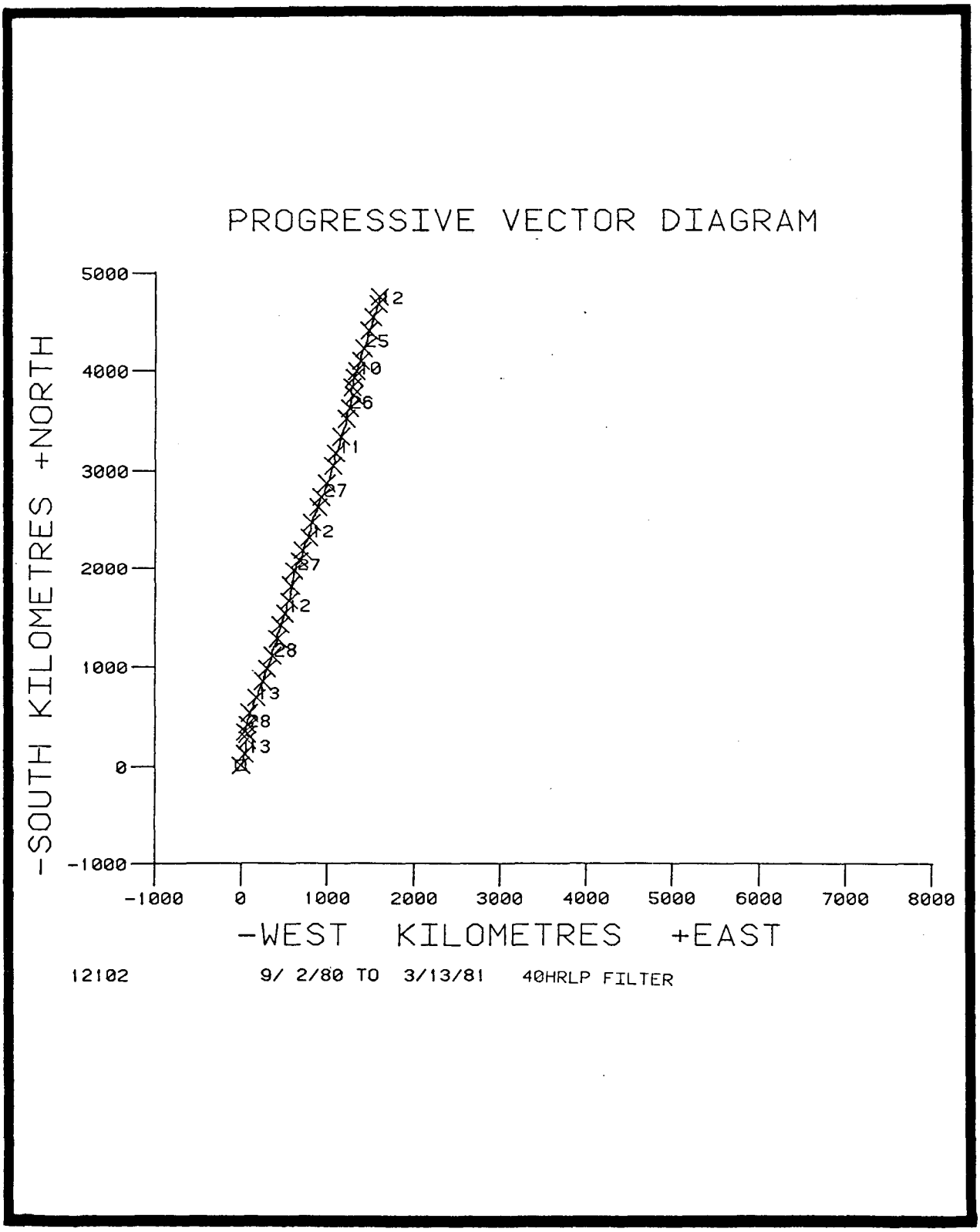

Figure A-15. Progressive vector diagram of currents measured by current meter 12102 during first deployment.

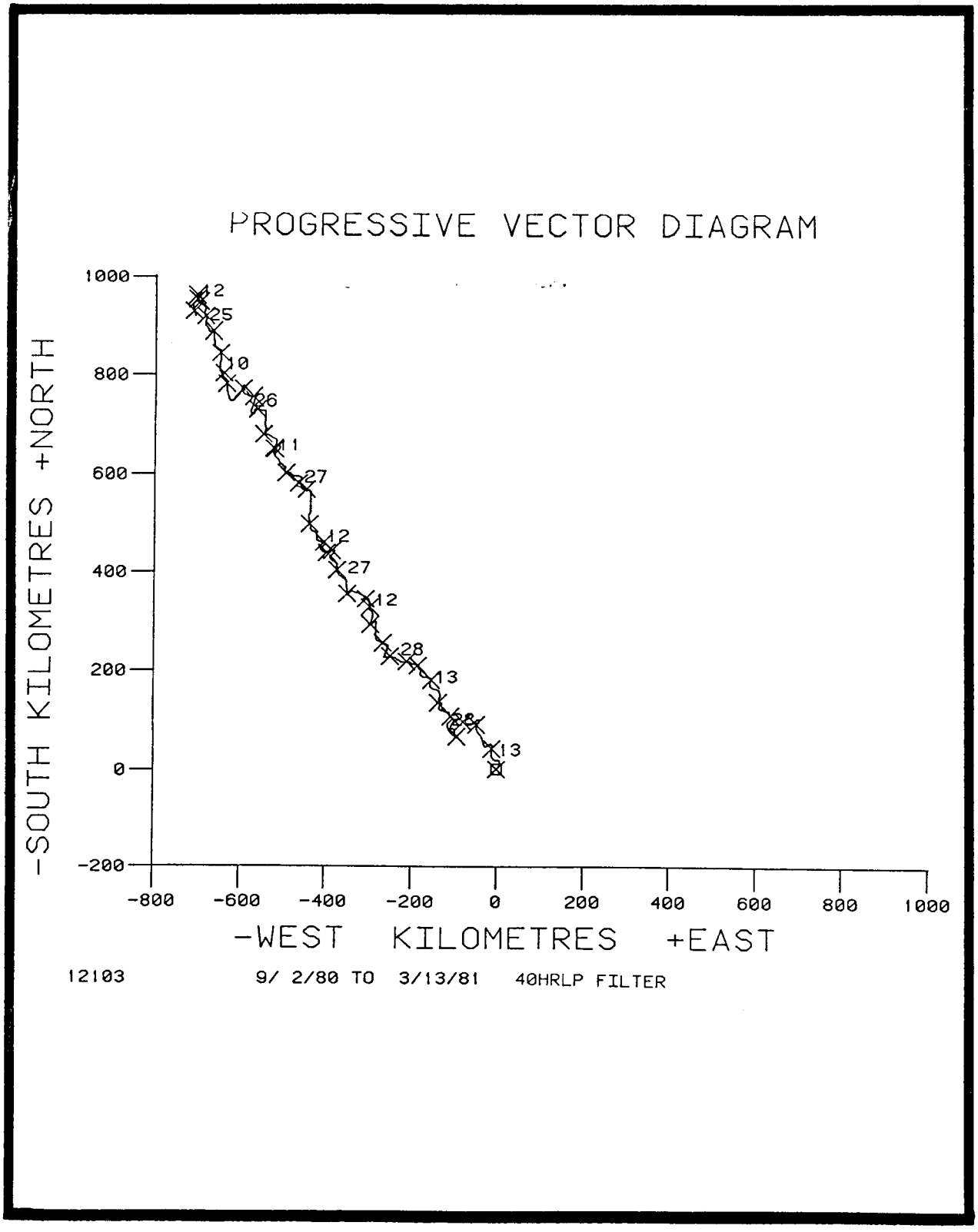

Figure A-16. Progressive vector diagram of currents measured by current meter 12103 during first deployment.

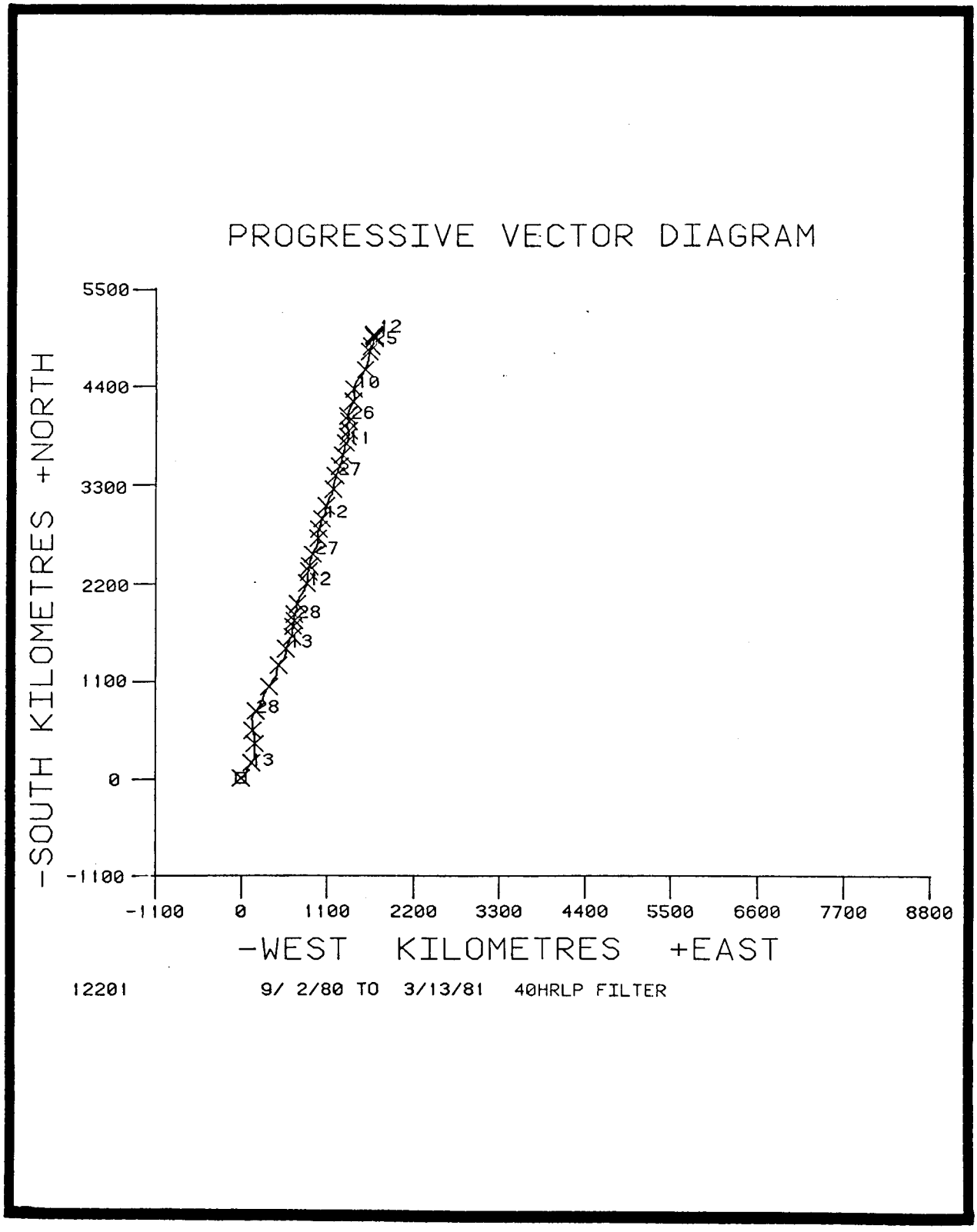

Figure A-17. Progressive vector diagram of currents measured by current meter 12201 during first deployment.

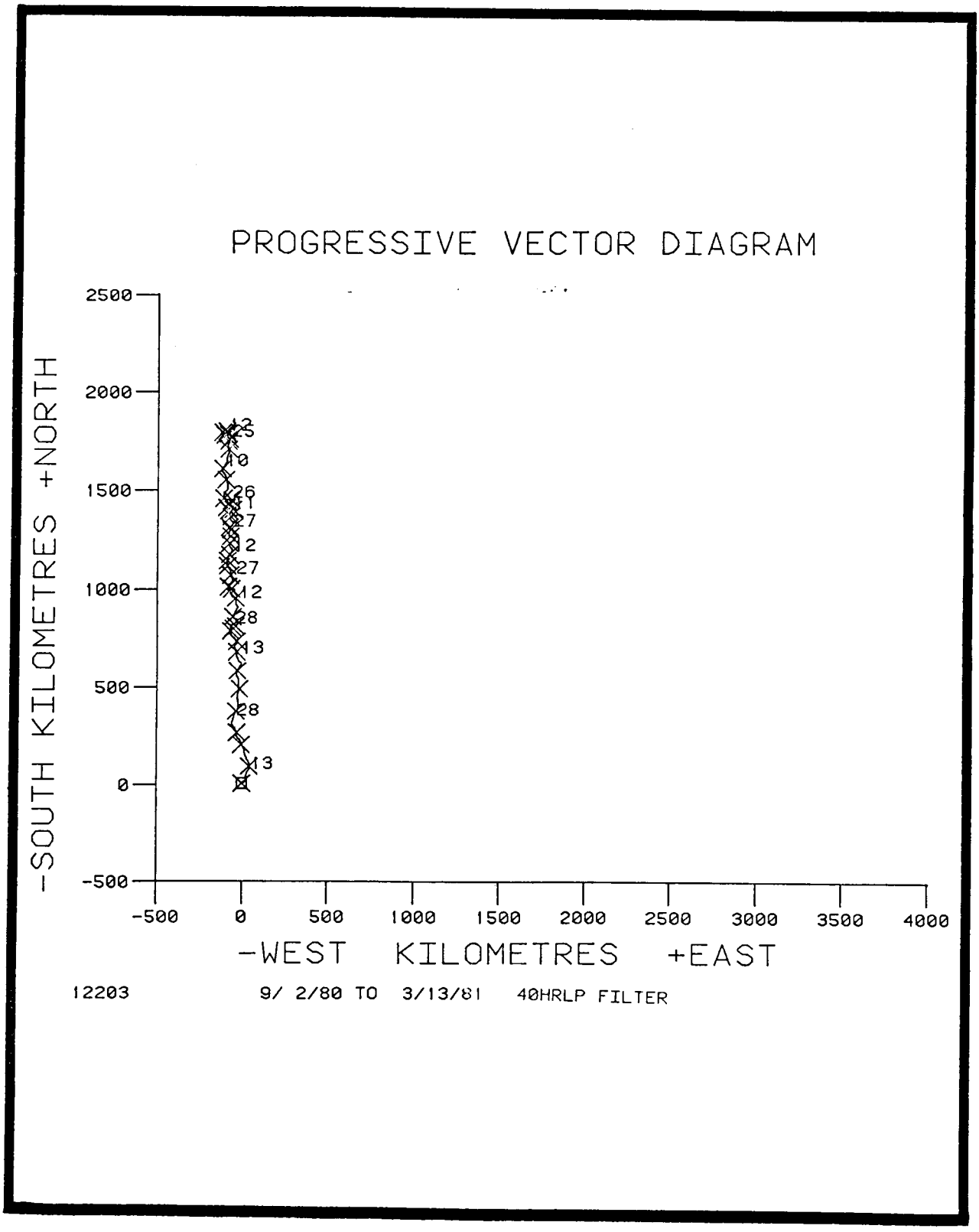

Firgure A-18. Progressive vector diagram of currents measured by current meter 12203 during first deployment.

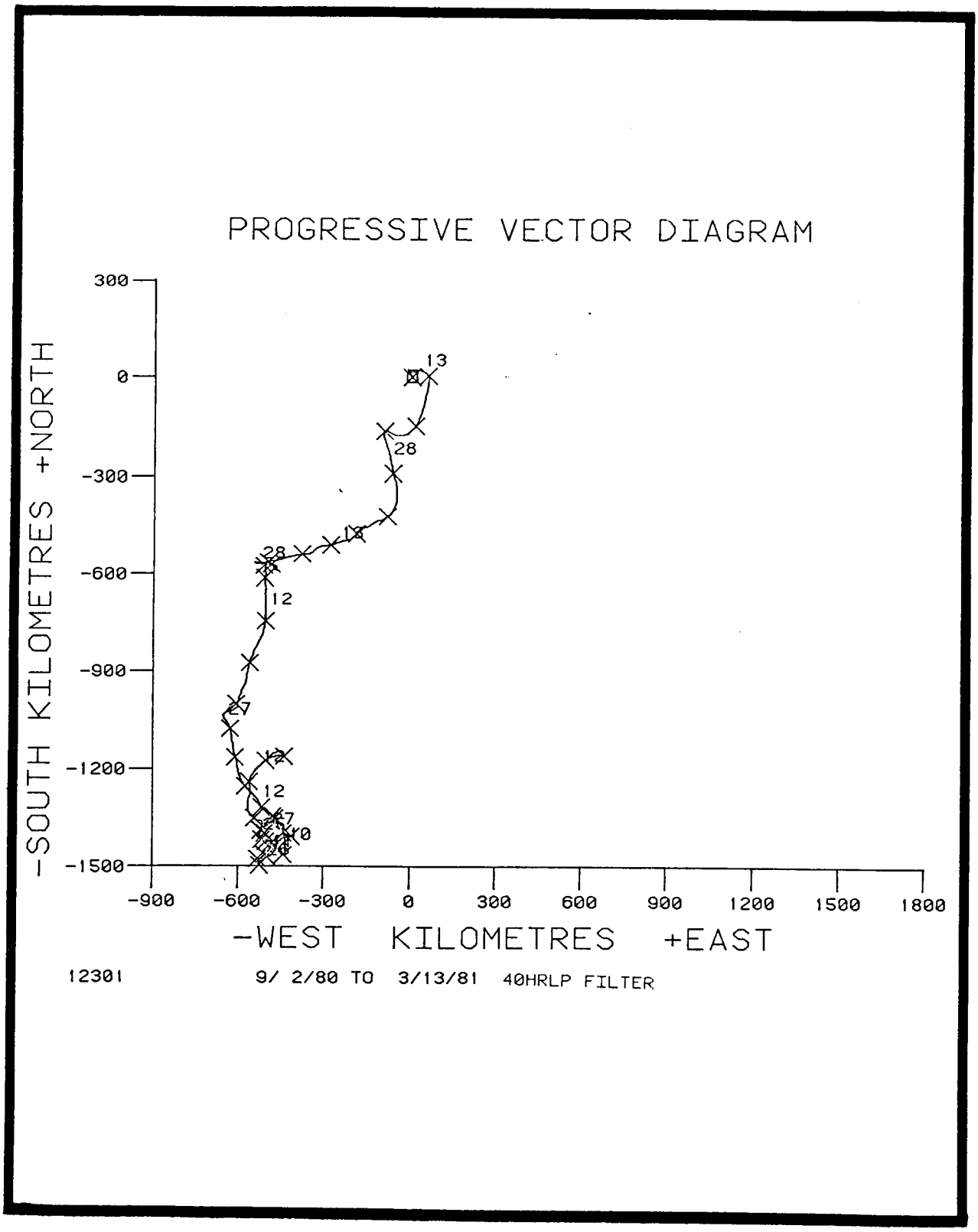

Figure A-19. Progressive vector diagram of currents measured by current meter 12301 during first deployment.

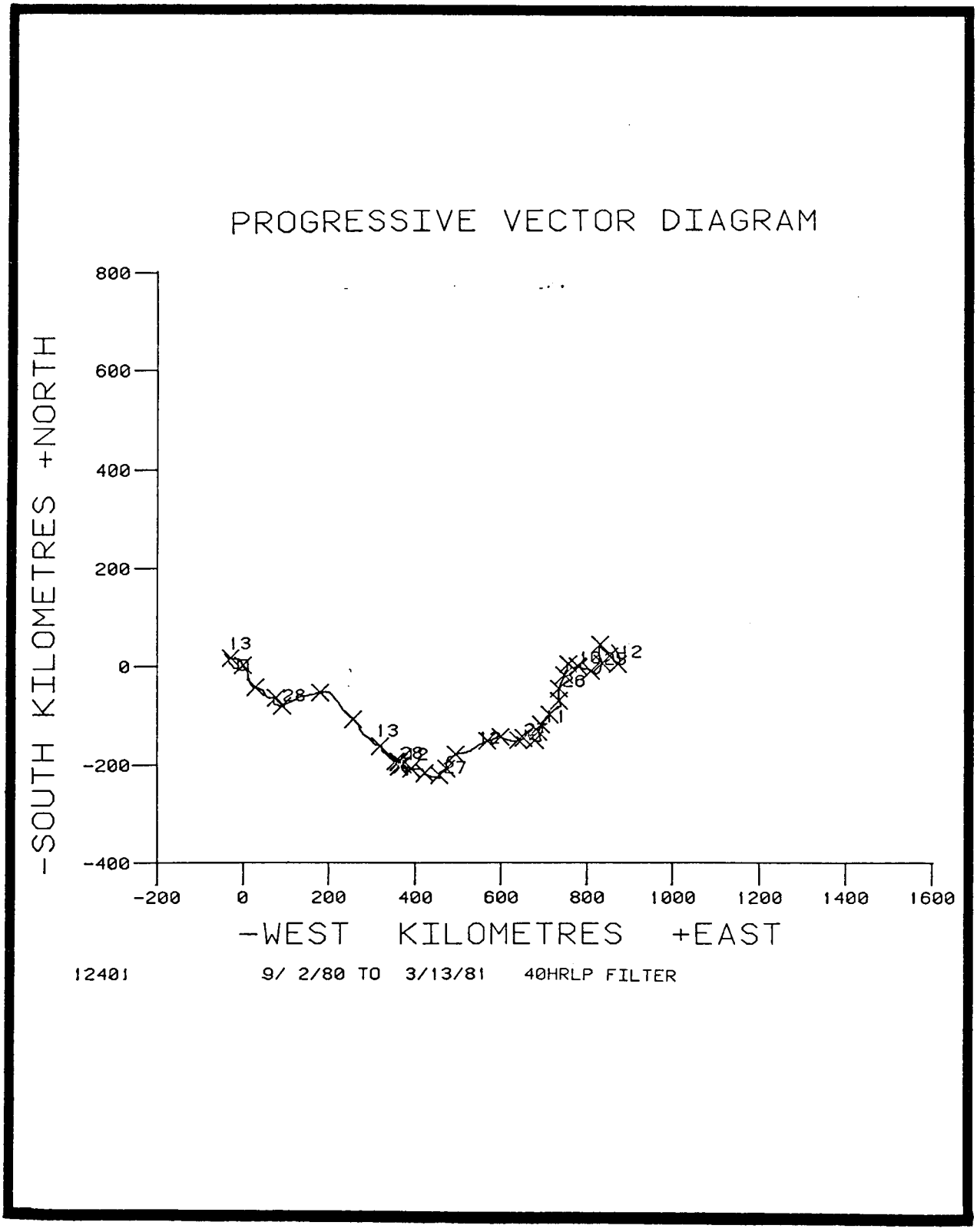

Figure A-20. Progressive vector diagram of currents measured by current meter 12401 during first deployment.

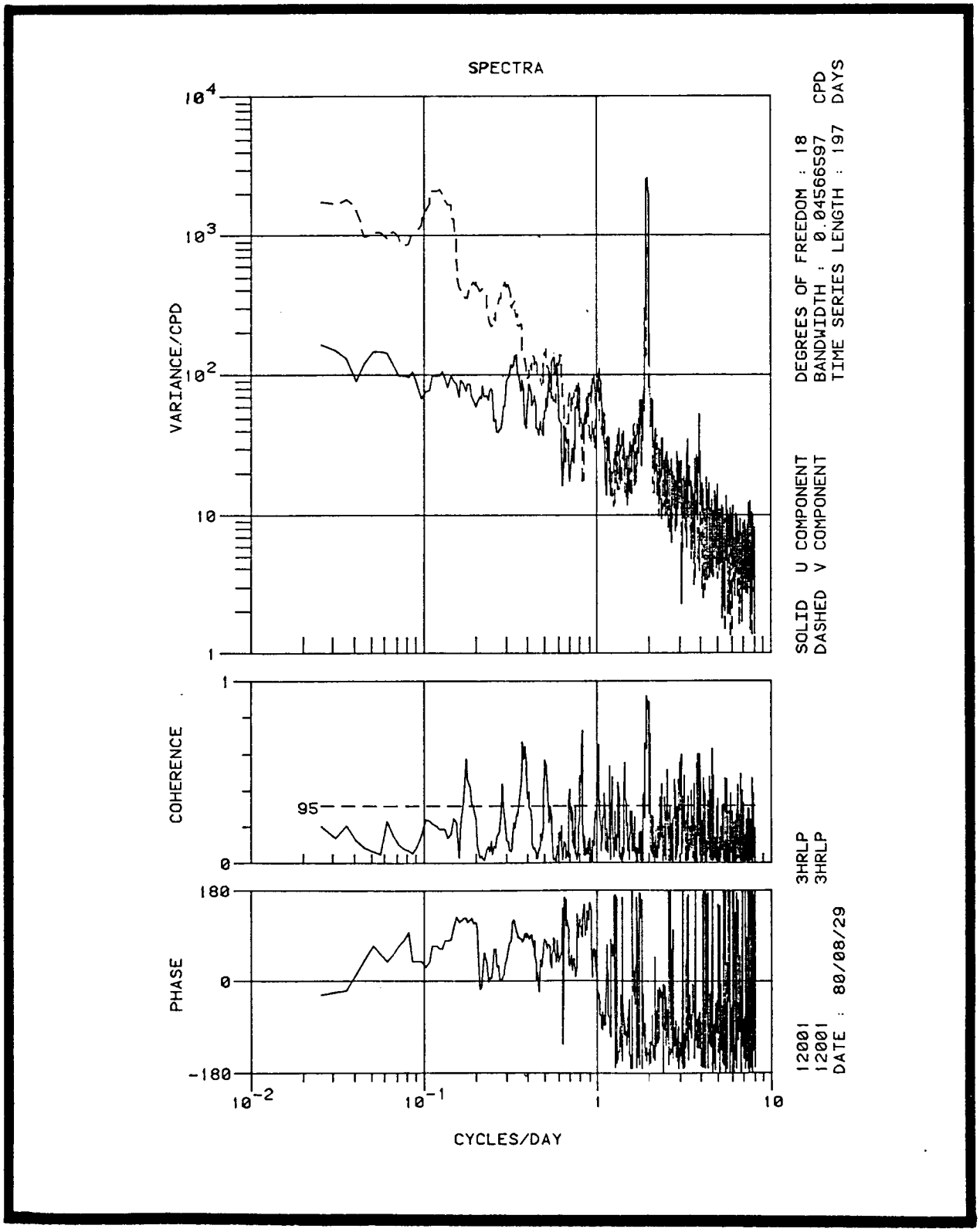

Figure A-21. Spectra of u component vs v component from current meter 12001 during first deployment.

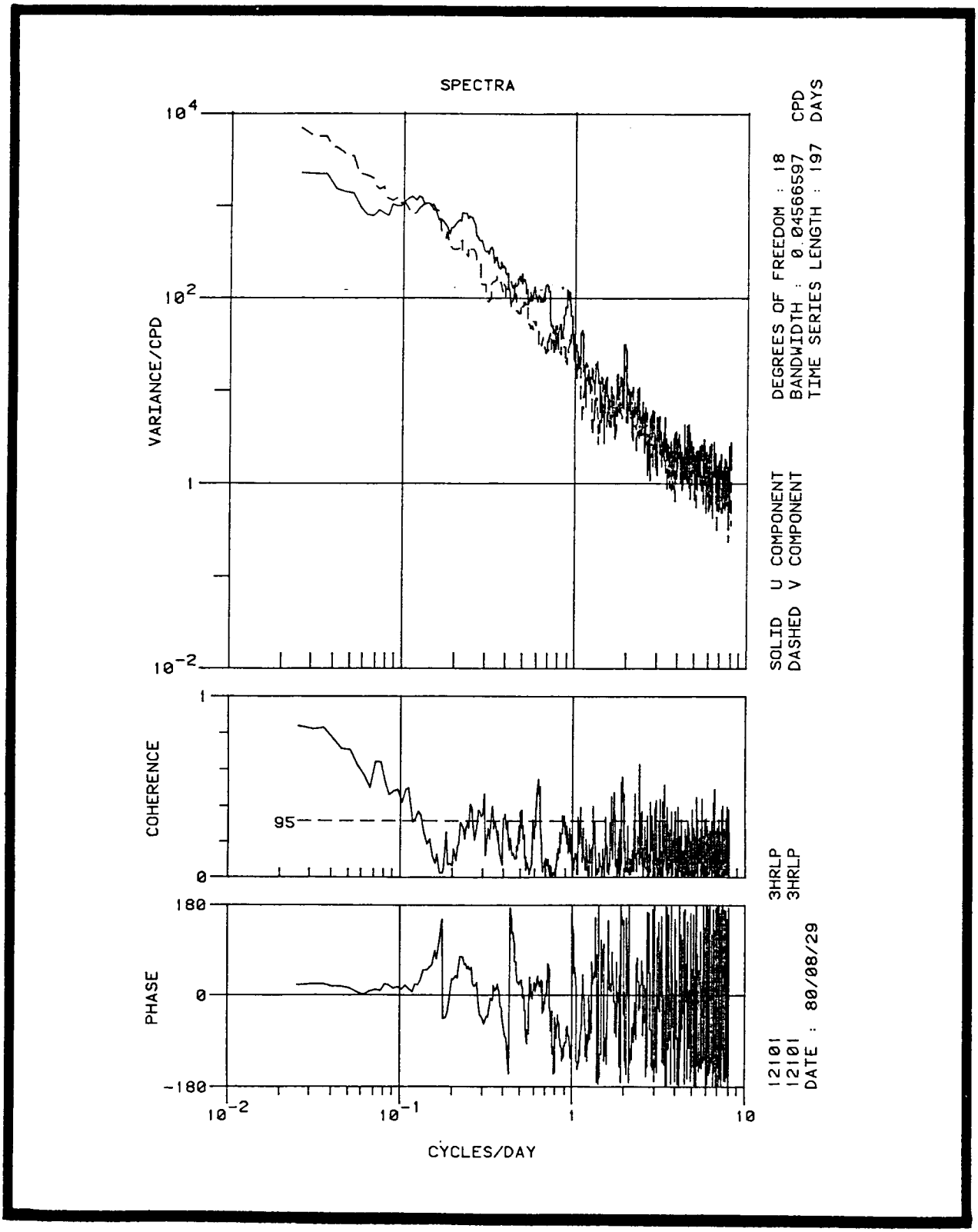

Figure A-22. Spectra of u component vs v component from current meter 12101 during first deployment.

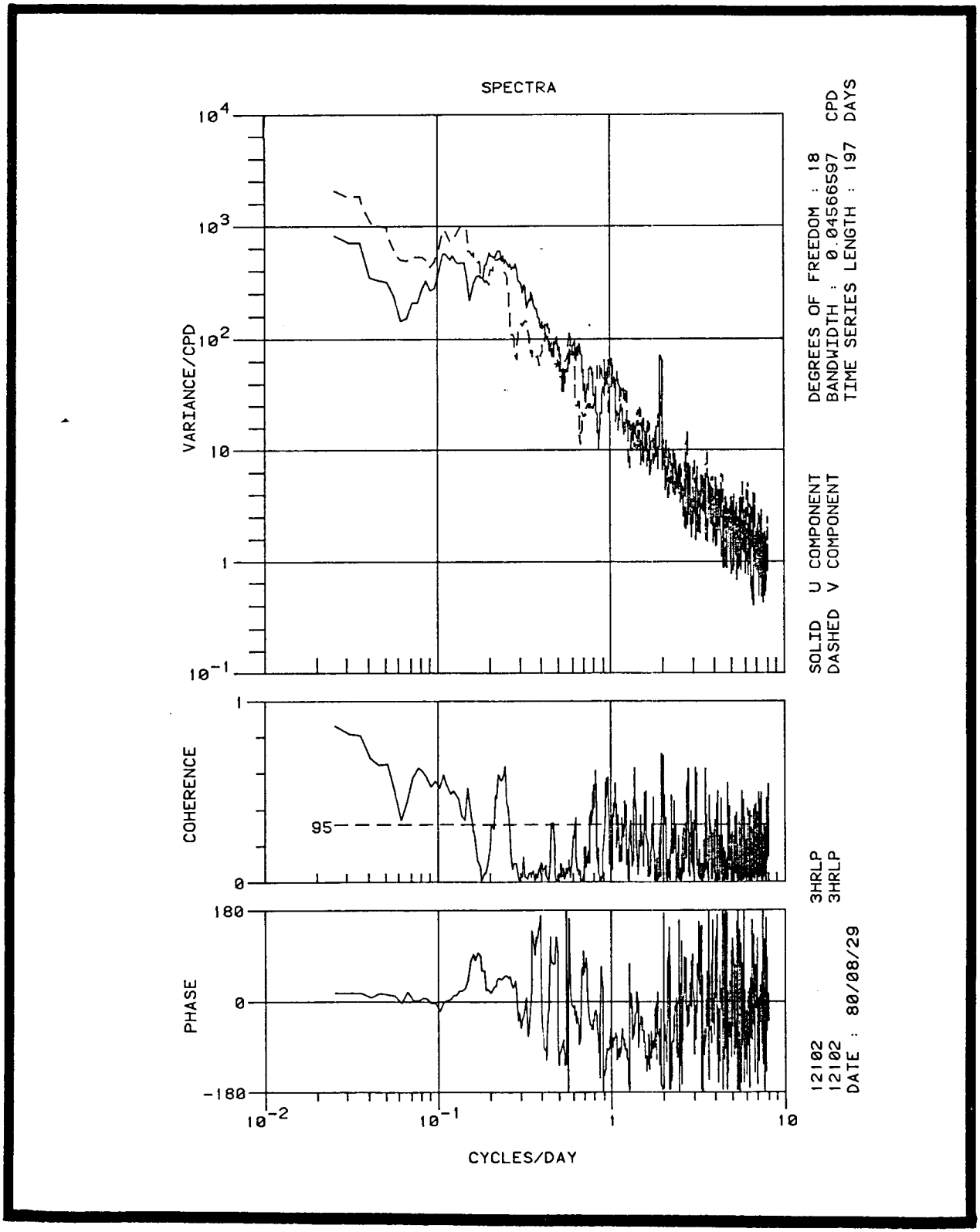

Figure A-23. Spectra of u component vs v component from current meter 12102 during first deployment.

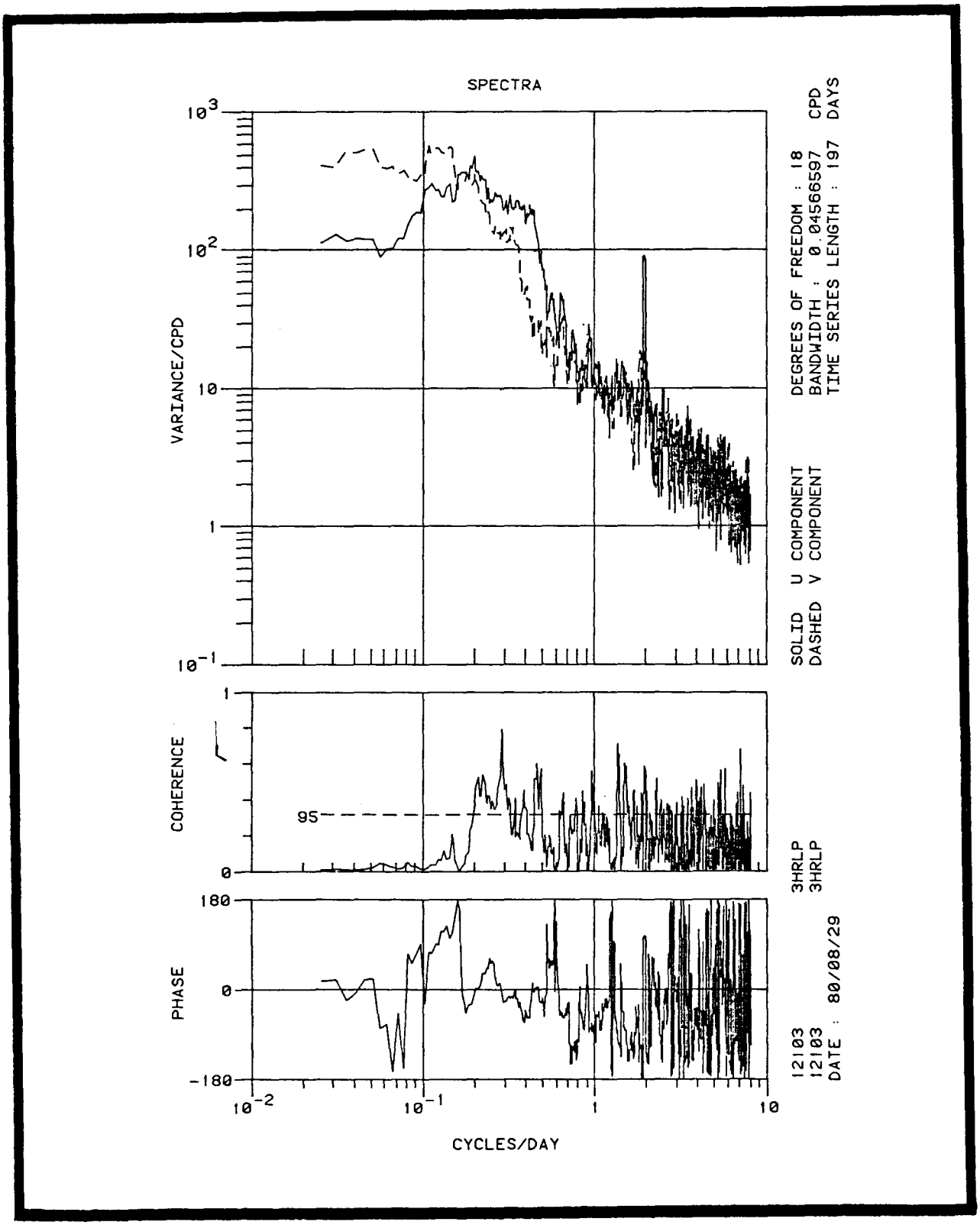

Figure A-24. Spectra of u component vs v component from current meter 12103 during first deployment.

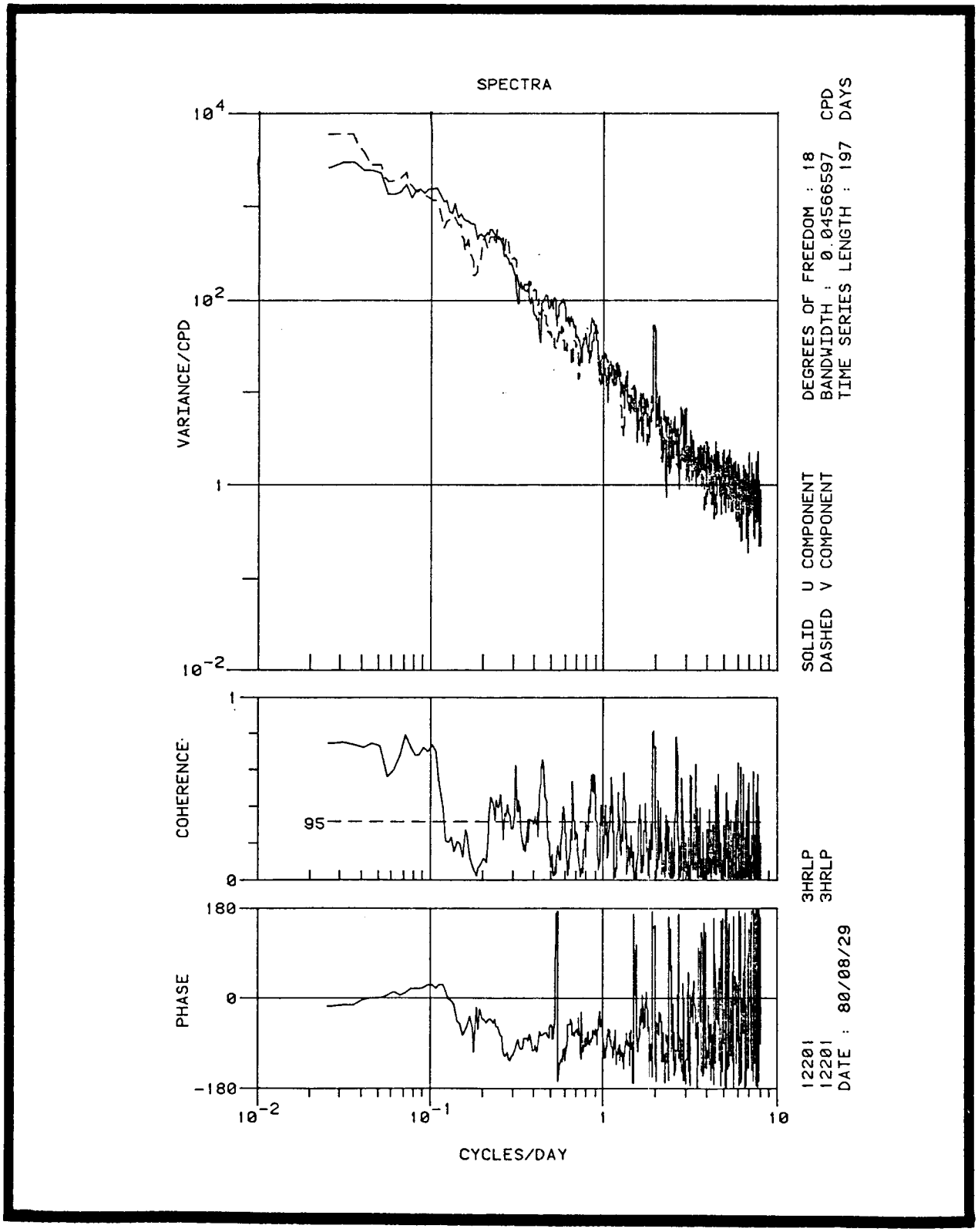

Figure A-25. Spectra of u component vs v component from current meter 12201 during first deployment.

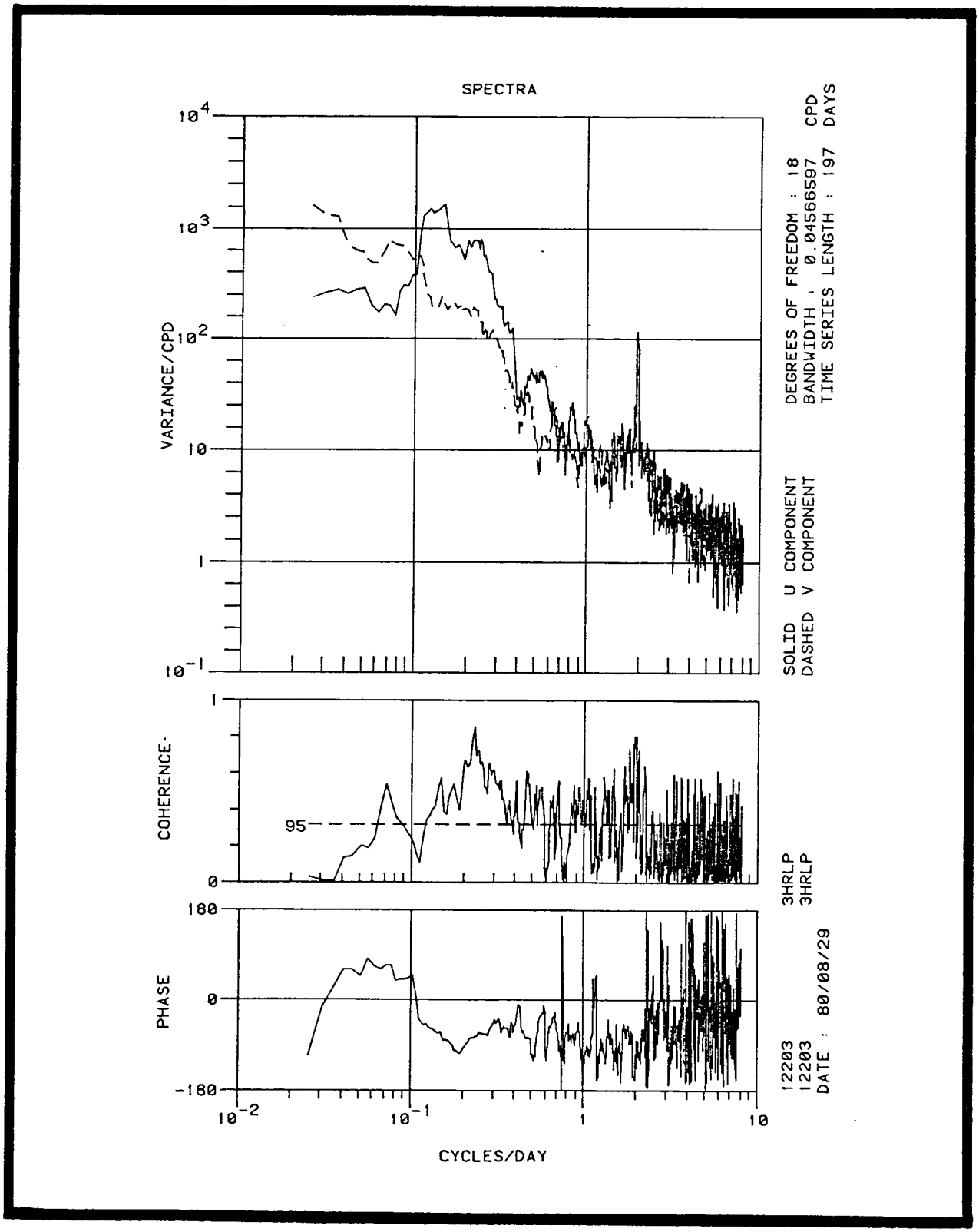

Figure A-26. Spectra of u component vs v component from current meter 12203 during first deployment.

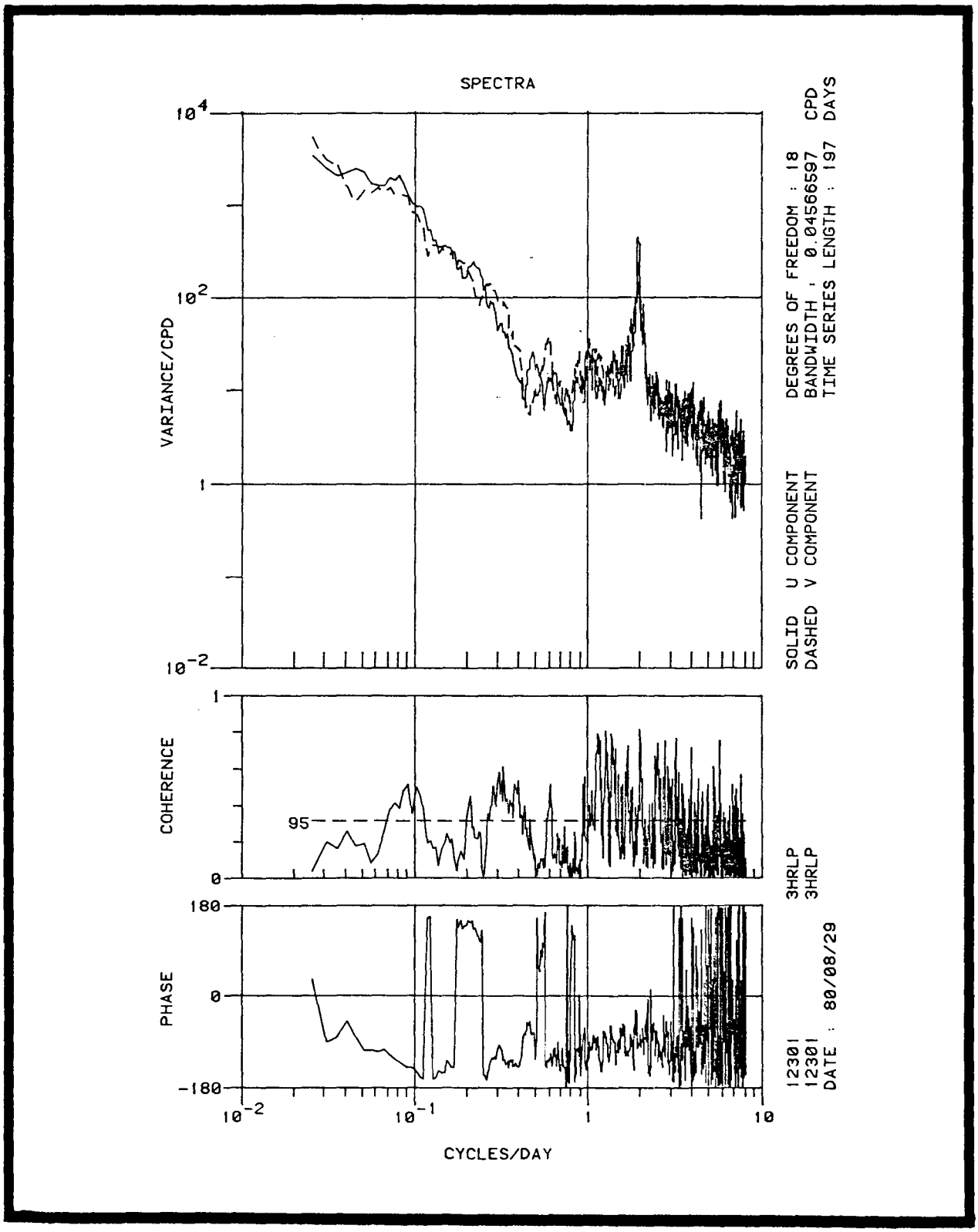

Figure A-27. Spectra of u component vs v component from current meter 12301 during first deployment.

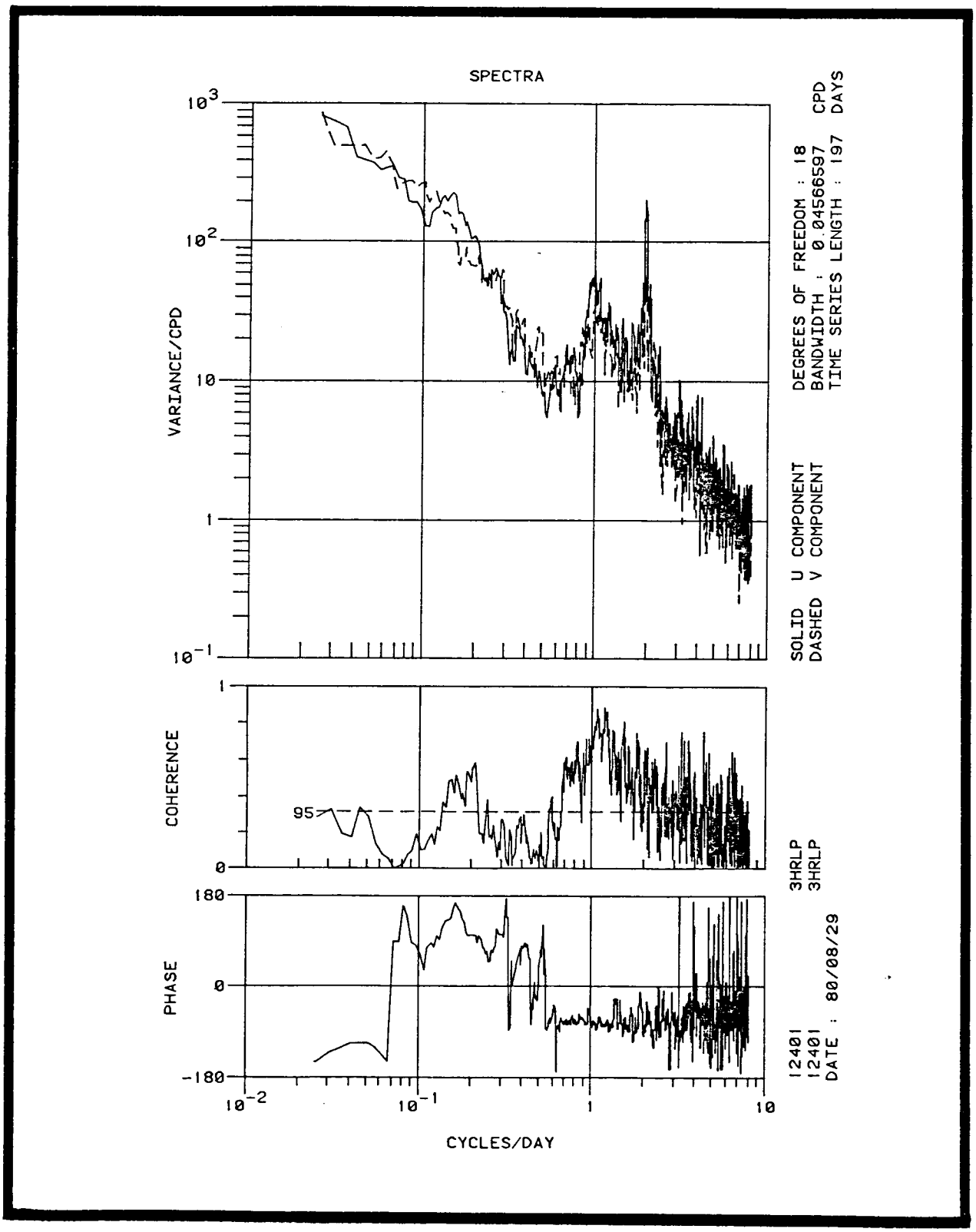

Figure A-28. Spectra of u component vs v component from current meter 12401 during first deployment.

12001 40HRLP

BIWEEKLY PERIOD NUMBER 1

FROM	THROUGH	VARIABLE	MINIMUM	MAXIMUM	MEAN	STD. DEV.
9/ 2/80	9/15/80	TEMP	19.26	22.68	20.68	.93
9/ 2/80	9/15/80	U	-1.00	4.86	4.55	3.39
9/ 2/80	9/15/80	V	-4.55	35.54	8.98	10.95

BIWEEKLY PERIOD NUMBER 2

FROM	THROUGH	VARIABLE	MINIMUM	MAXIMUM	MEAN	STD. DEV.
9/16/80	9/29/80	TEMP	19.84	23.80	21.53	.95
9/16/80	9/29/80	U	-.75	5.27	5.88	3.63
9/16/80	9/29/80	V	-15.17	24.23	2.78	10.57

BIWEEKLY PERIOD NUMBER 3

FROM	THROUGH	VARIABLE	MINIMUM	MAXIMUM	MEAN	STD. DEV.
9/30/80	10/13/80	TEMP	19.75	25.89	23.30	1.64
9/30/80	10/13/80	U	-4.30	10.43	5.00	4.52
9/30/80	10/13/80	V	-24.97	22.14	5.45	9.71

BIWEEKLY PERIOD NUMBER 4

FROM	THROUGH	VARIABLE	MINIMUM	MAXIMUM	MEAN	STD. DEV.
10/14/80	10/27/80	TEMP	19.19	26.78	22.38	1.99
10/14/80	10/27/80	U	-6.77	21.33	5.33	5.28
10/14/80	10/27/80	V	-24.37	32.37	8.82	13.39

BIWEEKLY PERIOD NUMBER 5

FROM	THROUGH	VARIABLE	MINIMUM	MAXIMUM	MEAN	STD. DEV.
10/28/80	11/10/80	TEMP	11.81	23.68	20.31	2.35
10/28/80	11/10/80	U	-8.01	11.50	5.67	5.63
10/28/80	11/10/80	V	-6.72	32.71	11.13	8.96

BIWEEKLY PERIOD NUMBER 6

FROM	THROUGH	VARIABLE	MINIMUM	MAXIMUM	MEAN	STD. DEV.
11/11/80	11/24/80	TEMP	13.14	25.60	21.49	2.62
11/11/80	11/24/80	U	-7.94	16.29	8.25	6.88
11/11/80	11/24/80	V	-22.43	32.06	5.17	12.70

BIWEEKLY PERIOD NUMBER 7

FROM	THROUGH	VARIABLE	MINIMUM	MAXIMUM	MEAN	STD. DEV.
11/25/80	12/ 8/80	TEMP	19.82	24.77	22.91	1.17
11/25/80	12/ 8/80	U	-2.50	26.93	9.53	8.63
11/25/80	12/ 8/80	V	-5.47	48.11	16.51	14.70

Figure A-29. Statistical parameters of temperature, u component, and v component for the first deployment period for current meter 12001.

BIWEEKLY PERIOD NUMBER 8

FROM	THROUGH	VARIABLE	MINIMUM	MAXIMUM	MEAN	STD. DEV.
12/ 9/80	12/22/80	TEMP	16.69	25.14	21.58	2.33
12/ 9/80	12/22/80	U	-5.32	9.62	6.71	6.40
12/ 9/80	12/22/80	V	-20.61	39.55	8.29	15.61

BIWEEKLY PERIOD NUMBER 9

FROM	THROUGH	VARIABLE	MINIMUM	MAXIMUM	MEAN	STD. DEV.
12/23/80	1/ 5/81	TEMP	18.46	23.63	22.23	1.15
12/23/80	1/ 5/81	U	-10.58	5.62	3.16	6.92
12/23/80	1/ 5/81	V	-40.93	33.79	-.33	16.40

BIWEEKLY PERIOD NUMBER 10

FROM	THROUGH	VARIABLE	MINIMUM	MAXIMUM	MEAN	STD. DEV.
1/ 6/81	1/19/81	TEMP	20.76	23.26	22.05	.67
1/ 6/81	1/19/81	U	-5.85	7.89	4.95	4.79
1/ 6/81	1/19/81	V	-19.22	49.55	12.07	18.81

BIWEEKLY PERIOD NUMBER 11

FROM	THROUGH	VARIABLE	MINIMUM	MAXIMUM	MEAN	STD. DEV.
1/20/81	2/ 2/81	TEMP	17.13	22.12	20.58	1.14
1/20/81	2/ 2/81	U	-6.56	2.84	5.97	7.38
1/20/81	2/ 2/81	V	-12.10	30.26	10.99	9.82

BIWEEKLY PERIOD NUMBER 12

FROM	THROUGH	VARIABLE	MINIMUM	MAXIMUM	MEAN	STD. DEV.
2/ 3/81	2/16/81	TEMP	16.48	20.34	18.61	1.19
2/ 3/81	2/16/81	U	-1.35	7.34	8.50	5.37
2/ 3/81	2/16/81	V	-12.48	19.67	3.75	7.86

BIWEEKLY PERIOD NUMBER 13

FROM	THROUGH	VARIABLE	MINIMUM	MAXIMUM	MEAN	STD. DEV.
2/17/81	3/ 2/81	TEMP	17.53	20.15	18.84	.52
2/17/81	3/ 2/81	U	-4.64	6.93	3.89	3.82
2/17/81	3/ 2/81	V	-31.57	15.18	-5.24	11.07

BIWEEKLY PERIOD NUMBER 14

FROM	THROUGH	VARIABLE	MINIMUM	MAXIMUM	MEAN	STD. DEV.
3/ 3/81	3/13/81	TEMP	17.00	21.31	19.29	1.48
3/ 3/81	3/13/81	U	-7.13	8.46	3.66	5.49
3/ 3/81	3/13/81	V	-5.37	25.95	9.56	8.78

FOR THE ENTIRE TIME PERIOD

FROM	THROUGH	VARIABLE	MINIMUM	MAXIMUM	MEAN	STD. DEV.
9/ 2/80	3/13/81	TEMP	11.81	26.78	21.16	2.13
9/ 2/80	3/13/81	U	-10.58	26.93	5.83	6.08
9/ 2/80	3/13/81	V	-40.93	49.55	6.94	13.71

Figure A-29. Continued.

12101 40HRLP

BIWEEKLY PERIOD NUMBER 1

FROM	THROUGH	VARIABLE	MINIMUM	MAXIMUM	MEAN	STD. DEV.
9/ 2/80	9/15/80	TEMP	10.70	17.38	14.86	1.92
9/ 2/80	9/15/80	U	-31.02	39.44	14.06	18.36
9/ 2/80	9/15/80	V	34.71	96.81	54.80	16.15

BIWEEKLY PERIOD NUMBER 2

FROM	THROUGH	VARIABLE	MINIMUM	MAXIMUM	MEAN	STD. DEV.
9/16/80	9/29/80	TEMP	9.17	15.88	11.78	1.22
9/16/80	9/29/80	U	-34.28	49.53	2.29	17.08
9/16/80	9/29/80	V	-20.19	80.79	26.27	21.36

BIWEEKLY PERIOD NUMBER 3

FROM	THROUGH	VARIABLE	MINIMUM	MAXIMUM	MEAN	STD. DEV.
9/30/80	10/13/80	TEMP	13.48	16.88	15.29	.80
9/30/80	10/13/80	U	2.13	53.26	27.38	10.32
9/30/80	10/13/80	V	38.40	79.24	66.31	11.10

BIWEEKLY PERIOD NUMBER 4

FROM	THROUGH	VARIABLE	MINIMUM	MAXIMUM	MEAN	STD. DEV.
10/14/80	10/27/80	TEMP	15.14	17.60	16.38	.65
10/14/80	10/27/80	U	-2.88	55.21	19.97	10.16
10/14/80	10/27/80	V	54.77	72.73	64.07	4.03

BIWEEKLY PERIOD NUMBER 5

FROM	THROUGH	VARIABLE	MINIMUM	MAXIMUM	MEAN	STD. DEV.
10/28/80	11/10/80	TEMP	12.94	17.44	15.30	1.19
10/28/80	11/10/80	U	-14.22	54.40	24.76	15.42
10/28/80	11/10/80	V	33.00	87.56	66.52	12.90

BIWEEKLY PERIOD NUMBER 6

FROM	THROUGH	VARIABLE	MINIMUM	MAXIMUM	MEAN	STD. DEV.
11/11/80	11/24/80	TEMP	12.81	17.72	15.32	1.40
11/11/80	11/24/80	U	-1.53	57.82	22.62	15.94
11/11/80	11/24/80	V	43.27	101.05	70.30	15.31

BIWEEKLY PERIOD NUMBER 7

FROM	THROUGH	VARIABLE	MINIMUM	MAXIMUM	MEAN	STD. DEV.
11/25/80	12/ 8/80	TEMP	15.00	17.38	16.46	.66
11/25/80	12/ 8/80	U	6.63	50.50	19.95	7.33
11/25/80	12/ 8/80	V	48.55	78.07	59.64	7.18

Figure A-30. Statistical parameters of temperature, u component, and v component for the first deployment period for current meter 12101.

BIWEEKLY PERIOD NUMBER 8

FROM	THROUGH	VARIABLE	MINIMUM	MAXIMUM	MEAN	STD. DEV.
12/ 9/80	12/22/80	TEMP	12.48	16.94	15.33	1.25
12/ 9/80	12/22/80	U	9.10	55.94	24.79	8.63
12/ 9/80	12/22/80	V	52.13	87.93	67.30	9.92

BIWEEKLY PERIOD NUMBER 9

FROM	THROUGH	VARIABLE	MINIMUM	MAXIMUM	MEAN	STD. DEV.
12/23/80	1/ 5/81	TEMP	13.86	16.98	15.92	.79
12/23/80	1/ 5/81	U	7.17	59.55	26.06	12.14
12/23/80	1/ 5/81	V	54.87	96.70	70.47	9.84

BIWEEKLY PERIOD NUMBER 10

FROM	THROUGH	VARIABLE	MINIMUM	MAXIMUM	MEAN	STD. DEV.
1/ 6/81	1/19/81	TEMP	13.43	17.73	16.05	1.30
1/ 6/81	1/19/81	U	.18	44.48	21.42	12.69
1/ 6/81	1/19/81	V	43.45	86.22	70.86	11.09

BIWEEKLY PERIOD NUMBER 11

FROM	THROUGH	VARIABLE	MINIMUM	MAXIMUM	MEAN	STD. DEV.
1/20/81	2/ 2/81	TEMP	10.44	18.01	15.68	2.03
1/20/81	2/ 2/81	U	-19.49	39.15	14.75	15.77
1/20/81	2/ 2/81	V	39.06	91.03	62.24	13.74

BIWEEKLY PERIOD NUMBER 12

FROM	THROUGH	VARIABLE	MINIMUM	MAXIMUM	MEAN	STD. DEV.
2/ 3/81	2/16/81	TEMP	11.29	16.72	14.08	1.56
2/ 3/81	2/16/81	U	-11.60	44.25	18.75	13.41
2/ 3/81	2/16/81	V	21.95	85.44	58.22	19.21

BIWEEKLY PERIOD NUMBER 13

FROM	THROUGH	VARIABLE	MINIMUM	MAXIMUM	MEAN	STD. DEV.
2/17/81	3/ 2/81	TEMP	10.15	17.60	15.37	1.74
2/17/81	3/ 2/81	U	13.91	58.03	28.26	8.02
2/17/81	3/ 2/81	V	55.76	92.67	69.73	8.97

BIWEEKLY PERIOD NUMBER 14

FROM	THROUGH	VARIABLE	MINIMUM	MAXIMUM	MEAN	STD. DEV.
3/ 3/81	3/12/81	TEMP	16.41	17.65	17.14	.32
3/ 3/81	3/12/81	U	2.92	49.61	15.09	7.83
3/ 3/81	3/12/81	V	49.45	70.52	57.16	6.32

FOR THE ENTIRE TIME PERIOD

FROM	THROUGH	VARIABLE	MINIMUM	MAXIMUM	MEAN	STD. DEV.
9/ 2/80	3/12/81	TEMP	9.17	18.01	15.31	1.79
9/ 2/80	3/12/81	U	-34.28	59.55	20.28	14.58
9/ 2/80	3/12/81	V	-20.19	101.05	61.62	17.09

Figure A-30. Continued.

12102 40HRLP

BIWEEKLY PERIOD NUMBER 1

FROM	THROUGH	VARIABLE	MINIMUM	MAXIMUM	MEAN	STD. DEV.
9/ 2/80	9/15/80	TEMP	7.46	11.90	9.50	1.35
9/ 2/80	9/15/80	U	-17.35	3.87	6.17	10.79
9/ 2/80	9/15/80	V	2.78	52.49	24.32	11.45

BIWEEKLY PERIOD NUMBER 2

FROM	THROUGH	VARIABLE	MINIMUM	MAXIMUM	MEAN	STD. DEV.
9/16/80	9/29/80	TEMP	7.15	11.27	8.15	.70
9/16/80	9/29/80	U	-20.50	24.34	.64	10.96
9/16/80	9/29/80	V	-5.82	39.35	15.04	11.78

BIWEEKLY PERIOD NUMBER 3

FROM	THROUGH	VARIABLE	MINIMUM	MAXIMUM	MEAN	STD. DEV.
9/30/80	10/13/80	TEMP	7.57	12.01	10.25	1.03
9/30/80	10/13/80	U	-7.20	33.13	15.43	11.32
9/30/80	10/13/80	V	17.69	51.14	35.87	7.76

BIWEEKLY PERIOD NUMBER 4

FROM	THROUGH	VARIABLE	MINIMUM	MAXIMUM	MEAN	STD. DEV.
10/14/80	10/27/80	TEMP	9.68	13.53	11.50	.93
10/14/80	10/27/80	U	-10.83	33.62	11.85	10.95
10/14/80	10/27/80	V	13.33	48.88	32.41	9.10

BIWEEKLY PERIOD NUMBER 5

FROM	THROUGH	VARIABLE	MINIMUM	MAXIMUM	MEAN	STD. DEV.
10/28/80	11/10/80	TEMP	8.13	12.41	9.96	1.14
10/28/80	11/10/80	U	-17.29	14.54	10.80	10.12
10/28/80	11/10/80	V	8.61	49.59	29.78	10.01

BIWEEKLY PERIOD NUMBER 6

FROM	THROUGH	VARIABLE	MINIMUM	MAXIMUM	MEAN	STD. DEV.
11/11/80	11/24/80	TEMP	7.60	13.90	10.46	1.93
11/11/80	11/24/80	U	-4.18	24.42	9.85	8.33
11/11/80	11/24/80	V	13.89	55.14	32.80	9.36

BIWEEKLY PERIOD NUMBER 7

FROM	THROUGH	VARIABLE	MINIMUM	MAXIMUM	MEAN	STD. DEV.
11/25/80	12/ 8/80	TEMP	10.01	13.08	11.55	.88
11/25/80	12/ 8/80	U	-8.19	25.67	11.23	8.64
11/25/80	12/ 8/80	V	5.59	42.71	29.13	8.21

Figure A-31. Statistical parameters of temperature, u component, and v component for the first deployment period for current meter 12102.

BIWEEKLY PERIOD NUMBER 8

FROM	THROUGH	VARIABLE	MINIMUM	MAXIMUM	MEAN	STD. DEV.
12/ 9/80	12/22/80	TEMP	7.30	12.00	9.79	1.27
12/ 9/80	12/22/80	U	.85	34.92	13.37	8.50
12/ 9/80	12/22/80	V	18.46	45.35	31.18	7.72

BIWEEKLY PERIOD NUMBER 9

FROM	THROUGH	VARIABLE	MINIMUM	MAXIMUM	MEAN	STD. DEV.
12/23/80	1/ 5/81	TEMP	8.00	12.32	10.93	1.03
12/23/80	1/ 5/81	U	-3.15	39.76	13.47	10.62
12/23/80	1/ 5/81	V	19.19	56.37	35.08	10.31

BIWEEKLY PERIOD NUMBER 10

FROM	THROUGH	VARIABLE	MINIMUM	MAXIMUM	MEAN	STD. DEV.
1/ 6/81	1/19/81	TEMP	8.28	12.90	11.03	1.52
1/ 6/81	1/19/81	U	-2.85	35.71	9.99	9.88
1/ 6/81	1/19/81	V	3.84	55.00	33.96	12.74

BIWEEKLY PERIOD NUMBER 11

FROM	THROUGH	VARIABLE	MINIMUM	MAXIMUM	MEAN	STD. DEV.
1/20/81	2/ 2/81	TEMP	8.10	12.68	10.41	1.10
1/20/81	2/ 2/81	U	-15.76	9.89	4.94	10.48
1/20/81	2/ 2/81	V	-.80	47.38	24.11	12.95

BIWEEKLY PERIOD NUMBER 12

FROM	THROUGH	VARIABLE	MINIMUM	MAXIMUM	MEAN	STD. DEV.
2/ 3/81	2/16/81	TEMP	7.82	10.54	9.02	.92
2/ 3/81	2/16/81	U	-8.47	22.58	7.06	7.86
2/ 3/81	2/16/81	V	.61	44.44	21.42	10.98

BIWEEKLY PERIOD NUMBER 13

FROM	THROUGH	VARIABLE	MINIMUM	MAXIMUM	MEAN	STD. DEV.
2/17/81	3/ 2/81	TEMP	7.22	11.88	9.86	1.45
2/17/81	3/ 2/81	U	2.68	25.76	13.81	7.16
2/17/81	3/ 2/81	V	12.12	52.95	33.63	10.88

BIWEEKLY PERIOD NUMBER 14

FROM	THROUGH	VARIABLE	MINIMUM	MAXIMUM	MEAN	STD. DEV.
3/ 3/81	3/12/81	TEMP	10.57	12.61	11.52	.66
3/ 3/81	3/12/81	U	-6.24	5.39	4.32	7.09
3/ 3/81	3/12/81	V	5.32	39.47	21.65	9.44

FOR THE ENTIRE TIME PERIOD

FROM	THROUGH	VARIABLE	MINIMUM	MAXIMUM	MEAN	STD. DEV.
9/ 2/80	3/12/81	TEMP	7.15	13.90	10.25	1.53
9/ 2/80	3/12/81	U	-20.50	39.76	9.62	10.47
9/ 2/80	3/12/81	V	-5.82	56.37	28.77	11.96

Figure A-31. Continued.

12103 40HRLP

BIWEEKLY PERIOD NUMBER 1

FROM	THROUGH	VARIABLE	MINIMUM	MAXIMUM	MEAN	STD. DEV.
9/ 2/80	9/15/80	TEMP	6.58	7.96	7.19	.46
9/ 2/80	9/15/80	U	-18.18	3.12	-4.93	7.45
9/ 2/80	9/15/80	V	-12.02	25.10	7.64	9.72

BIWEEKLY PERIOD NUMBER 2

FROM	THROUGH	VARIABLE	MINIMUM	MAXIMUM	MEAN	STD. DEV.
9/16/80	9/29/80	TEMP	6.35	7.57	6.91	.27
9/16/80	9/29/80	U	-27.02	12.46	-6.01	12.41
9/16/80	9/29/80	V	-28.57	19.19	3.03	10.74

BIWEEKLY PERIOD NUMBER 3

FROM	THROUGH	VARIABLE	MINIMUM	MAXIMUM	MEAN	STD. DEV.
9/30/80	10/13/80	TEMP	6.88	8.60	7.41	.43
9/30/80	10/13/80	U	-27.38	1.20	-5.42	8.75
9/30/80	10/13/80	V	-4.20	20.48	6.93	4.70

BIWEEKLY PERIOD NUMBER 4

FROM	THROUGH	VARIABLE	MINIMUM	MAXIMUM	MEAN	STD. DEV.
10/14/80	10/27/80	TEMP	7.28	8.71	8.24	.38
10/14/80	10/27/80	U	-20.26	7.16	-6.97	7.72
10/14/80	10/27/80	V	-4.02	19.25	3.97	4.67

BIWEEKLY PERIOD NUMBER 5

FROM	THROUGH	VARIABLE	MINIMUM	MAXIMUM	MEAN	STD. DEV.
10/28/80	11/10/80	TEMP	7.13	8.37	7.48	.32
10/28/80	11/10/80	U	-19.08	4.37	-2.06	7.48
10/28/80	11/10/80	V	-11.34	27.88	6.95	8.97

BIWEEKLY PERIOD NUMBER 6

FROM	THROUGH	VARIABLE	MINIMUM	MAXIMUM	MEAN	STD. DEV.
11/11/80	11/24/80	TEMP	7.00	9.48	8.05	.79
11/11/80	11/24/80	U	-20.79	8.41	-6.11	8.45
11/11/80	11/24/80	V	-7.58	25.81	8.03	7.19

BIWEEKLY PERIOD NUMBER 7

FROM	THROUGH	VARIABLE	MINIMUM	MAXIMUM	MEAN	STD. DEV.
11/25/80	12/ 8/80	TEMP	7.20	8.22	7.76	.28
11/25/80	12/ 8/80	U	-19.56	5.35	-4.11	7.02
11/25/80	12/ 8/80	V	-5.20	18.44	3.27	5.30

Figure A-32. Statistical parameters of temperature, u component, and v component for the first deployment period for current meter 12103.

BIWEEKLY PERIOD NUMBER 8

FROM	THROUGH	VARIABLE	MINIMUM	MAXIMUM	MEAN	STD. DEV.
12/ 9/80	12/22/80	TEMP	6.44	8.47	7.45	.51
12/ 9/80	12/22/80	U	-18.59	7.12	-3.24	7.60
12/ 9/80	12/22/80	V	-3.73	27.71	9.34	7.57

BIWEEKLY PERIOD NUMBER 9

FROM	THROUGH	VARIABLE	MINIMUM	MAXIMUM	MEAN	STD. DEV.
12/23/80	1/ 5/81	TEMP	6.91	9.60	7.89	.74
12/23/80	1/ 5/81	U	-19.79	11.09	-3.63	8.06
12/23/80	1/ 5/81	V	-16.88	21.55	6.13	9.24

BIWEEKLY PERIOD NUMBER 10

FROM	THROUGH	VARIABLE	MINIMUM	MAXIMUM	MEAN	STD. DEV.
1/ 6/81	1/19/81	TEMP	6.78	9.51	8.26	.76
1/ 6/81	1/19/81	U	-22.55	12.45	-4.65	7.97
1/ 6/81	1/19/81	V	-12.36	30.90	7.18	10.01

BIWEEKLY PERIOD NUMBER 11

FROM	THROUGH	VARIABLE	MINIMUM	MAXIMUM	MEAN	STD. DEV.
1/20/81	2/ 2/81	TEMP	6.99	8.86	7.80	.45
1/20/81	2/ 2/81	U	-23.39	5.67	-5.84	8.15
1/20/81	2/ 2/81	V	-17.65	20.23	3.77	9.59

BIWEEKLY PERIOD NUMBER 12

FROM	THROUGH	VARIABLE	MINIMUM	MAXIMUM	MEAN	STD. DEV.
2/ 3/81	2/16/81	TEMP	6.85	7.87	7.33	.29
2/ 3/81	2/16/81	U	-12.54	3.94	-3.07	4.29
2/ 3/81	2/16/81	V	-7.78	18.58	7.63	6.51

BIWEEKLY PERIOD NUMBER 13

FROM	THROUGH	VARIABLE	MINIMUM	MAXIMUM	MEAN	STD. DEV.
2/17/81	3/ 2/81	TEMP	6.69	8.29	7.19	.44
2/17/81	3/ 2/81	U	-10.35	.70	-1.15	6.72
2/17/81	3/ 2/81	V	-15.70	22.28	4.41	8.53

BIWEEKLY PERIOD NUMBER 14

FROM	THROUGH	VARIABLE	MINIMUM	MAXIMUM	MEAN	STD. DEV.
3/ 3/81	3/12/81	TEMP	6.73	8.22	7.34	.41
3/ 3/81	3/12/81	U	-11.69	4.03	-1.85	4.35
3/ 3/81	3/12/81	V	-19.64	6.83	-3.99	6.76

FOR THE ENTIRE TIME PERIOD

FROM	THROUGH	VARIABLE	MINIMUM	MAXIMUM	MEAN	STD. DEV.
9/ 2/80	3/12/81	TEMP	6.35	9.60	7.60	.64
9/ 2/80	3/12/81	U	-27.38	12.46	-4.29	8.11
9/ 2/80	3/12/81	V	-28.57	30.90	5.54	8.55

Figure A-32. Continued.

12201 40HRLP

BIWEEKLY PERIOD NUMBER 1

FROM	THROUGH	VARIABLE	MINIMUM	MAXIMUM	MEAN	STD. DEV.
9/ 2/80	9/15/80	TEMP	15.11	18.35	17.56	.74
9/ 2/80	9/15/80	U	-21.28	20.98	13.14	19.99
9/ 2/80	9/15/80	V	19.94	64.97	41.26	15.50

BIWEEKLY PERIOD NUMBER 2

FROM	THROUGH	VARIABLE	MINIMUM	MAXIMUM	MEAN	STD. DEV.
9/16/80	9/29/80	TEMP	10.70	17.65	14.63	2.04
9/16/80	9/29/80	U	-22.02	51.93	23.10	20.46
9/16/80	9/29/80	V	39.20	87.31	55.06	12.17

BIWEEKLY PERIOD NUMBER 3

FROM	THROUGH	VARIABLE	MINIMUM	MAXIMUM	MEAN	STD. DEV.
9/30/80	10/13/80	TEMP	16.19	18.46	17.72	.60
9/30/80	10/13/80	U	-7.07	20.40	16.65	14.62
9/30/80	10/13/80	V	15.41	73.68	39.55	15.15

BIWEEKLY PERIOD NUMBER 4

FROM	THROUGH	VARIABLE	MINIMUM	MAXIMUM	MEAN	STD. DEV.
10/14/80	10/27/80	TEMP	16.94	18.48	18.21	.40
10/14/80	10/27/80	U	-1.12	8.00	3.36	2.89
10/14/80	10/27/80	V	.67	36.48	18.51	6.74

BIWEEKLY PERIOD NUMBER 5

FROM	THROUGH	VARIABLE	MINIMUM	MAXIMUM	MEAN	STD. DEV.
10/28/80	11/10/80	TEMP	17.20	18.52	17.96	.39
10/28/80	11/10/80	U	-21.04	12.57	13.83	17.79
10/28/80	11/10/80	V	9.62	75.90	37.14	16.20

BIWEEKLY PERIOD NUMBER 6

FROM	THROUGH	VARIABLE	MINIMUM	MAXIMUM	MEAN	STD. DEV.
11/11/80	11/24/80	TEMP	17.05	19.19	18.03	.52
11/11/80	11/24/80	U	-5.58	34.99	10.18	9.22
11/11/80	11/24/80	V	2.98	62.63	28.87	14.94

BIWEEKLY PERIOD NUMBER 7

FROM	THROUGH	VARIABLE	MINIMUM	MAXIMUM	MEAN	STD. DEV.
11/25/80	12/ 8/80	TEMP	17.76	18.54	18.27	.20
11/25/80	12/ 8/80	U	-14.47	36.57	8.29	9.88
11/25/80	12/ 8/80	V	16.90	42.57	28.11	5.47

Figure A-33. Statistical parameters of temperature, u component, and v component for the first deployment period for current meter 12201.

BIWEEKLY PERIOD NUMBER 8

FROM	THROUGH	VARIABLE	MINIMUM	MAXIMUM	MEAN	STD. DEV.
12/ 9/80	12/22/80	TEMP	17.29	18.55	18.18	.31
12/ 9/80	12/22/80	U	-11.48	28.50	12.72	9.23
12/ 9/80	12/22/80	V	24.50	54.22	36.37	6.68

BIWEEKLY PERIOD NUMBER 9

FROM	THROUGH	VARIABLE	MINIMUM	MAXIMUM	MEAN	STD. DEV.
12/23/80	1/ 5/81	TEMP	17.50	18.57	18.17	.27
12/23/80	1/ 5/81	U	-9.76	26.28	10.58	8.50
12/23/80	1/ 5/81	V	.39	46.36	28.08	11.97

BIWEEKLY PERIOD NUMBER 10

FROM	THROUGH	VARIABLE	MINIMUM	MAXIMUM	MEAN	STD. DEV.
1/ 6/81	1/19/81	TEMP	17.19	18.69	18.17	.40
1/ 6/81	1/19/81	U	-13.48	15.65	1.37	8.26
1/ 6/81	1/19/81	V	.27	28.36	18.16	6.75

BIWEEKLY PERIOD NUMBER 11

FROM	THROUGH	VARIABLE	MINIMUM	MAXIMUM	MEAN	STD. DEV.
1/20/81	2/ 2/81	TEMP	15.92	18.56	17.89	.71
1/20/81	2/ 2/81	U	-20.82	21.79	4.81	15.45
1/20/81	2/ 2/81	V	4.05	64.28	27.72	17.90

BIWEEKLY PERIOD NUMBER 12

FROM	THROUGH	VARIABLE	MINIMUM	MAXIMUM	MEAN	STD. DEV.
2/ 3/81	2/16/81	TEMP	15.35	18.22	17.51	.68
2/ 3/81	2/16/81	U	-4.50	1.93	17.70	18.69
2/ 3/81	2/16/81	V	1.85	73.22	40.56	19.75

BIWEEKLY PERIOD NUMBER 13

FROM	THROUGH	VARIABLE	MINIMUM	MAXIMUM	MEAN	STD. DEV.
2/17/81	3/ 2/81	TEMP	16.92	18.39	17.96	.35
2/17/81	3/ 2/81	U	-2.62	.29	4.52	7.15
2/17/81	3/ 2/81	V	-1.18	32.83	10.88	10.37

BIWEEKLY PERIOD NUMBER 14

FROM	THROUGH	VARIABLE	MINIMUM	MAXIMUM	MEAN	STD. DEV.
3/ 3/81	3/11/81	TEMP	17.98	18.32	18.19	.09
3/ 3/81	3/11/81	U	-10.64	.65	-1.16	3.01
3/ 3/81	3/11/81	V	-1.55	8.93	2.77	3.21

FOR THE ENTIRE TIME PERIOD

FROM	THROUGH	VARIABLE	MINIMUM	MAXIMUM	MEAN	STD. DEV.
9/ 2/80	3/11/81	TEMP	10.70	19.19	17.73	1.16
9/ 2/80	3/11/81	U	-22.02	51.93	10.24	14.81
9/ 2/80	3/11/81	V	-1.55	87.31	30.24	17.98

Figure A-33. Continued.

12203 40HRLP

BIWEEKLY PERIOD NUMBER 1

FROM	THROUGH	VARIABLE	MINIMUM	MAXIMUM	MEAN	STD. DEV.
9/ 2/80	9/15/80	TEMP	7.12	8.67	7.92	.41
9/ 2/80	9/15/80	U	-22.95	12.65	-3.00	11.59
9/ 2/80	9/15/80	V	11.17	36.02	20.75	6.92

BIWEEKLY PERIOD NUMBER 2

FROM	THROUGH	VARIABLE	MINIMUM	MAXIMUM	MEAN	STD. DEV.
9/16/80	9/29/80	TEMP	6.71	9.14	7.46	.62
9/16/80	9/29/80	U	-21.35	15.53	.68	9.99
9/16/80	9/29/80	V	8.11	44.59	23.72	9.43

BIWEEKLY PERIOD NUMBER 3

FROM	THROUGH	VARIABLE	MINIMUM	MAXIMUM	MEAN	STD. DEV.
9/30/80	10/13/80	TEMP	7.14	9.56	8.36	.58
9/30/80	10/13/80	U	-22.36	11.56	-2.99	11.05
9/30/80	10/13/80	V	6.07	31.13	18.04	7.00

BIWEEKLY PERIOD NUMBER 4

FROM	THROUGH	VARIABLE	MINIMUM	MAXIMUM	MEAN	STD. DEV.
10/14/80	10/27/80	TEMP	8.48	9.37	8.94	.21
10/14/80	10/27/80	U	-16.35	6.76	.71	9.68
10/14/80	10/27/80	V	-6.38	14.13	4.94	5.29

BIWEEKLY PERIOD NUMBER 5

FROM	THROUGH	VARIABLE	MINIMUM	MAXIMUM	MEAN	STD. DEV.
10/28/80	11/10/80	TEMP	7.54	9.97	8.93	.70
10/28/80	11/10/80	U	-21.65	15.48	-.95	13.37
10/28/80	11/10/80	V	1.02	33.33	14.82	8.67

BIWEEKLY PERIOD NUMBER 6

FROM	THROUGH	VARIABLE	MINIMUM	MAXIMUM	MEAN	STD. DEV.
11/11/80	11/24/80	TEMP	7.30	10.16	9.16	.81
11/11/80	11/24/80	U	-20.18	4.59	-1.52	10.71
11/11/80	11/24/80	V	-16.16	17.61	8.83	8.73

BIWEEKLY PERIOD NUMBER 7

FROM	THROUGH	VARIABLE	MINIMUM	MAXIMUM	MEAN	STD. DEV.
11/25/80	12/ 8/80	TEMP	8.47	10.23	9.77	.39
11/25/80	12/ 8/80	U	-12.93	8.39	1.27	5.74
11/25/80	12/ 8/80	V	2.12	16.07	8.05	3.79

Figure A-34. Statistical parameters of temperature, u component, and v component for the first deployment period for current meter 12203.

BIWEEKLY PERIOD NUMBER 8

FROM	THROUGH	VARIABLE	MINIMUM	MAXIMUM	MEAN	STD. DEV.
12/ 9/80	12/22/80	TEMP	6.97	10.21	8.92	1.08
12/ 9/80	12/22/80	U	-25.96	5.86	.69	11.10
12/ 9/80	12/22/80	V	-6.49	19.45	7.64	5.77

BIWEEKLY PERIOD NUMBER 9

FROM	THROUGH	VARIABLE	MINIMUM	MAXIMUM	MEAN	STD. DEV.
12/23/80	1/ 5/81	TEMP	7.44	10.91	9.90	.81
12/23/80	1/ 5/81	U	-22.04	10.87	1.42	11.22
12/23/80	1/ 5/81	V	-7.40	17.72	9.07	5.43

BIWEEKLY PERIOD NUMBER 10

FROM	THROUGH	VARIABLE	MINIMUM	MAXIMUM	MEAN	STD. DEV.
1/ 6/81	1/19/81	TEMP	7.39	10.77	9.25	1.10
1/ 6/81	1/19/81	U	-27.82	2.03	-1.78	16.87
1/ 6/81	1/19/81	V	-17.10	18.21	3.51	7.92

BIWEEKLY PERIOD NUMBER 11

FROM	THROUGH	VARIABLE	MINIMUM	MAXIMUM	MEAN	STD. DEV.
1/20/81	2/ 2/81	TEMP	6.96	10.33	8.73	.89
1/20/81	2/ 2/81	U	-17.37	8.54	-4.94	9.47
1/20/81	2/ 2/81	V	-.66	37.32	13.09	9.65

BIWEEKLY PERIOD NUMBER 12

FROM	THROUGH	VARIABLE	MINIMUM	MAXIMUM	MEAN	STD. DEV.
2/ 3/81	2/16/81	TEMP	7.78	9.43	8.44	.49
2/ 3/81	2/16/81	U	-16.86	10.80	2.38	8.59
2/ 3/81	2/16/81	V	-9.80	29.34	11.86	10.81

BIWEEKLY PERIOD NUMBER 13

FROM	THROUGH	VARIABLE	MINIMUM	MAXIMUM	MEAN	STD. DEV.
2/17/81	3/ 2/81	TEMP	7.13	8.35	7.90	.42
2/17/81	3/ 2/81	U	-16.05	2.16	-.20	7.19
2/17/81	3/ 2/81	V	-7.68	17.20	3.09	6.86

BIWEEKLY PERIOD NUMBER 14

FROM	THROUGH	VARIABLE	MINIMUM	MAXIMUM	MEAN	STD. DEV.
3/ 3/81	3/11/81	TEMP	8.08	8.65	8.26	.20
3/ 3/81	3/11/81	U	-8.32	.64	-3.67	4.16
3/ 3/81	3/11/81	V	-2.84	6.17	1.77	2.55

FOR THE ENTIRE TIME PERIOD

FROM	THROUGH	VARIABLE	MINIMUM	MAXIMUM	MEAN	STD. DEV.
9/ 2/80	3/11/81	TEMP	6.71	10.91	8.72	.97
9/ 2/80	3/11/81	U	-27.82	15.53	-.77	10.81
9/ 2/80	3/11/81	V	-17.10	44.59	10.90	9.88

Figure A-34. Continued.

12301 40HRLP

BIWEEKLY PERIOD NUMBER 1

FROM	THROUGH	VARIABLE	MINIMUM	MAXIMUM	MEAN	STD. DEV.
9/ 2/80	9/15/80	TEMP	4.54	6.99	5.41	.85
9/ 2/80	9/15/80	U	-32.20	21.02	-6.93	20.45
9/ 2/80	9/15/80	V	-38.44	27.12	-13.44	19.13

BIWEEKLY PERIOD NUMBER 2

FROM	THROUGH	VARIABLE	MINIMUM	MAXIMUM	MEAN	STD. DEV.
9/16/80	9/29/80	TEMP	4.80	8.16	6.37	1.26
9/16/80	9/29/80	U	-27.03	14.13	-5.57	14.78
9/16/80	9/29/80	V	-36.54	7.34	-24.11	10.36

BIWEEKLY PERIOD NUMBER 3

FROM	THROUGH	VARIABLE	MINIMUM	MAXIMUM	MEAN	STD. DEV.
9/30/80	10/13/80	TEMP	8.06	9.80	9.14	.41
9/30/80	10/13/80	U	-29.07	14.55	-22.89	3.71
9/30/80	10/13/80	V	-25.66	1.05	-7.76	6.42

BIWEEKLY PERIOD NUMBER 4

FROM	THROUGH	VARIABLE	MINIMUM	MAXIMUM	MEAN	STD. DEV.
10/14/80	10/27/80	TEMP	6.23	9.58	7.63	1.34
10/14/80	10/27/80	U	-28.57	10.36	-6.31	19.21
10/14/80	10/27/80	V	-20.30	22.58	-1.84	9.11

BIWEEKLY PERIOD NUMBER 5

FROM	THROUGH	VARIABLE	MINIMUM	MAXIMUM	MEAN	STD. DEV.
10/28/80	11/10/80	TEMP	6.83	9.56	8.18	.99
10/28/80	11/10/80	U	-18.55	5.96	-4.79	6.93
10/28/80	11/10/80	V	-34.52	11.44	-25.42	10.35

BIWEEKLY PERIOD NUMBER 6

FROM	THROUGH	VARIABLE	MINIMUM	MAXIMUM	MEAN	STD. DEV.
11/11/80	11/24/80	TEMP	7.12	10.89	9.26	.84
11/11/80	11/24/80	U	-25.00	16.68	-4.43	11.74
11/11/80	11/24/80	V	-32.79	-9.09	-22.59	6.20

BIWEEKLY PERIOD NUMBER 7

FROM	THROUGH	VARIABLE	MINIMUM	MAXIMUM	MEAN	STD. DEV.
11/25/80	12/ 8/80	TEMP	9.95	10.96	10.41	.20
11/25/80	12/ 8/80	U	2.69	12.03	10.70	3.83
11/25/80	12/ 8/80	V	-25.92	-4.39	-15.59	5.56

Figure A-35. Statistical parameters of temperature, u component, and v component for the first deployment period for current meter 12301.

BIWEEKLY PERIOD NUMBER 8

FROM	THROUGH	VARIABLE	MINIMUM	MAXIMUM	MEAN	STD. DEV.
12/ 9/80	12/22/80	TEMP	7.61	10.60	9.90	.97
12/ 9/80	12/22/80	U	-11.00	5.25	-2.65	5.62
12/ 9/80	12/22/80	V	-13.48	3.21	-6.12	5.50

BIWEEKLY PERIOD NUMBER 9

FROM	THROUGH	VARIABLE	MINIMUM	MAXIMUM	MEAN	STD. DEV.
12/23/80	1/ 5/81	TEMP	7.60	10.67	9.22	1.10
12/23/80	1/ 5/81	U	-8.48	5.21	.59	6.24
12/23/80	1/ 5/81	V	-11.23	.31	-4.80	3.41

BIWEEKLY PERIOD NUMBER 10

FROM	THROUGH	VARIABLE	MINIMUM	MAXIMUM	MEAN	STD. DEV.
1/ 6/81	1/19/81	TEMP	8.28	9.79	9.09	.44
1/ 6/81	1/19/81	U	-9.73	11.04	1.03	5.66
1/ 6/81	1/19/81	V	-7.97	9.85	-.02	5.16

BIWEEKLY PERIOD NUMBER 11

FROM	THROUGH	VARIABLE	MINIMUM	MAXIMUM	MEAN	STD. DEV.
1/20/81	2/ 2/81	TEMP	6.28	8.33	7.82	.37
1/20/81	2/ 2/81	U	-2.88	7.56	5.23	3.68
1/20/81	2/ 2/81	V	-9.47	27.40	3.88	8.39

BIWEEKLY PERIOD NUMBER 12

FROM	THROUGH	VARIABLE	MINIMUM	MAXIMUM	MEAN	STD. DEV.
2/ 3/81	2/16/81	TEMP	4.95	8.28	6.42	.79
2/ 3/81	2/16/81	U	-28.00	7.95	-7.80	16.35
2/ 3/81	2/16/81	V	-21.24	35.61	1.62	15.12

BIWEEKLY PERIOD NUMBER 13

FROM	THROUGH	VARIABLE	MINIMUM	MAXIMUM	MEAN	STD. DEV.
2/17/81	3/ 2/81	TEMP	5.50	8.10	6.57	.78
2/17/81	3/ 2/81	U	-25.92	14.68	-1.26	10.02
2/17/81	3/ 2/81	V	-.89	38.29	15.77	9.38

BIWEEKLY PERIOD NUMBER 14

FROM	THROUGH	VARIABLE	MINIMUM	MAXIMUM	MEAN	STD. DEV.
3/ 3/81	3/11/81	TEMP	6.59	8.71	7.94	.72
3/ 3/81	3/11/81	U	4.42	4.42	15.04	4.63
3/ 3/81	3/11/81	V	-2.85	17.22	6.83	6.97

FOR THE ENTIRE TIME PERIOD

FROM	THROUGH	VARIABLE	MINIMUM	MAXIMUM	MEAN	STD. DEV.
9/ 2/80	3/11/81	TEMP	4.54	10.96	8.10	1.69
9/ 2/80	3/11/81	U	-32.20	21.02	-2.67	13.94
9/ 2/80	3/11/81	V	-38.44	38.29	-7.09	15.33

Figure A-35. Continued.

12401 40HRLP

BIWEEKLY PERIOD NUMBER 1

FROM	THROUGH	VARIABLE	MINIMUM	MAXIMUM	MEAN	STD. DEV.
9/ 2/80	9/15/80	TEMP	4.85	6.36	5.25	.42
9/ 2/80	9/15/80	U	-18.84	12.27	5.58	12.93
9/ 2/80	9/15/80	V	-22.49	20.74	-5.46	11.43

BIWEEKLY PERIOD NUMBER 2

FROM	THROUGH	VARIABLE	MINIMUM	MAXIMUM	MEAN	STD. DEV.
9/16/80	9/29/80	TEMP	5.28	7.75	6.20	.70
9/16/80	9/29/80	U	-8.14	20.73	13.35	9.43
9/16/80	9/29/80	V	-25.34	10.24	-1.67	9.46

BIWEEKLY PERIOD NUMBER 3

FROM	THROUGH	VARIABLE	MINIMUM	MAXIMUM	MEAN	STD. DEV.
9/30/80	10/13/80	TEMP	7.55	8.74	8.33	.33
9/30/80	10/13/80	U	-2.86	1.68	11.22	5.58
9/30/80	10/13/80	V	-22.63	2.99	-9.28	5.33

BIWEEKLY PERIOD NUMBER 4

FROM	THROUGH	VARIABLE	MINIMUM	MAXIMUM	MEAN	STD. DEV.
10/14/80	10/27/80	TEMP	4.36	8.56	5.98	1.57
10/14/80	10/27/80	U	-8.18	3.37	-.12	3.46
10/14/80	10/27/80	V	-11.16	6.26	-.83	4.51

BIWEEKLY PERIOD NUMBER 5

FROM	THROUGH	VARIABLE	MINIMUM	MAXIMUM	MEAN	STD. DEV.
10/28/80	11/10/80	TEMP	4.45	4.68	4.50	.06
10/28/80	11/10/80	U	-2.32	10.52	2.29	3.16
10/28/80	11/10/80	V	-4.36	4.56	-.12	2.18

BIWEEKLY PERIOD NUMBER 6

FROM	THROUGH	VARIABLE	MINIMUM	MAXIMUM	MEAN	STD. DEV.
11/11/80	11/24/80	TEMP	4.71	6.15	5.36	.34
11/11/80	11/24/80	U	-5.30	3.65	6.20	5.97
11/11/80	11/24/80	V	-12.83	11.02	-.29	4.93

BIWEEKLY PERIOD NUMBER 7

FROM	THROUGH	VARIABLE	MINIMUM	MAXIMUM	MEAN	STD. DEV.
11/25/80	12/ 8/80	TEMP	5.34	7.87	6.44	.70
11/25/80	12/ 8/80	U	-4.57	1.90	10.62	8.59
11/25/80	12/ 8/80	V	-1.85	14.43	6.37	3.65

Figure A-36. Statistical parameters of temperature, u component, and v component for the first deployment period for current meter 12401.

BIWEEKLY PERIOD NUMBER 8

FROM	THROUGH	VARIABLE	MINIMUM	MAXIMUM	MEAN	STD. DEV.
12/ 9/80	12/22/80	TEMP	4.20	7.52	5.48	1.05
12/ 9/80	12/22/80	U	-4.64	5.44	5.21	5.01
12/ 9/80	12/22/80	V	-10.48	9.41	.10	4.69

BIWEEKLY PERIOD NUMBER 9

FROM	THROUGH	VARIABLE	MINIMUM	MAXIMUM	MEAN	STD. DEV.
12/23/80	1/ 5/81	TEMP	5.02	6.75	5.97	.52
12/23/80	1/ 5/81	U	-4.88	1.79	3.28	5.78
12/23/80	1/ 5/81	V	-16.17	10.20	1.24	6.26

BIWEEKLY PERIOD NUMBER 10

FROM	THROUGH	VARIABLE	MINIMUM	MAXIMUM	MEAN	STD. DEV.
1/ 6/81	1/19/81	TEMP	5.44	8.31	7.32	.82
1/ 6/81	1/19/81	U	-4.57	1.41	3.07	5.18
1/ 6/81	1/19/81	V	-1.24	10.42	6.04	2.66

BIWEEKLY PERIOD NUMBER 11

FROM	THROUGH	VARIABLE	MINIMUM	MAXIMUM	MEAN	STD. DEV.
1/20/81	2/ 2/81	TEMP	4.31	8.97	6.46	1.75
1/20/81	2/ 2/81	U	-3.23	6.08	3.06	2.46
1/20/81	2/ 2/81	V	-4.89	10.99	3.61	4.91

BIWEEKLY PERIOD NUMBER 12

FROM	THROUGH	VARIABLE	MINIMUM	MAXIMUM	MEAN	STD. DEV.
2/ 3/81	2/16/81	TEMP	4.28	6.83	5.20	.70
2/ 3/81	2/16/81	U	-6.38	7.64	4.66	4.45
2/ 3/81	2/16/81	V	-11.53	9.43	-.62	4.38

BIWEEKLY PERIOD NUMBER 13

FROM	THROUGH	VARIABLE	MINIMUM	MAXIMUM	MEAN	STD. DEV.
2/17/81	3/ 2/81	TEMP	5.29	8.11	6.61	.76
2/17/81	3/ 2/81	U	-7.86	4.59	2.57	3.91
2/17/81	3/ 2/81	V	-12.03	12.04	2.27	6.97

BIWEEKLY PERIOD NUMBER 14

FROM	THROUGH	VARIABLE	MINIMUM	MAXIMUM	MEAN	STD. DEV.
3/ 3/81	3/10/81	TEMP	4.53	5.75	5.06	.35
3/ 3/81	3/10/81	U	-14.25	4.32	-.90	7.36
3/ 3/81	3/10/81	V	-12.13	19.38	4.26	8.99

FOR THE ENTIRE TIME PERIOD

FROM	THROUGH	VARIABLE	MINIMUM	MAXIMUM	MEAN	STD. DEV.
9/ 2/80	3/10/81	TEMP	4.20	8.97	6.04	1.29
9/ 2/80	3/10/81	U	-18.84	20.73	5.20	7.59
9/ 2/80	3/10/81	V	-25.34	20.74	.28	7.38

Figure A-36. Continued.

APPENDIX B

DATA PRODUCTS
SECOND DEPLOYMENT

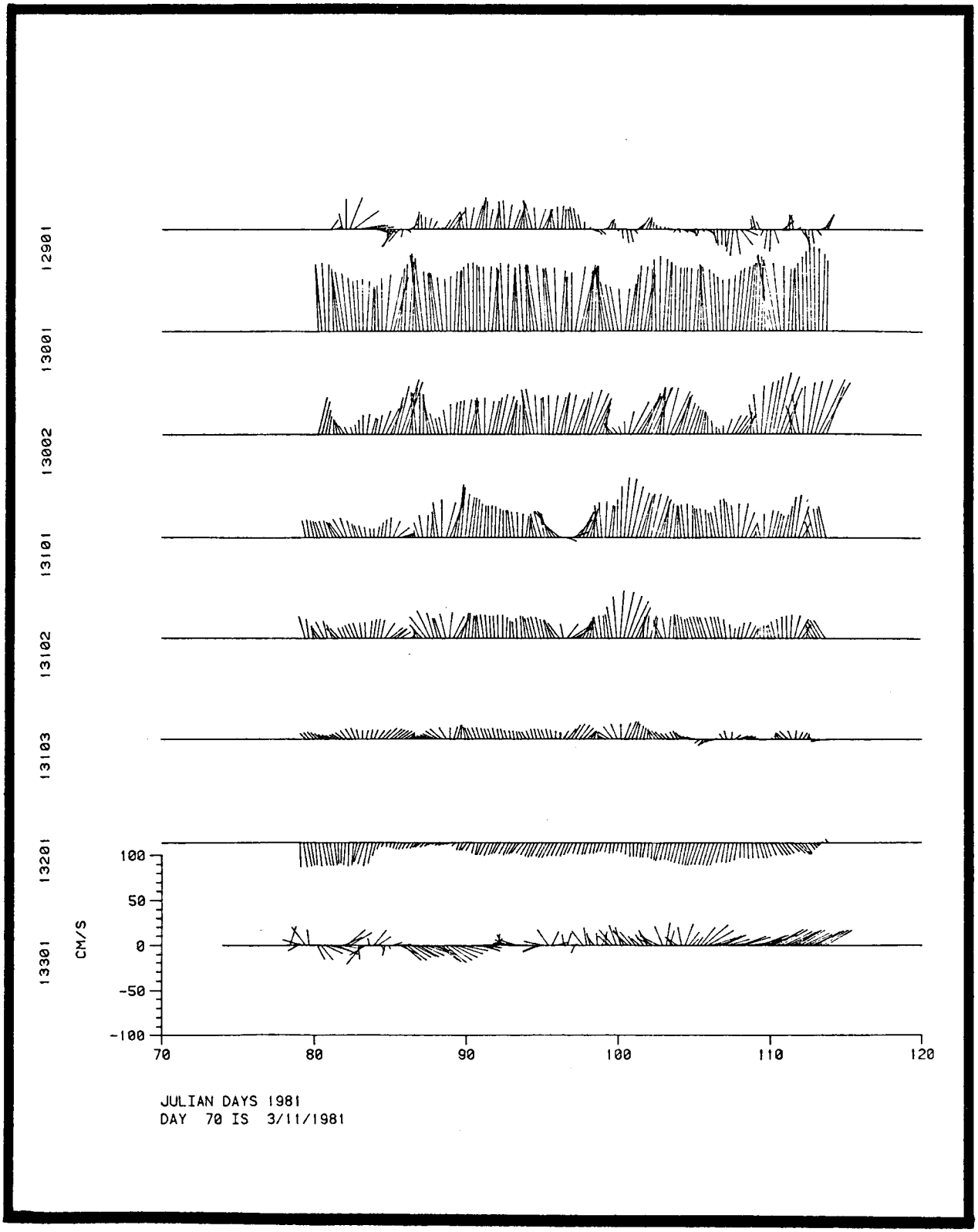

Figure B-1. Stick plot of currents during indicated period of second deployment (40-HLP data).

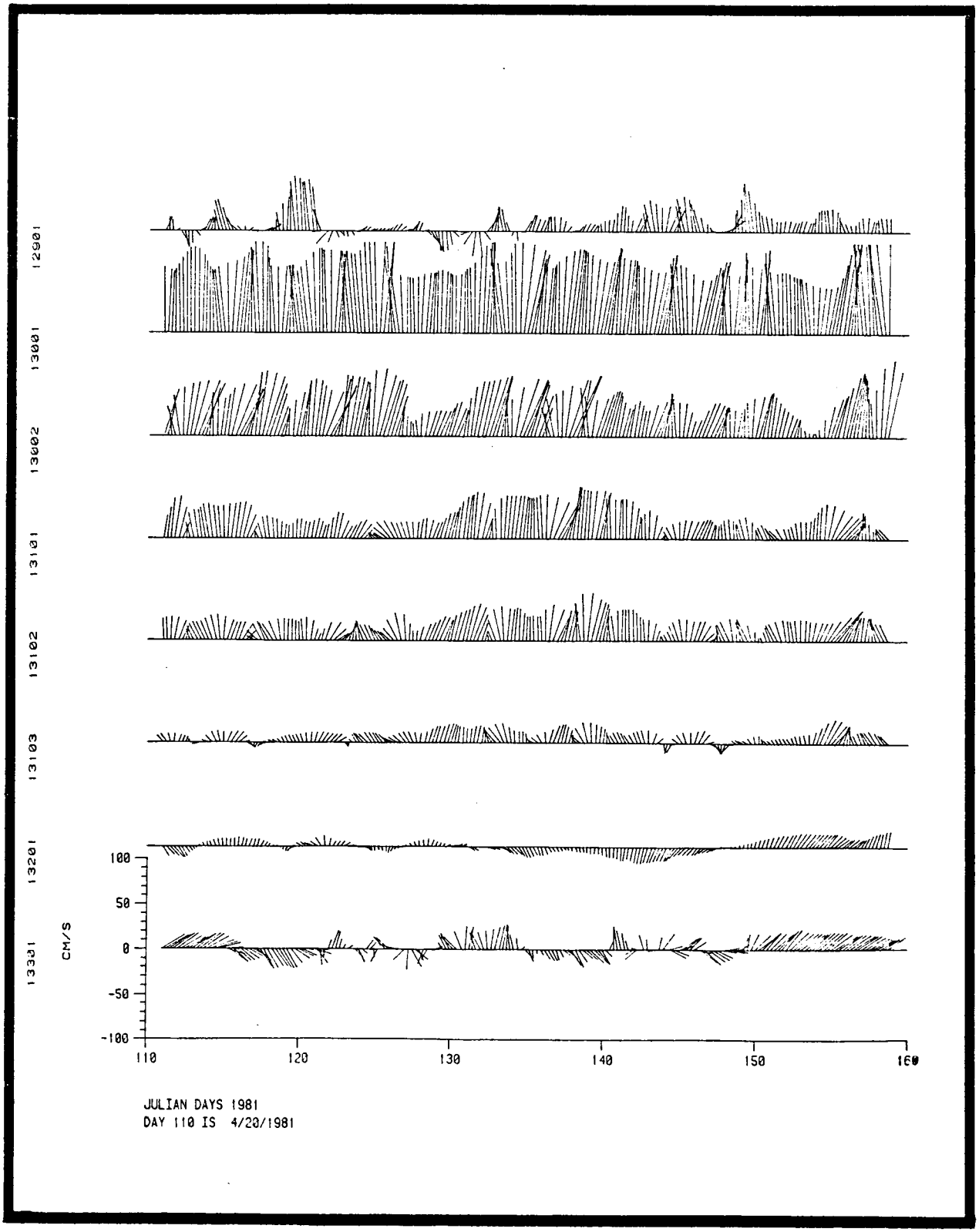

Figure B-2. Stick plot of currents during indicated period of second deployment (40-HLP data).

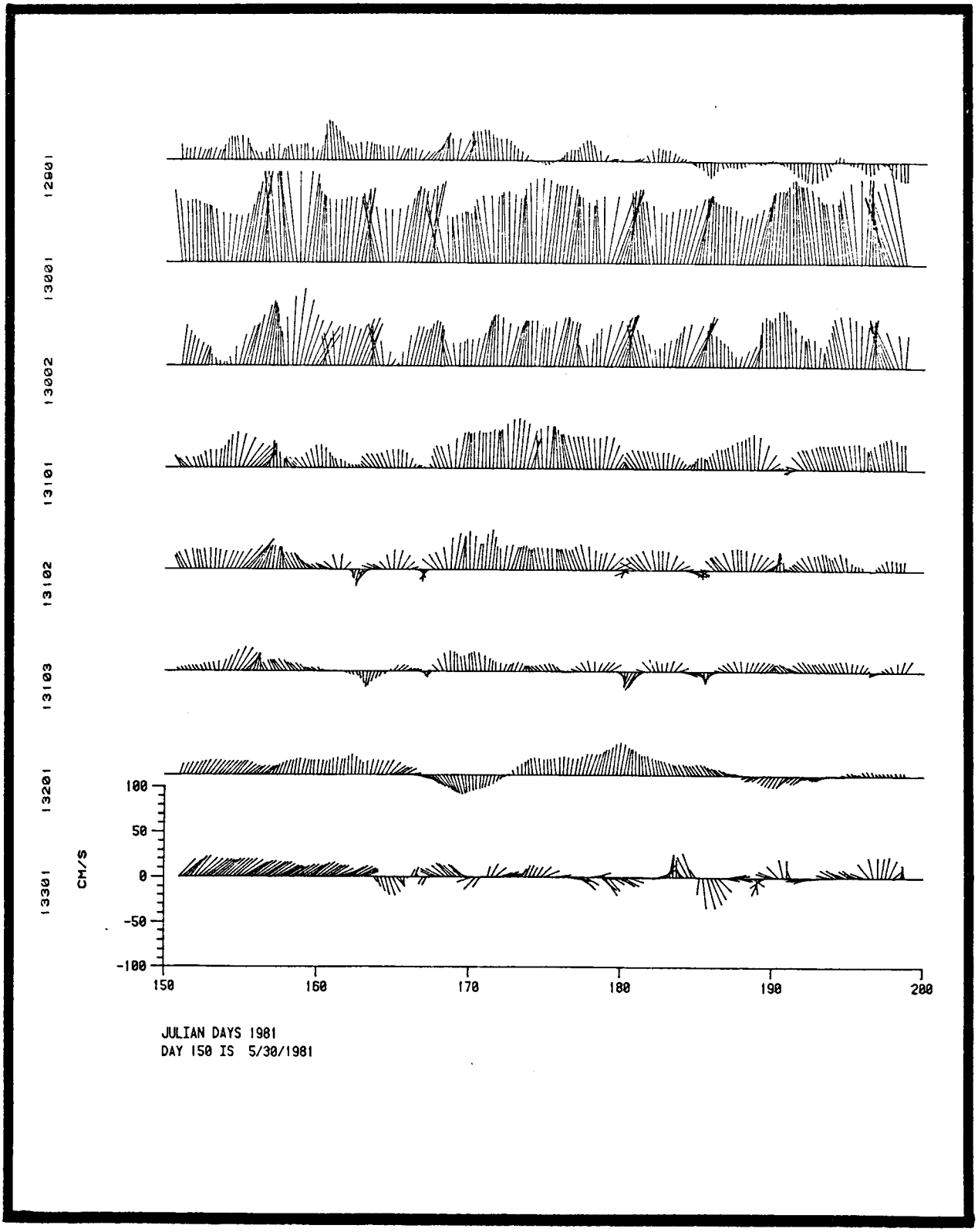

Figure B-3. Stick plot of currents during indicated period of second deployment (40-HLP data).

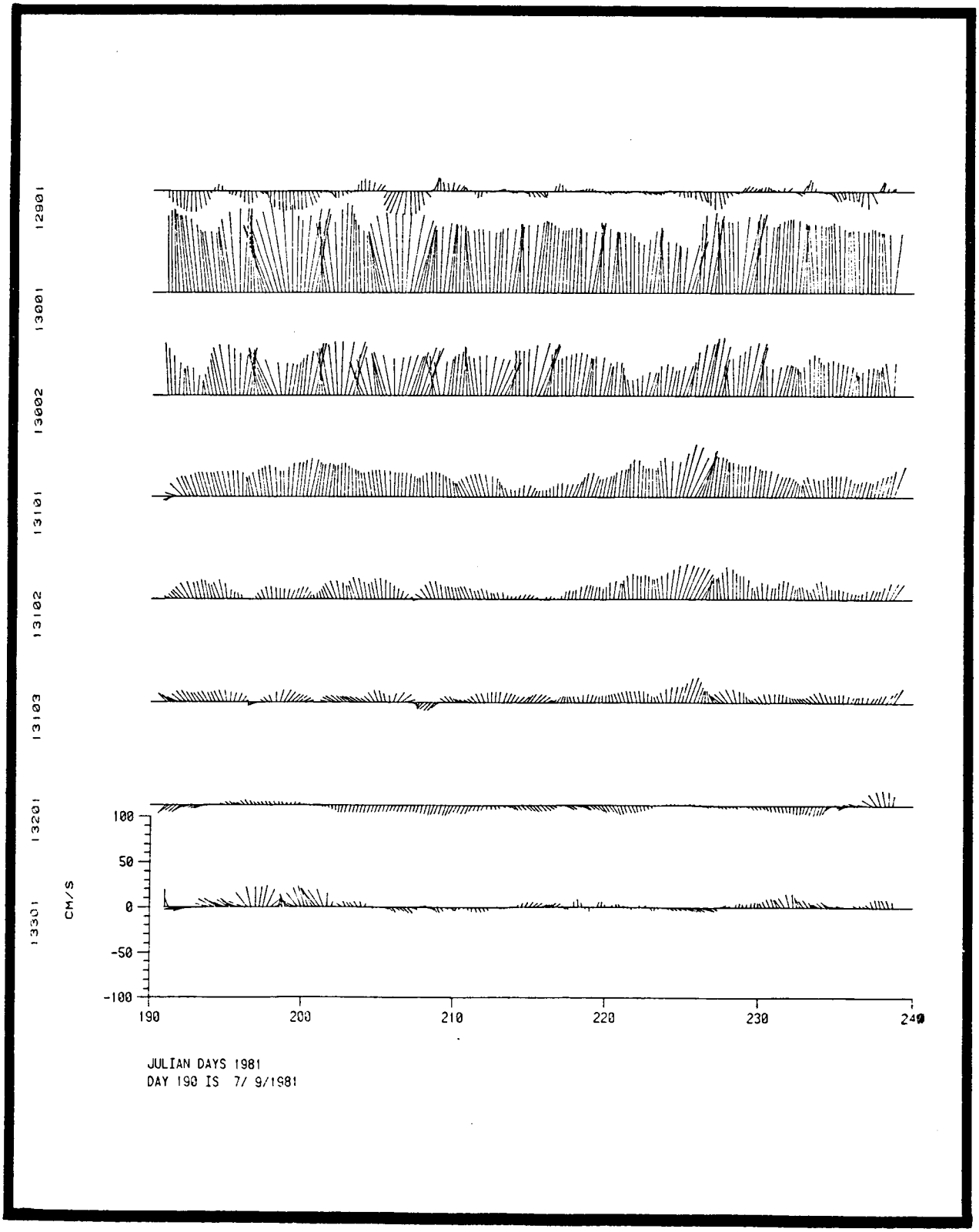

Figure B-4. Stick plot of currents during indicated period of second deployment (40-HLP data).

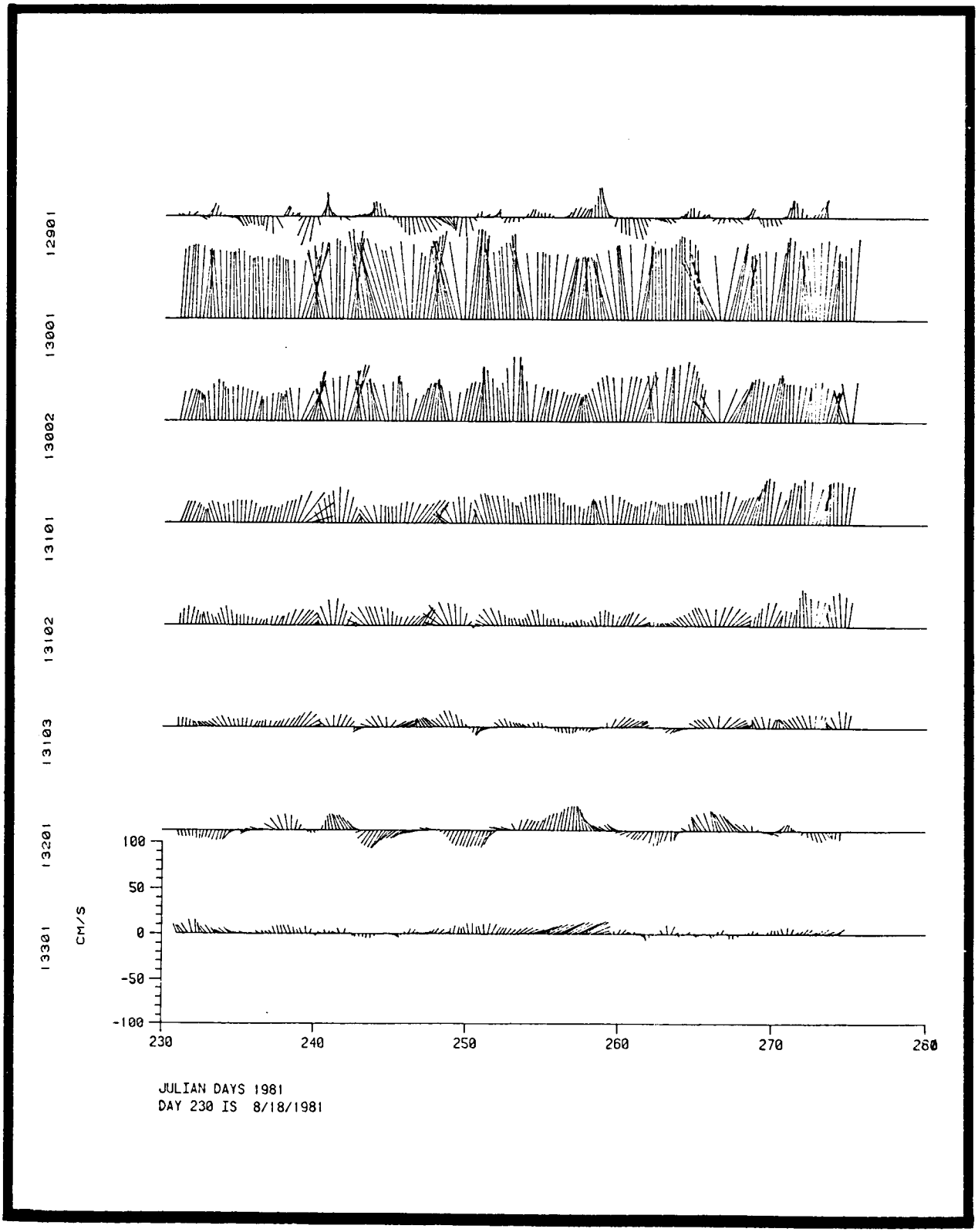

Figure B-5. Stick plot of currents during indicated period of second deployment (40-HLP data).

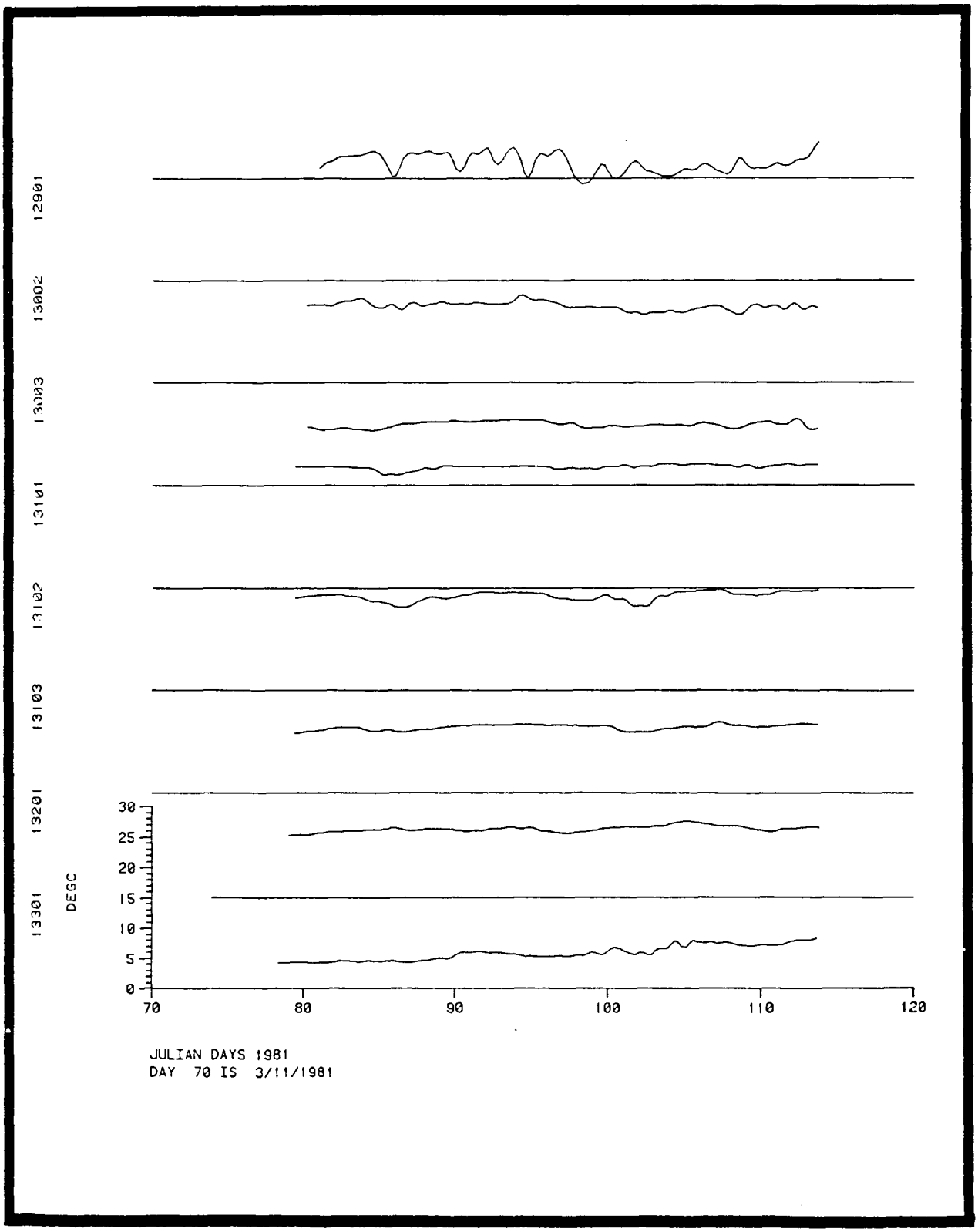

Figure B-6. Temperature time series plot during indicated period of second deployment (40-HLP data).

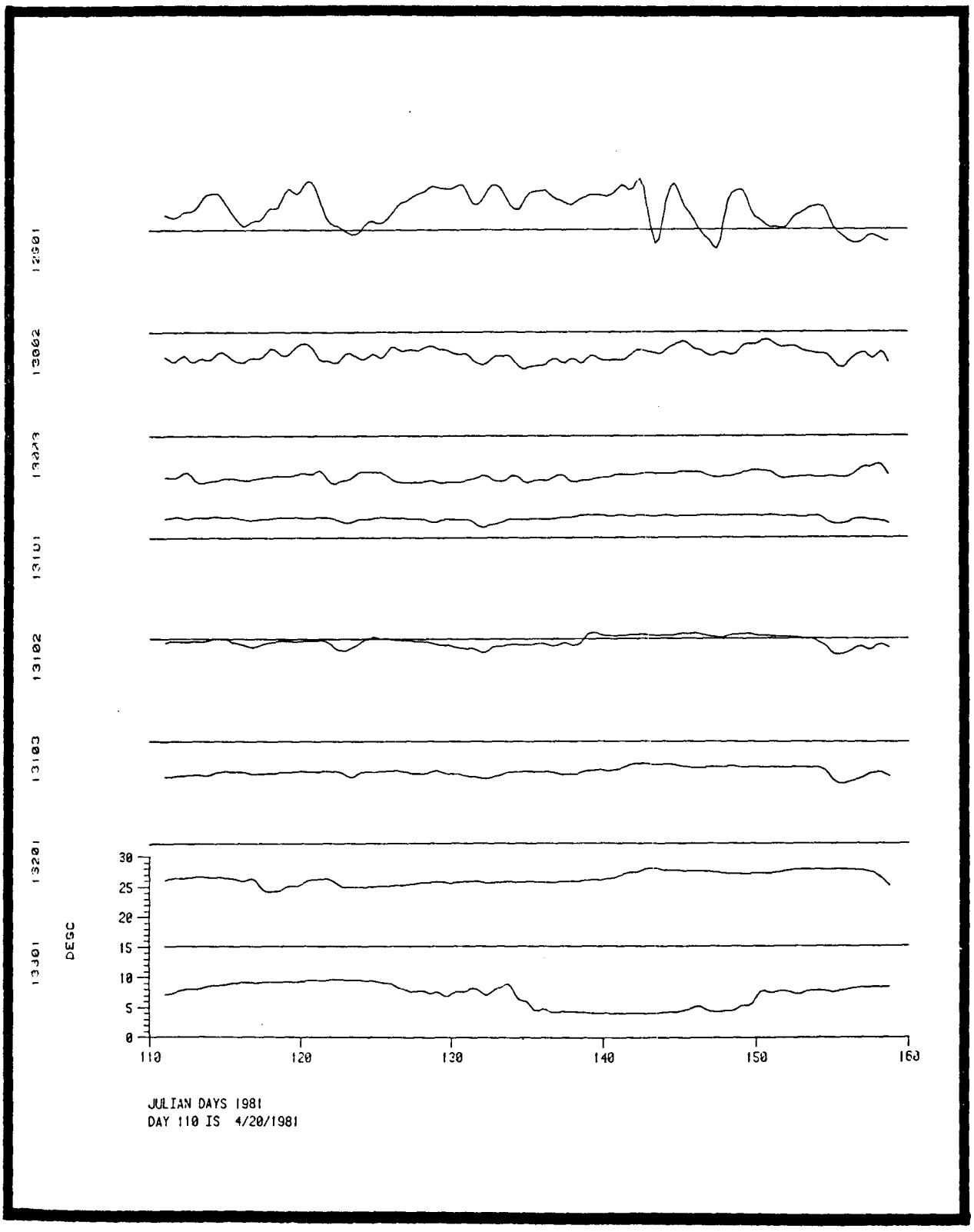

Figure B-7. Temperature time series plot during indicated period of second deployment (40-HLP data).

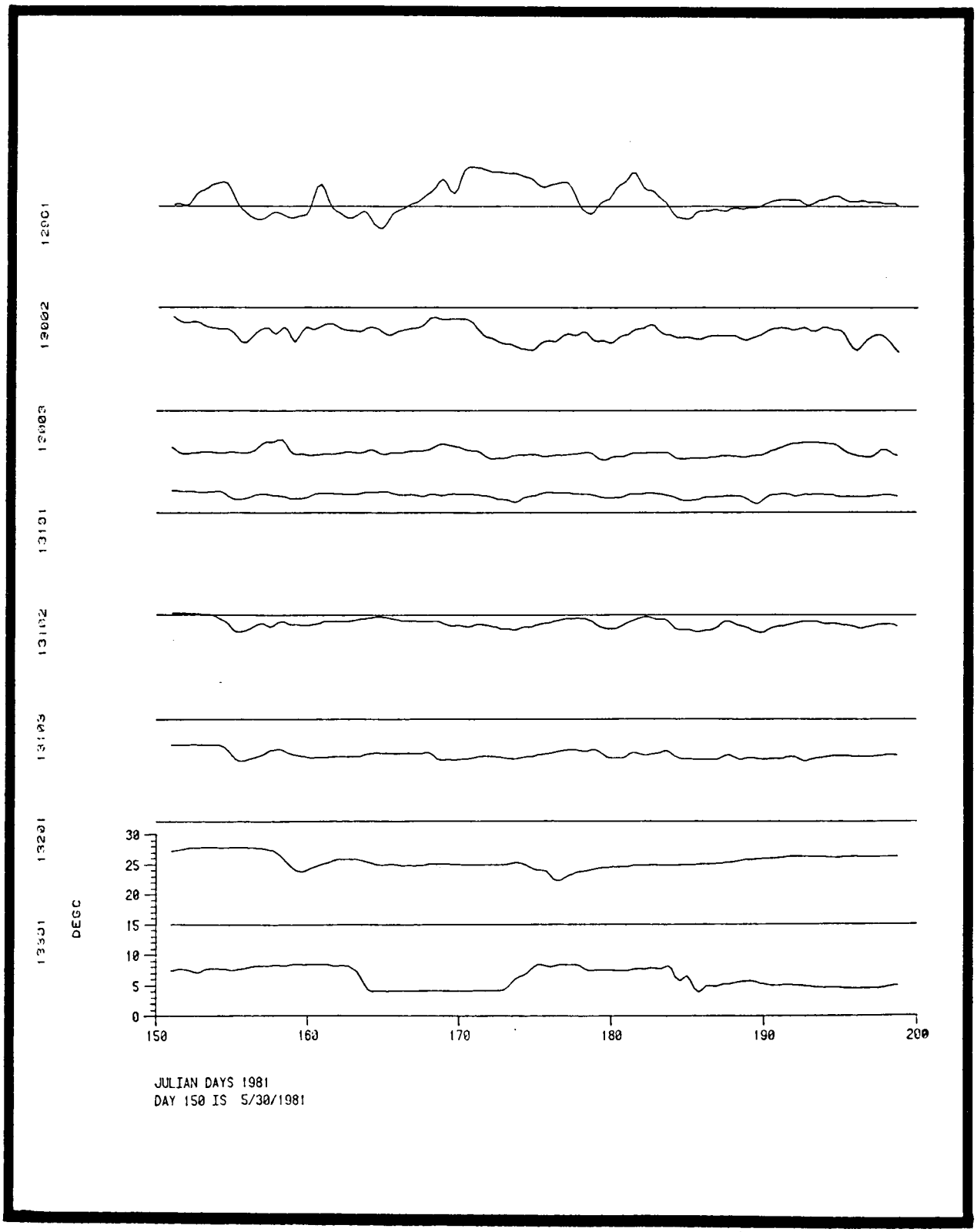

Figure B-8. Temperature time series plot during indicated period of second deployment (40-HLP data).

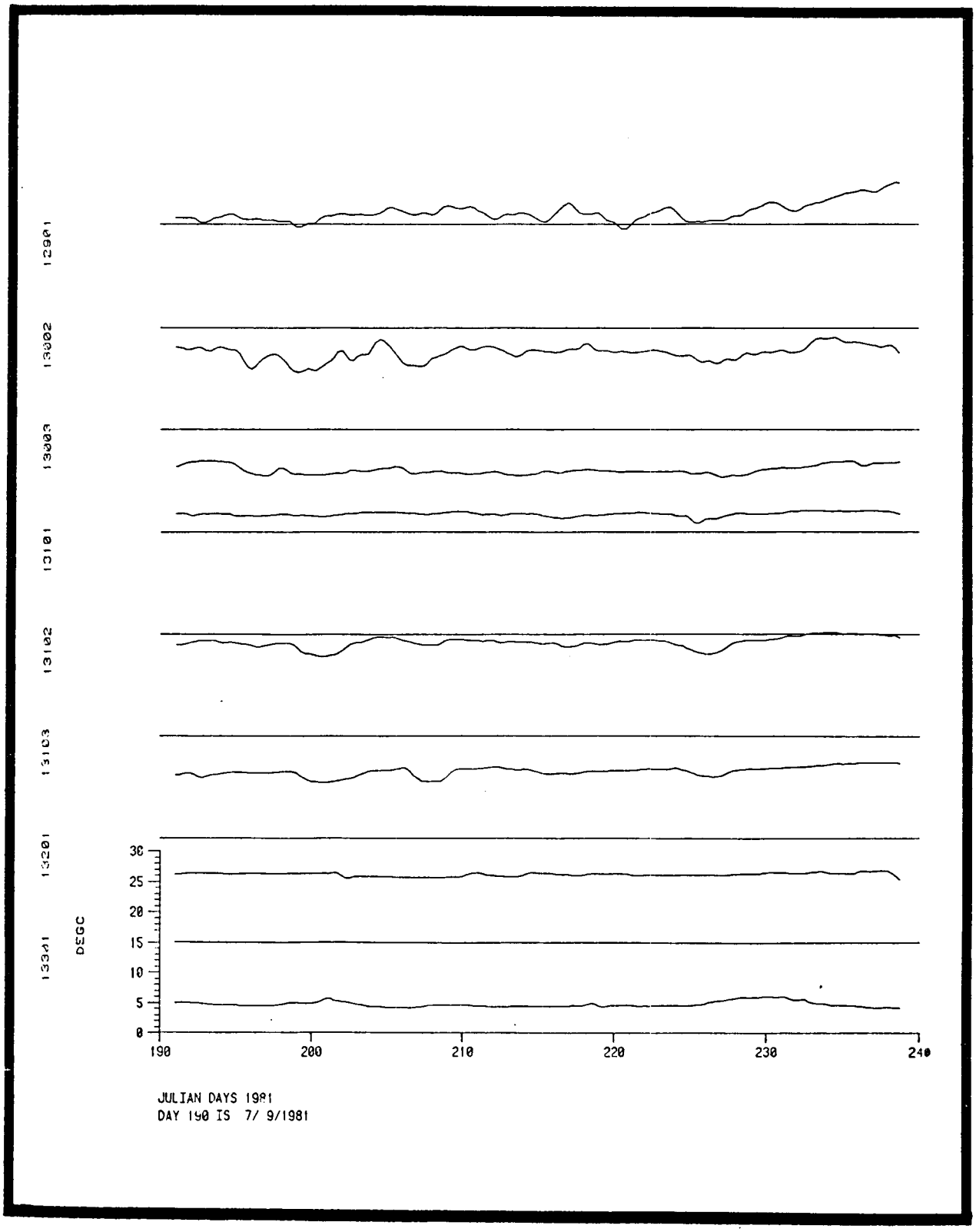

Figure B-9. Temperature time series plot during indicated period of second deployment (40-HLP data).

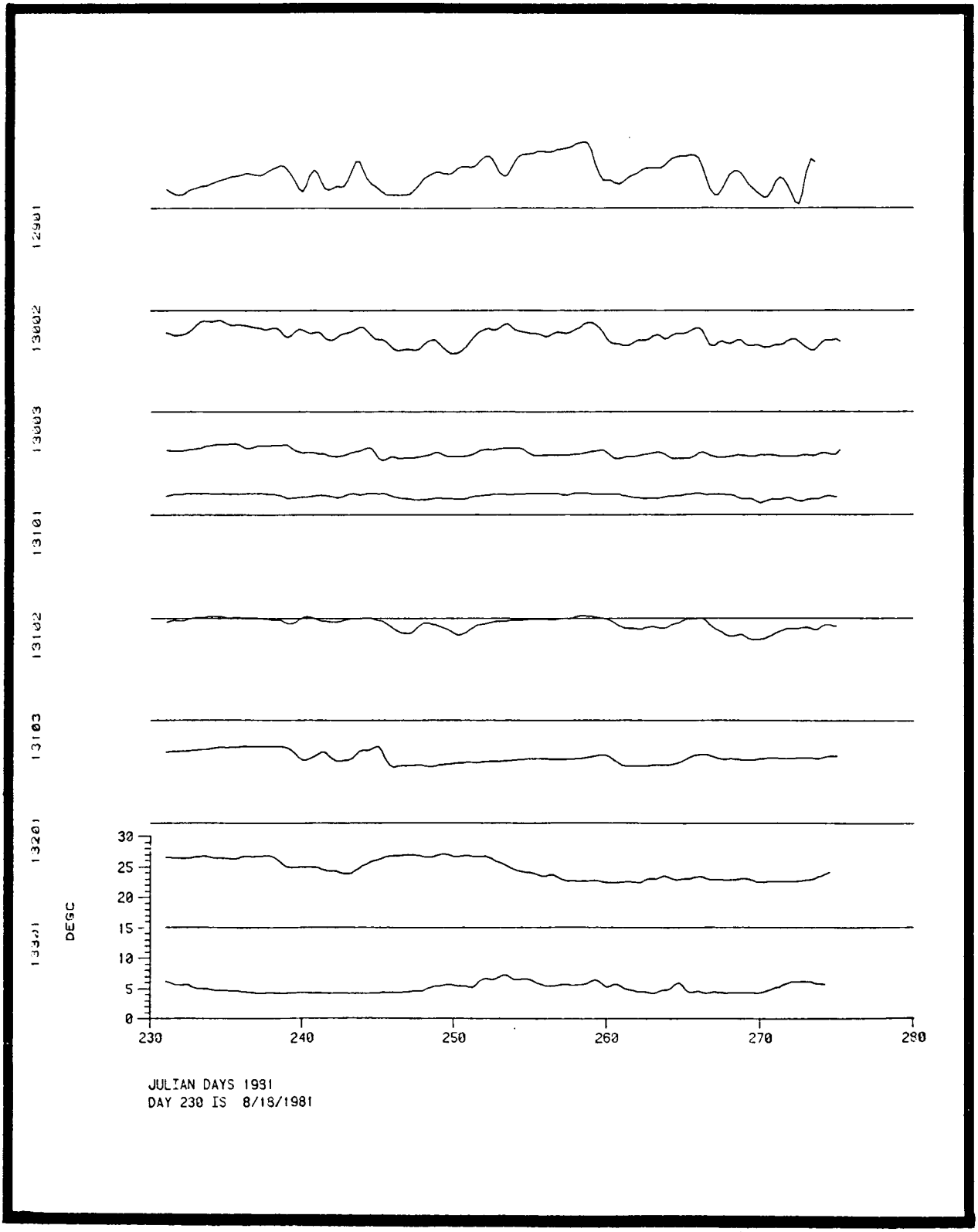

Figure B-10. Temperature time series plot during indicated period of second deployment (40-HLP data).

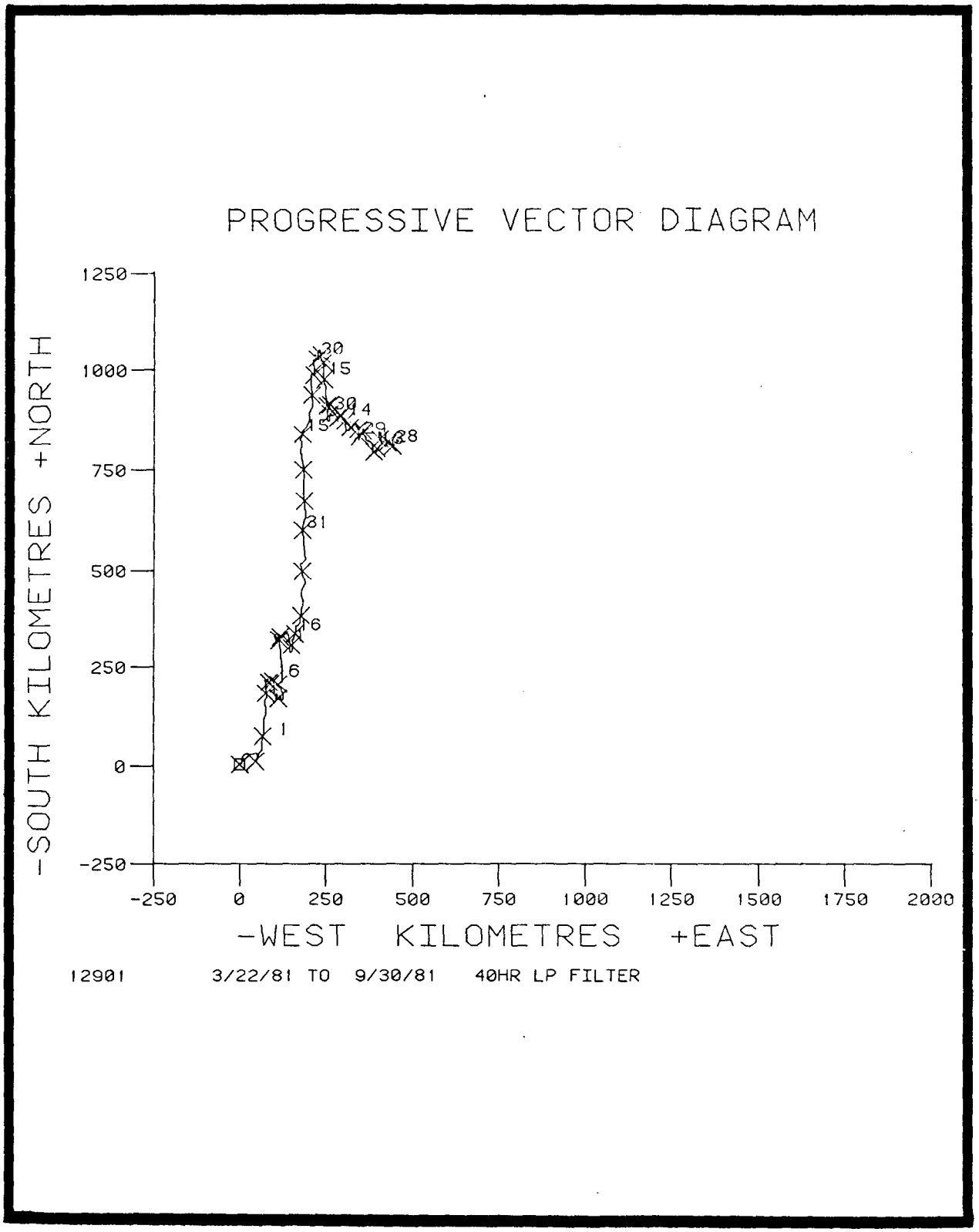

Figure B-11. Progressive vector diagram of currents measured by current meter 12901 during second deployment.

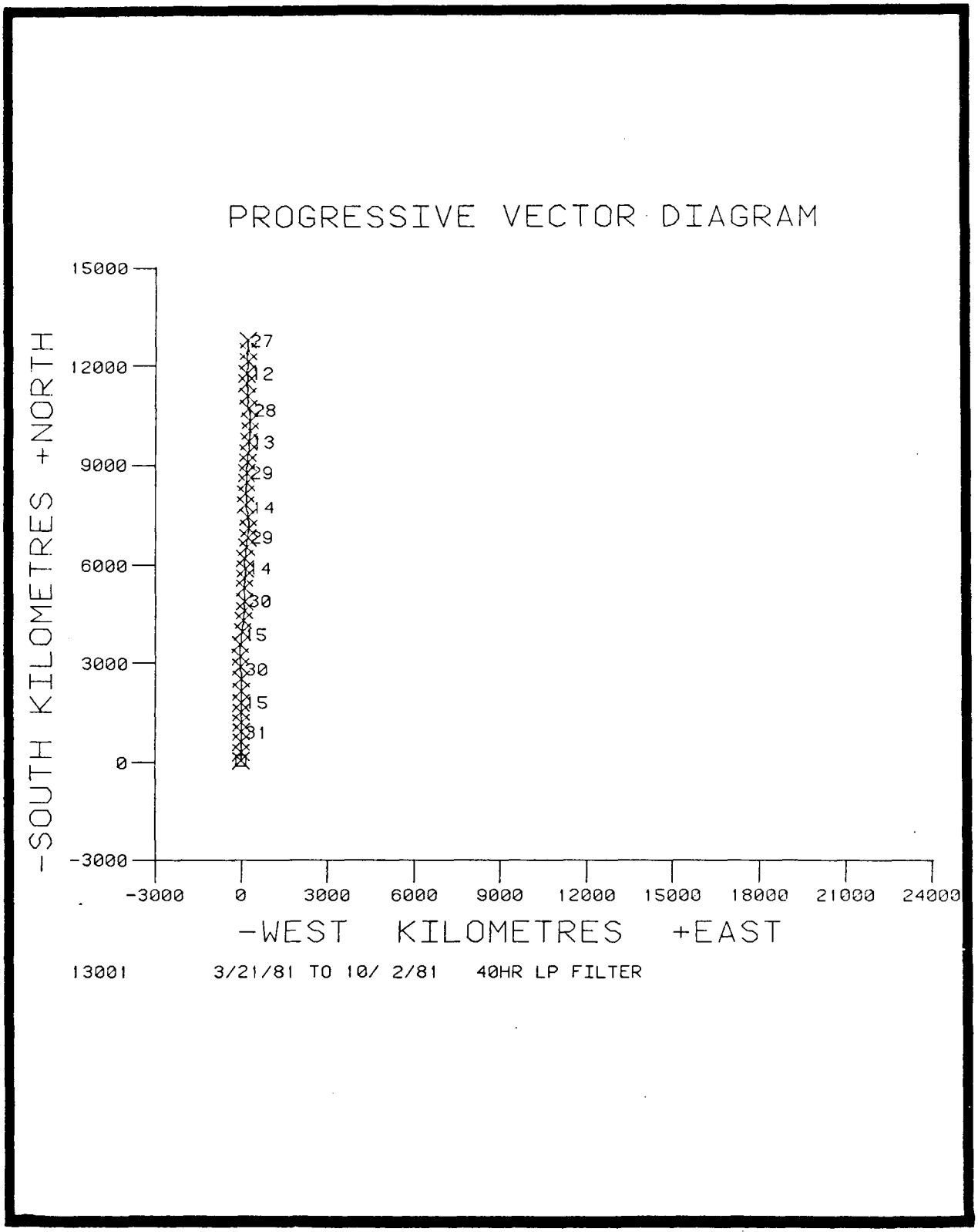

Figure B-12. Progressive vector diagram of currents measured by current meter 13001 during second deployment.

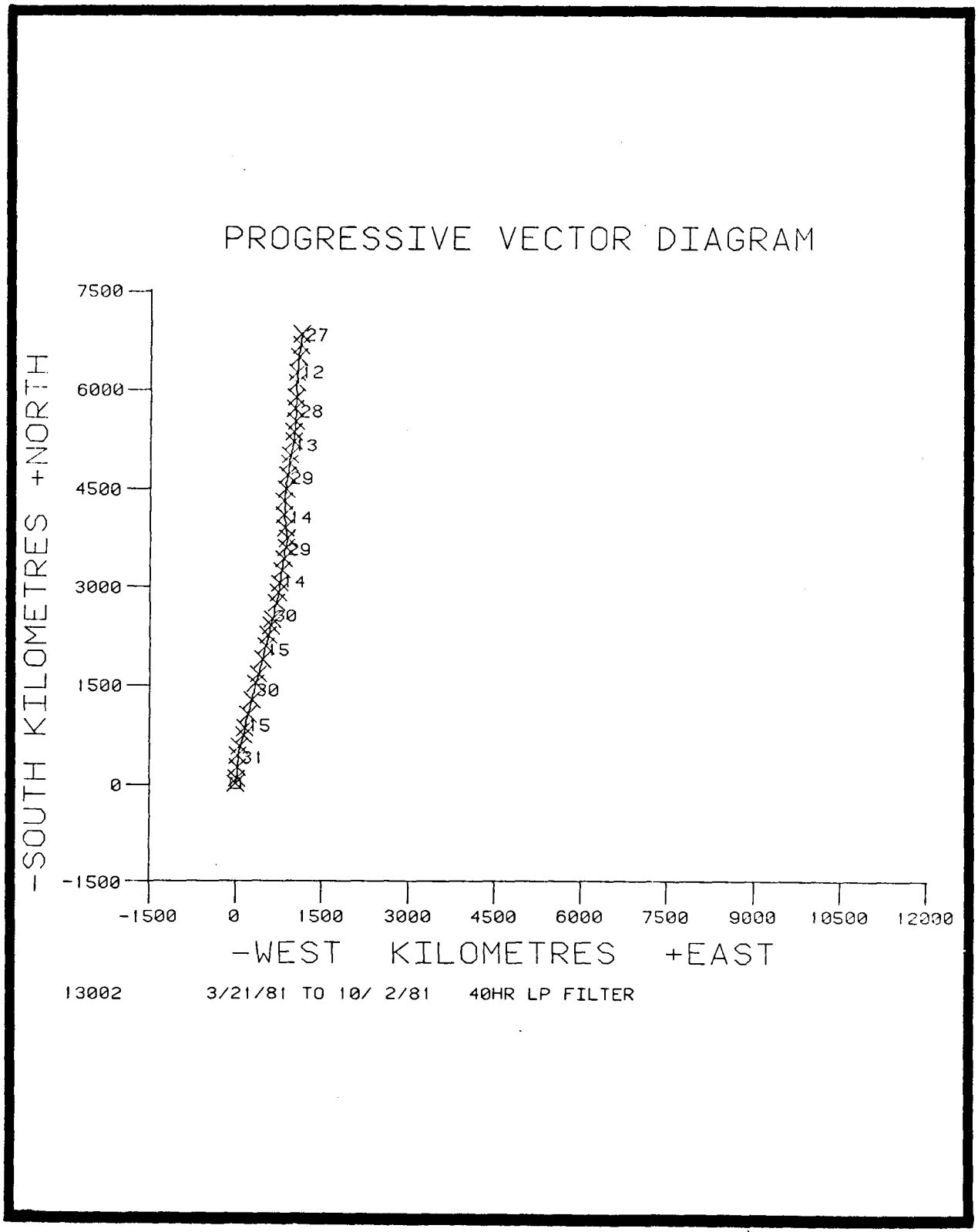

Figure B-13. Progressive vector diagram of currents measured by current meter 13002 during second deployment.

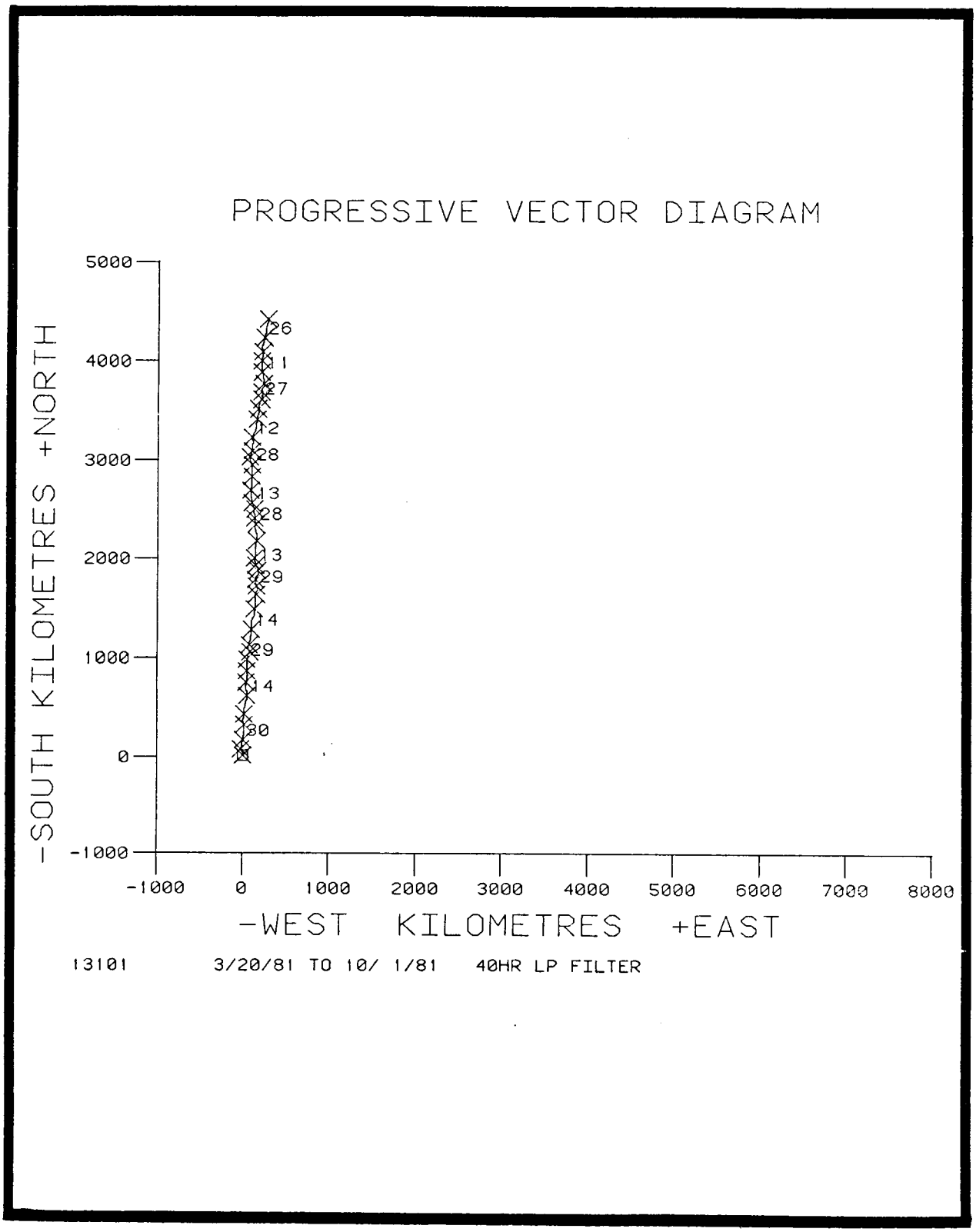

Figure B-14. Progressive vector diagram of currents measured by current meter 13101 during second deployment.

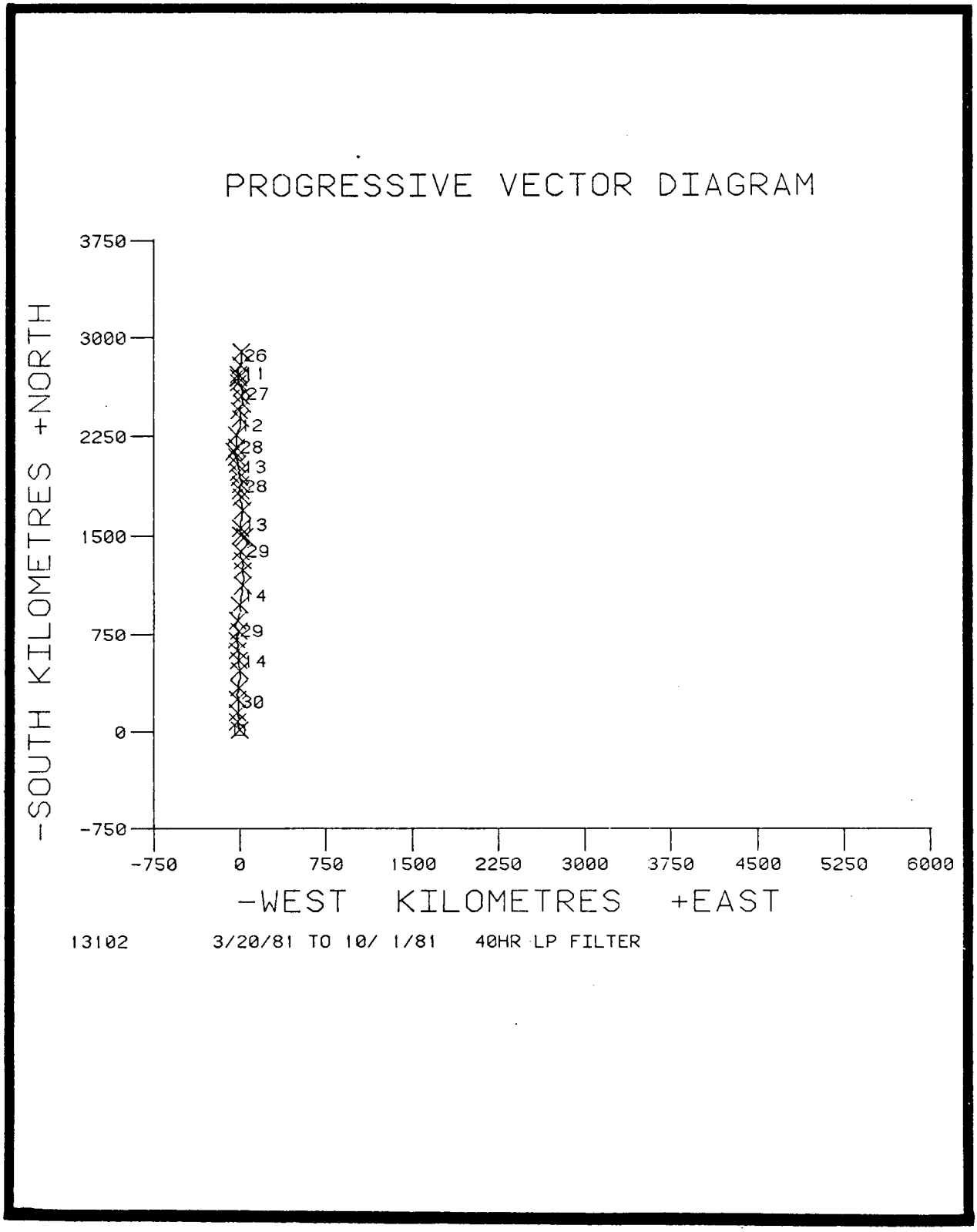

Figure B-15. Progressive vector diagram of currents measured by current meter 13102 during second deployment.

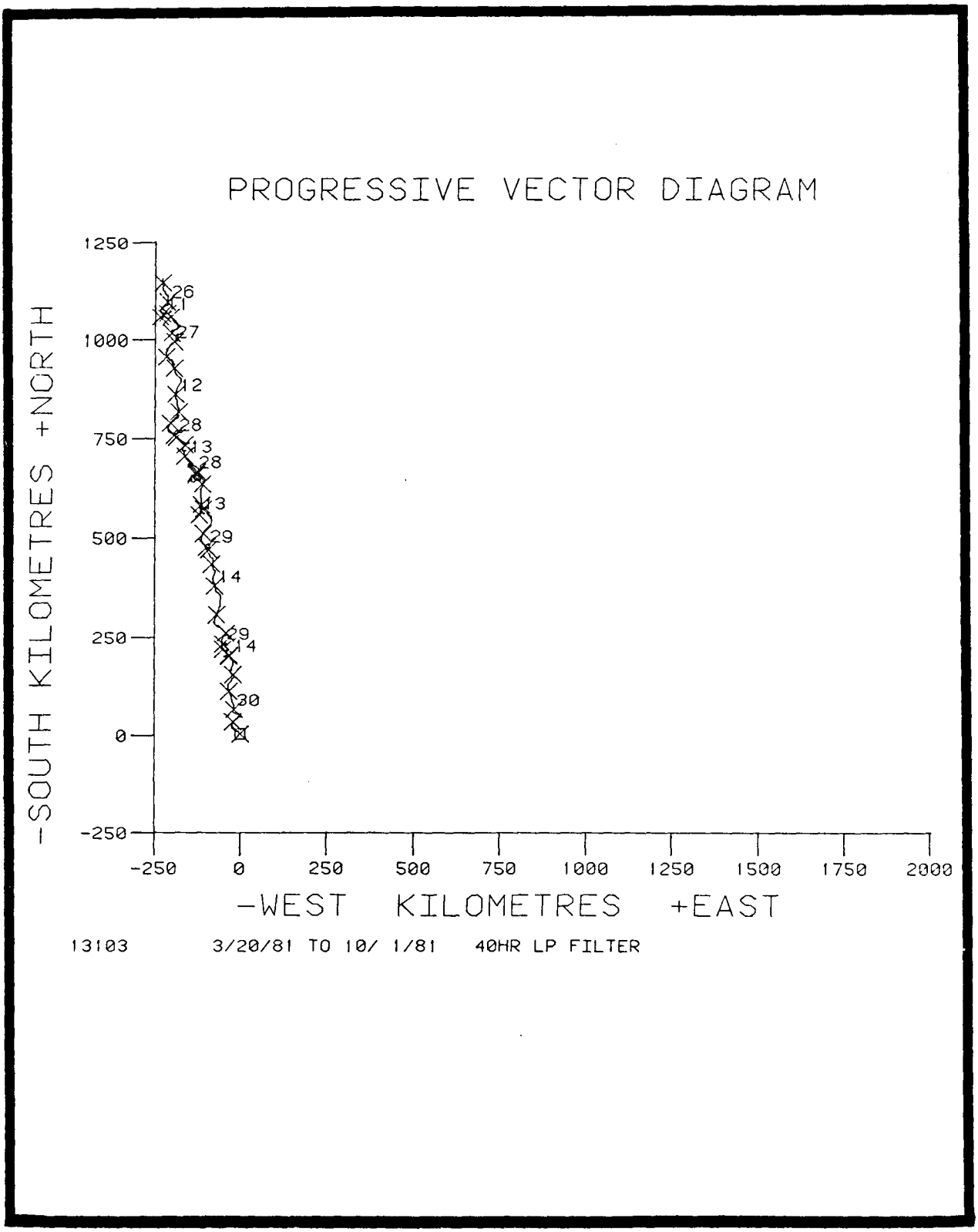

Figure B-16. Progressive vector diagram of currents measured by current meter 13103 during second deployment.

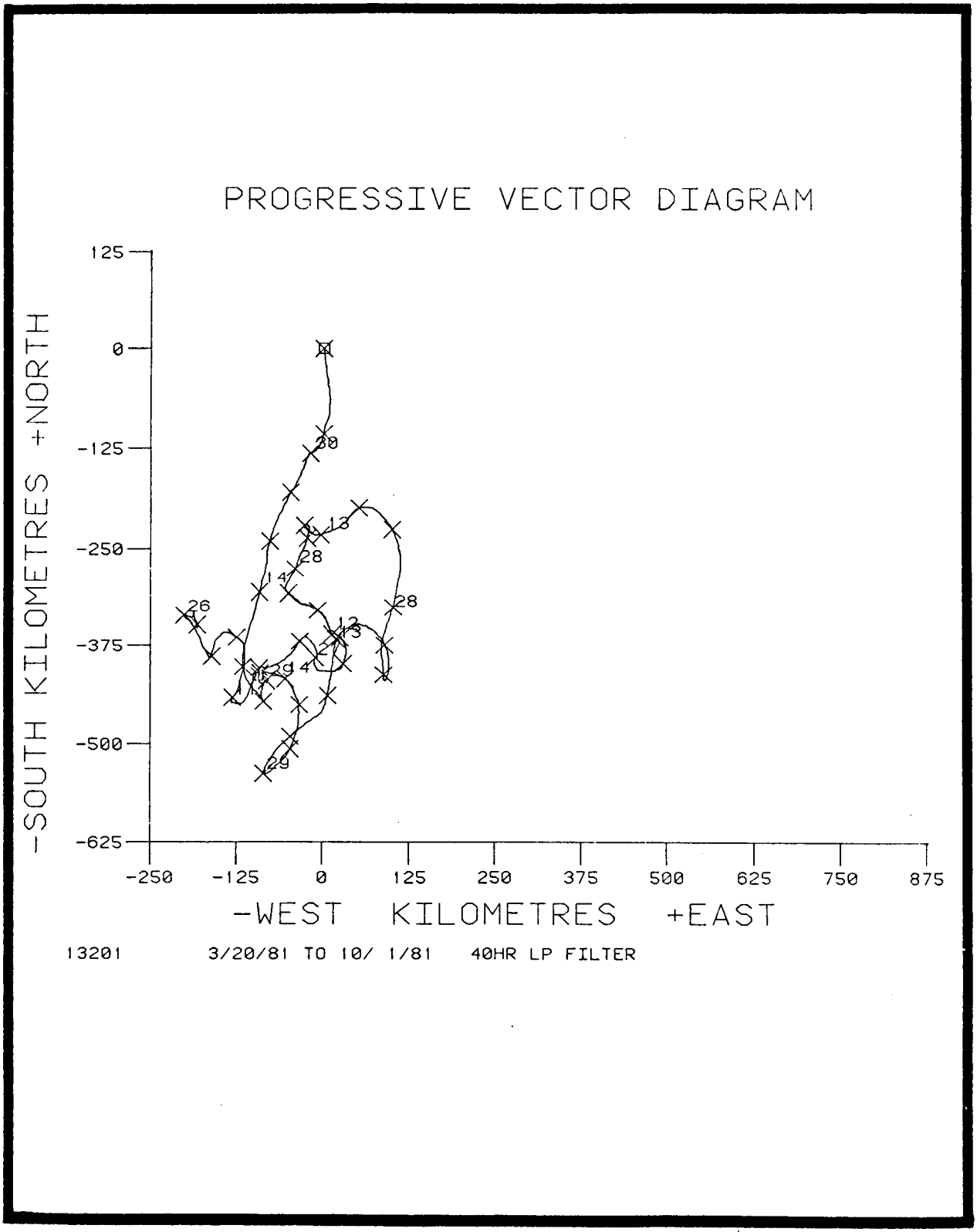

Figure B-17. Progressive vector diagram of currents measured by current meter 13201 during second deployment.

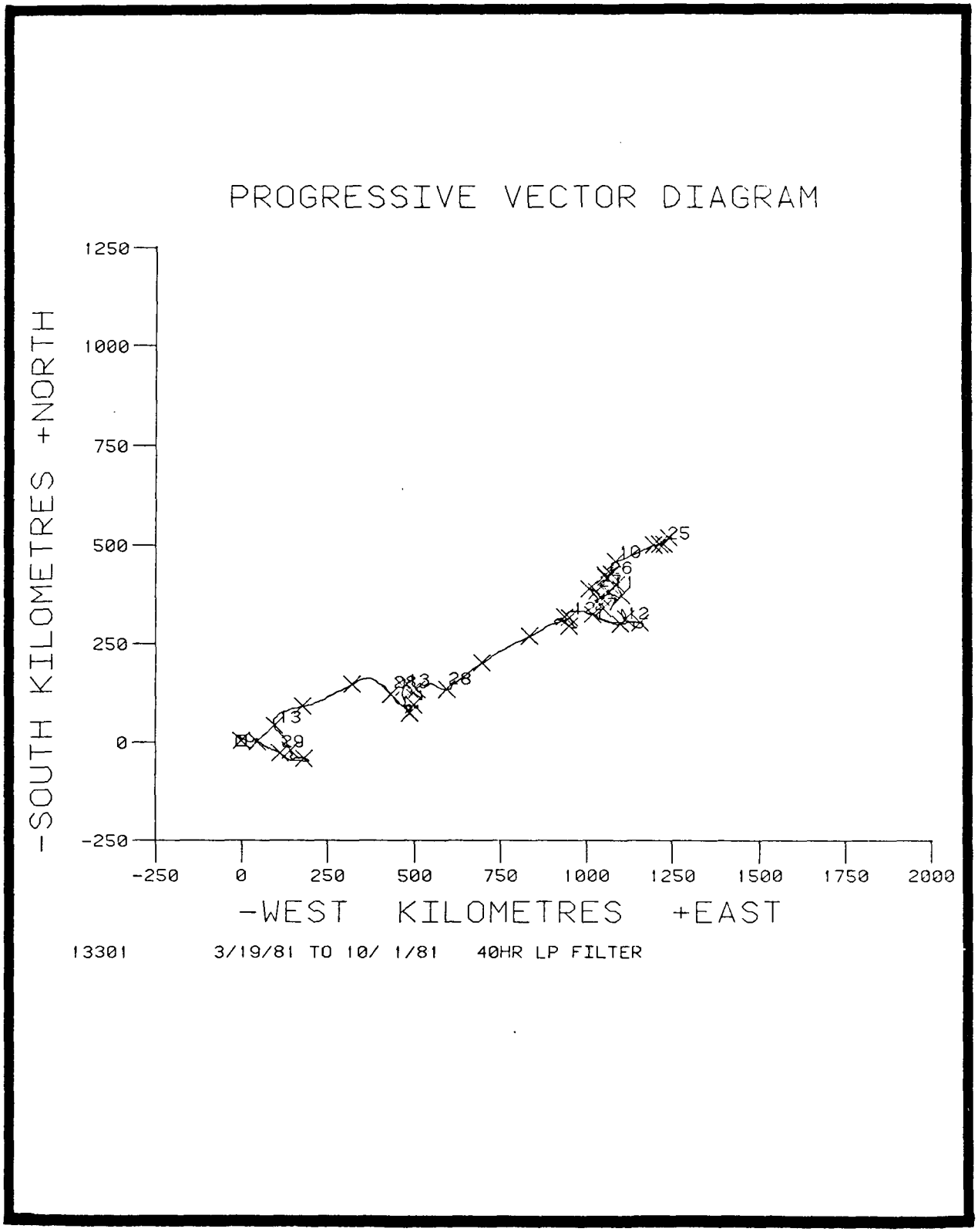

Figure B-18. Progressive vector diagram of currents measured by current meter 13301 during second deployment.

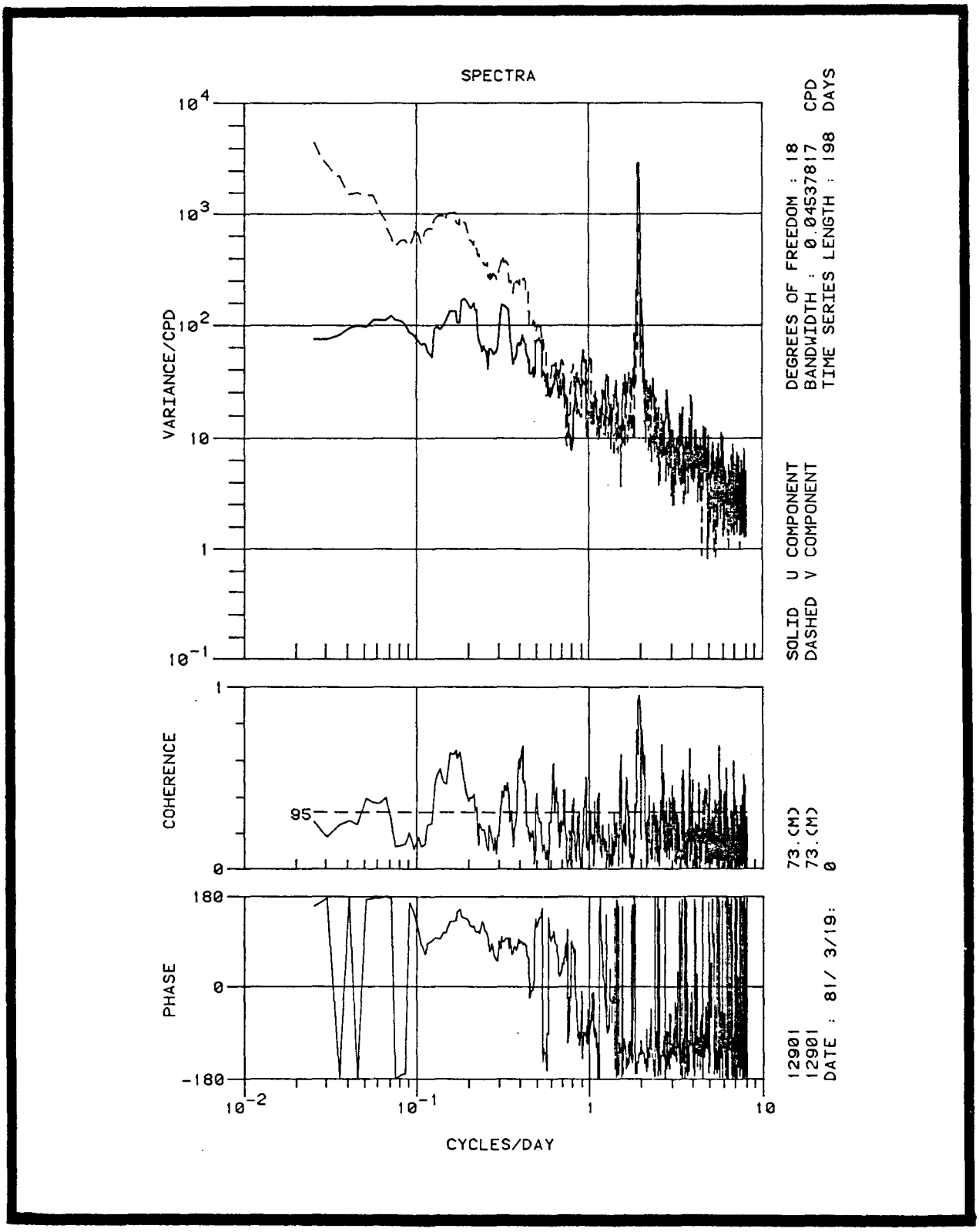

Figure B-19. Spectra of u component vs v component from current meter 12901 during second deployment.

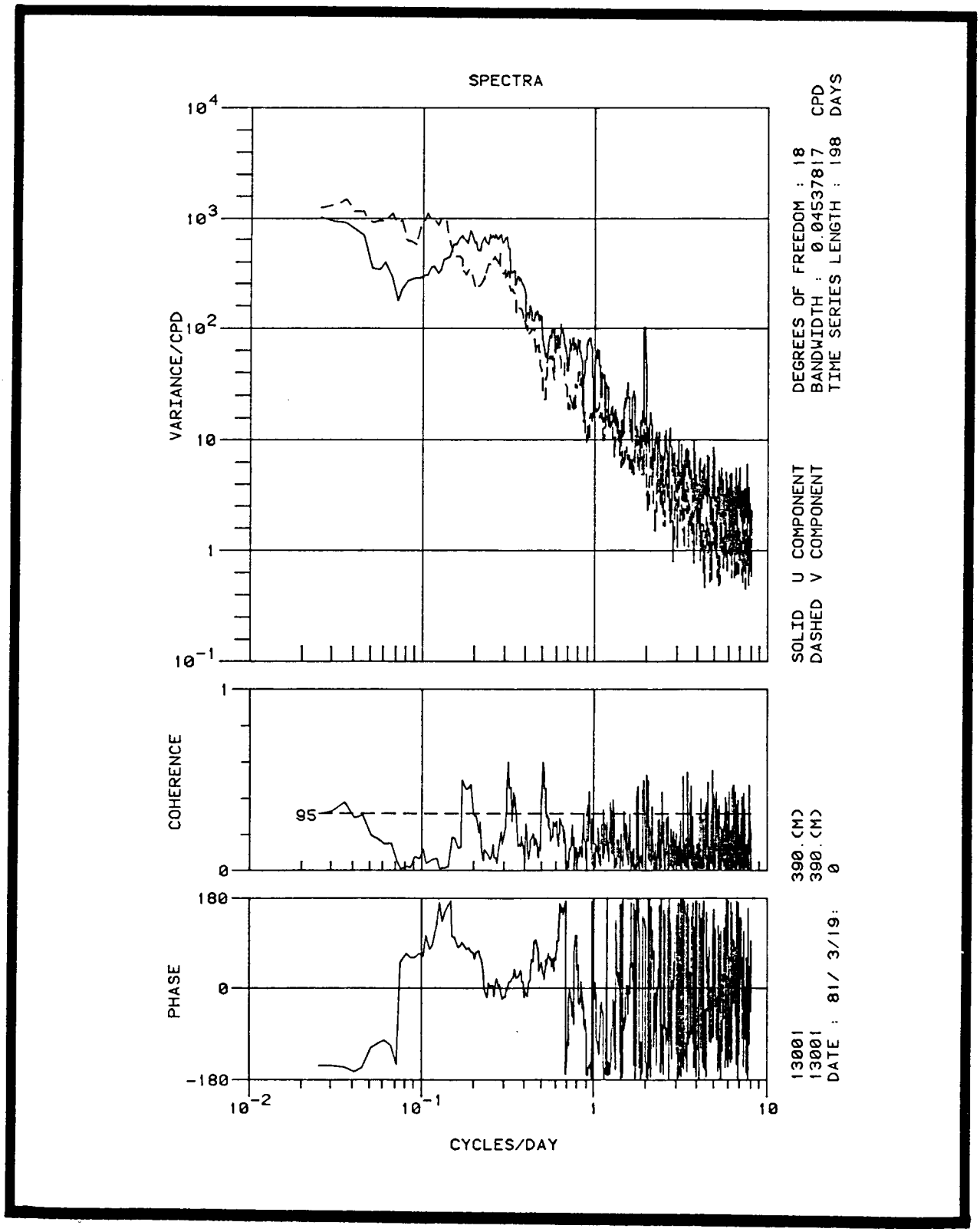

Figure B-20. Spectra of u component vs v component from current meter 13001 during second deployment.

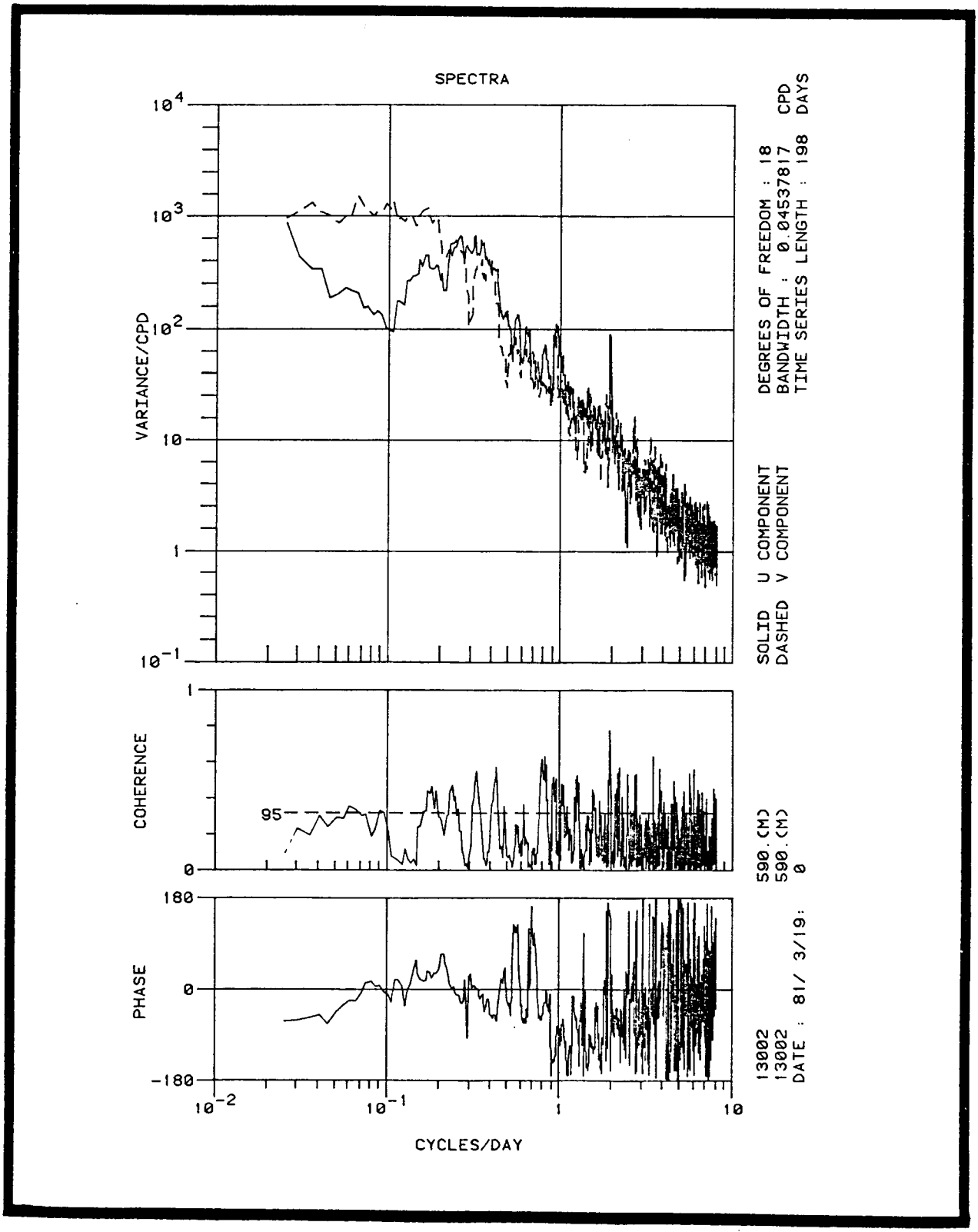

Figure B-21. Spectra of u component vs v component from current meter 13002 during second deployment.

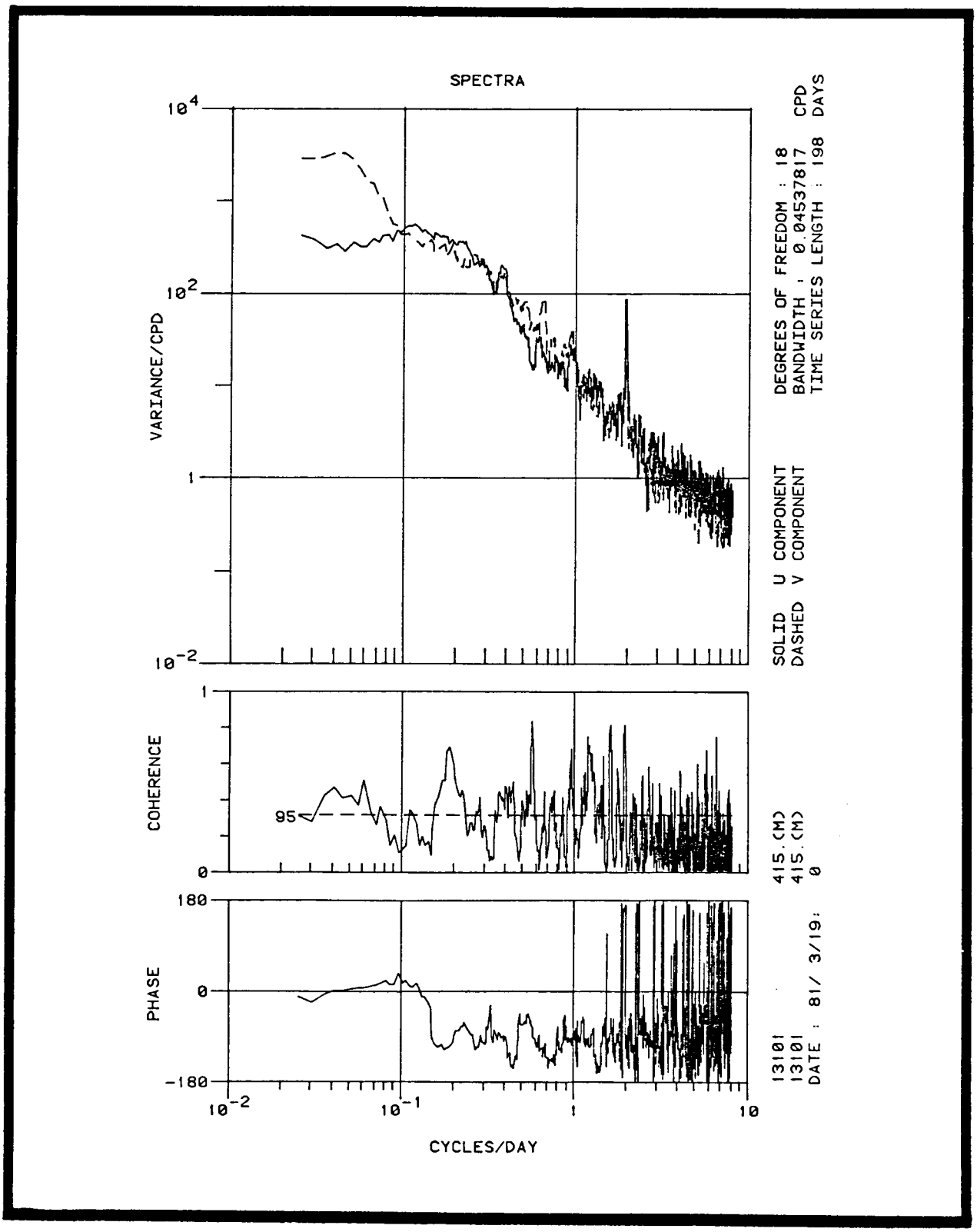

Figure B-22. Spectra of u component vs v component from current meter 13101 during second deployment.

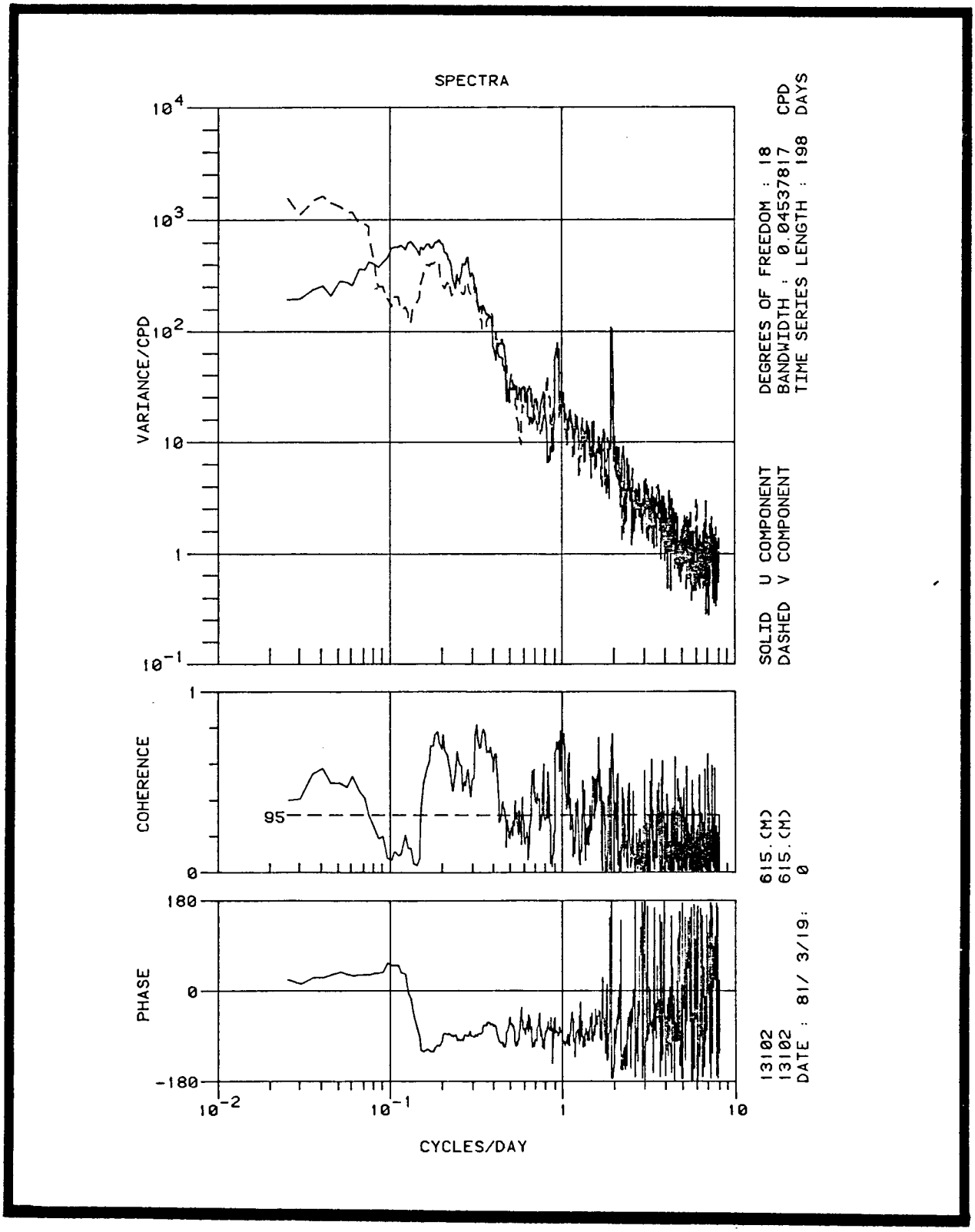

Figure B-23. Spectra of u component vs v component from current meter 13102 during the second deployment.

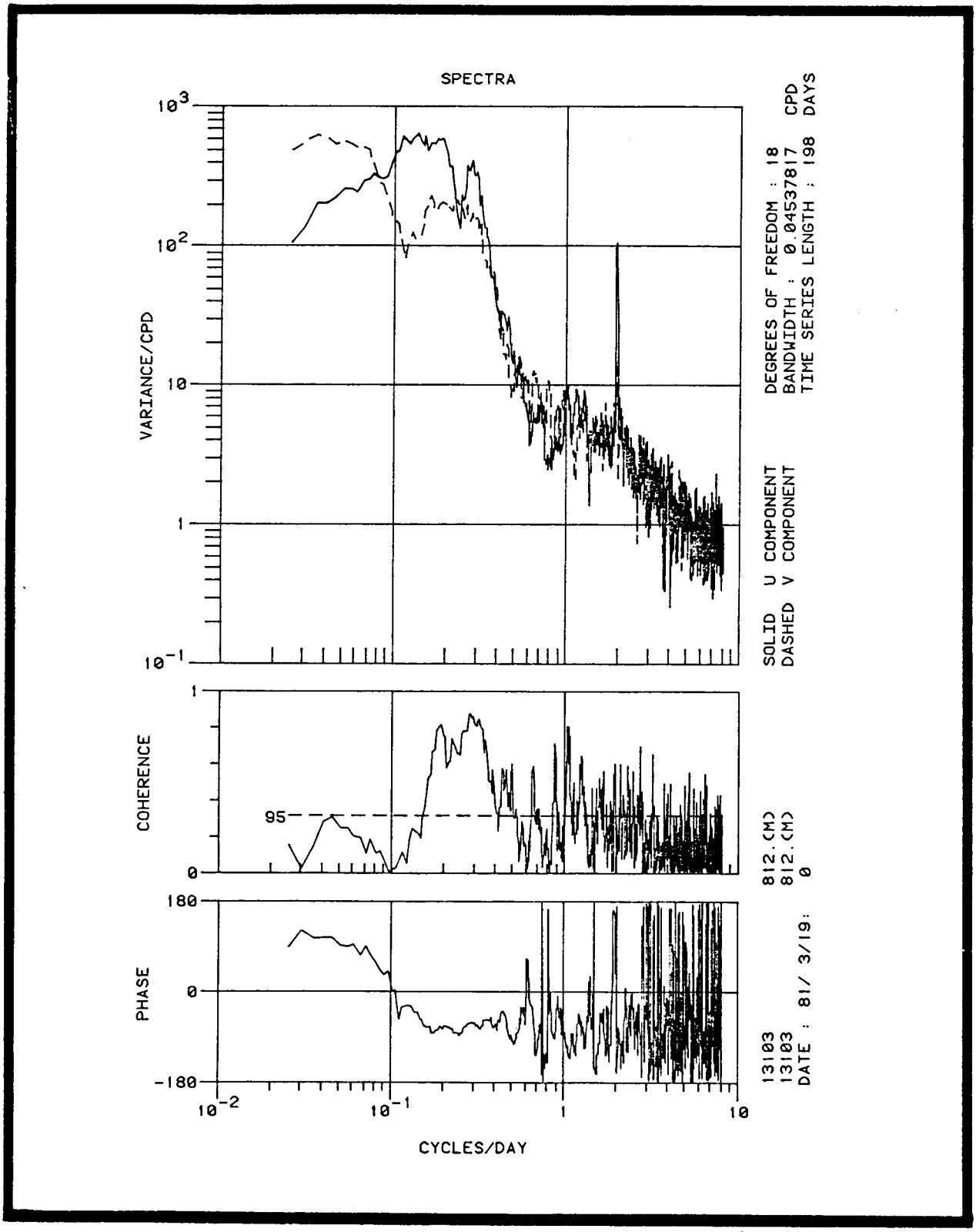

Figure B-24. Spectra of u component vs v component from current meter 13103 during second deployment.

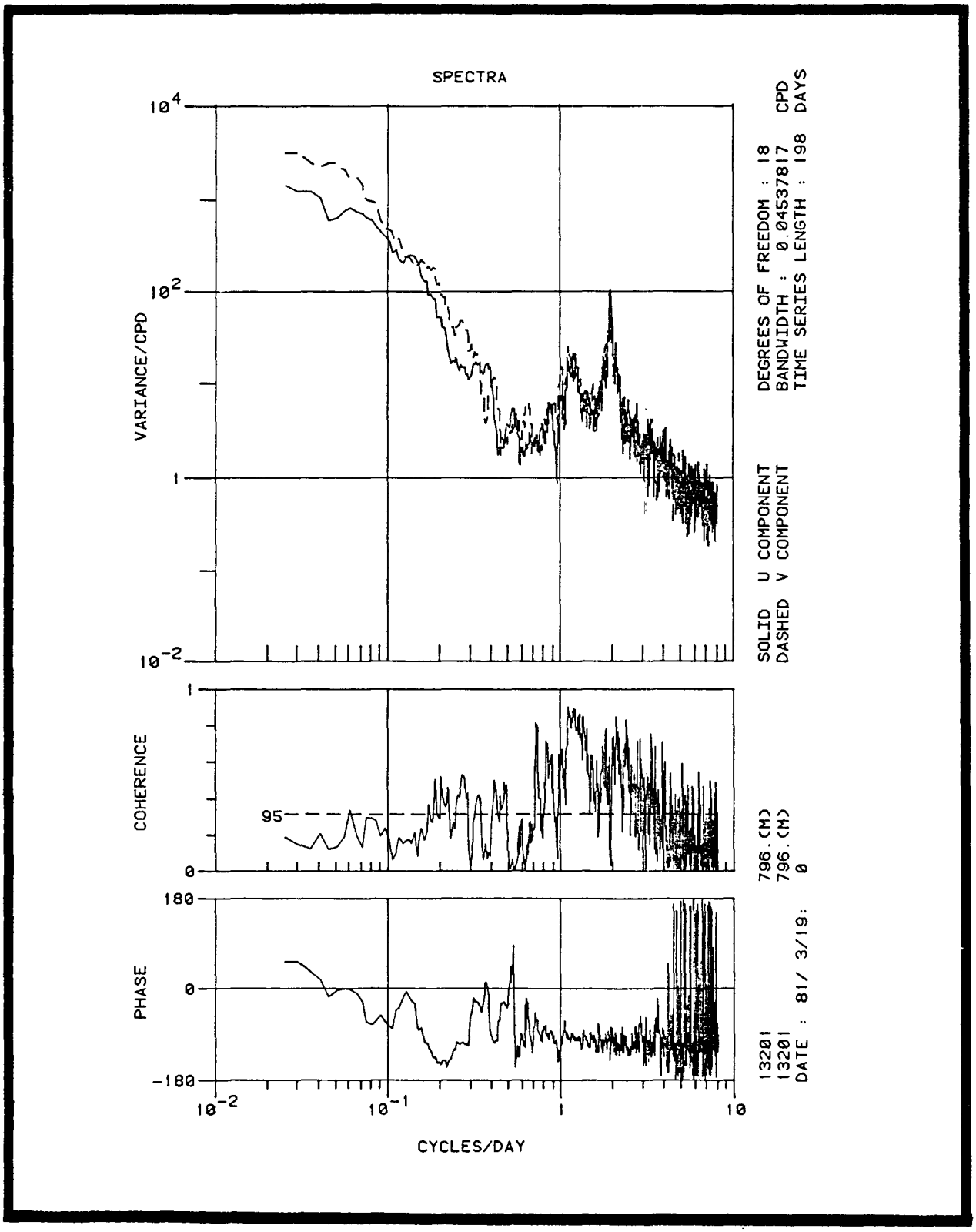

Figure B-25. Spectra of u component vs v component from current meter 13201 during second deployment.

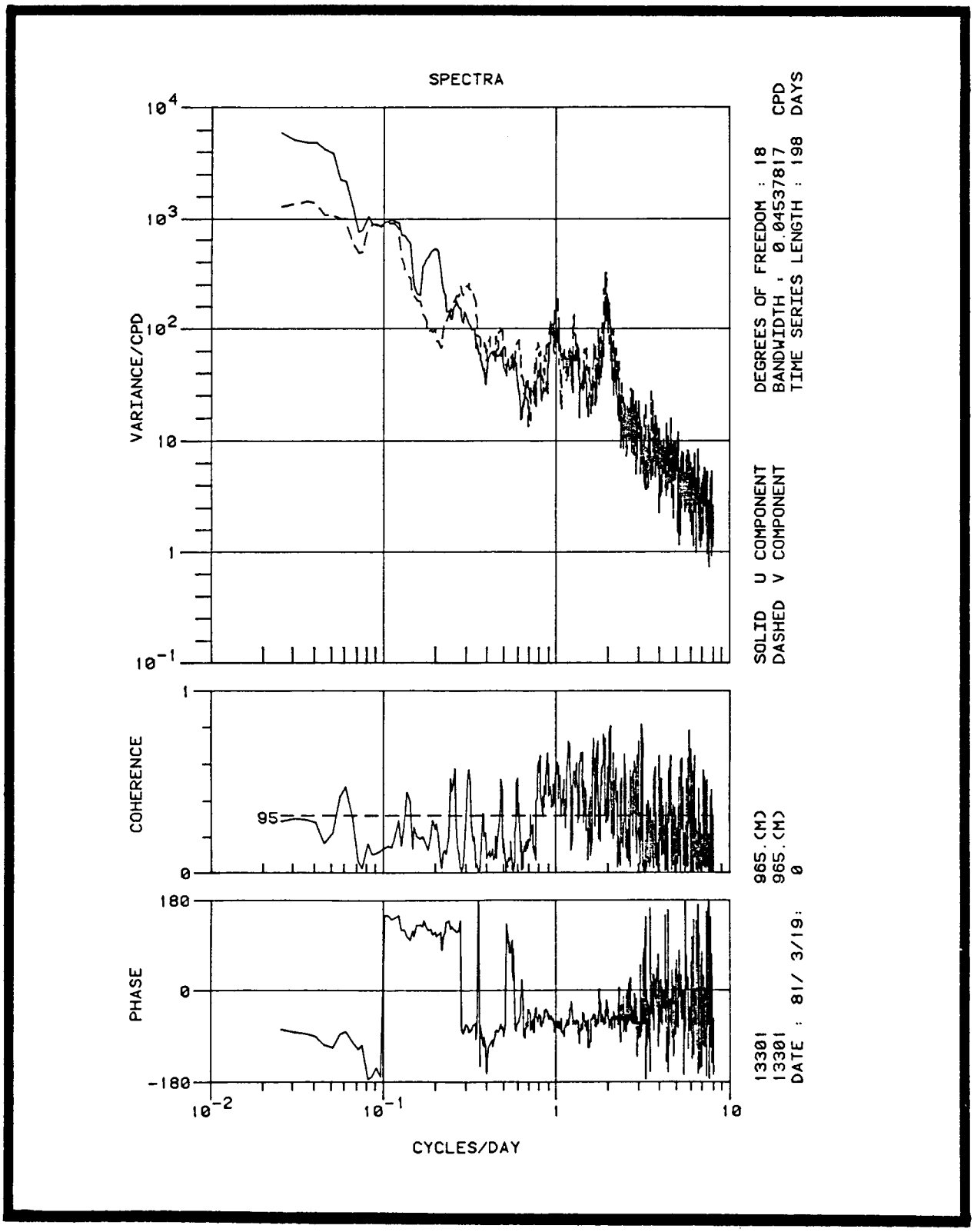

Figure B-26. Spectra of u component vs v component from current meter 13301 during second deployment.

12901 40HRLP
14 DAY AVERAGES

PERIOD NUMBER 1

FROM	THROUGH	VARIABLE	MINIMUM	MAXIMUM	MEAN	STD. DEV.
3/22/81	4/ 4/81	TEMP	15.05	20.14	18.41	1.24
3/22/81	4/ 4/81	U	-16.17	35.07	5.96	11.06
3/22/81	4/ 4/81	V	-18.91	35.50	13.38	14.45

PERIOD NUMBER 2

FROM	THROUGH	VARIABLE	MINIMUM	MAXIMUM	MEAN	STD. DEV.
4/ 5/81	4/18/81	TEMP	14.16	19.83	16.68	1.40
4/ 5/81	4/18/81	U	-4.50	17.32	2.87	4.70
4/ 5/81	4/18/81	V	-29.77	25.11	1.05	13.87

PERIOD NUMBER 3

FROM	THROUGH	VARIABLE	MINIMUM	MAXIMUM	MEAN	STD. DEV.
4/19/81	5/ 2/81	TEMP	15.32	23.30	18.55	2.20
4/19/81	5/ 2/81	U	-20.24	19.71	-.56	8.62
4/19/81	5/ 2/81	V	-25.06	61.06	12.06	22.45

PERIOD NUMBER 4

FROM	THROUGH	VARIABLE	MINIMUM	MAXIMUM	MEAN	STD. DEV.
5/ 3/81	5/16/81	TEMP	14.28	22.73	19.79	2.45
5/ 3/81	5/16/81	U	-12.71	16.50	4.92	6.12
5/ 3/81	5/16/81	V	-28.61	27.45	2.07	14.36

PERIOD NUMBER 5

FROM	THROUGH	VARIABLE	MINIMUM	MAXIMUM	MEAN	STD. DEV.
5/17/81	5/30/81	TEMP	11.77	23.69	18.98	3.17
5/17/81	5/30/81	U	-12.36	25.60	1.55	8.15
5/17/81	5/30/81	V	.40	54.83	20.76	12.77

PERIOD NUMBER 6

FROM	THROUGH	VARIABLE	MINIMUM	MAXIMUM	MEAN	STD. DEV.
5/31/81	6/13/81	TEMP	11.17	19.03	14.96	2.14
5/31/81	6/13/81	U	-5.89	5.97	-.31	3.41
5/31/81	6/13/81	V	8.62	44.53	19.00	8.06

PERIOD NUMBER 7

FROM	THROUGH	VARIABLE	MINIMUM	MAXIMUM	MEAN	STD. DEV.
6/14/81	6/27/81	TEMP	11.86	21.52	18.09	2.42
6/14/81	6/27/81	U	-5.50	16.91	2.85	5.85
6/14/81	6/27/81	V	-5.39	35.08	16.41	11.02

Figure B-27. Statistical parameters of temperature u component, and v component for the second deployment period for current meter 12901.

PERIOD NUMBER 8

FROM	THROUGH	VARIABLE	MINIMUM	MAXIMUM	MEAN	STD. DEV.
6/28/81	7/11/81	TEMP	12.93	20.62	15.78	1.87
6/28/81	7/11/81	U	-4.08	10.32	2.44	2.99
6/28/81	7/11/81	V	-23.63	16.10	-3.12	9.72

PERIOD NUMBER 9

FROM	THROUGH	VARIABLE	MINIMUM	MAXIMUM	MEAN	STD. DEV.
7/12/81	7/25/81	TEMP	14.63	17.84	16.25	.74
7/12/81	7/25/81	U	-13.90	7.44	.98	4.49
7/12/81	7/25/81	V	-26.43	12.95	-7.90	10.44

PERIOD NUMBER 10

FROM	THROUGH	VARIABLE	MINIMUM	MAXIMUM	MEAN	STD. DEV.
7/26/81	8/ 8/81	TEMP	14.19	18.60	16.77	.95
7/26/81	8/ 8/81	U	-2.38	10.27	3.17	3.35
7/26/81	8/ 8/81	V	-26.90	14.69	-.59	7.17

PERIOD NUMBER 11

FROM	THROUGH	VARIABLE	MINIMUM	MAXIMUM	MEAN	STD. DEV.
8/ 9/81	8/22/81	TEMP	14.71	19.72	17.15	1.23
8/ 9/81	8/22/81	U	-3.90	10.26	3.94	3.72
8/ 9/81	8/22/81	V	-19.89	12.67	-2.06	6.70

PERIOD NUMBER 12

FROM	THROUGH	VARIABLE	MINIMUM	MAXIMUM	MEAN	STD. DEV.
8/23/81	9/ 5/81	TEMP	17.17	22.67	19.62	1.55
8/23/81	9/ 5/81	U	-12.08	15.54	3.85	6.48
8/23/81	9/ 5/81	V	-31.35	24.39	-4.09	12.26

PERIOD NUMBER 13

FROM	THROUGH	VARIABLE	MINIMUM	MAXIMUM	MEAN	STD. DEV.
9/ 6/81	9/19/81	TEMP	18.94	25.91	22.38	1.98
9/ 6/81	9/19/81	U	-8.96	13.00	2.63	4.74
9/ 6/81	9/19/81	V	-22.91	31.51	-.05	12.14

PERIOD NUMBER 14

FROM	THROUGH	VARIABLE	MINIMUM	MAXIMUM	MEAN	STD. DEV.
9/20/81	9/30/81	TEMP	15.60	23.77	20.15	2.45
9/20/81	9/30/81	U	-6.28	12.57	3.51	4.22
9/20/81	9/30/81	V	-10.07	18.96	3.31	8.51

FOR THE ENTIRE TIME PERIOD

FROM	THROUGH	VARIABLE	MINIMUM	MAXIMUM	MEAN	STD. DEV.
3/22/81	9/30/81	TEMP	11.17	25.91	18.08	2.75
3/22/81	9/30/81	U	-20.24	35.07	2.69	6.26
3/22/81	9/30/81	V	-31.35	61.06	5.04	15.37

Figure B-27. Continued.

13001 40HRLP
14 DAY AVERAGES

PERIOD NUMBER 1

FROM	THROUGH	VARIABLE	MINIMUM	MAXIMUM	MEAN	STD. DEV.
3/22/81	4/ 4/81	TEMP	38.68	43.20	41.12	1.19
3/22/81	4/ 4/81	U	-13.28	18.24	-1.50	6.49
3/22/81	4/ 4/81	V	46.57	85.62	67.51	8.06

PERIOD NUMBER 2

FROM	THROUGH	VARIABLE	MINIMUM	MAXIMUM	MEAN	STD. DEV.
4/ 5/81	4/18/81	TEMP	36.92	43.21	39.53	1.33
4/ 5/81	4/18/81	U	-12.69	19.69	1.72	6.86
4/ 5/81	4/18/81	V	47.26	83.61	67.60	7.84

PERIOD NUMBER 3

FROM	THROUGH	VARIABLE	MINIMUM	MAXIMUM	MEAN	STD. DEV.
4/19/81	5/ 2/81	TEMP	36.07	42.76	39.85	1.68
4/19/81	5/ 2/81	U	-20.06	12.39	-1.92	7.62
4/19/81	5/ 2/81	V	68.20	102.91	81.64	9.25

PERIOD NUMBER 4

FROM	THROUGH	VARIABLE	MINIMUM	MAXIMUM	MEAN	STD. DEV.
5/ 3/81	5/16/81	TEMP	35.91	43.91	40.83	1.90
5/ 3/81	5/16/81	U	-18.21	26.82	.36	9.44
5/ 3/81	5/16/81	V	60.19	108.68	81.83	14.83

PERIOD NUMBER 5

FROM	THROUGH	VARIABLE	MINIMUM	MAXIMUM	MEAN	STD. DEV.
5/17/81	5/30/81	TEMP	38.75	44.63	41.66	1.33
5/17/81	5/30/81	U	-7.83	23.63	8.74	8.89
5/17/81	5/30/81	V	59.16	94.73	79.46	9.41

PERIOD NUMBER 6

FROM	THROUGH	VARIABLE	MINIMUM	MAXIMUM	MEAN	STD. DEV.
5/31/81	6/13/81	TEMP	38.10	44.51	41.07	1.62
5/31/81	6/13/81	U	-22.94	20.09	1.21	11.64
5/31/81	6/13/81	V	50.81	107.49	77.04	17.09

PERIOD NUMBER 7

FROM	THROUGH	VARIABLE	MINIMUM	MAXIMUM	MEAN	STD. DEV.
6/14/81	6/27/81	TEMP	34.76	43.96	39.96	2.71
6/14/81	6/27/81	U	-24.72	25.56	2.50	10.90
6/14/81	6/27/81	V	49.50	93.42	72.29	12.01

Figure B-28. Statistical parameters of temperature, u component, and v component for the second deployment period for current meter 13001.

PERIOD NUMBER 8

FROM	THROUGH	VARIABLE	MINIMUM	MAXIMUM	MEAN	STD. DEV.
6/28/81	7/11/81	TEMP	36.66	43.24	39.71	1.87
6/28/81	7/11/81	U	-15.39	38.67	7.80	13.52
6/28/81	7/11/81	V	50.51	93.22	70.96	10.90

PERIOD NUMBER 9

FROM	THROUGH	VARIABLE	MINIMUM	MAXIMUM	MEAN	STD. DEV.
7/12/81	7/25/81	TEMP	31.92	42.49	39.09	2.68
7/12/81	7/25/81	U	-41.48	26.87	-8.35	14.26
7/12/81	7/25/81	V	60.01	104.73	81.02	11.49

PERIOD NUMBER 10

FROM	THROUGH	VARIABLE	MINIMUM	MAXIMUM	MEAN	STD. DEV.
7/26/81	8/ 8/81	TEMP	37.51	43.05	40.51	1.40
7/26/81	8/ 8/81	U	-10.85	29.88	6.34	8.08
7/26/81	8/ 8/81	V	65.61	87.00	72.42	3.96

PERIOD NUMBER 11

FROM	THROUGH	VARIABLE	MINIMUM	MAXIMUM	MEAN	STD. DEV.
8/ 9/81	8/22/81	TEMP	35.36	44.09	40.10	2.24
8/ 9/81	8/22/81	U	-7.58	27.47	5.00	8.26
8/ 9/81	8/22/81	V	50.59	89.76	72.72	10.91

PERIOD NUMBER 12

FROM	THROUGH	VARIABLE	MINIMUM	MAXIMUM	MEAN	STD. DEV.
8/23/81	9/ 5/81	TEMP	35.32	43.46	40.40	2.11
8/23/81	9/ 5/81	U	-34.80	31.13	-4.10	15.59
8/23/81	9/ 5/81	V	64.58	99.73	79.83	9.62

PERIOD NUMBER 13

FROM	THROUGH	VARIABLE	MINIMUM	MAXIMUM	MEAN	STD. DEV.
9/ 6/81	9/19/81	TEMP	33.52	44.11	40.47	2.92
9/ 6/81	9/19/81	U	-30.14	22.78	-2.10	12.24
9/ 6/81	9/19/81	V	64.54	106.29	80.14	10.22

PERIOD NUMBER 14

FROM	THROUGH	VARIABLE	MINIMUM	MAXIMUM	MEAN	STD. DEV.
9/20/81	10/ 2/81	TEMP	35.55	43.38	38.92	2.02
9/20/81	10/ 2/81	U	-42.21	27.08	1.88	13.18
9/20/81	10/ 2/81	V	64.18	93.53	78.01	8.44

FOR THE ENTIRE TIME PERIOD

FROM	THROUGH	VARIABLE	MINIMUM	MAXIMUM	MEAN	STD. DEV.
3/22/81	10/ 2/81	TEMP	31.92	44.63	40.24	2.14
3/22/81	10/ 2/81	U	-42.21	38.67	1.25	11.79
3/22/81	10/ 2/81	V	46.57	108.68	75.87	11.80

Figure B-28. Continued.

13002 40HRLP
14 DAY AVERAGES

PERIOD NUMBER 1

FROM	THROUGH	VARIABLE	MINIMUM	MAXIMUM	MEAN	STD. DEV.
3/22/81	4/ 4/81	TEMP	10.16	12.71	11.25	.50
3/22/81	4/ 4/81	U	-11.82	22.83	2.52	7.81
3/22/81	4/ 4/81	V	7.52	59.11	32.07	12.89

PERIOD NUMBER 2

FROM	THROUGH	VARIABLE	MINIMUM	MAXIMUM	MEAN	STD. DEV.
4/ 5/81	4/18/81	TEMP	9.40	11.90	10.38	.66
4/ 5/81	4/18/81	U	-9.69	29.25	9.77	9.31
4/ 5/81	4/18/81	V	4.98	51.41	31.65	13.82

PERIOD NUMBER 3

FROM	THROUGH	VARIABLE	MINIMUM	MAXIMUM	MEAN	STD. DEV.
4/19/81	5/ 2/81	TEMP	9.74	13.28	11.04	.83
4/19/81	5/ 2/81	U	-13.14	37.70	13.62	11.55
4/19/81	5/ 2/81	V	22.18	70.27	50.41	11.60

PERIOD NUMBER 4

FROM	THROUGH	VARIABLE	MINIMUM	MAXIMUM	MEAN	STD. DEV.
5/ 3/81	5/16/81	TEMP	9.03	12.82	11.14	1.02
5/ 3/81	5/16/81	U	-14.27	36.80	12.92	10.69
5/ 3/81	5/16/81	V	12.82	73.00	44.74	16.83

PERIOD NUMBER 5

FROM	THROUGH	VARIABLE	MINIMUM	MAXIMUM	MEAN	STD. DEV.
5/17/81	5/30/81	TEMP	10.03	13.87	11.67	1.07
5/17/81	5/30/81	U	-6.45	41.84	10.96	9.74
5/17/81	5/30/81	V	17.04	66.26	39.39	10.82

PERIOD NUMBER 6

FROM	THROUGH	VARIABLE	MINIMUM	MAXIMUM	MEAN	STD. DEV.
5/31/81	6/13/81	TEMP	9.33	13.60	11.52	.87
5/31/81	6/13/81	U	-13.51	37.79	9.96	11.64
5/31/81	6/13/81	V	3.80	84.63	38.90	19.26

PERIOD NUMBER 7

FROM	THROUGH	VARIABLE	MINIMUM	MAXIMUM	MEAN	STD. DEV.
6/14/81	6/27/81	TEMP	8.11	13.52	10.84	1.64
6/14/81	6/27/81	U	-11.77	17.08	5.80	7.09
6/14/81	6/27/81	V	1.23	56.33	39.72	11.06

Figure B-29. Statistical parameters of temperature, u component, and v component for the second deplyment period for current meter 13002.

PERIOD NUMBER 8

FROM	THROUGH	VARIABLE	MINIMUM	MAXIMUM	MEAN	STD. DEV.
6/28/81	7/11/81	TEMP	9.27	12.33	10.73	.79
6/28/81	7/11/81	U	-15.72	35.75	5.12	12.67
6/28/81	7/11/81	V	11.07	61.12	38.85	13.54

PERIOD NUMBER 9

FROM	THROUGH	VARIABLE	MINIMUM	MAXIMUM	MEAN	STD. DEV.
7/12/81	7/25/81	TEMP	7.69	13.19	10.08	1.45
7/12/81	7/25/81	U	-32.21	23.81	-3.05	13.47
7/12/81	7/25/81	V	14.90	59.41	44.30	9.67

PERIOD NUMBER 10

FROM	THROUGH	VARIABLE	MINIMUM	MAXIMUM	MEAN	STD. DEV.
7/26/81	8/ 8/81	TEMP	8.53	12.46	11.10	.75
7/26/81	8/ 8/81	U	-15.67	31.02	7.71	10.17
7/26/81	8/ 8/81	V	31.12	57.28	44.35	6.11

PERIOD NUMBER 11

FROM	THROUGH	VARIABLE	MINIMUM	MAXIMUM	MEAN	STD. DEV.
8/ 9/81	8/22/81	TEMP	9.10	13.48	11.00	1.15
8/ 9/81	8/22/81	U	-5.59	20.78	6.01	6.69
8/ 9/81	8/22/81	V	17.50	64.19	37.59	11.87

PERIOD NUMBER 12

FROM	THROUGH	VARIABLE	MINIMUM	MAXIMUM	MEAN	STD. DEV.
8/23/81	9/ 5/81	TEMP	8.34	12.94	10.97	1.33
8/23/81	9/ 5/81	U	-16.51	25.02	2.38	10.22
8/23/81	9/ 5/81	V	22.50	62.04	40.07	9.50

PERIOD NUMBER 13

FROM	THROUGH	VARIABLE	MINIMUM	MAXIMUM	MEAN	STD. DEV.
9/ 6/81	9/19/81	TEMP	7.88	13.22	10.87	1.41
9/ 6/81	9/19/81	U	-13.02	20.10	2.88	8.50
9/ 6/81	9/19/81	V	23.26	71.63	43.51	11.60

PERIOD NUMBER 14

FROM	THROUGH	VARIABLE	MINIMUM	MAXIMUM	MEAN	STD. DEV.
9/20/81	10/ 2/81	TEMP	8.48	12.28	10.06	.92
9/20/81	10/ 2/81	U	-25.25	28.86	6.12	10.68
9/20/81	10/ 2/81	V	21.68	66.04	42.83	9.71

FOR THE ENTIRE TIME PERIOD

FROM	THROUGH	VARIABLE	MINIMUM	MAXIMUM	MEAN	STD. DEV.
3/22/81	10/ 2/81	TEMP	7.69	13.87	10.91	1.17
3/22/81	10/ 2/81	U	-32.21	41.84	6.63	11.13
3/22/81	10/ 2/81	V	1.23	84.63	40.58	13.40

Figure B-29. Continued.

13101 40HRLP
14 DAY AVERAGES

PERIOD NUMBER 1

FROM	THROUGH	VARIABLE	MINIMUM	MAXIMUM	MEAN	STD. DEV.
3/22/81	4/ 4/81	TEMP	16.79	18.35	17.89	.45
3/22/81	4/ 4/81	U	-13.30	17.26	.87	6.98
3/22/81	4/ 4/81	V	3.28	57.36	24.76	13.17

PERIOD NUMBER 2

FROM	THROUGH	VARIABLE	MINIMUM	MAXIMUM	MEAN	STD. DEV.
4/ 5/81	4/18/81	TEMP	17.72	18.56	18.20	.26
4/ 5/81	4/18/81	U	-26.31	21.74	2.76	10.34
4/ 5/81	4/18/81	V	-4.19	64.72	34.09	12.58

PERIOD NUMBER 3

FROM	THROUGH	VARIABLE	MINIMUM	MAXIMUM	MEAN	STD. DEV.
4/19/81	5/ 2/81	TEMP	17.66	18.57	18.32	.21
4/19/81	5/ 2/81	U	-9.72	13.31	2.21	6.10
4/19/81	5/ 2/81	V	4.70	45.52	24.34	9.78

PERIOD NUMBER 4

FROM	THROUGH	VARIABLE	MINIMUM	MAXIMUM	MEAN	STD. DEV.
5/ 3/81	5/16/81	TEMP	16.87	18.52	18.00	.38
5/ 3/81	5/16/81	U	-21.44	23.01	3.06	9.21
5/ 3/81	5/16/81	V	4.30	51.48	28.74	15.14

PERIOD NUMBER 5

FROM	THROUGH	VARIABLE	MINIMUM	MAXIMUM	MEAN	STD. DEV.
5/17/81	5/30/81	TEMP	18.34	18.90	18.73	.11
5/17/81	5/30/81	U	-9.35	29.09	3.94	8.23
5/17/81	5/30/81	V	3.13	57.91	28.96	15.81

PERIOD NUMBER 6

FROM	THROUGH	VARIABLE	MINIMUM	MAXIMUM	MEAN	STD. DEV.
5/31/81	6/13/81	TEMP	17.29	18.84	18.13	.42
5/31/81	6/13/81	U	-15.61	30.45	-.82	11.41
5/31/81	6/13/81	V	2.79	38.72	16.57	8.77

PERIOD NUMBER 7

FROM	THROUGH	VARIABLE	MINIMUM	MAXIMUM	MEAN	STD. DEV.
6/14/81	6/27/81	TEMP	16.81	18.59	17.96	.40
6/14/81	6/27/81	U	-14.97	15.40	-.58	6.80
6/14/81	6/27/81	V	.64	55.69	32.99	14.27

Figure B-30. Statistical parameters of temperature, u component, and v component for the second deployment period for current meter 13101.

PERIOD NUMBER 8

FROM	THROUGH	VARIABLE	MINIMUM	MAXIMUM	MEAN	STD. DEV.
6/28/81	7/11/81	TEMP	16.52	18.35	17.72	.44
6/28/81	7/11/81	U	-21.33	16.08	-1.75	8.95
6/28/81	7/11/81	V	-5.35	38.44	16.05	10.48

PERIOD NUMBER 9

FROM	THROUGH	VARIABLE	MINIMUM	MAXIMUM	MEAN	STD. DEV.
7/12/81	7/25/81	TEMP	17.54	18.40	17.98	.26
7/12/81	7/25/81	U	-11.76	12.05	-1.86	5.87
7/12/81	7/25/81	V	20.19	42.63	30.68	5.04

PERIOD NUMBER 10

FROM	THROUGH	VARIABLE	MINIMUM	MAXIMUM	MEAN	STD. DEV.
7/26/81	8/ 8/81	TEMP	17.35	18.46	17.97	.28
7/26/81	8/ 8/81	U	-13.75	10.32	.50	5.91
7/26/81	8/ 8/81	V	6.39	30.41	18.88	6.54

PERIOD NUMBER 11

FROM	THROUGH	VARIABLE	MINIMUM	MAXIMUM	MEAN	STD. DEV.
8/ 9/81	8/22/81	TEMP	16.48	18.64	18.01	.51
8/ 9/81	8/22/81	U	-9.01	28.93	5.66	8.77
8/ 9/81	8/22/81	V	12.66	58.87	33.51	11.04

PERIOD NUMBER 12

FROM	THROUGH	VARIABLE	MINIMUM	MAXIMUM	MEAN	STD. DEV.
8/23/81	9/ 5/81	TEMP	17.52	18.58	18.19	.34
8/23/81	9/ 5/81	U	-18.05	38.64	5.52	12.08
8/23/81	9/ 5/81	V	-.37	38.59	19.65	8.07

PERIOD NUMBER 13

FROM	THROUGH	VARIABLE	MINIMUM	MAXIMUM	MEAN	STD. DEV.
9/ 6/81	9/19/81	TEMP	17.61	18.70	18.29	.32
9/ 6/81	9/19/81	U	-11.79	6.49	-1.50	4.84
9/ 6/81	9/19/81	V	10.03	34.14	24.94	5.52

PERIOD NUMBER 14

FROM	THROUGH	VARIABLE	MINIMUM	MAXIMUM	MEAN	STD. DEV.
9/20/81	10/ 2/81	TEMP	16.99	18.55	17.93	.42
9/20/81	10/ 2/81	U	-6.32	20.04	5.54	6.88
9/20/81	10/ 2/81	V	20.65	50.84	35.26	8.79

FOR THE ENTIRE TIME PERIOD

FROM	THROUGH	VARIABLE	MINIMUM	MAXIMUM	MEAN	STD. DEV.
3/22/81	10/ 2/81	TEMP	16.48	18.90	18.10	.43
3/22/81	10/ 2/81	U	-26.31	38.64	1.65	8.77
3/22/81	10/ 2/81	V	-5.35	64.72	26.31	12.64

Figure B-30. Continued.

13102 40HRLP
14 DAY AVERAGES

PERIOD NUMBER 1

FROM	THROUGH	VARIABLE	MINIMUM	MAXIMUM	MEAN	STD. DEV.
3/22/81	4/ 4/81	TEMP	11.95	14.51	13.64	.74
3/22/81	4/ 4/81	U	-20.88	18.02	-.97	8.64
3/22/81	4/ 4/81	V	.07	29.85	18.84	7.15

PERIOD NUMBER 2

FROM	THROUGH	VARIABLE	MINIMUM	MAXIMUM	MEAN	STD. DEV.
4/ 5/81	4/18/81	TEMP	12.09	14.91	13.76	.77
4/ 5/81	4/18/81	U	-14.28	24.27	.73	9.45
4/ 5/81	4/18/81	V	10.86	51.77	23.47	8.93

PERIOD NUMBER 3

FROM	THROUGH	VARIABLE	MINIMUM	MAXIMUM	MEAN	STD. DEV.
4/19/81	5/ 2/81	TEMP	13.13	15.09	14.47	.43
4/19/81	5/ 2/81	U	-16.53	19.48	-.11	9.56
4/19/81	5/ 2/81	V	4.00	27.87	17.59	5.88

PERIOD NUMBER 4

FROM	THROUGH	VARIABLE	MINIMUM	MAXIMUM	MEAN	STD. DEV.
5/ 3/81	5/16/81	TEMP	12.85	15.38	14.21	.60
5/ 3/81	5/16/81	U	-17.01	18.99	1.68	10.02
5/ 3/81	5/16/81	V	6.06	41.13	23.77	9.50

PERIOD NUMBER 5

FROM	THROUGH	VARIABLE	MINIMUM	MAXIMUM	MEAN	STD. DEV.
5/17/81	5/30/81	TEMP	13.97	16.15	15.50	.49
5/17/81	5/30/81	U	-14.50	17.77	.78	7.97
5/17/81	5/30/81	V	3.89	52.69	23.66	12.17

PERIOD NUMBER 6

FROM	THROUGH	VARIABLE	MINIMUM	MAXIMUM	MEAN	STD. DEV.
5/31/81	6/13/81	TEMP	12.32	15.44	14.09	.83
5/31/81	6/13/81	U	-20.03	39.93	-1.25	14.25
5/31/81	6/13/81	V	-18.07	34.05	15.03	12.51

PERIOD NUMBER 7

FROM	THROUGH	VARIABLE	MINIMUM	MAXIMUM	MEAN	STD. DEV.
6/14/81	6/27/81	TEMP	12.73	14.73	13.75	.54
6/14/81	6/27/81	U	-19.94	15.05	.20	8.79
6/14/81	6/27/81	V	-13.45	45.01	23.14	12.89

Figure B-31. Statistical parameters of temperature, u component, and v component for the second deployment period for current meter 13102.

PERIOD NUMBER 8

FROM	THROUGH	VARIABLE	MINIMUM	MAXIMUM	MEAN	STD. DEV.
6/28/81	7/11/81	TEMP	12.18	14.82	13.35	.72
6/28/81	7/11/81	U	-28.27	24.76	.17	15.11
6/28/81	7/11/81	V	-9.49	25.17	10.86	10.45

PERIOD NUMBER 9

FROM	THROUGH	VARIABLE	MINIMUM	MAXIMUM	MEAN	STD. DEV.
7/12/81	7/25/81	TEMP	11.35	14.62	13.32	.92
7/12/81	7/25/81	U	-11.54	8.42	-2.22	4.70
7/12/81	7/25/81	V	-1.44	23.72	12.96	6.37

PERIOD NUMBER 10

FROM	THROUGH	VARIABLE	MINIMUM	MAXIMUM	MEAN	STD. DEV.
7/26/81	8/ 8/81	TEMP	12.94	14.29	13.67	.35
7/26/81	8/ 8/81	U	-12.96	6.19	-.63	4.89
7/26/81	8/ 8/81	V	-2.14	19.96	8.98	5.75

PERIOD NUMBER 11

FROM	THROUGH	VARIABLE	MINIMUM	MAXIMUM	MEAN	STD. DEV.
8/ 9/81	8/22/81	TEMP	11.79	15.38	13.90	1.05
8/ 9/81	8/22/81	U	-6.29	23.42	2.36	7.39
8/ 9/81	8/22/81	V	8.59	38.79	22.33	8.08

PERIOD NUMBER 12

FROM	THROUGH	VARIABLE	MINIMUM	MAXIMUM	MEAN	STD. DEV.
8/23/81	9/ 5/81	TEMP	12.58	15.42	14.57	.74
8/23/81	9/ 5/81	U	-24.51	17.86	1.22	10.46
8/23/81	9/ 5/81	V	-1.14	29.19	12.68	7.11

PERIOD NUMBER 13

FROM	THROUGH	VARIABLE	MINIMUM	MAXIMUM	MEAN	STD. DEV.
9/ 6/81	9/19/81	TEMP	12.32	15.51	14.32	.85
9/ 6/81	9/19/81	U	-17.08	15.43	-.98	6.30
9/ 6/81	9/19/81	V	-2.43	24.47	9.35	5.99

PERIOD NUMBER 14

FROM	THROUGH	VARIABLE	MINIMUM	MAXIMUM	MEAN	STD. DEV.
9/20/81	10/ 2/81	TEMP	11.56	15.07	13.33	.98
9/20/81	10/ 2/81	U	-12.51	23.24	1.34	9.00
9/20/81	10/ 2/81	V	1.81	40.26	18.31	9.91

FOR THE ENTIRE TIME PERIOD

FROM	THROUGH	VARIABLE	MINIMUM	MAXIMUM	MEAN	STD. DEV.
3/22/81	10/ 2/81	TEMP	11.35	16.15	14.00	.94
3/22/81	10/ 2/81	U	-28.27	39.93	.15	9.54
3/22/81	10/ 2/81	V	-18.07	52.69	17.20	10.56

Figure B-31. Continued.

13103 40HRLP
14 DAY AVERAGES

PERIOD NUMBER 1

FROM	THROUGH	VARIABLE	MINIMUM	MAXIMUM	MEAN	STD. DEV.
3/22/81	4/ 4/81	TEMP	8.06	9.42	8.82	.41
3/22/81	4/ 4/81	U	-16.01	15.24	-2.11	8.12
3/22/81	4/ 4/81	V	2.78	14.97	8.84	3.10

PERIOD NUMBER 2

FROM	THROUGH	VARIABLE	MINIMUM	MAXIMUM	MEAN	STD. DEV.
4/ 5/81	4/18/81	TEMP	8.14	9.80	8.96	.43
4/ 5/81	4/18/81	U	-13.42	13.32	-.26	7.77
4/ 5/81	4/18/81	V	-7.44	18.46	7.27	6.03

PERIOD NUMBER 3

FROM	THROUGH	VARIABLE	MINIMUM	MAXIMUM	MEAN	STD. DEV.
4/19/81	5/ 2/81	TEMP	8.91	10.09	9.66	.37
4/19/81	5/ 2/81	U	-12.23	14.15	.07	7.68
4/19/81	5/ 2/81	V	-5.76	11.93	4.30	5.19

PERIOD NUMBER 4

FROM	THROUGH	VARIABLE	MINIMUM	MAXIMUM	MEAN	STD. DEV.
5/ 3/81	5/16/81	TEMP	8.97	10.23	9.75	.38
5/ 3/81	5/16/81	U	-17.31	9.94	-3.49	8.03
5/ 3/81	5/16/81	V	-5.34	20.85	11.97	5.23

PERIOD NUMBER 5

FROM	THROUGH	VARIABLE	MINIMUM	MAXIMUM	MEAN	STD. DEV.
5/17/81	5/30/81	TEMP	9.58	11.45	10.71	.51
5/17/81	5/30/81	U	-14.56	12.34	-2.22	7.06
5/17/81	5/30/81	V	-10.92	22.39	6.88	8.74

PERIOD NUMBER 6

FROM	THROUGH	VARIABLE	MINIMUM	MAXIMUM	MEAN	STD. DEV.
5/31/81	6/13/81	TEMP	8.07	10.90	9.50	.88
5/31/81	6/13/81	U	-13.63	23.88	-1.27	8.88
5/31/81	6/13/81	V	-16.61	26.58	6.03	9.87

PERIOD NUMBER 7

FROM	THROUGH	VARIABLE	MINIMUM	MAXIMUM	MEAN	STD. DEV.
6/14/81	6/27/81	TEMP	8.21	9.96	9.07	.51
6/14/81	6/27/81	U	-12.22	10.66	-1.15	6.67
6/14/81	6/27/81	V	-6.67	22.54	8.61	7.17

Figure B-32. Statistical parameters of temperature, u component, and v component for the second deployment period for current meter 13103.

PERIOD NUMBER 8

FROM	THROUGH	VARIABLE	MINIMUM	MAXIMUM	MEAN	STD. DEV.
6/28/81	7/11/81	TEMP	8.17	10.01	8.82	.42
6/28/81	7/11/81	U	-19.60	19.54	-1.20	12.03
6/28/81	7/11/81	V	-18.85	13.80	2.53	9.65

PERIOD NUMBER 9

FROM	THROUGH	VARIABLE	MINIMUM	MAXIMUM	MEAN	STD. DEV.
7/12/81	7/25/81	TEMP	7.30	9.73	8.68	.69
7/12/81	7/25/81	U	-15.87	16.53	-2.78	9.45
7/12/81	7/25/81	V	-4.16	13.29	6.56	4.51

PERIOD NUMBER 10

FROM	THROUGH	VARIABLE	MINIMUM	MAXIMUM	MEAN	STD. DEV.
7/26/81	8/ 8/81	TEMP	7.40	9.87	9.02	.67
7/26/81	8/ 8/81	U	-11.36	13.85	.12	7.29
7/26/81	8/ 8/81	V	-9.31	11.59	4.85	5.57

PERIOD NUMBER 11

FROM	THROUGH	VARIABLE	MINIMUM	MAXIMUM	MEAN	STD. DEV.
8/ 9/81	8/22/81	TEMP	8.29	10.57	9.54	.57
8/ 9/81	8/22/81	U	-15.28	12.80	-2.90	6.34
8/ 9/81	8/22/81	V	3.26	27.09	10.90	5.02

PERIOD NUMBER 12

FROM	THROUGH	VARIABLE	MINIMUM	MAXIMUM	MEAN	STD. DEV.
8/23/81	9/ 5/81	TEMP	7.23	10.74	9.26	1.26
8/23/81	9/ 5/81	U	-15.41	21.90	1.47	10.49
8/23/81	9/ 5/81	V	-6.06	16.20	7.41	4.72

PERIOD NUMBER 13

FROM	THROUGH	VARIABLE	MINIMUM	MAXIMUM	MEAN	STD. DEV.
9/ 6/81	9/19/81	TEMP	7.37	9.24	8.30	.52
9/ 6/81	9/19/81	U	-13.74	18.74	-.49	7.77
9/ 6/81	9/19/81	V	-9.06	17.57	1.80	6.19

PERIOD NUMBER 14

FROM	THROUGH	VARIABLE	MINIMUM	MAXIMUM	MEAN	STD. DEV.
9/20/81	10/ 2/81	TEMP	7.61	9.42	8.65	.44
9/20/81	10/ 2/81	U	-14.04	21.52	-2.22	9.29
9/20/81	10/ 2/81	V	-6.55	18.84	7.91	6.24

FOR THE ENTIRE TIME PERIOD

FROM	THROUGH	VARIABLE	MINIMUM	MAXIMUM	MEAN	STD. DEV.
3/22/81	10/ 2/81	TEMP	7.23	11.45	9.20	.86
3/22/81	10/ 2/81	U	-19.60	23.88	-1.31	8.58
3/22/81	10/ 2/81	V	-18.85	27.09	6.84	7.12

Figure B-32. Continued.

13201 40HRLP
14 DAY AVERAGES

PERIOD NUMBER 1

FROM	THROUGH	VARIABLE	MINIMUM	MAXIMUM	MEAN	STD. DEV.
3/22/81	4/ 4/81	TEMP	8.50	9.58	9.06	.21
3/22/81	4/ 4/81	U	-10.35	5.24	-4.91	3.03
3/22/81	4/ 4/81	V	-26.61	-1.65	-12.46	7.30

PERIOD NUMBER 2

FROM	THROUGH	VARIABLE	MINIMUM	MAXIMUM	MEAN	STD. DEV.
4/ 5/81	4/18/81	TEMP	8.49	10.46	9.42	.56
4/ 5/81	4/18/81	U	-10.02	.64	-5.18	2.79
4/ 5/81	4/18/81	V	-25.56	-9.71	-17.28	4.65

PERIOD NUMBER 3

FROM	THROUGH	VARIABLE	MINIMUM	MAXIMUM	MEAN	STD. DEV.
4/19/81	5/ 2/81	TEMP	7.03	9.55	8.81	.71
4/19/81	5/ 2/81	U	-11.70	14.40	1.43	6.48
4/19/81	5/ 2/81	V	-17.07	10.75	-1.06	8.66

PERIOD NUMBER 4

FROM	THROUGH	VARIABLE	MINIMUM	MAXIMUM	MEAN	STD. DEV.
5/ 3/81	5/16/81	TEMP	7.75	8.78	8.40	.33
5/ 3/81	5/16/81	U	-5.34	13.09	4.96	5.18
5/ 3/81	5/16/81	V	-12.26	7.39	-2.46	5.17

PERIOD NUMBER 5

FROM	THROUGH	VARIABLE	MINIMUM	MAXIMUM	MEAN	STD. DEV.
5/17/81	5/30/81	TEMP	8.63	10.99	9.91	.69
5/17/81	5/30/81	U	-14.01	5.10	-3.64	5.29
5/17/81	5/30/81	V	-18.81	9.15	-7.27	7.17

PERIOD NUMBER 6

FROM	THROUGH	VARIABLE	MINIMUM	MAXIMUM	MEAN	STD. DEV.
5/31/81	6/13/81	TEMP	6.72	10.85	9.43	1.36
5/31/81	6/13/81	U	1.39	19.38	8.99	6.01
5/31/81	6/13/81	V	8.13	21.36	14.18	2.90

PERIOD NUMBER 7

FROM	THROUGH	VARIABLE	MINIMUM	MAXIMUM	MEAN	STD. DEV.
6/14/81	6/27/81	TEMP	5.16	8.19	7.46	.77
6/14/81	6/27/81	U	-4.33	19.83	6.03	8.43
6/14/81	6/27/81	V	-21.25	25.77	2.10	15.41

Figure B-33. Statistical parameters of temperature, u component, and v component for the second deployment period for current meter 13201.

PERIOD NUMBER 8

FROM	THROUGH	VARIABLE	MINIMUM	MAXIMUM	MEAN	STD. DEV.
6/28/81	7/11/81	TEMP	7.04	9.31	8.15	.59
6/28/81	7/11/81	U	-15.23	8.58	-7.19	6.64
6/28/81	7/11/81	V	-12.87	35.29	8.65	13.88

PERIOD NUMBER 9

FROM	THROUGH	VARIABLE	MINIMUM	MAXIMUM	MEAN	STD. DEV.
7/12/81	7/25/81	TEMP	8.51	9.38	9.04	.27
7/12/81	7/25/81	U	-15.05	4.00	-3.72	4.70
7/12/81	7/25/81	V	-9.39	5.16	-2.41	4.96

PERIOD NUMBER 10

FROM	THROUGH	VARIABLE	MINIMUM	MAXIMUM	MEAN	STD. DEV.
7/26/81	8/ 8/81	TEMP	8.56	9.41	8.98	.27
7/26/81	8/ 8/81	U	-7.04	12.68	3.07	6.68
7/26/81	8/ 8/81	V	-11.88	-1.66	-7.08	2.63

PERIOD NUMBER 11

FROM	THROUGH	VARIABLE	MINIMUM	MAXIMUM	MEAN	STD. DEV.
8/ 9/81	8/22/81	TEMP	8.96	9.61	9.21	.17
8/ 9/81	8/22/81	U	-7.75	5.90	1.76	2.99
8/ 9/81	8/22/81	V	-12.25	1.32	-5.15	4.11

PERIOD NUMBER 12

FROM	THROUGH	VARIABLE	MINIMUM	MAXIMUM	MEAN	STD. DEV.
8/23/81	9/ 5/81	TEMP	6.78	9.93	8.69	1.03
8/23/81	9/ 5/81	U	-20.41	3.90	-9.62	6.99
8/23/81	9/ 5/81	V	-20.44	16.87	.18	10.16

PERIOD NUMBER 13

FROM	THROUGH	VARIABLE	MINIMUM	MAXIMUM	MEAN	STD. DEV.
9/ 6/81	9/19/81	TEMP	5.27	10.00	7.20	1.74
9/ 6/81	9/19/81	U	-20.11	8.20	-5.53	8.12
9/ 6/81	9/19/81	V	-18.96	26.26	2.24	14.70

PERIOD NUMBER 14

FROM	THROUGH	VARIABLE	MINIMUM	MAXIMUM	MEAN	STD. DEV.
9/20/81	10/ 1/81	TEMP	5.42	7.08	5.90	.35
9/20/81	10/ 1/81	U	-15.63	14.09	-2.34	7.84
9/20/81	10/ 1/81	V	-15.92	21.80	2.01	10.76

FOR THE ENTIRE TIME PERIOD

FROM	THROUGH	VARIABLE	MINIMUM	MAXIMUM	MEAN	STD. DEV.
3/22/81	10/ 1/81	TEMP	5.16	10.99	8.57	1.27
3/22/81	10/ 1/81	U	-20.41	19.83	-1.12	8.10
3/22/81	10/ 1/81	V	-26.61	35.29	-1.89	11.91

Figure B-33. Continued.

13301 40HRLP
14 DAY AVERAGES

PERIOD NUMBER 1

FROM	THROUGH	VARIABLE	MINIMUM	MAXIMUM	MEAN	STD. DEV.
3/22/81	4/ 4/81	TEMP	4.27	6.07	5.01	.63
3/22/81	4/ 4/81	U	-23.97	33.45	12.34	18.65
3/22/81	4/ 4/81	V	-21.29	17.01	-3.89	9.47

PERIOD NUMBER 2

FROM	THROUGH	VARIABLE	MINIMUM	MAXIMUM	MEAN	STD. DEV.
4/ 5/81	4/18/81	TEMP	5.25	7.95	6.37	.90
4/ 5/81	4/18/81	U	-25.49	35.39	3.17	18.03
4/ 5/81	4/18/81	V	-7.95	24.81	11.10	6.47

PERIOD NUMBER 3

FROM	THROUGH	VARIABLE	MINIMUM	MAXIMUM	MEAN	STD. DEV.
4/19/81	5/ 2/81	TEMP	6.94	9.52	8.55	.85
4/19/81	5/ 2/81	U	-.73	35.54	25.01	9.46
4/19/81	5/ 2/81	V	-22.63	19.92	-.09	14.51

PERIOD NUMBER 4

FROM	THROUGH	VARIABLE	MINIMUM	MAXIMUM	MEAN	STD. DEV.
5/ 3/81	5/16/81	TEMP	4.08	9.47	7.57	1.44
5/ 3/81	5/16/81	U	-25.62	18.90	-1.18	11.18
5/ 3/81	5/16/81	V	-22.64	27.79	4.32	14.30

PERIOD NUMBER 5

FROM	THROUGH	VARIABLE	MINIMUM	MAXIMUM	MEAN	STD. DEV.
5/17/81	5/30/81	TEMP	3.94	7.71	4.56	.89
5/17/81	5/30/81	U	-15.78	29.73	12.66	11.92
5/17/81	5/30/81	V	-19.31	25.17	1.25	12.83

PERIOD NUMBER 6

FROM	THROUGH	VARIABLE	MINIMUM	MAXIMUM	MEAN	STD. DEV.
5/31/81	6/13/81	TEMP	4.05	8.51	7.62	1.13
5/31/81	6/13/81	U	5.31	35.63	26.85	7.48
5/31/81	6/13/81	V	-20.63	22.53	11.57	9.52

PERIOD NUMBER 7

FROM	THROUGH	VARIABLE	MINIMUM	MAXIMUM	MEAN	STD. DEV.
6/14/81	6/27/81	TEMP	4.04	8.46	5.56	1.81
6/14/81	6/27/81	U	-25.93	26.89	5.58	17.03
6/14/81	6/27/81	V	-16.53	14.33	1.78	8.39

Figure B-34. Statistical parameters of temperature, u component, and v component for the second deployment period for current meter 13301.

PERIOD NUMBER 8

FROM	THROUGH	VARIABLE	MINIMUM	MAXIMUM	MEAN	STD. DEV.
6/28/81	7/11/81	TEMP	3.94	8.25	6.13	1.25
6/28/81	7/11/81	U	-26.01	31.62	6.64	18.51
6/28/81	7/11/81	V	-34.51	26.33	-1.71	13.59

PERIOD NUMBER 9

FROM	THROUGH	VARIABLE	MINIMUM	MAXIMUM	MEAN	STD. DEV.
7/12/81	7/25/81	TEMP	4.15	5.64	4.66	.34
7/12/81	7/25/81	U	-24.46	14.89	-7.72	11.26
7/12/81	7/25/81	V	-6.64	22.94	7.12	8.47

PERIOD NUMBER 10

FROM	THROUGH	VARIABLE	MINIMUM	MAXIMUM	MEAN	STD. DEV.
7/26/81	8/ 8/81	TEMP	4.35	4.95	4.51	.12
7/26/81	8/ 8/81	U	-1.90	12.05	3.90	3.76
7/26/81	8/ 8/81	V	-7.06	8.50	-.36	3.82

PERIOD NUMBER 11

FROM	THROUGH	VARIABLE	MINIMUM	MAXIMUM	MEAN	STD. DEV.
8/ 9/81	8/22/81	TEMP	4.51	6.11	5.21	.59
8/ 9/81	8/22/81	U	-10.61	13.39	1.04	6.95
8/ 9/81	8/22/81	V	-5.27	14.63	2.18	5.27

PERIOD NUMBER 12

FROM	THROUGH	VARIABLE	MINIMUM	MAXIMUM	MEAN	STD. DEV.
8/23/81	9/ 5/81	TEMP	4.12	5.41	4.37	.26
8/23/81	9/ 5/81	U	-11.40	8.13	-.20	4.70
8/23/81	9/ 5/81	V	-5.42	9.17	1.64	3.82

PERIOD NUMBER 13

FROM	THROUGH	VARIABLE	MINIMUM	MAXIMUM	MEAN	STD. DEV.
9/ 6/81	9/19/81	TEMP	4.36	7.26	5.76	.69
9/ 6/81	9/19/81	U	-3.06	31.53	11.60	11.67
9/ 6/81	9/19/81	V	-6.31	13.84	6.10	4.83

PERIOD NUMBER 14

FROM	THROUGH	VARIABLE	MINIMUM	MAXIMUM	MEAN	STD. DEV.
9/20/81	10/ 1/81	TEMP	4.19	6.18	4.98	.71
9/20/81	10/ 1/81	U	-4.25	14.07	3.94	4.15
9/20/81	10/ 1/81	V	-5.23	9.51	2.00	3.53

FOR THE ENTIRE TIME PERIOD

FROM	THROUGH	VARIABLE	MINIMUM	MAXIMUM	MEAN	STD. DEV.
3/22/81	10/ 1/81	TEMP	3.94	9.52	5.79	1.59
3/22/81	10/ 1/81	U	-26.01	35.63	7.45	15.39
3/22/81	10/ 1/81	V	-34.51	27.79	3.09	10.38

Figure B-34. Continued.